Development and intensification of a foam flotation system in harvesting microalgae for biofuel

A Thesis Submitted By

Muayad Abed Shihab Al-karawi

For the Degree of Doctor of Philosophy

School of Chemical Engineering and Advanced Materials
Newcastle University

November 2018

Abstract

Due to their photosynthetic efficiency, microalgae tend to have high lipid content and growth rates, hence their importance to the biofuel sector. However, the viability of microalgae-derived biofuel is hindered by high capital and/or operating costs required for cultivation, harvesting, and drying. Harvesting the microalgae cells represents a substantial process cost, accounting for an estimated 30% of the total cost of production particularly because of the low concentration of microalgal biomass relative to water in the algae culture.

Foam flotation can be utilised as an energy-efficient harvesting and enriching technique for microalgae biomass with the potential to significantly reduce the production cost of algal fuel. In this thesis, foam flotation was used for the first time in a continuous mode to harvest freshwater and marine microalgae species in an attempt to overcome the trade-off between recovery efficiency and enrichment in batch and semi-batch foam flotation. The influences of cell surface characteristics on flotation performance were investigated by quantifying hydrophobicity, zeta potential, and contact angle. Fractional factorial and response surface designs of experiment were used to determine the best operating conditions to achieve an effective combination of a high recovery efficiency (for greater biomass removal from the growth medium) and concentration factor (to lower downstream dewatering and drying costs).

Tubular setups of different smooth-successive contraction and expansion ratios (foam riser) were used for the first time to enhance foam drainage. A recovery efficiency of 91% was obtained for *Chlorella vulgaris* with a concentration factor of 722. Foam flotation demonstrated a much lower power consumption (0.052 kWh m^{-3} of algae culture) in comparison to other flotation techniques including dissolved air flotation and electro-flotation.

The algal biomass harvested by foam flotation was processed directly using hydrothermal liquefaction (HTL) without extra stages for dewatering and drying or intermediate storage. Thus, it can offer precise investigations on the process feasibility and it also represents a more realistic scenario for the application of HTL. The fate of surfactant in harvested microalgae and its effects on the HTL product yield and distribution were also investigated. HTL of *C. vulgaris* recovered by foam flotation demonstrated that the surfactant had additional benefits on HTL product yield, distribution, and composition.

Overall, foam flotation is an effective, rapid, low cost, media (and arguably species) independent, scalable harvesting system which is able to operate continuously. Foam flotation also delivers algal biomass having additional advantages for biofuel production.

Acknowledgements

First and foremost, I would like to express my sincere gratitude to my academic advisors: Dr. Jonathan G.M. Lee and Dr. Gary S. Caldwell for the continuous support of my PhD study, their keen supervision, patience, advice, motivation, encouragement, and immense knowledge. This dissertation would not have been accomplished without their tremendous help, guidance, and wealth of knowledge. It has been a great honour and a pleasure to work with both of you.

My profound appreciation also goes to the most precious humans being in the world: my life-coach, my late father Abed Shihab Ahmed, my mother, my brother: Mohannad Abed Shihab, my sisters, my wife, my daughters: Dimah and Tiba, I am very grateful for their prayers and encouragement.

I would like to extend thanks to Dr. Valentine Eze and Dr. Jonathan McDonough for their help. Similar, profound appreciation goes to all process intensification group members. I would like also to acknowledge useful contributions from my friends at Newcastle University and office colleagues.

I would like to acknowledge the help I have received from CEAM and marine technical and IT support staff: Rob Dixon, Michael Percival, David Whitaker, Peter McParlin, Paul Roberts, Paul Sterling, Simon Daley, Daniel Padgett, and CEAM administrative staff. I am hugely appreciative to all of you.

I gratefully acknowledge the funding source that made my PhD study possible. I was funded by Higher Committee for Education Development in Iraq (HCED).

Table of contents

List of figures

List of figures

List of figures

List of figures

List of figures

List of tables

List of tables

Abbreviations and notation

Abbreviation	
ABS	Adsorptive bubble separation
AD	Anaerobic digestion
ASP	Aquatic species program
BSA	Bovine serum albumin
BSD	Bubble size distribution
CCD	Central composite design
COD	Chemical oxygen demand
CTAB	Cetyltrimethylammonium bromide
DAF	Dissolved air flotation
DAG	Diacylglycerol
DAH	Dodecylammonium hydrochloride
DCM	Dichloromethane
DFF	Direct flow filtration
DiAF	Dispersed air flotation
DOE	Design of experiment or US Department of energy
DPC	Dodecyl pyridinium chloride
DW	Dry weight basis
EOM	Extracellular organic matter
EPS	Extracellular polymer substances
FAEE	Fatty acid ethyl ester
FAME	Fatty acid methyl ester
FFA	Free fatty acids
FID	Flame ionisation detector
GHG	Greenhouse gas
HHV	Higher heating value
HTG	Hydrothermal gasification
HTL	Hydrothermal liquefaction
MAG	Monoacylglycerol
OMEGA	Offshore membrane enclosures for growing microalgae
PCs	Pharmaceutical contaminants
SCWG	Supercritical water gasification
SDS	Sodium dodecylsulfate

Abbreviations and notation

SLS	Significance level to stay
TAG	Triacylglycerol
TCD	Thermal conductivity detector
TFF	Tangential (cross) flow filtration

Notation

A	Parameter in bubble-particle collision efficiency model
A_{aq}	Absorbance reading of the aqueous phase after n-hexane addition
A_c	Flotation column cross sectional area
A_o	Absorbance reading of the microalgae suspension before n-hexane addition
C	Concentration of particles in the bubbly liquid
C_∞	Concentration of particle remained in the bubbly liquid after infinite time
CF	Concentration factor
C_f	Concentration of particles in the feed stream
d	Microalgae cell diameter
D	Diameter of the foam column
Di	Axial dispersion coefficient
d_{32}	Sauter mean bubble diameter
d_b	Mean bubble diameter
d_p	Particle diameter
DWC	Dry weight concentration
E_a	Attachment efficiency
E_c	Collision efficiency
E_{col}	Collection efficiency
ER	Energy recovery
E_s	Stability efficiency of the particle-bubble aggregate
g	Acceleration due to gravity
H	Humidity of air
H_s	Humidity of the saturated air
h	Liquid pool depth
H_{ydro}	Hydrophobicity of the algal suspension

Abbreviations and notation

j_d	Superficial drainage velocity
J_g	Superficial gas velocity
J_l	Superficial liquid velocity
k	Flotation rate constant
k_f	Rate constant of fast-floating particles
k_s	Rate constant of slow-floating particles
K_w	Dissociation constant of water
m	Adjustable parameter in measuring superficial drainage velocity for vertical foam column (calculated by a forced drainage method)
M_A	Molecular weight of air
M_{algae}	Algal feedstock mass
M_{ash}	Ash mass
M_{sR}	Solid residue mass
M_w	Molecular weight of water
n	Adjustable parameter in measuring superficial drainage velocity for vertical foam column (calculated by a forced drainage method)
n_b	Bubble flow rate
P	Total pressure
P_0	Pressure upstream of the compressor
P_1	Pressure of the compressed gas
P_s	Vapour pressure of the water at system temperature
Pe_p	Equivalent particle Peclet number
R	Universal gas constant
R	Particle recovery in the foamate
R_∞	Maximum recovery after infinite time
r_b	Bubble radius
RE	Recovery efficiency
Re_b	Bubble Reynolds number
Re_p	Particle Reynolds number
r_o	Sparger mean pore size
s_b	Bubble surface area flux
St	Stokes number
t	Flotation time
t_{con}	Contact time

Abbreviations and notation

t_{ind}	Induction time
T_o	Absolute initial temperature
t_{sl}	Sliding time
TSS	Total suspended solids
V	Particle settling velocity
V_b	Bubble rise velocity
W_{comp}	Compressor work
Wt_1	Aluminium dish weight
Wt_2	Wet microalgae sample and dish weight
Wt_3	Dry microalgae sample and dish weight
x_i	Independent variable in the polynomial quadratic regression model
x_j	Independent variable in the polynomial quadratic regression model
Y	Predicted response

Greek letters

β_i	Linear effect coefficient in the polynomial quadratic regression model
β_{ii}	Squared effect coefficient in the polynomial quadratic regression model
β_{ij}	Interaction effect coefficient in the polynomial quadratic regression model
β_o	Intercept term in the polynomial quadratic regression model
ε_L	Liquid fraction of the foam
ε_G	Gas fraction of the bubbly liquid
θ_c	Angle of bubble-particle collision
θ_{ca}	Contact angle of microalgae cell
ρ_f	Liquid density
ρ_g	Gas density
ρ_p	Particle density
ρ_s	Microalgae cell density
τ_w	Wall shear stress
τ_p	Particle residence time
τ_l	Liquid residence time
γ	Ratio of the isobaric to isochoric heat capacities

Abbreviations and notation

η_{is}	Efficiency of air compressor
λ	Gamma distribution function
μ	Liquid viscosity
σ	Liquid surface tension
φ	Fraction of flotation particles

Chapter 1

Introduction

1.1 Project background

Global challenges coincident with fossil fuels burning (energy security, environmental pollution, climate change) are some of the main drivers behind the ongoing search for affordable, reliable, and environmentally friendly fuels (Jing Lu *et al.*, 2011; Pragya *et al.*, 2013; Reyes and Labra, 2016). Microalgae have been called a "third-generation" source of biofuels that can play a vital role in the biofuel market due to their higher lipid content and high growth rate relative to terrestrial crops (Wenchao Yang *et al.*, 2014). Microalgae can be cultivated on non-arable land and consequently avoid direct competition with agricultural crops. Moreover, many of the species of microalgae can be grown in wastewater by consuming inorganic nitrogen and phosphorus as nutrients to reduce the costs for commercialisation (F. Chen *et al.*, 2012; Farid *et al.*, 2013; C. Zhang *et al.*, 2016a). Several downstream processing steps are required to produce and convert microalgae into biofuels comprising harvesting, further dewatering, drying, and lastly a conversion process of algal biomass into biofuel (Halim *et al.*, 2012). However, microalgae-derived biofuel is not viable yet due to high capital and/or operating costs, including the energy input required for harvesting, dewatering, and drying. Harvesting of the algae biomass represents a substantial process cost, accounting for an estimated 20-30% of the total cost of production and it has been suggested up to 50% of algal biomass cost. For microalgae production in open systems, it has been estimated that 90% of the equipment cost may come from harvesting and dewatering (Molina Grima *et al.*, 2003; Greenwell *et al.*, 2010; Milledge and Heaven, 2012). Harvesting from dilute algae suspensions is challenging due to the small cell size translating to a low specific gravity, as well as the cell surface being negatively charged thereby maintaining a stable colloidal suspension. Other impediments stem from the ionic strength of the culture medium due to salinity, pH, and hydrophobicity of microalgae species (Milledge and Heaven, 2012; Udom *et al.*, 2013). A wide range of solid-liquid separation techniques have been trialled, both individually or in combination, such as coagulation and flocculation, followed by sedimentation, flotation, centrifugation, or filtration. Both efficiency and energy consumption of the harvesting technology have major impacts on the economic feasibility of microalgal derived biofuels.

A successful harvesting system needs to be effective, rapid, low cost, species independent, scalable, and should be able to operate continuously if required. Adsorptive bubble separation is a process of separation and concentration based on differences in the physicochemical

properties of interfaces. Due to its simplicity and low capital and operating costs, it is widely used in industrial and domestic wastewater treatment, and in the mining, pharmaceutical, rubber, glass, plastics, and food industries (Jenkins *et al.*, 1972; Rubio *et al.*, 2002; Fuerstenau *et al.*, 2007; Schramm and Mikula, 2012; Bu X, 2016). Foam flotation, which is a subclass of adsorptive bubble separation, is a selective separation process which shows notable promise as a microalgae biomass harvesting and enrichment method. Foam flotation columns have a number of advantages over other algal harvesting techniques including simple construction and lower capital, operating and maintenance costs when compared to centrifugation and filtration. It requires less time and floor space compared to that required for flocculation and sedimentation. Foam flotation processes have additional advantages such as the ability of the process to scale up and operate in a continuous mode. The majority of previously reported works on the bulk harvesting of microalgae have been adopted in a batch or semi-batch modes and consequently they focused only on the recovery efficiency or concentration factor of the harvested microalgae due to the trade-off between them, very few studies have considered both those effectiveness criteria. Achieving an effective combination of a high recovery efficiency (for greater biomass removal from the growth medium) and concentration factor (to lower downstream dewatering and drying costs) is pivotal for driving down the cost of handling and processing bulk quantities of microalgae. Therefore, research into an effective combination of high recovery efficiency and high concentration factor in a foam flotation column that operates in a continuous mode, at the same time determining the process economics, is highly important.

Harvested microalgae can be converted chemically, thermo-chemically and biologically into a wide range of biofuel products such as biodiesel and bio-oils. However, due to the very high-water content in algal biomass and to avoid the major costs and power consumption associated with dewatering and drying, hydrothermal liquefaction (HTL) of microalgal biomass is the most appropriate biomass into biofuel conversion process that allows microalgae to be processed wet with high water content (López Barreiro *et al.*, 2013; Tian *et al.*, 2014). Hydrothermal liquefaction is a technique for converting the whole microalgae biomass and is more rapid than other biomass to biofuel conversion processes such as the fermentation and *in-situ* transesterification. The majority of the previous HTL works on microalgal biomass has been carried out using pulverised-dried or freeze-dried microalgae mixed with deionised water. Using different microalgal physical state will probably affect the composition and yield of the bio-oil since the extractability of some constituents might be changed due to the pulverising and freeze-drying of harvested microalgae. Therefore, yield and chemical composition of bio-oil from direct HTL of algae slurry recovered by any harvesting technique like foam flotation

in this work is more meaningful. Research into the influence of microalgae harvested by foam flotation on hydrothermal product yield and composition is required to observe any positive or negative implications that the harvesting process may have on both quantity and quality of biofuels.

1.2 Project development

The present work developed a foam flotation column to continuously harvest freshwater and marine microalgae species. The influence of controllable process variables on the recovery efficiency and concentration factor were evaluated and optimised. Attention was also paid to the harvesting economics including the power consumption and chemical costs to assess the economic feasibility of the process. Next, the influence of tubular inserts in the foam column, with smooth contraction and expansion profiles, on the draining of microalgae-containing foam was investigated. Lastly, the harvested microalgae from the foam flotation column were converted directly to bio-oil without extra stages of dewatering and drying, using a HTL process. Direct liquefaction of the harvested microalgae hydrothermally can offer precise investigations on the process feasibility and it represents a more realistic scenario for the application of HTL.

1.3 Aims and objectives

The foam flotation column, can be utilised as an effective harvesting and enriching technique for microalgae biomass. However, for foam flotation operating in batch or semi-batch modes, it is difficult to find an effective combination of high recovery efficiency and concentration factor. The aim of the work described in this thesis is therefore to develop a foam flotation column to continuously harvest microalgae species not only for high throughputs but also to attempt to overcome the barrier described above. This study also aims to demonstrate unambiguously the economic feasibility and the capability of continuous foam flotation to recover high microalgae biomass without any negative implications on the harvested algae for biofuel production. An understanding of the influences of process key factors on both microalgae recovery and enrichment can result in a pivotal combination between factors to achieve high recovery efficiency and concentration factor together. It is also imperative to understand the effect of the foam flotation process on biofuel yield and composition. Accordingly, the specific objectives of this research are:

1- To review the current state of knowledge.
2- To develop a foam flotation column to continuously harvest freshwater and marine microalgae species.

3- To investigate the effects of surface characteristics on microalgae flotation performance by quantifying the hydrophobicity, zeta potential, and the contact angle.
4- To determine the significance of each individual process variable and the interactions among variables on the recovery efficiency and concentration factor of the harvested microalgae.
5- To optimise the key process variables to achieve an effective combination of a high recovery efficiency (for greater biomass removal from the growth medium) and concentration factor (to lower downstream dewatering and drying costs).
6- To compare the power consumption and chemical costs of the foam flotation column with the other commonly used harvesting techniques.
7- To intensify the process by enhancing the drainage of the foam containing microalgae (i.e. increasing the concentration factor of the harvested microalgae) to lower downstream dewatering and drying costs.
8- To study the flotation kinetics and probabilities of bubble-microalgae cell collision, attachment, and detachment, for better understanding of this complex physicochemical process.
9- To assess the direct conversion of the harvested microalgae into biofuel without extra stages for dewatering, drying, and storing using a hydrothermal liquefaction process.
10- To understand the effect of the foam flotation process on the hydrothermal liquefaction product yield, quality and composition.

1.4 Outline of the thesis

This thesis is presented as a series of chapters formatted in the style of journal papers. All chapters were written by the primary author, Muayad Al-karawi, and edited by Dr Jonathan Lee and Dr Gary Caldwell. All experimental work was conducted by Muayad Al-karawi.

This introduction is followed by a literature review (chapter two) in which microalgae as a sustainable source of biofuels is assessed. The review includes brief discussions on culturing systems, harvesting, drying techniques and biofuel production methods, with the focus on the advantages and disadvantages of commonly available harvesting technologies and conversion methods of algal biomass to biofuel. This demonstrates awareness about the research which has already been performed and identifies knowledge gaps to advance the scientific understanding in these areas. This chapter supports a platform for comparing the outcomes from the current research with the existing results.

Chapter three describes the design of a continuous foam flotation column. The hydrophobicity of microalgae was enhanced at first using cationic, anionic, and non-ionic surfactants. The

effects of surface characteristics on microalgae flotation performance were then investigated by measuring the zeta potential and the contact angle. Fractional factorial and central composite design experiments were conducted to study the effect of individual variables and variables interactions on the effectiveness criteria of the harvest process (the current work focusses on both recovery efficiency and the concentration factor). Flotation process factors were then optimised to maximise microalgae recovery at a considerable concentration factor. The power consumption and chemical costs were also considered in this chapter and compared to those of commonly used harvesting techniques.

Chapter four investigates the potential to intensify a continuous foam flotation column through enhancing microalgae-containing foam drainage. Tubular inserts with different contraction and expansion ratios were used for this purpose. The effect of the tubular inserts on concentration factor and recovery efficiency of harvested microalgae were studied only with key variables of the foam flotation process noted in chapter three. Liquid fraction in the rising foam containing microalgae was measured using the pressure profile in the foam column to examine the foam drainage upon using these drainage enhancer modules.

Chapter five includes a theoretical study of the probabilities of collision, attachment, and detachment between microalgae cells and bubbles in the flotation column based on experimental measurements of bubble size, rise velocity, and microalgae cell size. This chapter also covers the kinetics models of foam flotation of microalgae and determines the flotation rate constant for continuous foam flotation under different experimental conditions. Foam flotation is a complex process that involves the interactions between three phases (solid, gas, and liquid) in the presence of surfactant chemicals; therefore, studying these phenomenological models (i.e. probabilistic and kinetic models) is important to better understand and develop the continuous foam flotation process.

Chapter 6 investigates the use of microalgae harvested by a continuous foam flotation column as a feedstock for biofuel production. Direct hydrothermal liquefaction (HTL) of microalgae harvested by foam flotation and by centrifugation were carried out to observe any potential influences that harvesting via foam flotation may have on product yields and compositions. The direct HTL of algal biomass without extra stages for dewatering, drying and intermediate storage will yield information on the process feasibility and it represents a more realistic scenario for the application of the HTL process. Surfactants and three model compounds (starch, bovine serum albumin (BSA), and rapeseed oil) representing the three categories of

biochemical compounds present in microalgae (carbohydrate, protein, and lipid) were also liquefied hydrothermally in isolation to support interpretation of experimental data.

The overall impact of the work described in the previous chapters is discussed and summarised in chapter 7. The recommendations for future work and projects are also discussed in this chapter including the potential of harvesting more freshwater and marine microalgae species in order to give foam flotation the advantage of being a species independent harvester. Continuous conversion of harvested microalgae into bio-oil is recommended through the connection of a continuous high-pressure reactor for the HTL with the continuous foam flotation column.

Chapter 2

Literature review

Abstract

In the last two decades, there has been massive interest from the research community in biofuel production due to the growing concerns associated with the sustainability of petroleum-based fuels as well as their contribution to atmospheric pollution and CO_2 levels. Biofuels such as biodiesel and bioethanol are currently produced from food crops such as oil palm and sugarcane, however there are many economic and ethical concerns related to the use of food crops and large agrarian lands for fuel production. Second generation biofuels that utilise the whole plant bring more advantages than first generation; however, the lack of efficient technologies for large-scale production, the transportation of biomass, and high investment requirements are the major drawbacks associated with this generation. Third generation biofuels derived from microalgae are considered as the most promising alternative energy resource that can overcome the major drawbacks of first- and second-generation biofuels. Nevertheless, the production of algal biomass is still limited to approximately 10 to 20 thousand tons per year (dry weight basis). Microalgae-derived low value high demand products such as biofuels are currently not economically feasible due to the high capital and operating costs of cultivation, harvesting and drying stages. This chapter serves as a platform to present a comprehensive review on state-of-the-art production techniques for microalgae-based biofuels from species isolation to biofuel conversion technologies. In this review, foam flotation is highlighted as a promising technique for low-cost and rapid harvesting of microalgae. Apart from harvesting, this review also shows that hydrothermal liquefaction of algal biomass as has additional advantages for biofuel production.

2.1 Introduction

2.1.1 Energy crisis and biofuels

Post the Industrial Revolution in 18^{th} century, energy started to play an essential role in all life aspects including but not limited to transportation, heating, and electricity generation. Energy sources can be categorised into non-renewable fossil fuels and renewables like biomass. The term fossil fuel refers to coal, natural gas, and crude oil that were formed from buried plants and animals through different lysis processes under high pressure and temperature as well as bacterial action for millions of years (Ayhan Demirbas and Demirbas, 2010; Davudov and Moghanloo, 2017). Over the last two decades, massive attention has been given to renewable

energy resources due to the concerns about the sustainability of fossil fuel, fluctuating market price of fossil fuel, global climate change, and environmental pollution (Y. L. Cheng *et al.*, 2011; Pragya *et al.*, 2013). According to expert's reports, most fossil fuel reservoirs will be depleted over the next 50 years with the current consumption rate and consequently fossil fuels will become more expensive (Wilson, 2012). The overwhelming level of greenhouse gases (particularly CO_2) emissions is another issue arising from the use of conventional fuels. CO_2 has a warming influence on the atmosphere due to its absorption and emission of infrared radiation. As a result, there is a continuous increase in global surface temperature and sea levels (F. Li, 2012). According to measurements made by the Mauna Loa observatory, Hawaii, the measured CO_2 concentration at 2018 was 409 ppm while the suggested upper safety concentration is 350 ppm (Loa, 2018, July). Moreover, CO_2 emissions are forecast to increase due to the growing demand of energy caused by the increase in the world's population and increasing use of technology. In addition to CO_2 emissions, a number of air pollutants emitted at the same time when fossil fuels (especially coal) are burnt, such as sulphur dioxide (SO_2) and nitrogen oxides (NO_x) which have many harmful impacts on public health and the environment. Additional water and air pollution come from the extraction, transportation and processing of fossil fuels (Perera, 2018).

Renewable energy can be defined as the energy that relies mainly on natural sources such as wind power, biomass, hydropower, geothermal, solar and tidal. Currently, about 24% of the global electricity generation depends on renewable resources (World Energy Statistics, 2017). Among all renewable energies, biomass represents a promising energy source to produce biofuels that may substitute fossil fuels especially in the transportation sector since most renewable energies are exploited to supply fully or partly the demands of electric power and heating. In the future, it is expected that biomass will be at the top of sustainable energy sources with 3,271 million ton oil equivalent by 2040 (Ayhan Demirbas and Demirbas, 2010). Biomass is a term that refers to all biological substances derived from living or lately living plants (such as algae and agricultural crops) and their wastes (Tekin *et al.*, 2014). Biomass can be processed thermo-chemically, chemically, or biologically to produce biofuels such as biodiesel, bioethanol, bio-methane, bio-oil, and bio-syngas (Uduman *et al.*, 2010b). These biofuels are renewable resources and biodegradable (F. Li, 2012). Moreover, less emissions of CO, NOx, lower unburned hydrocarbon residues as well as lower smoke opacity were noticed from the combustion of microalgae oil methyl ester compared to those from the combustion of diesel (Satputaley *et al.*, 2017).

2.1.2 Biomass sources and their potential for biofuel production

First generation biofuels such as biodiesel and bioethanol derived from food crops like oil palm and sugarcane have shown potential as a viable alternative to liquid fuels. However, economic and ethical concerns come from using food crops and large agrarian lands for fuel production (A. J. Dassey, 2013). Although the growth in production and consumption of first generation biofuels is increasing, their potential to meet the overall energy demand particularly for the transport sector is still limited due to competition with food crops for the use of agricultural lands, otherwise they may cause food insufficiency as well as deforestation if mass production is applied (Noraini *et al.*, 2014). For instance, about 220 trillion litres of diesel were consumed in US through 2010. Using soybeans as an example, with an average oil productivity of 600 litres per hectare (l/Ha) per year, to yield this volume of diesel requires 367 million Ha whereas only 178 million Ha is currently available for culturing crops in the US (Leite *et al.*, 2013). In the UK, only 6 million Ha of arable land is available and 2.4 million Ha is forest in contrast with the total land area of 24.3 million Ha. Consequently, to produce biodiesel to meet only a 10% rapeseed methyl ester blend, 15 to 36% of the UK arable land is required (Thea Coward, 2012). Second generation biofuels derived from inedible biomass like switch grass and wood have attempted to overtake these concerns by replacing agricultural crops with lignocellulosic materials due to their abundance worldwide. However, intense pre-treatment steps are required to decompose these types of biomass due to their lignin (a complex aromatic polymer) content and the crystalline structure of cellulose. Commercial production of second generation biofuels is currently limited (Xin Bei Tan *et al.*, 2018). Other concerns are derived from both feedstock's economics as well as their effects on nature. For instance, commercial scale production uses large amounts of water, nitrate fertilisers and agrochemical which may result in reduction in water availability and soil activity over time (D. P. Ho *et al.*, 2014; Ullah *et al.*, 2015).

Algae have been classified as the third-generation source of biofuel that can overcome the major drawbacks associated with first- and second-generation sources. Algae are very diverse photosynthetic organisms growing in aqueous environments, soils, snow, and hot springs. They are broadly classified into microalgae and macroalgae (seaweed). Algae have sizes ranging from several microns to giant kelp which can extend up to 46 m. Microalgae are preferable over macroalgae due to the differences in their biochemical compositions especially lipid content which make the former more versatile. Microalgae are planktonic microorganisms which can grow under severe conditions owing to their simple structure. Over 35,000 microalgae species have been described and the real number will be significantly higher (Pahl *et al.*, 2013; Xin Bei Tan *et al.*, 2018). The use of algae goes back into ancient history; the Chinese first used the

edible blue green algae, *Nostoc* (technically a cyanobacterium), as food to survive during a famine 2000 years ago (Spolaore *et al.*, 2006). Currently, microalgae are highlighted as the most efficient photosynthetic organisms, which may play a vital role in the biofuel market due to their high lipid content and superior growth rate. Solid paleobotanical evidence demonstrated that microalgae are the main constituents of many of the fossil fuel hydrocarbon sources used today. For instance, *Botryococcus* was observed to be dominant in oil shale in Puertollano, Spain (Borrego *et al.*, 1996).

The growing interest in microalgae as a feedstock is due to their ability to fix CO_2 and capturing the energy from sunlight 10-50 times more rapidly than other plants, which means they can be considered for carbon culture (Chinnasamy *et al.*, 2010a; M. K. Lam and Lee, 2012). Microalgae have been reported to produce oil amounts larger than those produced from oil crops as illustrated in table 2.1 (Brennan and Owende, 2010; Lohrey, 2012; Cui, 2013). Most microalgae species have a high growth rate of about 0.54 day^{-1} and high lipid production without the need to provide large amount of raw materials in comparison to other plants (Andrew K. Lee *et al.*, 2013; Coons *et al.*, 2014). For instance, approximately 591-3650 kg of seawater is required for microalgae cultivation to produce 1 kg of biodiesel whereas 13676, 14201, and 19924 kg of freshwater are required for the cultivation of soybean, rapeseed, and jatropha respectively to produce 1 kg of biodiesel (Gerbens-Leenes *et al.*, 2009; Jia Yang *et al.*, 2011a). Unlike terrestrial plants, different microalgae have the remarkable ability to be cultivated in freshwater, seawater, brackish, municipal and agricultural wastewater where microalgae offer an additional benefit by contributing to the wastewater treatment process, as a cost-effective method, through absorbing the nitrates, phosphates, and other organic matters like organic dyes as nutrients (F. Chen *et al.*, 2012; Farid *et al.*, 2013; Pleissner and Rumpold, 2018). Recently, many investigations have been conducted to study the capability of microalgae strains for removing pharmaceutical contaminants (PCs) and if so, this will increase the applications of microalgae for removing unwanted materials from industrial wastewater (Xiong *et al.*, 2018). During the cultivation period, it is easy to control the cultivation conditions to enhance microalgae biomass yield or lipid content (Y. L. Cheng *et al.*, 2011; Nurra *et al.*, 2014). Some unicellular green microalgae have the capability to produce hydrogen (H_2) photo-biologically over the cultivation period (Wonjun Park and Moon, 2007; Ust'ak *et al.*, 2007). In the case of microalgae biodiesel production, the residuals after lipid extraction can also be used as valuable co-products. These chemical compounds like pigments (β-carotenes, phycoerthrin, and astaxanthin) and vitamins can be exploited in the nutraceuticals, pharmaceuticals, and cosmetics fields (Spolaore *et al.*, 2006). Microalgae are not a conventional food source like

corn, palm oil and soybean (but are used as nutritional supplements) and used as biomass feedstock for biofuel, it will not affect global food markets (A. J. Dassey, 2013). Lastly, microalgae can be used as enhancers in upgrading heavy oil under supercritical water conditions to lower coke formation and increased lighter products (Caniaz *et al.*, 2018).

Source	Oil productivity per year
	l/Ha
Corn	168
Soybeans	449
Camelina	580
Sunflower	954
Canola	1,187
Jatropha	1,890
Coconut	2,685
Oil Palm	5,940
Microalgae (based on 30% lipid content)	58,707

Table 2.1: Biodiesel productivity from different biomass sources (Brennan and Owende, 2010; Lohrey, 2012; Cui, 2013)

2.2 Microalgae biomass cultivation technologies

The selection of appropriate microalgae strains for biofuel production is the most important step before cultivation. Suitable species should have high growth rate, high ability to survive in different environments, high lipid productivity, and have ability to be cultivated under different production conditions i.e. photoautotrophy, heterotrophy, and mixotrophy. Throughout cultivation, water, light, CO_2, nutrients (nitrogen, phosphorus, etc.), an appropriate temperature and mixing are required for sustained rapid growth. Light is the most important factor for growth and productivity since it provides the energy required for photosynthesis. Sunlight and/or artificial light (e.g. fluorescent lamps or multi-LED light) are used in microalgae cultivation systems. The latter is more efficient than sunlight for producing microalgae of high biomass and oil productivity. However, fluorescent lamps consume higher energy and therefore they are often replaced by multi-LED light sources or fibre optic lighting excited by solar energy (Qari *et al.*, 2017). CO_2 is the carbon source for algal biomass production that can be obtained directly from air as well as from industrial exhaust gases, which may contain around 15% CO_2. A previous study has demonstrated that 1.8 kg of CO_2 (from atmosphere, industrial flue gases, or soluble carbonate) was required to produce 1 kg of microalgae indicating that cultivation represents an efficient and feasible path for carbon fixation (Abdel-Raouf *et al.*, 2012). Microalgae biomass comprises 30-50% dry weight basis (DW) carbon, 30-50% DW

oxygen, 3-7% DW hydrogen, and 4-9% DW nitrogen, and 1-3% DW phosphorus in addition to trace amounts of other elements such as sulphur, calcium, magnesium, and potassium. Therefore, it is essential to include all these nutrients in the culture medium to obtain maximum culture performance. The nutrients are supplied by dissolving them in the algae culture and CO_2 is supplied as a gas although only dissolved CO_2 will be available for the cells as the carbon source (Acién *et al.*, 2017). CO_2 reacts with water and produces carbonic acid, carbonate, or bicarbonate according to the medium pH before being used by the microalgae. During photosynthesis, O_2 is released and it can inhibit photosynthesis (photorespiration) when its concentration exceeds (0.2247 mole O_2 m^{-3} at 20 ˚C) (Ippoliti *et al.*, 2016). Urea, nitrate, or ammonium are often the nitrogen source whereas phosphorus is usually provided as phosphate, for example as potassium or sodium phosphate (Acién *et al.*, 2017).

Many different algal biomass production systems such as open ponds and closed photobioreactors have been trialled at different scales to evaluate their efficiencies and economics (Thea Coward, 2012; Xin Bei Tan *et al.*, 2018). Microalgae are cultivated in these systems under different production mechanisms including photo-autotrophy, heterotrophy, and mixotrophy. Photo-autotrophy is autotrophic photosynthesis, that is to say the microalgae use light as an energy source, CO_2 as the carbon source, and other nutrients to grow whereas microalgae cultivated under heterotrophic conditions are independent of light energy and therefore the system does not need a high surface to volume ratio but does require an additional source of a substrate such as glucose or glycerol as the carbon and energy source to stimulate growth. The combination of these mechanisms is called mixotrophic cultivation (Brennan and Owende, 2010; Xin Bei Tan *et al.*, 2018). In this production approach, microalgae are cultivated heterotrophically in the first stage to increase the growth rate due to high organic content before being diverted to the second stage where photosynthesis is induced by reducing the nutrient organic content to a certain level. Mixotrophy couples the pros of photo-autotrophy and heterotrophy production mechanisms as well as overcoming the cons of photo-autotrophy (Zhan *et al.*, 2017).

The photoautotrophic cultivation of microalgae is economically and technically feasible for large-scale production as this approach does not require any additional costly carbon source. It is the most dominant method commonly used for microalgal cultivation. Heterotrophic cultivation yields larger biomass productivity and accelerates lipid accumulation even though the oil productivity of microalgae varies for different microalgae species and consequently it reduces the harvesting costs. However, heterotrophic microalgae cultures are costly and easily contaminated by bacteria and hence it may affect microalgae productivity in large-scale

production systems. Moreover, there are a limited number of algal species that can utilize organic carbon sources (Kang *et al.*, 2004; Qari *et al.*, 2017).

The technologies for algal biomass cultivation can be further categorised into suspended and non-suspended (attached) algae production.

2.2.1 Suspended algal cultivation technologies

In these cultivation systems, algae grow in suspension and are not attached to any solid carrier surface. Suspended culture is the most common type and consists of open systems where the culture is in direct contact with the environment and closed systems in which the medium is fully enclosed within culture vessels. The advantages, disadvantages, mass production rate, and cost of these production systems are summarised in table 2.2 (Brennan and Owende, 2010; Suali and Sarbatly, 2012; Aitken, 2014; Wenguang Zhou *et al.*, 2014).

2.2.1.1 Open system

Historically, the first suspended culture systems were open pond systems that were used for small-scale production of microalgae around the 1950s. Later, large scale projects were developed in the USA between 1976 and 1980 to produce microalgae simultaneously with wastewater treatment due to the simplicity of the open pond system in addition to its lower construction and operating costs (Cui, 2013). For the cultivation of photoautotrophic microalgae at large scale, open systems including natural features (lakes, lagoons, and ponds) or artificial ponds are the preferred systems as the microalgae can use the sunlight directly as the energy source and CO_2 from the atmosphere or submerged aerators as the carbon source, besides the other advantages set out in table 2.2. Circular central pivot, inclined (cascade) and raceway ponds are the most common types of open cultivation system as shown in figure 2.1. Circular central pivot has a rotating arm to agitate the culture whereas inclined systems combine both gravity and pumping flow. Among these types, raceway/oval-shaped pond types are widely used and comprise a closed loop lined recirculation channel with a typical depth of between 20 and 50 cm to increase light penetration. Paddlewheels or sometimes propellers are used to provide continuous circulation and mixing to the raceway pond with typical flow velocity of 20-30 cm s^{-1} to avoid sedimentation (Xin Bei Tan *et al.*, 2018). Lower length to width channel ratio and lower number of bends are preferable to reduce imposing extra head losses. The surface to volume ratio in the open pond systems is low and therefore it is recommended that this production system be used with low depth of water to increase light penetration and the stability of the culture (Acién *et al.*, 2017). Open ponds have a nearly constant average biomass concentration of around 0.5 g l^{-1} to enhance light penetration;

however, this adds additional duty to the harvesting stage and make the culture more likely to be contaminated by other microorganisms.

Cultivation Technique	Biomass production rate, Cost	Advantages	Disadvantages
Open system	35-40 g m^{-3} day^{-1} (it is considerably based on the microalgae strains, pond depth, and climate conditions) 1 kg of algae oil: 7.64 $ 1 kg of algae biomass: 1.54 $	• Low capital cost (0.13-0.37) Million Euro/Ha at 100 Ha scale • Low operating energy inputs (0.25-1.2) W m^{-2} • Easy to maintenance and clean • Well understood • Lower oxygen accumulation • Easier to scale up	• Low spatial efficiency due to the poor mixing and light penetration which leads to low biomass productivity rate. • Required large land area • Poor contact between gas and medium in channels and bends (mass transfer coefficient ≈ 0.7 h^{-1}) • Dilute biomass due to slow growth rate translated to low oil productivity • Low light and CO_2 absorbance • Easily contaminated by fungi and insects. • High CO_2 losses due to the difficulties in maintaining the gas bubbles for a long time. • Suitable for a small number of microalgae species especially those have fast growth rates. • Lack of operational conditions control may lead to large difference in temperature between day and night • Low to mild surface to volume ratio • Other disadvantages arise from excessive water loss due to evaporation in addition to storm and rainfall events which may damage the culture system.
Closed system	200-800 g m^{-3} day^{-1}, (600 g m^{-3} day^{-1} was obtained with *Arthrospira platensis)* 1 kg of algae oil: 24.6 $ 1 kg of algae biomass: 7.32 $	• High biomass productivity rate • Concentrated biomass • Required small land area • Easy to control operational conditions • Low risk of contamination • High mass transfer coefficient between gas and medium even though it is lower into the loop than in the mixing unit • High surface to volume ratio (up to 80 m^{-1}) • Suitable for a wide range of microalgae strains • Very low water loss from evaporation	• High capital costs 0.51 Million Euro/Ha at 100 Ha scale • High operating energy inputs (10-100) W m^{-2}, total energy consumption for biomass production was determined to be approximately 15 kWh day^{-1} m^{-3} • Some issues related to culture mixing, light penetration and gas exchange may be noticed with the large-scale production systems

Table 2.2: The advantages, disadvantages, mass production rate and cost of open and closed cultivation systems (Weissman and Goebel, 1987; Brennan and Owende, 2010; Y. Chisti, 2012; Sompech *et al.*, 2012; Suali and Sarbatly, 2012; Aitken, 2014; Wenguang Zhou *et al.*, 2014; Acién *et al.*, 2017)

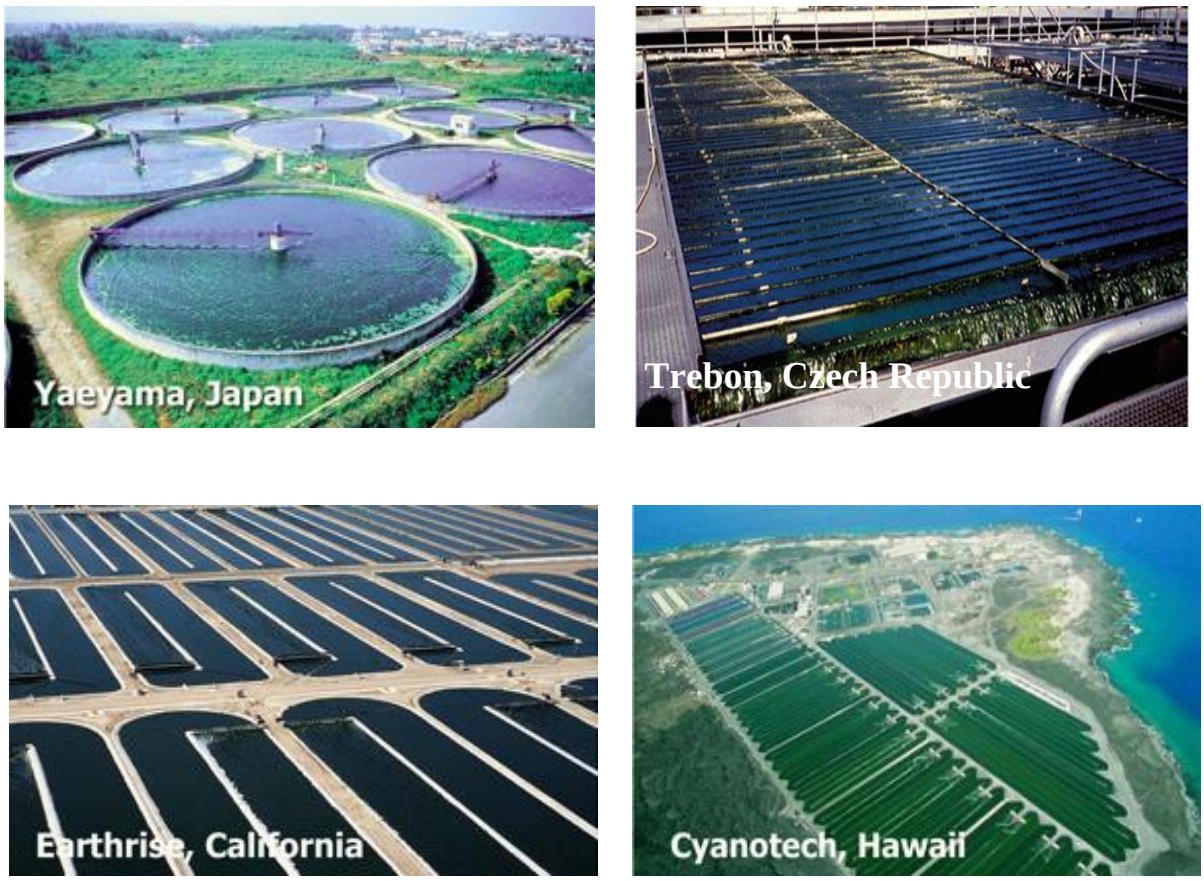

Figure 2.1: Circular central pivot (upper left), inclined (cascade)(upper right) and raceway ponds, (Pahl *et al.*, 2013).

2.2.1.2 Closed systems

Some of the drawbacks of open system ponds particularly culture contamination, low light penetration and CO_2 absorbance are tackled by using closed photobioreactor systems, with consequent increased biomass growth rate and lipid productivity. Closed photobioreactors are typically sets of straight-parallel transparent plastic or glass tubes, with a typical diameter less than 10 cm, aligned vertically, horizontally, inclined, or helically. Tubular, flat plate and cylindrical are the most common types as shown in figure 2.2. Pumps provide circulation for the algal medium with typical velocity ranges of 10 to 80 cm s^{-1} to prevent sedimentation. Airlifts have also been employed to exchange CO_2 and O_2 between the culture and gas and deliver the required mixing. Closed photobioreactors have many merits over open systems as shown in table 2.2, particularly the ability to cultivate a single species and delivering better control of cultivation conditions such as temperature, pH, and CO_2/O_2 exchange. Tubular photobioreactors have been proposed to be more appropriate for large-scale cultivation of microalgae due to their high surface to volume ratio (Zhan *et al.*, 2017). It was reported that cell concentrations of 20 g L^{-1} and biomass yield of 250-3640 g m^{-3} d^{-1} can be attained in flat

plate photobioreactors with a 1.2-12.3 cm light path (Xin Bei Tan *et al.*, 2018). The high capital cost and operating energy are the main drawbacks that prevent scale up of these production systems for low-value products. In addition, there is a design limitation of the tube length for exchanging CO_2 and O_2 and pH control (Brennan and Owende, 2010; Suali and Sarbatly, 2012; Cui, 2013). Biomass washout in the closed photobioreactors is another problem that restricts the implementation of this cultivation system (Bilad *et al.*, 2014).

Figure 2.2: Tubular and flat plate photobioreactors respectively (top), tubular manifold photobioreactors (bottom) (*The Different Kinds of Chlorella's Production » Photobioreactor*, 2011; *Photobioreactor*, 2012; Acién *et al.*, 2017)

Floating closed photobioreactors, also known as Offshore Membrane Enclosures for Growing Microalgae (OMEGA) were proposed by NASA and used for microalgae cultivation in the Gulf

of California, US. Floating on the sea keeps temperature stable for the culture as well as providing mixing with the help of waves (Su *et al.*, 2017).

A "hybrid cultivation system" combining open and closed photobioreactors in a two-stage process, can reduce the overall microalgae production cost and enhance biomass and oil productivity. The first stage has a high biomass production rate and takes place in a highly controlled environment in a closed system to reduce any possible contamination of the culture. The culture of dense microalgae cells from the first stage is then diverted to the second stage which takes place in an open pond system for further biomass production. The second stage often comprises nutrient deficiency to promote lipid or astaxanthin production. An average oil productivity rate of 10 tonnes ha^{-1} $annum^{-1}$ was achieved with *Haematococcus pluvialis* in a two stage system with an ability to gain 76 tonnes ha^{-1} $annum^{-1}$ if a species with a high oil content is used (Huntley and Redalje, 2007; Brennan and Owende, 2010; Xin Bei Tan *et al.*, 2018).

In general, the high water to algal biomass ratio is the main drawback with the cultivation regimes described above. In other words, huge amounts of water are required for the cultivation and consequently the cost for biomass production as well as downstream processes i.e. harvesting and drying costs are high.

2.2.2 Non-suspended/immobilised/attached micro-algal cultivation technologies

In these systems, microalgae grow on a solid carrier surface rather than being suspended in the culture as shown in figure 2.3. High long-term stability of biofilm, low risk of contamination in addition to low energy consumption are the main advantages of attached growth systems (Su *et al.*, 2017). Attached cultivation technology has a moderate algal production rate of 71 g m^{-2} day^{-1}. A previous study demonstrated that biomass productivity of 50-80 g m^{-2} day^{-1} was obtained for *Senedesmus obliguus* by using an outdoor attached cultivation system.

The attached cultivation technique is often adopted in two different approaches, the first is known as "non-enclosure" where microalgae form a biofilm on the surface by attaching microalgae cells to sets of vertical-arranged substratum with low water flow rate to maintain wet surfaces. The second is called "enclosure" in which algae is encapsulated to confine them using a polymeric matrix composite to restrict algal cells in a specific area. This technology has been applied extensively for enzyme, yeast, and bacteria medium. Highly controlled cultivation conditions can be obtained with the enclosure method. However, many studies have demonstrated the difficulty of separating algae from the matrix in addition to drawback of expensive scaling up due to the high cost of the polymer matrix (Tianzhong Liu *et al.*, 2013b;

Katarzyna *et al.*, 2015; Su *et al.*, 2017). For non-enclosure cultivation, not all microalgae species are able to attach and grow on surfaces, for example *Chlorella* and *Dunaliella species*, and therefore binders are required. Aero-terrestrial microalgae like *Coccomyxa sp.* grow naturally on surfaces and hence they are more suitable for this type of cultivation system. Such cultivation systems may reduce the overall cost of microalgae production as well as downstream processes i.e. harvesting, as it is easier to harvest microalgae from surfaces due to their crowded accumulation in a small area. A lower footprint area and high CO_2 mass transfer rate are other advantages in comparison to suspended cultivation. However, a cost-effective and simple design for attached cultivation system is not yet available (Xue-Qiao Xu *et al.*, 2017).

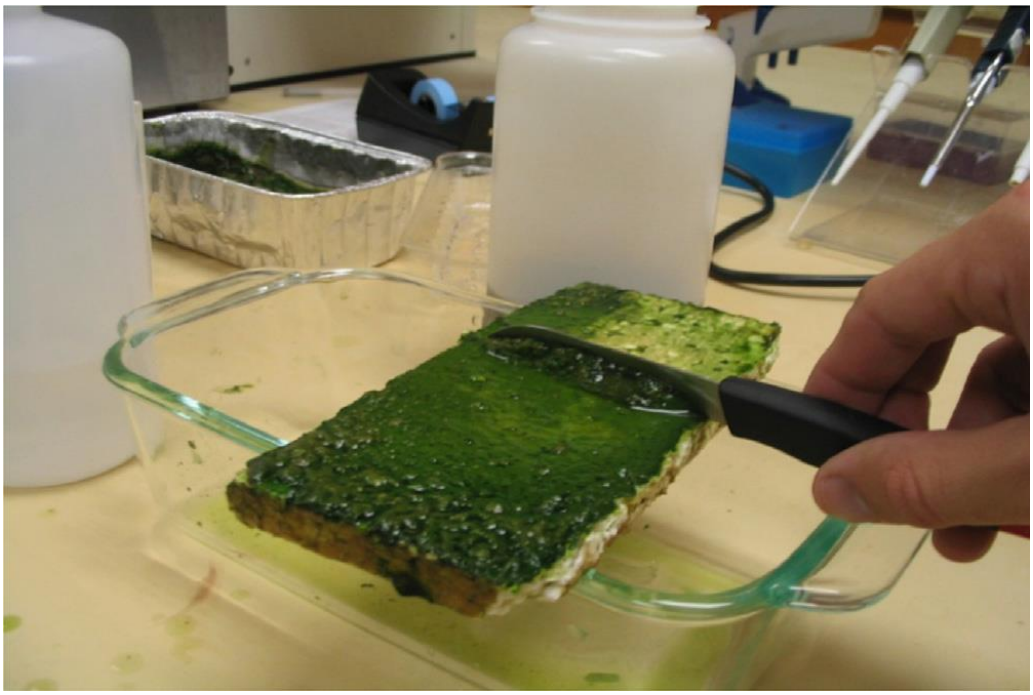

Figure 2.3: Non-suspended cultivation technologies (Johnson, 2009)

The production of microalgae biomass represents a first obstacle in producing algal biofuel with a competitive price due to the cost of the nutrients (N, P and trace elements), and water for the cultivation of freshwater species. Katarzyna *et al.* (2015) have reported that approximately 3800 kg of freshwater is required to produce 1 kg of biodiesel (Wenguang Zhou *et al.*, 2014). However, other researchers have shown that the obstacles to cultivation can be overcome by recycling the spent culture medium after harvesting which provides about 84% and 55% of water and nutrients requirements respectively. In other words, the freshwater footprint can be reduced to 608 kg freshwater/kg of biodiesel if the freshwater discharged after harvesting is fully reused.

Seawater is a successful alternative due to the advantages that it has over freshwater, in particular it contains most of the nutrients required for microalgae cultivation such as $MgSO_4$, $NaCO_3$, and $CaCl_2$ but not including phosphate. It reduces water requirement by about 90% (Jia Yang *et al.*, 2011a). A variety of marine species have been investigated as promising feedstocks for the production of chemicals and biofuels. The profusion of microalgae species in the sea, in addition to its obvious abundance, makes seawater a promising cost-effective culture medium compared to freshwater.

Industrial scale microalgae cultivation needs large quantities of nutrients, particularly nitrogen and phosphorus. Therefore, a rich nutrient source is required for large scale biofuel production. Alternatively, wastewater rich in organic matters or organic compost as the nutrient source can provide nutrients required for high microalgae growth rate and hence it may reduce the cultivation cost significantly (Wenguang Zhou *et al.*, 2014). Microalgae also have the potential to adsorb heavy or trace metals from wastewater (Liandong Zhu, 2015). However, the microalgae strains should have specific characteristics to use wastewater as the nutrient source including high growth rate and high tolerance to potential contamination by toxic compounds and metal ions as well as high tolerance to variations in environmental conditions and salinity levels. Among different microalgae species, strains of the genera *Scenedesmus* and *Chlorella* have shown high ability to grow in various wastewater treatment ponds (Y. Wang *et al.*, 2016b). A study by Li et al. (2011) demonstrated C*hlorella* sp. to grow in "centrate" municipal wastewater and remove nitrogen and phosphorus with efficacies of 89 and 81% respectively and chemical oxygen demand (COD) of 91% (Yecong Li *et al.*, 2011b). Removal efficiencies of 72 and 28% for nitrogen and phosphorus respectively were observed by Aslan and Kapdan through growing *Chlorella vulgaris* in municipal wastewater (Aslan and Kapdan, 2006).

For industrial wastewater, the potential of being a nutrient source is centrally dependant on the nature of the product. Industrial wastewater has adverse impacts on microalgae cultivation with a variety of toxic chemicals present in it and hence it may be considered an inappropriate nutrient source compared to municipal or agricultural wastewater. Therefore, most current studies have focused on eliminating heavy metals and toxic chemicals by using various species of microalgae instead of growing them for biofuel production. However, a recent study demonstrated the potential of untreated industrial wastewater produced from a carpet mill to grow different microalgae species including *Botryococcus braunii, Chlorella saccharophila, Dunaliella tertiolecta*, and *Pleurochrysis carterae* due to its low concentration of toxic components and sufficient amount of nitrogen and phosphorus. Algal biomass productivity (mg L^{-1} d^{-1}), lipid content (% DW), and lipid productivity (mg L^{-1} d^{-1}) were 34, 13.2%, 4.5 and 23,

18.1%, 4.2 and 28, 15.2%, 4.3 and 33, 12%, 4 respectively for the microalgae (in the same order above) (Chinnasamy *et al.*, 2010b). Moreover, the ability of some microalgae species to treat the wastewater from an oil well was discovered by OriginOil Inc. According to the US Department of Energy (DOE), every barrel of oil produced from onshore drilling is accompanied with three barrels of wastewater. Therefore, large amounts of microalgae biomass can be produced daily if this huge volume of wastewater can be exploited for cultivation (Wenguang Zhou *et al.*, 2014). Use of waste-based organic compost and livestock waste derived from animal manure as a nutrient source has exhibited promising outcomes in term of microalgae growth rate and lipid content (Agwa and Abu, 2014; Kumaran *et al.*, 2016).

However, high levels of chemical contaminations and inconsistent nutrient composition are the main drawbacks from adopting this wastewater as the nutrient source. For instance, high concentrations of trace metals such as copper can inhibit microalgae growth (M. K. Lam and Lee, 2012).

2.3 Harvesting of microalgal biomass

Following the cultivation of algal biomass and prior to any further processing into products including pigments, nutritional supplements, and biofuels, microalgae should be detached from the culture medium and this stage is referred to as harvesting. Despite extensive studies and all the advantages related to algal biomass described previously, the production of algal biomass is still limited to approximately 10 to 20 thousand tons per year (dry weight basis). Microalgae-derived low-value products such as biofuels are currently not commercially viable due to the high capital and/or operating costs, partly due to the energy input required for the harvesting and drying stages (Muylaert *et al.*, 2017).

A wide range of solid-liquid separation techniques have been trialled to harvest microalgae from the culture medium (Figure 2.4) (Pahl *et al.*, 2013). These techniques can be categorised into those that separate cells based on gravity or buoyancy such as centrifugation, sedimentation, and flotation (liquid constrained), whereas the other techniques separate cells mechanically by means of a screen or filter (solid constrained). Harvesting microalgae can be carried out in one- or two- step processes. In a two-step process, dilute microalgae culture is concentrated to a slurry of 2-7% dry-matter content and this can be achieved by using coagulation and flocculation processes followed by sedimentation or flotation. After that, the microalgae slurry can be further concentrated to a paste or cake of 15-25% dry-matter content using centrifugation or filtration.

Harvesting represents a substantial process cost, accounting for an estimated 20-30% of the total cost of production and possibly as high as 50% of algal biomass cost. For microalgae production in open systems, it has been estimated that 90% of the equipment cost may come from harvesting and dewatering (Molina Grima *et al.*, 2003; Greenwell *et al.*, 2010; Milledge and Heaven, 2012).

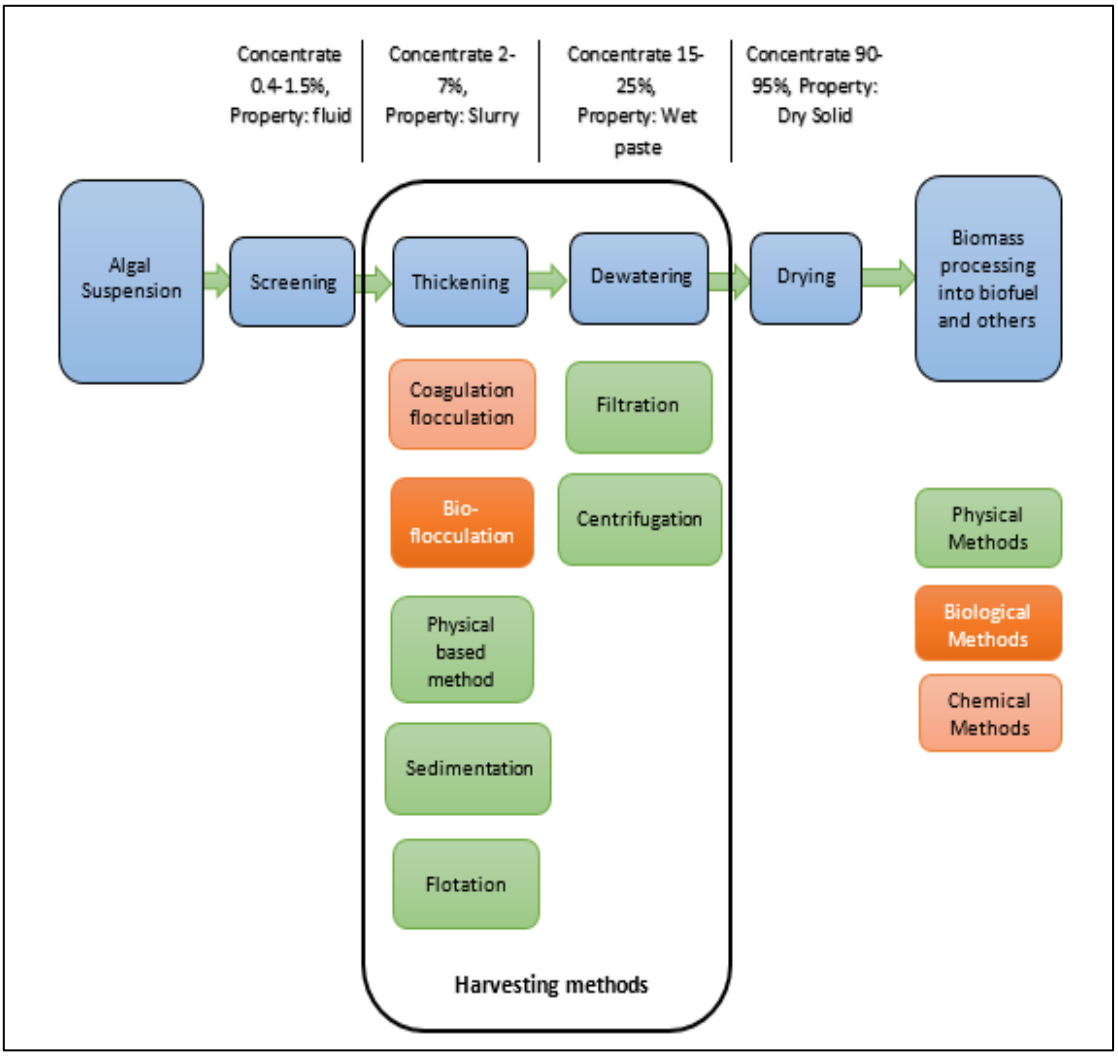

Figure 2.4: Block diagram of algae biomass recovery stages (Pahl *et al.*, 2013; Barros *et al.*, 2015).

The challenges in separating microalgal biomass from the growth medium and the cause of the high microalgae recovery costs arise from several factors including:

1- Microalgae cell nature:

- Microalgae species have small cell size with an average diameter range of 2 to 30 µm. For instance, the average cell diameter for *Chlorella vulgaris* is 5 µm (Milledge and Heaven, 2012) and 22 µm for *Dunaliella Salina* (Elena S. Barbieri, 2006).

- Most microalgae species have a specific gravity close to that of the cultivation medium. For example, the density of *Chlorella vulgaris* is 1,070 kg m^{-3} whereas most marine species have densities of 1,030-1,230 kg m^{-3} (Milledge and Heaven, 2012; Farid *et al.*, 2013).
- Microalgae have high dispersion stability in suspension due to their negative surface charge. Zeta potential for most species is within the range of (-10 to -35) mV (Pranowo *et al.*, 2013). In addition, a recent study has demonstrated the ability of microalgae to retrieve their negative charge after coagulation (Udom *et al.*, 2013).

2- Microalgae growth culture has low biomass concentration especially in large-scale production systems, typically with a range of 0.2-5 g L^{-1} dry weight basis due to the mutual- and self-shading of microalgae cells (F. Chen *et al.*, 2012; Faried *et al.*, 2017).

3- Additional challenges in the harvesting stage may come from the salinity of the growth medium, culture pH, nutrients, and culture age (Pahl *et al.*, 2013; Muylaert *et al.*, 2017). Moreover, the presence of different concentrations and compositions of extracellular organic matter (EOM) excreted by microalgae into the culture medium may affect the efficiency of some harvesting techniques (Udom *et al.*, 2013). Also, it is worth noting that the heterogeneity of microalgae species in terms of different cell size, shape, surface characteristics (e.g. hydrophobicity and charge), and wall rigidity may represent a major impediment in the way of adopting a universal harvesting technology.

Coagulation and flocculation are often coupled with most harvesting technologies such as sedimentation, flotation and filtration to promote the aggregation of microalgae cells and therefore facilitate separation (Uduman *et al.*, 2010a; Milledge and Heaven, 2012; Pahl *et al.*, 2013). The selection of the most appropriate harvesting technique depends on the microalgae species in addition to the desired product quality and concentration and the additional uses of the spent culture. Both efficiency and energy consumption of the harvesting technology have major impacts on the economic feasibility of microalgae-derived products. The most successful harvesting technique should have the capability to harvest large volumes of microalgae culture at low cost and energy demand. Open pond cultivation systems, for example, produce microalgae with a biomass concentration of approximately 0.5 g L^{-1} dry weight basis, therefore large volumes of water should be removed by the harvesting technique to thicken the biomass approximately 400-600 times into a paste of 200-300 g L^{-1} dry weight basis at least (Pahl *et al.*, 2013).

The effectiveness of the harvesting process is determined by the concentration factor (CF) and the recovery efficiency (RE). The concentration factor is the ratio of the microalgae

concentration in the final product to the microalgae concentration in the culture as given in equation 2.1.

$$Concentration\ factor\ (CF) = \frac{Concentration\ of\ algae\ in\ final\ product}{Concentration\ of\ algae\ in\ culture} \quad \cdots (2.1)$$

The recovery efficiency is the ratio of the microalgae cells/mass in the final product to the microalgae cells/mass in the culture as given in equation 2.2.

$$Recovery\ efficiency\ (RE) = \frac{mass/cells\ of\ algae\ in\ final\ product}{mass/cells\ of\ algae\ culture} 100\% \cdots (2.2)$$

2.3.1 Sedimentation

Sedimentation is a simple solid-liquid separation technology which uses gravity to force solid particles to separate from the liquid phase in settling tanks. The main advantages of this method are the low infrastructure cost and power consumption. However, the long settling time is the major drawback of this method and accordingly a large area is required. Microalgae cells have an average sedimentation rate of (0.1-2.6) cm hr^{-1}. For example, the sedimentation rate for *Cyclotella* is 0.04 m day^{-1} (Greenwell *et al.*, 2010). Separation of microalgae by sedimentation needs large land areas if it is adopted for a large-scale harvesting. In addition, there is the potential of biomass deterioration in high temperature environments whilst the algae settle. Furthermore, water turbulence and microalgal cell motility can affect the sedimentation efficiency (Milledge and Heaven, 2012; Pahl *et al.*, 2013). Gravity sedimentation produces a rather dilute slurry which increases the cost of further downstream processes and therefore should be used as a primary harvesting technology (T. Coward *et al.*, 2013; Muylaert *et al.*, 2017).

Nevertheless, for relatively large microalgae sedimentation is considered a suitable harvesting method (Moraes, 2013; Rawat *et al.*, 2013), for instance, the filamentous *Arthrospira* (*Siprulina*) *platensis* (diameter of 10 µm and length of tens to hundreds of µm) has a theoretical settling rate of 0.64 m h^{-1} due to the high content of accumulated glycogen (more than 50% under nitrogen starvation conditions) giving it a specific density of 1.5 (Depraetere *et al.*, 2015). Some species that naturally favour aggregation, such as *Scenedesmus*, are also suitable for gravity sedimentation (Zhaowei Wang *et al.*, 2013c). The settling velocity of microalgae cells in the culture medium can be described by Stokes' law as given in equation 2.3 (Wei *et al.*, 2014):

$$V = \frac{gd^2(\rho_s - \rho_f)}{18\mu} \quad \ldots (2.3)$$

where: V: is the settling velocity (m sec^{-1}), d: microalgae diameter (m), g is the acceleration due to gravity (9.18 m sec^{-1}), ρ_s, ρ_f are the microalgae cell and the liquid densities respectively (kg m^{-3}), and μ is the fluid viscosity (kg m^{-1} sec^{-1}). According to equation 2.1, it is obvious that microalgae cells have low settling velocity since the diameter of most microalgae is less than 30 µm and the density difference between cells and culture medium is very small. Several studies have shown that gravity sedimentation can be enhanced by using inclined tubes, channels, or plates (for example lamella sedimentation tank), such that microalgae cells do not need to travel long distances like in conventional tanks and the inclined tubes or plates can shorten the distance for cells to hit the wall surface and then glide down as illustrated in figure 2.5. However, this gravity separator is not able to overcome most of the sedimentation drawbacks (Show *et al.*, 2013; Benjamin T. Smith and Davis, 2013).

Gravity sedimentation is rarely used alone for harvesting microalgae, therefore coagulation and flocculation processes are often used prior to the sedimentation step to increase the settling efficiency by increasing the size of the particles that are settling (Uduman *et al.*, 2010b; Benjamin T. Smith and Davis, 2012). Kavithaa et al. (2018) reported that a coagulation-flocculation-sedimentation process using $FeCl_3$ as coagulant and chitosan as flocculant gave better removal efficiency (98%) with a reduced settling time of five minutes in comparison to individual coagulation or flocculation (Loganathan *et al.*, 2018).

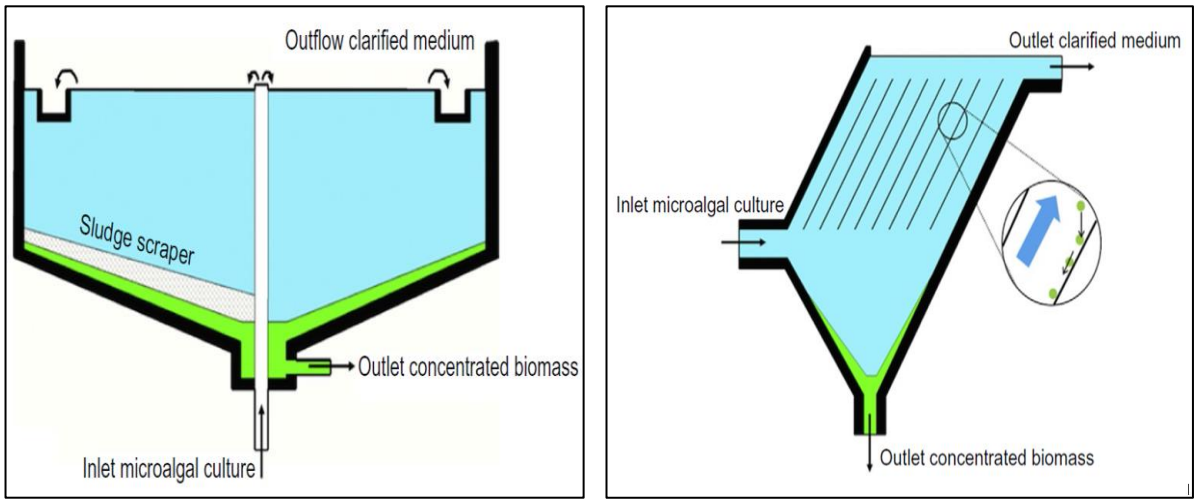

Figure 2.5: Separation of microalgae cells by conventional settling tanks (left), and lamella separator (right) (Muylaert *et al.*, 2017)

2.3.2 Coagulation and flocculation

Due to their negative surface charge and density that is similar to that of the growth medium, microalgae have high dispersion stability. Although this stable dispersion is vital during the

growth phase to reduce the dark region and thus increase the photosynthesis efficiency, it is a dilemma through the harvesting phase since it represents a barrier against self-aggregation in the suspension (Greenwell *et al.*, 2010). Nevertheless, this drawback can be overcome using coagulation and flocculation processes. In coagulation, chemical compounds (coagulants) are added to destabilise the cells by neutralising their negative charge which results in the formation of small clumps of cells (Udom *et al.*, 2013). Flocculation involves adding natural or synthetic high molecular weight polymers to promote the aggregation of the small clumps destabilised by coagulation with the flocculants and form masses called floc as shown in figure 2.6 (Zemmouri *et al.*, 2012; L. Chen *et al.*, 2013). The time required for coagulation is shorter than for flocculation. Coagulation takes place typically in less than 10 seconds whereas flocculation needs a longer time (typically 20-40 minutes) (Crittenden, 2012).

Figure 2.6: Coagulation and flocculation of microalgae (Laurent, 2010).

Many inorganic and organic compounds are utilised to initiate coagulation and flocculation for example, aluminium and ferric salts, lime, chitosan, Magnafloc, Praestol, Aminoclay, and cationic starch (Ahmad *et al.*, 2011; Milledge and Heaven, 2012; Anthony *et al.*, 2013; Pahl *et al.*, 2013; Alam *et al.*, 2014; Gerde *et al.*, 2014). Increasing the particle size by agglomeration due to coagulation and flocculation can improve microalgae separation from culture by sedimentation, flotation, and filtration separation techniques. For example, according to Stokes' law, to achieve a settling rate of 1 m h^{-1} of a diatom *Cyclotella* (average diameter of 6 μm and density of 1,114 kg m^{-3}), flocs of 88 μm diameter are required at the same density (JK Edzwald, 1993). The ideal flocculant must be biodegradable, non-toxic, inexpensive, efficient at low

concentrations, and appropriate for a wide range of environmental conditions (e.g. pH and ionic strength) (Milledge and Heaven, 2012). Using coagulation and flocculation in microalgae recovery is dependent on species, surface charge, concentration in the growth culture, coagulant and flocculant type and dosage, degree and time of mixing, in addition to salinity, pH, and temperature of the growth media (Pahl *et al.*, 2013).

2.3.2.1 Inorganic coagulants (metal salts)

Inorganic coagulants are often used to reduce or neutralise microalgae surface charge for subsequent processing by flocculation or other harvesting techniques such as dissolved air flotation. Inorganic multivalent cations such as aluminium sulphate, ferric chloride, ferric sulphate, and ferrous sulphate are widely used in different industries and particularly in wastewater treatment. When metal salts are dissolved in water, the positively charged metal ion interacts with microalgae, therefore neutralising their negative surface charge. The effectiveness of metal salts varies based on their ionic strength (Pragya *et al.*, 2013). The recovery efficiency of microalgae is affected by the anion of metal salts. Chloride salts of iron, zinc, and aluminium are more effective than sulphate salts for recovering freshwater *Chlorella minutissima* (Papazi *et al.*, 2010). Use of inorganic coagulants at high dosages results in the precipitation of inorganic metal hydroxides, such as aluminium hydroxide and ferric hydroxide which clump making a mesh-like structure trapping microalgal cells (Thea Coward, 2012; Muylaert *et al.*, 2017).

One of the disadvantages of using inorganic coagulants for pre-treating microalgae prior to harvesting is their relatively high cost because of the large amount needed, particularly in saline solutions. Therefore, they are frequently used in wastewater treatment and water purification systems due to their low salinity. The Aquatic Species Program (ASP) reported that using inorganic metals for algal biofuels production was not viable due to cost (Sheehan *et al.*, 2009). Additionally, the optimal dosage of chemicals for coagulation is highly influenced by the ionic strength (salinity) of the growth medium. Sukenik et al. (1988) reported that the optimal coagulation dosage of alum increased from 75 to 225 mg L^{-1} when the medium ionic strength was altered from 0.2 to 0.7M (the ionic strength of natural seawater) at pH of 5.5 (Sukenik *et al.*, 1988).

Another drawback arises from contamination of the growth medium with residual metals which may limit the recycling of the growth medium. Moreover, dissolved salts may be recovered with the harvested microalgae and consequently affect the biomass quality. For example, coagulation of microalgae with high dosage of alum produces biomass with high aluminium

concentrations, consequently making the biomass unsuitable for use as an animal feed. The coagulation process using inorganic coagulants is highly sensitive to the pH level of the growth medium which may result in additional costs for pH adjustment, as shown in table 2.3 (the optimum pH range for various inorganic coagulants) (Pahl *et al.*, 2013). Finally, inorganic-based coagulants may work efficiently with some microalgae species, but not with others unless the dosage is increased.

Metal salts	Formula	Optimal pH range
Alum	$Al_2(SO_4)_3.18H_2O$	4.0 – 7.0
Ferric chloride	$FeCl_3$	3.5-6.5 and > 8.5
Ferric sulphate	$Fe_2(SO_4)_3.3H_2O$	3.5-7 and > 9
Ferrous sulphate	$FeSO_4.7H_2O$	> 8.5

Table 2.3: Common inorganic coagulants used in wastewater treatment and optimum pH range, (Pahl *et al.*, 2013)

2.3.2.2 Organic flocculants

Organic flocculants are synthetic or natural high molecular weight polymers and can be divided broadly into ionic and non-ionic types. Ionic flocculants have ionisable functional groups such as carboxyl, amino or sulphonic structures. Ionisable flocculants (known as polyelectrolytes) are categorised into cationic, anionic, or ampholytic. Although organic-based flocculants can be used to enhance microalgae separation by neutralising or reducing their negative surface charge, they are used more often in combination with coagulation processes to aid the linking between the coagulated cells and flocculants by electrostatic or chemical forces to produce larger particles in a process known as inter-particle bridging (Uduman *et al.*, 2010a). Most cationic polyelectrolytes are non-toxic and biodegradable. They are widely used in low dosage (2-25 mg L^{-1}) in the flocculation of freshwater species which effectively facilities microalgae separation with a concentration factor up to 35. However, poor flocculation efficiency was noticed using anionic polyelectrolytes even though they could destabilise negative colloids (Granados *et al.*, 2012; Milledge and Heaven, 2012). Chitosan, which is commercially produced by the deacetylation of the naturally abundant polymer chitin, is a linear polysaccharide used widely as a cationic flocculant (Rehn *et al.*, 2013). Beach et al. (2012) induced the flocculation of the freshwater microalga *Neochloris oleoabundans* using chitosan with an optimum dosage of 100 mg L^{-1}. The flocculation process demonstrated a high flocculation rate and efficiency

over inorganic coagulants such as alum and ferric sulphate (Beach *et al.*, 2012). Cationic starch is another efficient organic flocculant which has been demonstrated to possess advantages over inorganic coagulants. It does not contaminate the growth medium, lower doses are required, it is cheap, and its efficiency is pH-independent (Vandamme *et al.*, 2010).

In a similar way to inorganic coagulants, polyelectrolyte effectiveness dramatically decreases when the ionic strength (salinity) of the growth medium is increased and more flocculant is required. For example, recovery efficiencies of between 70 and 95% were obtained for marine species with a chitosan dosage of between 40 and 150 mg L^{-1} (Pahl *et al.*, 2013). It is essential to apply the optimum dosage for flocculation of microalgae as lower dosage of organic flocculants may result in weak bridging whereas higher dosage may hinder the bridging process due to electrostatic/static hindering (Thea Coward, 2012). Knuckey et at (2006) reported that the flocculation of microalgae was inhibited at a salinity above 5 g L^{-1} (seawater salinity = 35 g L^{-1}) when an organic polymer was used (Knuckey *et al.*, 2006). Organic flocculants are expensive compared to inorganic coagulants and using them to harvest microalgae, especially marine species, for low-value products is not economically viable even though smaller amounts of flocculants than coagulants are usually required. Suali and Sarbatly (2012) reported that extra organic flocculants dosage had negative effects on the efficiency of filter media in downstream filtration processes (Suali and Sarbatly, 2012). Therefore, flocculation by organic polymers is not a good choice for pre-treating marine microalgae.

2.3.2.3 Integration of inorganic coagulants-organic flocculants

Harvesting of some marine species by sedimentation and filtration was observed to be more efficient when the growth culture was pre-treated by a two-stage process of coagulation followed by flocculation rather than a one-stage process (Pragya *et al.*, 2013). Integration of coagulation and flocculation also overcome the inhibition of the flocculation process due to medium salinity, however higher doses (approximately 5-10 times) were required for both processes (Knuckey *et al.*, 2006).

2.3.2.4 Auto-flocculation

Microalgae flocculation may sometimes occur naturally in the cultivation medium whereby the cells self-combine at higher pH level resulting in agglomeration without the addition of chemicals. Naming the process auto-flocculation does not mean that microalgae flocculate by themselves at higher pH level, but that the flocculation is somehow induced by the precipitation of pH-dependent chemicals (Muylaert *et al.*, 2017). Auto-flocculation processes are induced at elevated pH levels usually above 10 (i.e. outside ideal culture conditions) due for example to

reduction in dissolved CO_2 concentration (Uduman *et al.*, 2010a). It is also associated with the presence of divalent cations such as calcium and magnesium which have a positive charge and can induce flocculation by reducing or neutralising the microalgae surface charge (Vandamme, 2013). In microalgae cultures, depletion of CO_2 due to photosynthesis can cause the culture pH to increase to 8-9, the precipitation of Ca as calcium phosphates or calcium carbonates and Mg as magnesium hydroxide or brucite is induced at that pH level. Therefore, the auto-flocculation process is also affected by the concentrations of calcium and magnesium ions in the growth culture (Brady *et al.*, 2014). This process has an advantage that both calcium and magnesium precipitates have lower toxicity than other metals in inorganic coagulation resulting in fewer problems with contamination of the biomass (Vandamme *et al.*, 2015).

Some researchers have stated that changing the temperature of the growth medium and its dissolved oxygen level may stimulate flocculation (Salim *et al.*, 2011). Vandamme et al. (2012) achieved a recovery efficiency of 98% for *Chlorella vulgaris* at pH 10.8 using KOH, NaOH, and $Ca(OH)_2$ and at pH 9.7 using $Mg(OH)_2$ within 30 min (Vandamme *et al.*, 2012). Similarly, Perez et al. (2014) stated that a recovery efficiency of 95% for *C. vulgaris* was achieved at pH 10.5 using $Mg(OH)_2$ within 30 min (García-Pérez *et al.*, 2014). On the other hand, other studies demonstrated that auto-flocculation can be induced at pH levels lower than 4 due to the protonation of carboxylic acid on the microalgae cell surface and consequently the surface charge of the cells becoming neutral. It was reported that denser and more compact flocculated microalgae cells (defined based on the dry weight and volume of the harvested biomass) were obtained at pH 4 with 95% recovery efficiency in comparison to those obtained at a pH greater than 10 (Jiexia Liu *et al.*, 2013a; Pezzolesi *et al.*, 2015). However, auto-flocculation is slow, dependent on microalgae species, and is difficult to control. It is also inappropriate for "semi-continuous and continuous cultures" where maintaining neutral pH is required for maximum productivity. Given current levels of understanding, auto-flocculation is thought to be too unreliable for commercial use.

2.3.2.5 Bio-flocculation

Induced flocculation of microalgae occurs in rivers or lakes and it is achieved by the existence of biologically excreted organic compounds, known as extracellular polymer substances (EPS). EPS, which are usually high molecular weight polysaccharides of uronic or pyruvic acids, can be excreted into the growth medium by biological species such as microalgae, bacteria, and filamentous fungi during temperature, pH or nutrient stress (Andrew K. Lee *et al.*, 2009b; Vandamme, 2013). Some studies demonstrated the importance of EPS compounds in the induction of flocculation of microbial organisms (Singh and Patidar, 2018). *Ettlia texensis* or

Pediastrum microalgae tend to aggregate spontaneously due to their excreted EPS (Salim *et al.*, 2014; Jason B. K. Park *et al.*, 2015). The main EPS components are carbohydrates especially polysaccharides, however, they could be proteins, DNA, and humic substances as well. Lee et al. (2009) stated that depletion of an organic carbon source such as acetate or glucose from the growth medium induced EPS excretion. They succeeded in inducing flocculation of the marine microalga *Pleurochrysis carterae* using microbes and achieved recovery efficiencies up to 90% and a concentration factor of 226 (AK Lee *et al.*, 2009a). Wan et al. (2013) harvested *Nannochloropsis oceanica* with 88% recovery efficiency using the bacterium (*Solibacillus silvestris*) (Wan *et al.*, 2013). *Botryococcus braunii, Scenedesmus quadricauda* and *Selenastrum capricornutum* microalgae were harvested using bacteria (*Paenibacillus* sp.) with removal efficiencies ranging between 91-95% (Oh *et al.*, 2001). Similarly, *Chlorella vulgaris* was harvested using filamentous fungi (*Cunninghamella echinulata*) and pellet forming fungi (*Aspergillus oryzae*) with recovery efficiencies of 97% (Xie *et al.*, 2013; Wenguang Zhou *et al.*, 2013).

The induction of flocculation by other microorganisms may avoid algal biomass and growth culture from being contaminated by chemicals but it may result in other problems with contamination by fungi or bacteria. However, use of either crude or purified EPS may help in avoiding contamination by other organisms but renders the process uneconomical due to the high costs associated with EPS separation and purification (Pahl *et al.*, 2013). Like auto-flocculation, the performance of bio-flocculation process is also difficult to predict. Salim et al. (2012) reported that bio-flocculation is a highly species dependent process and produces biomass of low lipid content, therefore it is not recommended for bio-fuel production (Salim *et al.*, 2012). Moreover, the excretion of EPS by microalgae usually takes place under non-ideal cultivation conditions, therefore bio-flocculation is unsuitable for "semi-continuous and continuous cultures" which are adopted for high throughput. However, bio-flocculation is a promising and simple harvesting technology in bacteria-microalgae wastewater treatment systems (Craggs *et al.*, 2012).

2.3.2.6 Electro-coagulation

Electrolytic coagulation processes are considered among the most efficient methods and can reduce harvesting costs. It does not require the addition of coagulants, is fast, safe, cost effective, versatile, and requires low energy inputs (Muylaert *et al.*, 2017). Electro-coagulation has been efficiently employed in wastewater treatment to enhance the quality of drinking water (Poelman *et al.*, 1997). Harvesting is achieved by passing an electrical current through two sacrificial electrodes (e.g. aluminium or iron) or non-sacrificial electrodes (e.g. carbon) placed

vertically in the culture. Half reactions take place at each electrode as shown in equations 2.4, 2.5, and 2.6 (Vandamme *et al.*, 2011; Pahl *et al.*, 2013):

1- Half reactions on the anode (electrolytic oxidation):

$$M_{(s)} \rightarrow M_{(aq)}^{n+} + ne^{-} \quad \ldots 2.4$$

Where: M is the metal anode, n is the charge of the metal ion, for iron anode for example:

$$Fe_{(s)} \rightarrow Fe_{(aq)}^{+2} + 2e^{-} \quad or \quad Fe_{(s)} \rightarrow Fe_{(aq)}^{+3} + 3e^{-}$$

A side reaction consists of the oxidation of water to produce oxygen:

$$2H_2O_{(l)} \rightarrow O_{2(g)} + 4H_{(aq)}^{+} + 4e^{-} \quad \ldots 2.5$$

2- Half reactions on the cathode (reduction):

$$2H_2O_{(l)} + 2e^{-} \rightarrow H_{2(g)} + 2OH^{-} \quad \ldots 2.6$$

The cations released from the anode by electrolytic oxidation serve as coagulants that can destabilise microalgae cells by reducing or neutralising their surface charge. This process allows for aggregation of the destabilised microalgae cells and consequently eases their separation from culture. Based on the design of the process, clumps once formed may move to the bottom of the tank due to their weight or attach to hydrogen bubbles generated by the reduction on the cathode electrode and float to the surface (Pahl *et al.*, 2013; Vandamme *et al.*, 2013). This process is similar to the coagulation process using metal salts with the advantage that there are no anions (e.g. chloride or sulphate ions) introduced into the culture. Nevertheless, the aluminium/iron could be toxic to the microalgae biomass based on the electrical current density and operation time (Muylaert *et al.*, 2017). Electrical current, voltage, anode material, residence time, microalgae concentration and the design of system are the main factors that affect the performance of the electro-coagulation process (Pahl *et al.*, 2013; Singh and Patidar, 2018).

It was reported that approximately 1.5 wt.% of aluminium was present in the biomass after electro-coagulation with an electrical current density of 3 mA cm^{-2} for 10 min (Vandamme *et al.*, 2011). More than 98% removal efficiency of *Chlorococcum* sp. was obtained in the laboratory using electro-coagulation (Uduman *et al.*, 2011). Vandamme et al. (2011) evaluated this method to harvest freshwater and marine microalgae using aluminium and iron electrodes. The outcomes demonstrated that an aluminium anode was more effective than iron with energy consumption of 2 and 0.3 kWh kg^{-1} for freshwater and marine microalgae respectively

(Vandamme *et al.*, 2011). Xu et al. (2010) showed the capability of electro-coagulation to harvest *B. braunii* with recovery efficiencies of 93 and 98% when it was coupled with gravity sedimentation for 30 min and dissolved air flotation for 14 min respectively (Ling Xu *et al.*, 2010). The energy consumption of electro-coagulation slightly increases when non-sacrificial electrodes are used. The optimum energy consumption of this process using non-sacrificial electrodes was 3.4 kWh kg^{-1} after adjusting the electrical current applied, culture pH, and addition of an electrolyte (NaCl) (Misra *et al.*, 2015).

However, the contamination of the growth medium and algal concentrate with metal ions from the sacrificial anode, the high cost of anode replacement and maintenance, the formation of an oxide layer on the anode and an increase in algae culture temperature are the main problems of using electro-coagulation for harvesting microalgae biomass. Moreover, the process may become expensive if scaled up as the energy consumption increases with the distance between the electrodes (Milledge and Heaven, 2012; Pahl *et al.*, 2013; Singh and Patidar, 2018).

2.3.2.7 Ultrasound-flocculation

Sonication at low frequency can be implemented to stimulate flocculation of microalgae. Ultrasound can disrupt microalgae cells and induce flocculation but with concentration factors lower than other methods (Milledge and Heaven, 2012). In this method, microalgae are streamed into the resonator chamber and exposed to ultrasonic waves that disrupt the cells and induce the formation of aggregates. The aggregates sink to the bottom of the vessel due to their weight (Suali and Sarbatly, 2012). Harvesting using ultrasound offers additional advantages over other harvesting technologies including the fact that it can be carried out in a continuous mode resulting in a small footprint and it avoids addition of chemical coagulants which contaminate the recovered biomass and culture medium (Pahl *et al.*, 2013). However, Bosma et al. (2003) reported that, despite the capability of ultrasound to successfully harvest *Monodus subterraneus* with high removal efficiency of about 92% and a concentration factor of 20, the energy required was too high at approximately 345 kW d^{-1}. Additionally, they claimed that the resonator can only handle 1000 L d^{-1}, therefore the process is not appropriate for large-scale microalgae production (Bosma *et al.*, 2003). Furthermore, ultrasound can aggregate all matters present in the growth medium and if it is used to induce microalgae flocculation cultivated in wastewater open pond systems, it may recover most contaminants (e.g. mercury) with the harvested biomass (Suali and Sarbatly, 2012). Finally, ultrasonic waves at high frequency may promote the lysis of microalgae cells resulting in release of their internal contents into the growth medium (MUNIR *et al.*, 2013).

2.3.2.8 Flocculation by magnetic nanoparticles

Physical flocculation of microalgae using magnetic nanoparticles has been proposed as a technique that, like ultrasound and electro-coagulation, avoids contamination due to the addition of chemicals. In general, flocculation by magnetic particles is simple, fast, and has low operating costs (Ling Xu *et al.*, 2011). This process involves adsorption of magnetic nanoparticles such as iron oxide (Fe_3O_4) or iron oxide coated with silica or cationic polyelectrolyte onto the microalgae cell surface due to electrostatic attraction forces. Flocculation is then induced using a magnetic field (Cerff *et al.*, 2012; Lim Jit *et al.*, 2012; Wan *et al.*, 2014). Cerff et al. (2012) conducted experiments to magnetically harvest freshwater *Chlamydomonas reinhardtii* and *Chlorella vulgaris* and marine *Phaeodactylum tricornutum* and *Nannochloropsis salina* using silica-coated iron oxide nanoparticles with a maximum particle loading of 30 and 77 g/g for freshwater and marine microalgae respectively. Recovery efficiencies of more than 95% were obtained for all microalgae species (Cerff et al., 2012). Similarly, Hu et al. (2013) evaluated the efficiency of using uncoated magnetic nanoparticles (Fe_2O_3) to harvest marine *Nannochloropsis maritime*. A removal efficiency of 95% and a flocculation rate of 4 min were obtained with a Fe_2O_3 dosage of 120 mg L^{-1} (Y. R. Hu *et al.*, 2013).

Nevertheless, the high cost of the magnetic nanoparticles and the lack of a practical method for recycling nanoparticles from the recovered biomass are the main drawbacks associated with this process. Moreover, the adsorption of Fe_3O_4 nanoparticles onto the cell surface seems to be species specific and the coating of the nanoparticles with cationic polymers to enhance the adsorption makes the harvesting process more expensive (Wan *et al.*, 2014). It is worth noting that this process requires higher doses of magnetic nanoparticles for harvesting marine species due to the ionic strength (salinity) of seawater similar to flocculation using organic polymers.

2.3.3 Centrifugation

Centrifugation is a harvesting method which utilises centrifugal force to separate microalgae from the growth medium. Centrifugation is the most widely used separation technology for high-value products. The main advantages are its simplicity, rapidity, the lack of contamination by chemical coagulants, and its ability to harvest nearly all microalgae strains with high recovery efficiency and concentration factor. Moreover, due to its rapidity, centrifugation can avoid deterioration of the recovered biomass (Muylaert *et al.*, 2017). Heasman, et al. (2002) harvested various microalgae species under centrifugal forces of 13,000, 6000 and 1300 G. Harvesting efficiencies of >95, 60, and 40% were obtained respectively and it was concluded

that the separation feasibility is centrally dependent on the microalgae species and type of centrifuges (Heasman *et al.*, 2002).

Different types of industrial centrifuges are used for harvesting microalgae including decanters, cyclones, solid bowl and disc stack centrifuges (Pahl *et al.*, 2013). Decanter and disc stack centrifuges are efficient and widely used commercially in continuous mode to harvest microalgae biomass for high-value products. The decanter can handle high capacity with lower maintenance requirements, usually used to harvest microalgae from suspension with a higher solids content (from 10 to 50% algal dry weight) whereas a disc bowl centrifuge is used for suspensions with a low solids content (from 0.01 to 20% algal dry weight) (P. E. Wiley *et al.*, 2011; Milledge and Heaven, 2012). Hydro-cyclones, unlike other centrifuges, are cheap and do not have moving parts; however, they require precision engineering to be installed and are more suitable as a primary concentrator step (Pahl *et al.*, 2013).

Although harvesting by centrifugation is simple and has low footprint, the high capital and operating costs required for large centrifuges are the main disadvantage which limits its application to only higher-value products. It may also damage the cells due to high shear forces if it is used with high centrifugal force (Uduman *et al.*, 2010a; Gouveia, 2011). Moreover, the sticky nature of microalgae biomass may make discharging the recovered cells difficult. Increasing the surface area (e.g. by using spiral plated) and flow rates through the centrifuge are other approaches adopted to reduce the energy consumption. Dassey and Theegala (2013), harvested algal biomass using a continuous centrifuge at a rate of 18 L min^{-1}, a lower harvesting efficiency of 28.5% was obtained but with an 82% reduction in power consumption (Adam J. Dassey and Theegala, 2013). The different centrifuge types used for microalgae harvesting with their energy requirements are shown in table 2.4 (Pahl *et al.*, 2013).

Centrifuge type	**Energy requirement kWh m^{-3}**	**Biomass concentration %**
Decanter	8	22
Hydro-cyclone	0.3	0.4
Disc stacked	0.7-1.3	2-15

Table 2.4: Typical centrifuge equipment summary

Even if an energy-efficient harvesting technique is developed in the future, it is widely accepted that centrifugation will still play key role as a dewatering method for pre-concentrated algal slurry (Milledge, 2010; Gouveia, 2011; MUNIR *et al.*, 2013). Pre-concentration of microalgae

biomass reduces the culture volume that needs to be processed, consequently the energy required for centrifugation will also be lower (Muylaert *et al.*, 2017).

2.3.4 Filtration

Filtration techniques operating continuously or discontinuously under pressure, vacuum, magnetic fields or gravity fields, have been trialled to harvest microalgae using different filter media such as screens, filter cloths, and permeable membranes, which allow growth medium and small cells (less than filter pore size) to pass through while retaining the residual cells on the filter (Milledge and Heaven, 2012; Pahl *et al.*, 2013; Hamawand *et al.*, 2014). During filtration, the driving force (usually pressure drop) should be maintained across the surface of the medium to force fluid flow through it (Barros *et al.*, 2015). Filtration is considered an effective harvesting technique for large or filamentous microalgae since the retained cells are less disrupted. It is a high rate technique with recovery efficiency of 70-89% and there is no contamination by chemicals (Leite *et al.*, 2013; Singh and Patidar, 2018). It was reported that conventional filtration under gravity or low pressure (microstrainer) is often used to recover large or filamentous species like *Coelastrum* and *Arthrospira*. However, these species are unsuitable for biofuel production because of their low lipid content. Dense and impermeable cake on the filter media is often formed when very small particles like microalgae are filtered which may quickly clog the filter media (Christenson and Sims, 2011; Pahl *et al.*, 2013; Xin Bei Tan *et al.*, 2018). Clogging and fouling of the media can dramatically influence the filtration efficiency; for instance, very low concentrations (250-1000 cells ml^{-1}) of the diatom *Synedra acus* were able to clog a filter and consequently reduce filter run time from 35 hrs to 23.5 hrs (Thea Coward, 2012).

Tangential (cross) flow filtration (TFF) using reverse osmosis (< 0.001μm pore size), ultrafiltration (0.001–0.1μm pore size), microfiltration (0.1–10μm pore size), or macrofiltration (> 10μm pore size) membrane is a high rate filtration technique which is usually used for harvesting microalgae with small cell sizes. Nevertheless, frequent replacement of the expensive membranes is required (Milledge and Heaven, 2012; Pahl *et al.*, 2013; Xin Bei Tan *et al.*, 2018). In this filtration technique, shear force created by flowing microalgae culture parallel to the membrane surface is used to regularly clean the membrane surface, therefore eliminating cake formation. Membrane pore size, type, transmembrane pressure drop, feed flow rate and algae concentration are the main factors influencing permeate fluxes (the volume flowing through the membrane per unit area per unit time). However, high shear force may damage some microalgae cell membranes (Rossignol *et al.*, 1999). Petruševski et al. (1995) recovered freshwater *Stephanodiscus hantzschii*, *S. astraea*, *Cyclotella* sp., and *Rhodomonas*

minuta with efficiencies of 70 to 89% and concentration factors of 5 to 40 using tangential flow filtration equipped with a 0.45µm pore size membrane (Petruševski *et al.*, 1995). Similarly, Rossignol et al. (1999) recovered marine species (*Haslea ostrearia* and *Skeletonema costatum*) using cross flow filtration equipped with eight commercial microfiltration and ultrafiltration membranes. They estimated power consumption to be between 3-10 kWh m^{-3} and reported that membrane performance was centrally dependent on the hydrodynamic conditions, microalgae properties (e.g. age and shape) and concentration in culture (Rossignol *et al.*, 1999). Danquah et al. (2009) harvested *Tetraselmis suecica* using tangential flow filtration. A concentration factor of 151 was obtained with an energy requirement of 2.15 kWh m^{-3} (Danquah Michael *et al.*, 2009). Meanwhile, Bhave et al. (2012) succeeded in concentrating *Nannochloropsis oculata* 75 times using hollow fiber and tubular membranes with an energy consumption of 0.3-0.7 kWh m^{-3} (Bhave *et al.*, 2012). However, membrane processes for harvesting microalgae cells less than 10µm are challenging and hindered by low throughput and rapid fouling (Milledge and Heaven, 2012). Process efficiency is improved by pre-treating the cultures using coagulation and/or flocculation (Barros *et al.*, 2015). Direct flow filtration (DFF) is not economically feasible to harvest microalgae because of quick fouling of membranes due to the perpendicular flow of growth medium to the membrane (Singh and Patidar, 2018).

Direct filtration by a microbial membrane which only allows microalgae cells to pass through is cheap but it needs a long time to process the medium. Additionally, the backwash of the membrane is regularly required to keep its efficiency but resulting in additional costs (Suali and Sarbatly, 2012).

2.3.5 Flotation

Flotation is a gravity separation method in which small air or gas bubbles collide and adhere to solid particles such as microalgal cells and carry them to the liquid surface where a scum is formed and skimmed off (Jing Lu *et al.*, 2011; Laamanen *et al.*, 2016). The basic process is called adsorptive bubble separation (ABS) which can be defined as the chemical and physical processes that take place at the gas-liquid interface to separate particles due to their surface activity. ABS has been widely used for decades in industrial and domestic wastewater treatment, mineral processing, the pharmaceutical industry, and the food industry due to its simplicity, rapidity, and relatively low operating cost (Odd, 2013). Large-scale froth flotation of ores is an application of ABS in mineral beneficiation to separate high-value minerals from undesirable ash and gangue materials (P. Stevenson and Li, 2014). ABS processes can be classified based on the method of bubble formation, mechanism of separation, operation mode, size and characteristic of materials separated, and the bubble size (Somasundaran and

Ananthapadmanabhan, 1987). For example, Stevenson and Li (2014) classified ABS based on the mechanism of separation and characteristics of the materials separated as shown in figure 2.7 (P. Stevenson and Li, 2014).

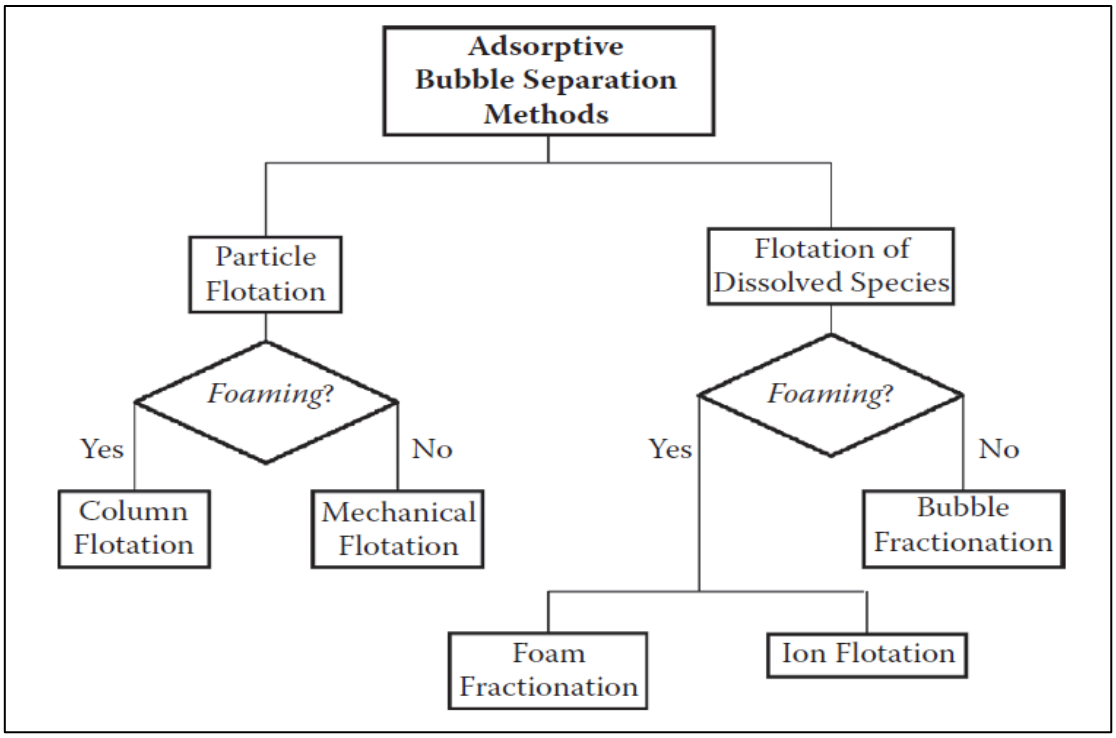

Figure 2.7: Adsorptive bubble separation hierarchy based on the characteristic of material separated and mechanism of separation

Harvesting microalgae by flotation is faster and more effective than sedimentation due to the low density of microalgae. Some microalgae cells naturally float on the water surface when the lipid content is high (the density of lipid is 860 kg m^{-3} (Reynolds, 1984; Milledge and Heaven, 2012)) or due to the presence of gas vesicles as found in *Anabaena* and *Arthrospira* (Thea Coward, 2012). Freshwater and marine microalgae species have been efficiently harvested via flotation processes (T. Coward *et al.*, 2013; Garg *et al.*, 2014; Garg *et al.*, 2015). Whilst separation by flotation is centrally dependent on the physicochemical properties of microalgae in addition to culture pH and salinity, the size of microalgae cells and gas bubbles are also important. Smaller gas bubbles are more favourable since they have a larger specific surface area as well as lower buoyancy, therefore the probability of collisions between a gas bubble and a microalgae cell increases (Hanotu *et al.*, 2012; Pahl *et al.*, 2013). In contrast, larger microalgae cells offer higher collision probability with gas bubbles which results in higher removal efficiency even though smaller cells are easily carried by gas bubbles. Previous studies have demonstrated that microalgae cells of diameter between 10-30µm can be removed by flotation with 80-90% removal efficiency (Rashid *et al.*, 2014).

Flotation processes are classified based on the method of bubble formation: dissolved air flotation (DAF), dispersed air flotation (DiAF), and electrolytic flotation (also called electro-flotation) (Singh and Patidar, 2018). Coagulants, commonly aluminium and ferric salts, are usually used with DAF to induce microalgae aggregation for higher collision efficiency between microalgae aggregates and air bubbles whereas surface active materials (surfactants) are used with DiAF as foaming agents to stabilise foam in the system (the process is also known as foam flotation) and to increase hydrophobicity of microalgae cells for better attachment efficiency between microalgae cells and hydrophobic air bubbles. Moreover, drainage of interstitial water from the foam containing microalgae produces more-concentrated microalgae (Laamanen *et al.*, 2016). A limited number of microalgae species have been harvested using DAF without the injection of a coagulant in optimal dose (Show *et al.*, 2013). Ozone has also been used instead of air in flotation to harvest microalgae biomass. Ozone can promote microalgae cell lysis for the release of intracellular protein-like substances which play the role of bio-surfactants (Y. L. Cheng *et al.*, 2010; Laamanen *et al.*, 2016). Moreover, it was observed that ozonation of microalgae cells promoted the production of saturated fatty acids such as palmitic acid and stearic acid during the lipid extraction phase (Lin and Hong, 2013; Kamaroddin *et al.*, 2016).

2.3.5.1 Dissolved air flotation

Dissolved air flotation (DAF) is commonly used as a clarification method in water and wastewater treatment. In DAF, air is compressed and dissolved in water under high pressure, typically > 500 kPa. When the pressure of the solution is reduced in a nozzle, the water is now supersaturated with air, small bubbles of diameters ranging from 10 to 100μm are formed in the flotation cell. The bubbles collide with the suspended particles and force them to float to the water surface where a scum is formed and skimmed off (J. K. Edzwald, 2010; X. Zhang *et al.*, 2012; Muylaert *et al.*, 2017; Singh and Patidar, 2018). DAF is proven at large scale and is preferred over sedimentation to process microalgae-rich waters (Christenson and Sims, 2011). However, removing microalgae from water for wastewater treatment differs from removing of microalgae from growth medium for biomass production as the microalgae concentration in the latter is typically thousands of times greater than in wastewater (X. Zhang *et al.*, 2014).

Traditionally, coagulation and sometimes flocculation processes are used in conjunction with DAF to attain larger microalgae aggregates and increase the likelihood of collision between the aggregates and bubbles (Show *et al.*, 2013). However, high dosage of coagulants and/or flocculants, clumps or flocs breakage due to large bubble size, and the possibility of bubble-flocs detachment when flocs become too large are the main problems of combining

coagulation/flocculation with DAF (Ndikubwimana *et al.*, 2016). Zhang et al. (2014) evaluated the harvesting of *Chlorella zofingiensis* using DAF. They demonstrated that the recovery efficiency increased with chemical dosage. When chitosan, Al^{3+}, Fe^{3+}, and cetyltrimethylammonium bromide (CTAB) were used at doses of 70, 180, 250, and 500 mg g^{-1}, recovery efficiencies of 81, 86, 91, and 87% were achieved respectively. They also reported that the process efficiency-coagulant dosage relationship was affected by microalgae growth culture conditions (X. Zhang *et al.*, 2014).

Zhang et al. (2016) recovered *Chlorella zofingiensis* using DAF with a recovery efficiency of > 90. They reported that a magnesium-based coagulant was more effective than chitosan, aluminium, and ferric salts. Moreover, the optimal coagulant dosage was observed to be affected by the growth culture; for example, Mg^{2+} dosage of 226 mg g^{-1} was required for harvesting an early exponential culture, whereas a late stationary culture required 36 mg g^{-1} (Xuezhi Zhang *et al.*, 2016b). Henderson et al. (2009) attempted to modify bubble characteristics by adding aluminium sulphate, a cationic surfactant (CTAB) and a cationic polymer (PolyDADMAC) into the saturator instead of microalgae culture attaining removal efficiencies of 60, 63 and 95% respectively (Rita K. Henderson *et al.*, 2009).

DAF is not an energy efficient harvesting technique with an energy requirement as high as 7.6 kWh m^{-3} due to the energy required to compress the air. However, this high energy requirement may be avoided by using smaller bubble generation systems which may result in lower recovery efficiencies (Ndikubwimana *et al.*, 2016).

2.3.5.2 Electro-flotation

In electro-flotation, small hydrogen bubbles are generated for the flotation at a cathode made from a non-sacrificial cathode (inactive metal) such as titanium alloy (Uduman *et al.*, 2010a). Electro-flotation is often coupled with electro-coagulation by using a sacrificial anode to induce the coagulation process. Hydrogen bubbles generated by water electrolysis attach to the microalgae cells and their aggregates and carry them to the surface. Electro-flotation has many advantages over other harvesting techniques (especially for marine microalgae) because of the higher electrical conductivity of saltwater. It is not species-specific, is rapid, and able to produce bubbles which have high resistance to coalescence. Alfafara et al. (2002) evaluated electro-flotation for the recovery of microalgae for both continuous and batch systems. A sacrificial polyvalent aluminium anode and a non-sacrificial titanium alloy cathode were used to induce coagulation and flotation simultaneously. The results showed that removal efficiency can be enhanced by increasing the power input. They also demonstrated that electro-flotation could

not be used alone as it attained a removal efficiency of only 40-50% (i.e. without electro-coagulation) (Alfafara Catalino *et al.*, 2002). Similarly, Ryu et al. (2018) demonstrated that an electro-coagulation-flotation process at 15 mA cm^{-2} for 40 min led to complete harvesting of *Scenedesmus quadricauda* (Ryu *et al.*, 2018). However, the high energy requirements, the high costs for scaling electrodes, the increased medium temperature and increased pH during harvesting may limit electro-flotation application in large-scale systems (Pragya *et al.*, 2013; Rashid *et al.*, 2014; Barros *et al.*, 2015).

2.3.5.3 Dispersed air flotation

In dispersed air flotation (DiAF), bubbles ranging from 700 and 1500μm are generated by passing gas continuously through a porous media (e.g. diffuser or sparger) or by using a high speed mechanical agitator (Singh and Patidar, 2018). DiAF (Figure 2.8) requires less power than DAF, however, the bubble size is larger. Natural and synthetic surface-active materials (surfactants), such as N-cetyl-N-N-N-trimethylammonium bromide (CTAB), sodium dodecylsulfate (SDS), saponin, and Triton X-100 have been employed to stabilise the foam in these systems (T. Coward *et al.*, 2013; Truc Linh Nguyen *et al.*, 2013; Kurniawati *et al.*, 2014). Due to the hydrophilic nature of most microalgae cells, surfactants work to impart hydrophobicity to the cell surface and enhance their adsorption to the liquid-gas interface (Ozkan and Berberoglu, 2013b). Surfactants are amphiphilic molecules, that is to say they possess at least one hydrophilic head-group and one hydrophobic tail-group (Buga, 2005). Broadly, the adsorption mechanism of surfactant to particle surface is based on different interactive forces which act individually or in combination such as covalent or electrostatic attraction forces (Somasundaran and Ananthapadmanabhan, 1987). In the case of microalgae, the electrostatic attraction or dipole interaction may represent the strongest driving force for surfactant adsorption on their cell walls. The presence of surfactants in DiAF has an additional advantage through the production of stable bubbles which have high resistance to coalescence due to the decreased surface tension of air-liquid interface (T. Coward *et al.*, 2013).

Microalgae have a negative surface charge and therefore cationic surfactants such as CTAB have shown high efficiency for algal cell removal (up to 90%) (R. W. Smith *et al.*, 1991; Y. M. Chen *et al.*, 1998; J. C. Liu *et al.*, 1999; Phoochinda and White, 2003). Anionic surfactants such as SDS can be used as effectively as cationic surfactants if the culture is pre-treated by coagulation and/or flocculation processes or the culture pH is adjusted to a more acidic pH to change the surface charge of the cells. Metal salts as well as cationic polymers can neutralise or reduce the negative surface charge of microalgae, therefore improving the absorption of anionic surfactants (Y. M. Chen *et al.*, 1998; J. C. Liu *et al.*, 1999). Some functional groups on

the surface of the cell wall such as amine (-NH_2), carboxyl (-COOH), and hydroxyl (-OH) groups, can be protonated or deprotonated according to the culture pH (Ozkan and Berberoglu, 2013b). For instance, when amine and hydroxyl groups on the cell surface get protonated, the residual surface charge is positive at acidic pH and anionic surfactants are adsorbed effectively (Huang *et al.*, 1999).

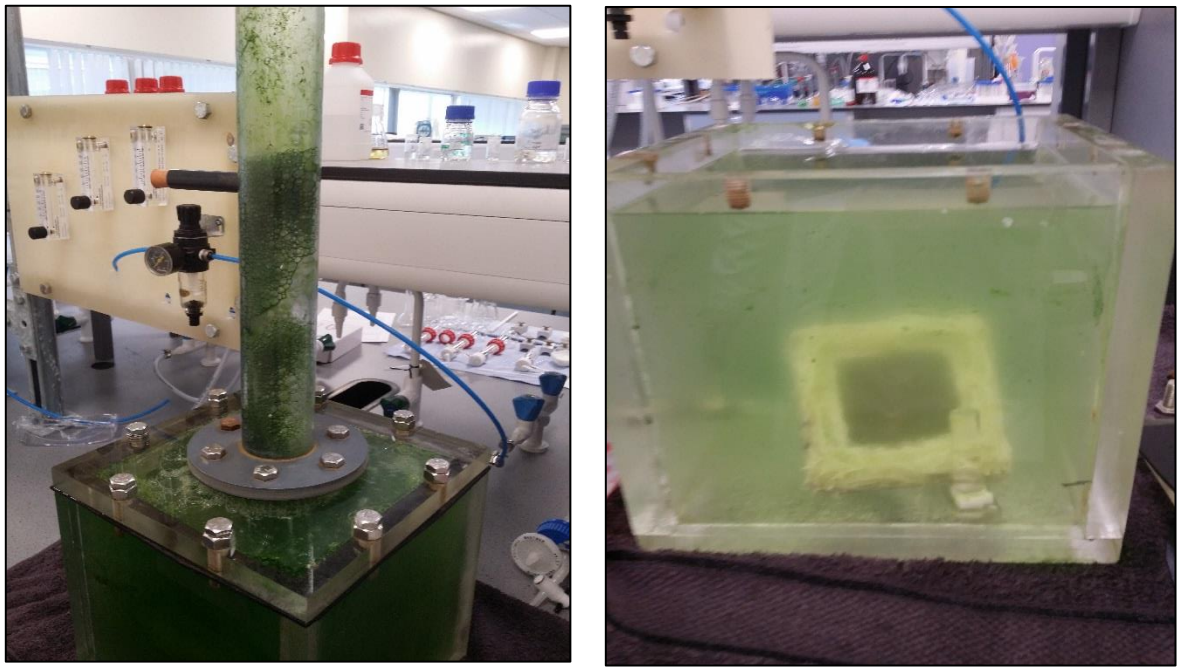

Figure 2.8: Dispersed foam flotation with rising foam (left), dispersed foam flotation reservoir after harvesting (right)

Hydrophobicity is an important factor in DiAF processes. Hydrophilic molecules are usually polar molecules which tend to create bonds with water to reduce the surface energy (surface tension). Hydrophobic molecules, usually non-polar, tend to clump forming micelles to evade water molecules and decrease the entropy of the system due to the disruption of the strong hydrogen bonds between water molecules. In flotation processes, hydrophobic air bubbles attract other molecules due to their original or acquired hydrophobicity and then carry them to the surface. Furthermore, both microalgae cells and air bubbles have negative surface charge, therefore microalgae cells do not adhere and flotation does not operate well unless chemicals (e.g. surfactants) are employed (Garg *et al.*, 2012).

Smith et al. (1991) harvested *Chlorella vulgaris* using both cationic dodecylamine or anionic sodium dodecyl sulphate SDS with alum (R. W. Smith *et al.*, 1991). Chen et al. (1998) conducted harvesting trials of *Scenedesmus quadricauda* using DiAF with three surfactants (cationic CTAB, anionic SDS, and non-ionic Triton X-100). Higher removal efficiency (90%) was obtained with CTAB at an optimum pH in the range of 5-8 (Y. M. Chen *et al.*, 1998).

Similarly, Liu et al. (1999) employed DiAF to separate *Chlorella* sp. from water. In their harvesting trials using either CTAB or SDS. Removal efficiencies of 20 and 86% were achieved upon addition of 40 mg L^{-1} of SDS and CTAB respectively. However, recovery efficiency with SDS increased to 90% when 10 mg L^{-1} of the cationic polymer chitosan was added to the algal suspension prior to harvesting (J. C. Liu *et al.*, 1999). Phoochinda and White (2003) examined DiAF as a function of the collector type, aeration rate and pH of the growth medium using CTAB, SDS and Triton X-100 to harvest microalgae *S. quadricauda*. CTAB and SDS were able to increase the aeration rates and reduce the size of air bubbles with removal efficiencies of 90 and 16%, respectively. With SDS, however, they found that decreasing pH of the growth medium increased removal efficiency to 80% but no increase in removal efficiency was observed for CTAB at lower pH (Phoochinda and White, 2003).

Xu et al. (2010) integrated DiAF with electro-flocculation as an alternative to surfactants to harvest *Botryococcus braunii*. A recovery efficiency of 98.9% was achieved after a flotation time of 14 min (Ling Xu *et al.*, 2010). Nguyen et al. (2013) examined the effects of pre-oxidation of algal suspension by ozone and peroxone. They observed that 76.4% of cells were recovered at 40 mg L^{-1} CTAB and the recovery efficiency increased to 95% after 30min of ozonation (Truc Linh Nguyen *et al.*, 2013). Likewise, Coward et al. (2013) used DiAF to harvest *C. vulgaris*. They studied the effects of different operational conditions on the concentration factor and yield of the harvested microalgae. Their model demonstrated that highest concentration factors were achieved with CTAB at low surfactant concentrations and high foam column heights (T. Coward *et al.*, 2013). Their batch foam flotation column demonstrated low power consumption of 0.015 kWh m^{-3} and produced microalgae biomass which had high lipid content and enhanced lipid profile (T. Coward *et al.*, 2014). These advantages make DiAF a promising technology for harvesting microalgae for low-value products. However, the performance of DiAF is sensitive to medium pH and is reduced when using marine microalgae due to the salinity of seawater (Garg *et al.*, 2012). Recently, Garg et al. (2015) harvested marine microalgae (*Tetraselmis* sp. M8) using a pilot scale Jameson flotation cell with the cationic surfactant, dodecyl pyridinium chloride (DPC). Over 99% removal efficiency with a 23-fold increase in harvested microalgae concentration were reported (Garg *et al.*, 2015). Csordas and Wang (2004) successfully harvested the marine diatom, *Chaetoceros* sp., by a foam fractionation column with a removal efficiency of 90% without the addition of flocculating agents or surfactants. Instead, they stabilised the foam by bio-surfactants excreted naturally by the microalgae (Csordas and Wang, 2004). They also concluded that the flotation efficiency was unaffected by the ionic strength of the medium

unlike other reported works where synthetically produced surfactants were used (Y. M. Chen *et al.*, 1998).

Cheng et al. (2010) reported that high removal efficiencies of *Chlorella sp.* with 24% increase in the fatty acids fraction were achieved by using dispersed ozone flotation with an ozone dosage of 0.03 mg/mg biomass (Y. L. Cheng *et al.*, 2010). Use of ozone as an alternative to air in dispersed flotation processes promotes microalgae cell lysis and releases EPS which can enhance the aggregation and removal of cells (Y. L. Cheng *et al.*, 2011). However, the production of ozone is very expensive and using ozone instead of air will limit the scale at which the method can be used.

All previous flotation-based harvesting has been conducted as a batch or semi-batch process. It is challenging to attain an effective combination of high recovery efficiency and concentration factor because the conditions required for a high recovery do not favour a high concentration factor. Very little work on flotation has focused on the recovery efficiency and concentration factor of the harvested microalgae together. For instance, Garg et al. (2013) recovered 85% of *Tetraselmis* sp. using mechanical flotation cells with dodecylammonium hydrochloride surfactant but at the expense of enrichment with the harvested biomass being only six-times more concentrated than the culture (Garg *et al.*, 2013).

DiAF consumes less energy than most other harvesting technologies. Wiley et al. (2009) reported that this method only required 0.003 kWh m^{-3} in comparison to 7.6 kWh m^{-3} for DAF (Patrick E. Wiley *et al.*, 2009) and 0.105 kWh m^{-3} for a microbubble production system (T. Coward *et al.*, 2015; Xin Bei Tan *et al.*, 2018). DiAF can take place in a flotation column (foam flotation) or in mechanical flotation cell based on the method of bubble formation. A flotation column has many advantages over conventional flotation cells and other harvesting methods including: simple construction, lower capital and operating cost, improved recovery, higher grade products, less wear and tear due to the absence of moving parts, and a smaller footprint (Sastri, 1998).

Foam flotation is a physicochemical separation technique which involves interaction between three phases which are solid (microalgae cell), gas (air bubble), and liquid (growth medium). Therefore, the efficiency of foam flotation is highly dependent on the shape, size, hydrophobicity, and zeta potential of the microalgae cells; the bubble size and flux, bubble zeta potential and coalescence rate in the column; growth pH, ionic strength; surfactant type and surfactant concentration (Chun Yang *et al.*, 2001; J. K. Edzwald, 2010; T. Coward *et al.*, 2013;

Ozkan and Berberoglu, 2013b; Garg *et al.*, 2014; Bui *et al.*, 2015; Ling Xia *et al.*, 2016; Wen H, 2017; L. Xia *et al.*, 2017a).

2.4 Drying

Harvesting and dewatering methods have the capability to increase dry weight content up to 10-25%, leaving 90-75% water (Pahl *et al.*, 2013). The conversion process for microalgae into biofuel, on a wet-basis such as hydrothermal liquefaction or a dry-basis such as pyrolysis, will determine the necessity for the energy-intensive process of drying after harvesting. Drying is an essential thermal process if downstream processes, such as lipid extraction, are influenced by the water content of the algal biomass. Some studies have stated the importance of this stage for the stability of the microalgae biomass as well as increasing the extraction efficiency of lipid and protein (Wahlen *et al.*, 2011; Kim *et al.*, 2013). Various techniques have been employed to dry harvested microalgae and eliminate deterioration of the biomass; such as solar dryers, spray dryers, drum dryers, fluidised bed dryers and freeze dryers. The solar dryer is a low cost drying method that uses natural sunlight to dry microalgae. Previous work succeeded in dehydrating *Arthrospira* at temperatures of 60-65 ˚C for 5-6 hrs to produce a dried product of 4-8 wt.% water content (Show *et al.*, 2013). Nevertheless, this method requires a large area, is time consuming, is not consistent throughout the year due to its dependency on climate, and there is a potential risk of matter loss and fermentation. Therefore, other drying methods powered by natural gas or electrical energy are more appropriate for the continuous production of dried microalgae throughout the year, even though the energy input is higher (Pahl *et al.*, 2013; Xin Bei Tan *et al.*, 2018).

Spray dryers are commonly utilised prior to extraction of high-value products (Brennan and Owende, 2010; Ayhan Demirbas and Demirbas, 2010). However, they may damage some intracellular microalgae contents such as pigments, particularly when high pressure atomisation of the microalgae slurry is used (Soeder, 1980; Xin Bei Tan *et al.*, 2018). Freeze drying is very efficient in disrupting microalgae cells for lipid, protein, and enzyme extractions. In freeze drying, a temperature of less than -40 °C and a pressure of 1 kPa are applied to slowly freeze the microalgae and remove water by sublimation. Formation of large ice crystals causes cell walls to be more porous. However, freeze drying is time-consuming with high power and maintenance costs and is difficult to scale up (D'Hondt *et al.*, 2017). Drum drying was observed to be more economically viable than spray dryer. Mohn and Soeder (1978) stated that drum dryer had lower energy demands and lower investment costs (Show *et al.*, 2013).

The high energy demands of most drying methods, especially spray drying may result in a negative energy balance when producing low-value products such as biofuels since the drying stage may contribute up to 59% of the total energy required for the production of microalgae-based biofuel (Yanfen *et al.*, 2012; Abdelaziz *et al.*, 2014). It was also reported that drying may constitute 70-75% of the processing cost (Show *et al.*, 2013). Therefore, eliminating or optimising the microalgae drying stage can, to a certain extent, render the production of microalgae-based biofuel economically feasible.

2.5 Lipid Extraction

For biodiesel production, lipid extraction from the algal biomass is the next step after harvesting and drying. In a typical lipid extraction process, microalgae are disrupted using physical, chemical, or biological methods. Next, a chemical solvent is used to extract lipid. An efficient lipid extraction method should not damage the extracted lipid, be rapid and easily scalable, and has selectivity for the lipid fraction that can be converted into biodiesel (Pragya *et al.*, 2013; Xin Bei Tan *et al.*, 2018). In microalgae, the lipid fraction is a mixture of triglycerides (TAG), diacylglycerol (DAG), monoacylglycerol (MAG), free fatty acids (FFA), in addition to polar lipids such as phospholipids (Rios *et al.*, 2013). In most microalgae species, these molecules are surrounded by a thick and strong cell wall; therefore, the lipid extraction method should be effective at disrupting the cell wall and cell membrane (Steriti *et al.*, 2014). A wide range of techniques are used for lipid extraction from microalgae including solvent extraction, bead-beating, supercritical fluid extraction, microwave-assisted extraction, chemical cold press (cold press with solvent), freezing, osmotic shock, enzymatic extraction and ultrasound. Solvent extraction and supercritical fluid extraction are commonly employed to extract lipid from microalgae (Halim *et al.*, 2012). Solvents such as hexane, chloroform, acetone, benzene, ethanol (96%), chloroform-methanol mixtures, and hexane-ethanol (96%) mixtures have been used. If only the algal lipids are required, ethanol is not a good choice as it can extract out molecules (contaminants to lipid) such as amino acids, salts, and hydrophobic proteins (Mata *et al.*, 2010). The Folch and modified Bligh and Dyer are common solvent extraction methods as they are simple and can extract total lipids as well. These methods are widely used for the estimation of lipids in food, pharmaceutical, and biofuel laboratories. However, they have serious safety issues due to the high toxicity and carcinogenicity of chloroform, making them unsuitable for large-scale application (Breil *et al.*, 2017). Solvent-based lipid extraction methods can extract lipid from microalgae with high moisture content (>85%); However, these methods use large volumes of solvents (Yusuf Chisti, 2007; Im *et al.*, 2014). Solvent-based

lipid extraction methods require a solvent which is inexpensive, non-toxic, non-volatile, and non-polar (Rawat *et al.*, 2011).

Lipid extraction by a supercritical fluid like CO_2 is an alternative method, it can extract 70-75% of microalgae oils with high selectivity and short processing time. CO_2 has a relatively low critical pressure of 72.9 bar that allows for a moderate compression cost, whereas its low critical temperature (31.1 °C) allows for extraction of lipid fractions without degradation. However, the process is difficult to scale up (Santana *et al.*, 2012).

Microwaves generate high frequency waves which break the cell wall by thermal shock. It has recently received attention as an efficient method for disrupting oil-containing plant cells (Pragya *et al.*, 2013). Sonication, widely used for microbial cells, disrupts both cell wall and membrane by cavitation. In liquid media, intense sonic pressure waves cause microbubbles to form and implode. Consequently, intense shock waves are generated due to the implosion which are enough to break cell walls. In bead-beating extraction, high-speed rotation of the biomass with fine beads causes mechanical disruption to the cells. Bead-beating has gained success, on both bench and industrial scales (Wahlen *et al.*, 2011; Sathish and Sims, 2012; Pragya *et al.*, 2013; C. L. Teo and Idris, 2014a; Willis *et al.*, 2014). Converti et al. (2009) combined ultrasound with solvent extraction by chloroform-methanol mixture, allowing for the complete extraction of the microalgae lipid fraction (Converti *et al.*, 2009). Ultrasound extraction was found to be better than Soxhlet extraction in disrupting the rigid cell wall of the marine microalgae *Crypthecodinium cohnii*, in which an extraction yield of 25.9% was achieved compared to 4.8% by Soxhlet (Mata *et al.*, 2010).

Chemical cold press is a simple lipid extraction technology in which microalgae cells are mechanically pressed in the presence of solvent; such as hexane, ether, or benzene. Approximately 95% of the total oil content was extracted using this method (Oilgae; Xin Bei Tan *et al.*, 2018). Enzymatic extraction is another bench scale method that uses enzymes to disrupt the cell wall with the ability to extract lipid from wet microalgae. Liang et al. (2012) extracted approximately 49.8% of total lipid from oleaginous alga utilising a combined sonication-enzyme treatment at pH 4 (Liang *et al.*, 2012). Zuorro et al. (2016) successfully recovered 90% of lipids from *Nannochloropsis* using cellulase and mannanase with optimum dosages of 13.8 and 1.5 mg g^{-1} respectively, a temperature of 53 °C, pH of 4.4, and treatment for 210 min (Zuorro *et al.*, 2016).

2.6 Conversion technologies of microalgae into biofuel

Currently, a range of processes are used to produce biofuels commercially. Fermentation of sugar crops and hydrolysis and fermentation of starch containing feedstocks are used to produce bioethanol. Acid/base/bio-catalytic transesterification of oily crops with an alcohol is used to produce biodiesel which is a mixture of fatty acid methyl esters (Laurens *et al.*, 2012; Brown Tristan and Brown Robert, 2013; Adam F. Lee and Wilson, 2015).

Microalgae biorefineries aim to develop sustainable production technologies for biofuels and the bioproducts from algae. Due to the versatile biochemical composition of microalgae (lipids, proteins, carbohydrates, other metabolites, and minerals), many technologies have been adopted to convert their biomass into biofuels such as biodiesel, bioethanol, bio-methane, bio-oil, and syngas. These technologies involve different processes that can be categorised into chemical (i.e. transesterification), thermochemical, and biochemical conversion technologies as shown in figure 2.9 (S. N. Naik *et al.*, 2010; Raheem *et al.*, 2015). The chemical conversion technology involves the reaction, organic equilibrium exchange reaction, between algal lipids and alcohol (methanol or ethanol) to produce fatty acid alkyl ester which is termed as biodiesel. In thermochemical conversion technologies, microalgae are decomposed by heat with or without catalysts into intermediate products, which are processed into biofuels using additional chemical or biological processing steps. Biochemical conversion technologies involve, for example, the use of micro-organisms or enzymes to hydrolyse the pre-treated microalgae and attain fermentable sugars which can be converted into bioethanol (Raheem *et al.*, 2018). Thermochemical conversion technologies are considered the most viable for overcoming some of the problems associated with biochemical conversion technologies including low conversion efficiency by micro-organisms and enzymes, long processing time, and high capital costs. In addition, thermochemical conversion technologies can produce several end products whereas biochemical conversion technologies only produce a single end product for each technology (Raheem *et al.*, 2015).

The selection of the most suitable technologies relies on the biomass feedstock (e.g. dry-matter content and microalgae species), the end-use of the bioenergy, and economic considerations (Brennan and Owende, 2010; D. P. Ho *et al.*, 2014). A full summary of the microalgae conversion techniques into biofuels are shown in table 2.6.

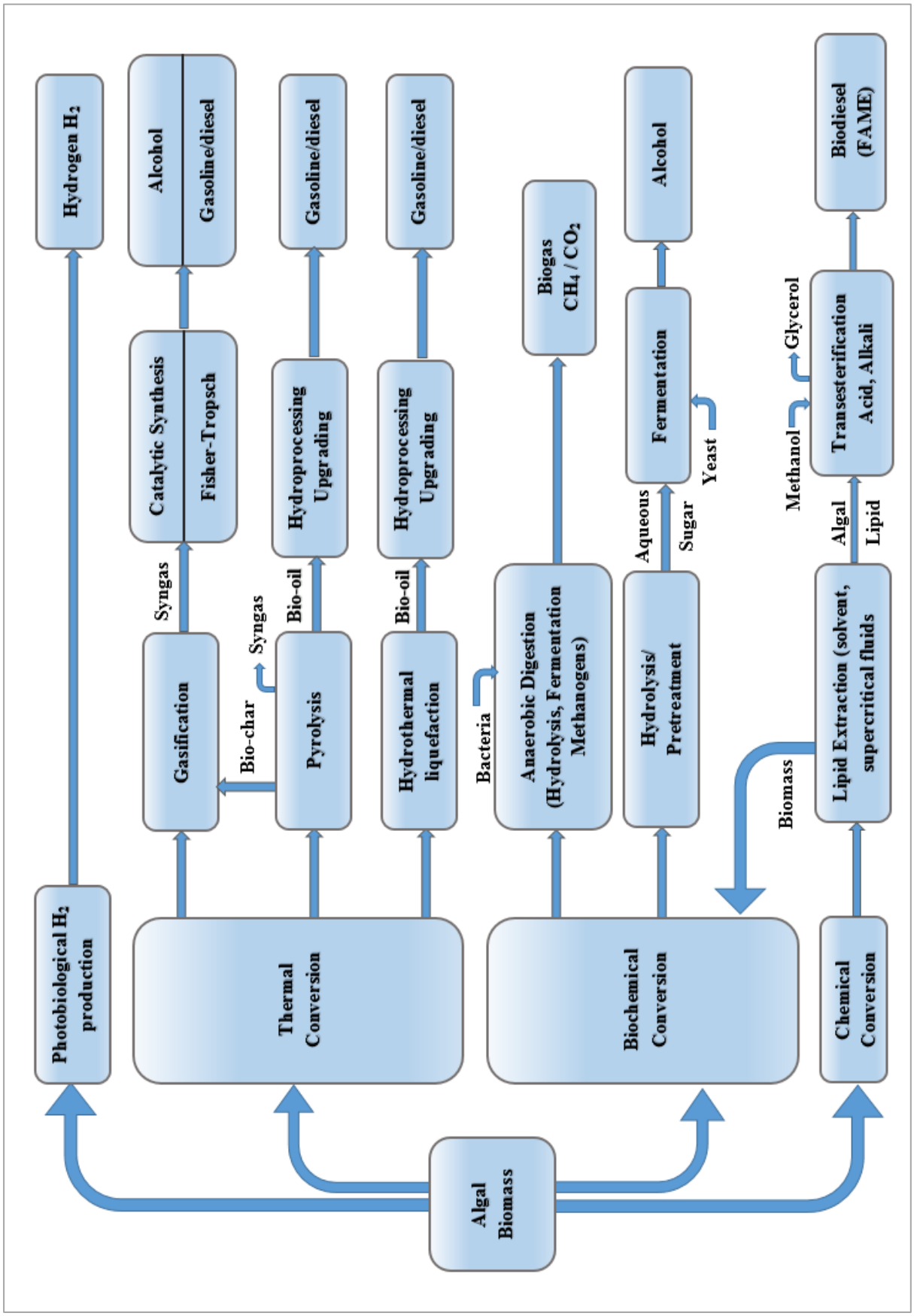

Figure 2.9: The conversion methods of microalgae biomass into fuels (Brennan and Owende, 2010; Suali and Sarbatly, 2012).

2.6.1 Thermochemical conversion technologies

As mentioned previously, thermochemical conversion technologies involve thermal decomposition of the organic components in microalgae biomass into intermediate products, which are then converted into biofuels via chemical or biological processes. Hydrothermal liquefaction, pyrolysis, gasification, and even direct combustion are the main technologies used for this purpose (Brennan and Owende, 2010). These techniques are capable of converting whole microalgae biomass as well as the residue after lipid extraction (mainly comprised of carbohydrates, proteins, and non-extracted lipids) into gaseous, solid and liquid fuels (Pradhan *et al.*, 2017).

2.6.1.1 Hydrothermal liquefaction

Hydrothermal liquefaction (HTL) or thermochemical liquefaction is a biomass-to-liquid conversion process conducted in water at a typical temperature range of 250-374 ˚C and high pressures 39-215 bar with or without a catalyst. The mass fraction of microalgae is within the range of 5–50% in the feed slurry (Wei-Hsin Chen *et al.*, 2015). HTL keeps the water in its liquid state. As the water approaches its critical point (374 ˚C, 220.6 bar), it acts more like a non-polar solvent with lower density due to the significant changes in its density, dielectric constant, and reactivity. This change in properties makes the water have a higher affinity for organic compounds and consequently breaks them down into smaller and shorter molecular weight materials. Energy-dense bio-oil is the main product in the HTL reaction in addition to a gas consisting mainly of CO_2, a nutrient-rich aqueous phase, and residual solid (Garcia Alba *et al.*, 2011; López Barreiro *et al.*, 2013; Anastasakis and Ross, 2015). Liquefying microalgae hydrothermally avoids the need for energy-intensive dewatering and drying stages. A considerable amount of attention has been given to hydrothermal liquefaction over the last 10 years owing to its capability for converting wet microalgae into biofuels (Elliott, 2016; Chiaramonti *et al.*, 2017). Lam and Lee (2012) reported that microalgae are a perfect feedstock for thermochemical liquefaction due to their small size which enables them to quickly attain the required reaction temperature (M. K. Lam and Lee, 2012).

Through liquefaction, some compounds are extracted from microalgae biomass while others are depolymerised into oligomers and monomers by hydrolysis, which is the dominant process during liquefaction. If the liquefaction processing time is extended, these compounds are further decomposed through decarboxylation, dehydration, deamination, and cleavage reactions to produce smaller active fragments which re-react (repolymerise) by different reactions such as

condensation to form new compounds. For instance, ketone and aldehyde compounds are produced from the HTL of carbohydrates (Raheem *et al.*, 2018).

The effects of different HTL parameters including temperature, holding time, heterogenous and homogenous catalyst, percentage solid loading, co-solvent, and the diverse biochemical compositions of various algae species have been evaluated on the product yields (Table 2.5) (Fortier *et al.*, 2014). Bio-oil yields of 9-65% were reported for *Arthrospira* and *B. braunii* respectively (Dote *et al.*, 1994; Duan and Savage, 2011). Dote et al. (1994) successfully liquefied *B. braunii* at 300˚C and achieved a maximum bio-oil yield of 64% (DW) with higher heating value (HHV) of 45.9 MJ kg^{-1} (Dote *et al.*, 1994). Similarly, Tomoaki et al. (1995) obtained a bio-oil yield of 37% (W.D.) with HHV of 36 MJ kg^{-1} by the HTL of *Dunaliella tertiolecta* at 340 ˚C reaction temperature and 10 MPa pressure for 60 minutes (Minowa *et al.*, 1995). Both studies reported positive energy balances (output/input ratio) of 6.67:1 and 2.94:1 respectively.

Species	Biochemical composition			Liquefaction conditions			Bio-oil yield% (DW)	HHV (MJ kg^{-1})	Reference
	Carbohydrate	Protein	Lipid	Temp. (˚C)	Holding time (min)	Catalyst			
Botryococcus braunii	-	-	-	300	60	Na_2CO_3	64	45.9	(Dote *et al.*, 1994)
Dunaliella tertiolecta	15.9	63.6	20.5	340	60	Na_2CO_3	37	36	(Minowa *et al.*, 1995)
Chlorella vulgaris	9	55	25	350	60	- Na_2CO_3 HCOOH	37 27 25	35.1 37.1 33.2	(P. Biller and Ross, 2011b)
Nannochloropsis oculata	8	57	32	350	60	- Na_2CO_3 HCOOH	36 26 24.6	34.5 35.5 39	(P. Biller and Ross, 2011b)
Porphyridium cruentum	40	43	8	350	60	- Na_2CO_3 HCOOH	22 26.5 20	35.7 22.8 36.3	(P. Biller and Ross, 2011b)
Arthrospira (Spirulina)	20	65	5	350	60	- Na_2CO_3 HCOOH	29 17 20	36.8 34.8 35.1	(P. Biller and Ross, 2011b)
Desmodesmus sp.	23-33	38-44	10-14	375	5	-	49.4	35.4	(Garcia Alba *et al.*, 2012)
Microcystis viridis	-	-	-	340	30	Na_2CO_3	33	31	(Y. F. Yang *et al.*, 2004)
Enteromorpha prolifera	-	-	-	300	30	Na_2CO_3	23	28-30	(Dong Zhou *et al.*, 2010)

Table 2.5: Feedstock biochemical composition, hydrothermal conditions, bio-oil product yields, and HHV for different algae species.

Energy dense bio-oil is a viscous and dark liquid and its yield according to Biller and Ross is 5-25% (W.D.) higher than the lipid content in the microalgae biomass, indicating that carbohydrates and proteins are also contributing to its fraction (P. Biller and Ross, 2011b). The bio-oil yield, composition, chemical and physical properties are strongly dependent on the biochemical composition of biomass feedstock as well as process parameters. Long-chain fatty acids, alkanes and alkenes, phenol and its alkylated derivatives, derivatives of phytol and cholesterol, and heterocyclic N-containing compounds are the main constituents of bio-oil (Brown *et al.*, 2010). Nitrogen heterocycles, pyrroles, and indoles are produced from proteins, fatty acids from lipids, whereas cyclic ketones and phenols are produced from carbohydrates (P. Biller and Ross, 2011b; Wei-Hsin Chen *et al.*, 2015). According to the results for HTL for diverse algae species at different operating conditions, bio-oil yield and HHVs are within the range of 20-65% (DW) and 20-46 MJ kg^{-1} (Table 2.5).

The aqueous phase from the HTL of microalgae is rich in nutrients such as NH_4^+, PO_4^{3-}, CH_3COO^- in addition to metallic cations such as K^+, Ca^{2+}, Na^+, Mg^{2+}. Therefore, it can be used as a nutrient source for cultivation since microalgae can assimilate organic and inorganic nutrients from a wide variety of sources. Gasification of the aqueous phase at supercritical conditions is an interesting route to produce gas rich in hydrogen while the residual from this process can be recycled to the growth medium as nutrients (López Barreiro *et al.*, 2013).

The gaseous products of the HTL comprise CO_2, H_2, CH_4, CO, N_2, C_2H_4, C_2H_6, and C_3H_6. CO_2 is the most abundant gas product with concentrations exceeding 90% followed by H_2 and CH_4 (Brown *et al.*, 2010). It was reported that the yield of light hydrocarbons such as CH_4 increased whereas CO_2 yield dropped off when liquefaction conditions surpassed the critical point of water (López Barreiro *et al.*, 2013). Brown et al. (2010) suggested that the CO gas produced during the liquefaction process is probably utilised in the water gas shift and/or methanation reactions, subsequently low amounts of CO are often detected (Brown *et al.*, 2010). However, others suggested that the high amount of CO_2 gas compared to CO is due to the possibility that the deoxygenation reaction mainly takes place by decarboxylation instead of decarbonylation (Garcia Alba *et al.*, 2012). HTL of microalgae also produces a solid residue having a high content of ash with small quantities of carbon, hydrogen, nitrogen, and sulphur (Wei-Hsin Chen *et al.*, 2015).

Although bio-oil produced by HTL can be used directly as a fuel, it has lower elemental oxygen content compared to the biomass feedstock, and has a HHV comparable to that of petroleum, it cannot be treated using conventional fossil fuel refineries due to high nitrogen content and

requires denitrification by a hydro-treating process (Wei-Hsin Chen *et al.*, 2015). Nevertheless, according to Jena and Das (2011), bio-oil produced by the HTL of microalgae was reported to be more stable and have higher energy content compared to pyrolysis oil from the same microalgae species (Jena and Das, 2011). However, thermochemical liquefaction processes have high capital costs due to the high operating pressure.

2.6.1.2 Gasification

Gasification is a versatile thermochemical technology that can process a wide range of carbon feedstocks. Organic or fossil based carbonaceous materials are converted without combustion through partial oxidation at high temperature (700-850 ºC) to a mixture of gases including H_2, CO, CO_2, and CH_4 (known as syngas). Further processing with temperatures up to 1000 ºC can produce 64% w/w methanol as reported by Hirano et al. (1998) when they gasified *Arthrospira* at this temperature (A. Hirano *et al.*, 1998). Biomass with 15% moisture content is appropriate for gasification; however, some studies suggested that algal biomass with moisture content up to 40% are acceptable for gasification even though high moisture content reduces syngas energy content as well as the process efficiency (Raheem *et al.*, 2015). Gasification temperature has a large effect on both process yield and selectivity. Demirbas (2009) succeeded in increasing the gasification yields of *Cladophorafracta* and *Chlorella* sp. from 28 to 57% through increasing reaction temperature from 552 to 952 ˚C (A. Demirbas, 2009). Syngas has low HHVs of 4-6 MJ m^{-3} and is appropriate to be used as a fuel for heating and electricity generation (Raheem *et al.*, 2018). Syngas can also be used to produce liquid fuels (e.g. gasoline and methanol) via the Fischer-Tropsch process and hydrogen via the water gas shift reaction (Sanchez-Silva *et al.*, 2013). The gasification of algal biomass occurs in three steps: drying, pyrolysis, and char combustion (Raheem *et al.*, 2015).

The selection of a gasifying agent such as steam-oxygen mixture, steam, or air has a pivotal influence on product composition. For instance, higher hydrogen yield was obtained with steam used as a gasifying agent compared to air when both agents were examined for the gasification of oil palm (Brennan and Owende, 2010; Motasemi and Afzal, 2013; Sanchez-Silva *et al.*, 2013; López-González *et al.*, 2014a; Tekin *et al.*, 2014). Sanchez et al. (2013) reported that syngas rich in H_2, CO and CO_2 and low in CH_4 was obtained from *Nannochlorophsis gaditana* using steam as the gasifying agent. This was likely due to the water gas shift and steam methane reforming reactions induced by the presence of steam (Sanchez-Silva *et al.*, 2013). The use of air is not recommended as it yields higher tar content even though it is the cheapest gasifying agent (Raheem *et al.*, 2018). Khoo et al. (2013) obtained 59 wt.% tar, 28 wt.% syngas and 14

wt.% bio-oil by the gasification of *Nannochloropsis* sp. in a fixed bed gasifier at 850 ˚C (Khoo *et al.*, 2013).

Accumulation of biomass residue is an issue often observed when gasifying microalgae with high ash content. However, elements such as K and Mg can catalyse the process and therefore enhance its yield. The presence of catalyst with high loading increases the gasification efficiency of algal biomass up to 85% (Chakinala *et al.*, 2010). Steam gasification of *Scenedesmus almeriensis*, *Nannochloropsis gaditana* and *Chlorella vulgaris* were studied by López et al. (2014) (López-González *et al.*, 2014b). They observed that CO_2, H_2, CO are the main products with lower amounts of CH_4, C_2H_2 and C_2H_5. They concluded that the highest gasification yields obtained with *S. almeriensis* was due to its high content of catalytic elements (e.g. K and Mg). Chakinala et al. (2010) achieved complete gasification of *C. vulgaris* at 700 ˚C in the presence of Ru/TiO2 catalyst (Chakinala *et al.*, 2010). Nickel-based catalysts were stated to be capable of decreasing tar formation at high temperatures (Asadullah *et al.*, 2002). The most common catalysts used in the gasification processes are listed in table 2.6.

A gasification process utilising water under supercritical conditions (SCWG) is another interesting conversion process working under high temperature (374-700 ºC) and sufficient pressure (22.1 MPa). This process is also called hydrothermal gasification (HTG) and is capable of converting wet algae biomass, 90% moisture, directly into syngas with high hydrogen and methane yields and low biochar content (Suali and Sarbatly, 2012; Guan *et al.*, 2013). SCWG of microalgae is therefore a promising technology to produce gaseous fuels since it has an important advantage of avoiding the high energy requirements associated with the dewatering and drying stages in the conventional gasification process.

2.6.1.3 Pyrolysis

Pyrolysis is a thermochemical process that thermally decomposes biomass with up to 10% water content at temperatures of 200-700 ºC in the absence of oxygen, with or without catalyst into a low energy value gas (mainly composed of CH_4 and CO_2), bio-oil, and biochar. The bio-oil is isolated by condensing the generated vapour, leaving behind biochar (Raheem *et al.*, 2018). Bio-oils produced from the pyrolysis of microalgae have been reported be more stable than those from lignocellulosic biomass but with a slightly lower HHV (Mohan *et al.*, 2006). Pyrolytic bio-oils have caloric values ranging between 31 and 42 MJ kg^{-1}, contain amounts of solids, chemically dissolved water, oxygen and nitrogen containing compounds which make them acidic and viscous. Catalytic upgrading of the oil via hydro-treating is required (Du *et al.*, 2011).

Heating rate and temperature are the most important parameters in pyrolysis. According to the process heating rate or vapour residence time, pyrolysis is categorised into slow pyrolysis (0.1-1 ˚C s^{-1}), fast pyrolysis (10-200 ˚C s^{-1}) and flash pyrolysis (>1000 ˚C s^{-1}). Tubular and fixed bed reactors are often employed to perform slow pyrolysis. Wire mesh, vacuum furnace, entrained flow, rotating, vortex, and circulating fluidised bed reactors are used for conducting fast pyrolysis. Special reactors such as fluidised bed reactors are used for flash pyrolysis (Goyal *et al.*, 2008). Due to its low heating rate, slow pyrolysis is easier to perform, but it produces lower oil yields (Campanella *et al.*, 2012; Chaiwong *et al.*, 2013). Grierson et al. (2009) pyrolysed six microalgae species, *Tetraselmis chuii*, *Chlorella* sp., *C. vulgaris*, *Chaetocerous muelleri*, *Dunaliella tertiolecta* and *Synechococcus* sp. at slow heating rate and temperature of 500 ˚C. Product yields of 24–43%, 13–25% and 30–63% for bio-oil, gas and biochar were obtained respectively. Fatty acids, alkenes, phenols and amides were the dominant compounds identified in the pyrolytic bio-oils (Grierson *et al.*, 2009). Fast and flash pyrolysis can drastically reduce the amount of biochar, increase the amount of bio-oil and its caloric value as well as reducing the oxygen contents in the bio-oil (Dickerson and Soria, 2013; Raheem *et al.*, 2015). Miao and Wu (2004) stated that fast pyrolysis of microalgae, *C. prothothecoides* produced bio-oil yields of 19-57%. They concluded that bio-oil yield obtained by fast pyrolysis of *C. prothothecoides* produced heterotrophically were 3.4 times higher than that obtained from autotrophic cells (Miao and Wu, 2004). The temperature range of 200 to 520 ˚C is believed to be optimal for thermal decomposition of microalgae. Demirbas studied the effect of temperature on bio-oil yield through the pyrolysis of *C. prothothecoides*, finding that increasing temperature from 255 to 500 ˚C led to increased yield from 6-55% (Demirbaş, 2006). However, Peng et al. (2000) reported that pyrolysis temperatures in the range of 300-500 ˚C had no significant effect on yield at holding times above 20 min (Peng *et al.*, 2000). High heating rates are required during flash pyrolysis and hence the biomass size should be very small, typically between 105–250μm. According to these requirements, microalgae are seen as a promising biomass for this technology (Gerçel, 2002).

The presence of catalyst was reported to improve the pyrolytic bio-oil quality through reducing oxygen contents as well as increasing HHV. Pan et al. (2010) observed lower oxygen content of 19 wt.% and a higher calorific value of 32.5 MJ kg^{-1} in the bio-oil produced by catalytic pyrolysis of *Nannochloropsis* sp. residue using zeolite, HZSM-5 catalyst in comparison to that produced by direct pyrolysis which had an oxygen content of 30 wt.% and a caloric value of 24.6 MJ kg^{-1} (Pan *et al.*, 2010). Na_2CO_3 catalyst was found to increase and reduce the yields of

gaseous and liquid products respectively during the pyrolysis of *Chlorella* sp. (Babich *et al.*, 2011).

Pyrolysis by microwave-assisted heating has been performed on microalgae in a few studies (Du *et al.*, 2011; Zhifeng Hu *et al.*, 2012; Fernanda Cabral Borges *et al.*, 2014). Microwave pyrolysis is operated at powers of 500-2250W, temperatures of 500-800 ˚C, and absorber contents of 5–30 wt.%. This technology produces bio-oil with yield and calorific values in the range of 18-59 wt.% and 30-42 MJ kg^{-1} respectively. Compared to pyrolysis by traditional heating methods, microwave pyrolysis offers quick heating, uniform internal heating of feedstock, no requirement for agitation by fluidisation, and less ash in the bio-oil (Wei-Hsin Chen *et al.*, 2015). Absorbers such as chars, metallic oxides, activated carbon, ionic liquids, and sulfuric acid are usually blended with microalgae in microwave pyrolysis to enhance liquid product yield or quality (Salema and Ani, 2012). Du et al. (2011) achieved a maximum bio-oil yield of 28.6 wt.% through microwave pyrolysis of *Chlorella* sp. with char as absorber. They observed that the bio-oil obtained had lower oxygen contents and the gas product was mainly composed H_2, CO, CO_2, and light hydrocarbons (Du *et al.*, 2011).

2.6.1.4 Direct combustion

The chemical energy stored in microalgae biomass can be directly converted into heat or power by combustion in the presence of excess air at temperature of around 850 ˚C; however, the heat yielded from this process cannot be stored and hence it is best to be used immediately (Raheem *et al.*, 2015). The combustion process is practically viable when moisture content is less than 50%, otherwise, a pre-treatment stage (i.e. drying) is required which in turn may render the process totally unfeasible due to the costs of drying the biomass (Goyal *et al.*, 2008). There are a few reports on the technical viability of using microalgae for direct combustion; however, coal-algae co-firing was proven to produce lower GHG emissions and air pollution (Kadam, 2002).

2.6.2 Chemical conversion technologies (transesterification)

Transesterification is the most commonly applied technology to produce biodiesel (Thea Coward, 2012). During transesterification, the lipid components especially triglycerides (TAG) from the extraction step react with alcohol (methanol or ethanol) catalysed by alkalis, acids, or enzymes to produce fatty acid alkyl ester which is termed as biodiesel (Raheem *et al.*, 2018). Methanol is a simple polar solvent which is commonly used in the transesterification process due to its low cost, availability, and advantageous physical and chemical properties over other solvents (Thea Coward, 2012). Biodiesel produced from various biomass including microalgae

is compatible and has comparable properties to diesel such as cetane number, caloric value, flash point and viscosity, therefore, it can be used directly in conventional diesel engines (Azadi *et al.*, 2014). Nevertheless, algal oils include higher polyunsaturated fatty acids than vegetable oils, and therefore it is more liable to oxidation during storage (Yusuf Chisti, 2007). Microalgae with high lipid contents are an appropriate source for biodiesel production. Moreover, algal biodiesel is more appropriate than 1st generation biodiesel for utilisation in the aviation industry due to its lower freezing point and high energy density (Brennan and Owende, 2010). High microalgae production costs especially cultivation, harvesting, and drying stages, scalability, microalgae diversion from growth regime to stress regime to improve lipid productivity which causes limited growth rates are the main drawbacks for large-scale biodiesel production from microalgae (Jing Lu *et al.*, 2011).

The selection of the catalyst type in the transesterification reaction depends on the content of free fatty acids (FFA) in the feedstock. Acidic catalysed reactions are less sensitive to the existence of water and FFA and consequently reduce the formation of soap and water and improve the product separation (Ruoyu Xu and Mi, 2010). Although acid catalysts (e.g. H_2SO_4) are preferable in the transesterification of various feedstocks, they have lower activity in comparison to alkaline catalysts. High reaction temperatures over 100 ˚C, long reaction times, corrosion risks to process equipment are the main drawbacks associated with acid catalysts (Raheem *et al.*, 2018). Transesterification reactions using alkaline catalysts (e.g. NaOH and KOH) are approximately 4000 times faster than acid catalysed reactions (Thea Coward, 2012). However, as stated earlier, oil feedstocks with high FFA content (approximately above 0.5 wt.%) prohibited such catalysts to be used for transesterification due to the reaction between FFA and base catalyst which forms soap, resulting in less biodiesel yield and difficulty in separating biodiesel from glycerol (co-product) (Ehimen *et al.*, 2010). For instance, Naik et al. (2008) noticed a reduction in biodiesel yield from 97 to 6% in a KOH catalysed transesterification when FFA content in the feedstock increased from 0.3 to 5.3 wt.% (Malaya Naik *et al.*, 2008). Alternatively, a two-step process comprising the use of acid and base catalysts together can be employed to overcome the drawbacks above. Oil feedstocks with high FFA content are initially treated with acidic catalyst to reduce FFA level before the alkaline catalysed reaction occurs. However, this process requires extra base catalyst to neutralise the acid catalyst during transesterification (M. K. Lam and Lee, 2012). Biocatalysts such as lipase used for the transesterification of triglycerides have shown attractive outcomes in comparison to conventional chemical catalysts. They require lower energy-input and ease the recovery of

co-products (e.g. glycerol). In addition, lipase catalyst is capable of aiding both transesterification of TAG and esterification of FFA (Khan *et al.*, 2009; Guldhe *et al.*, 2016).

Conventional biodiesel production is performed over two distinct stages, lipid extraction followed by transesterification. In contrast, *in-situ* transesterification allows lipid extraction and transesterification to take place in one single stage (Takisawa *et al.*, 2013; Chee Loong Teo and Idris, 2014b). The *in situ* transesterification process was developed by Harrington and D'Arcy in 1985 to produce biodiesel from biomass in a single step without prior isolation of oils (Leung *et al.*, 2010). A chemical solvent has two substantial roles through *in situ* transesterification; first, it is used as a solvent to extract lipid/oil from biomass and second, as a reactant in the transesterification reaction (M. K. Lam and Lee, 2012). The one stage transesterification process has many advantages over the conventional process including it shortens processing time which results in lower overall production costs and also eliminates the solvent-lipid separation stage (Shuit *et al.*, 2010). Ehimen et al. (2010) studied *in-situ* transesterification of dried *Chlorella*. They achieved a maximum biodiesel yield of 90 wt.% at a reaction temperature of 60 °C, methanol to lipid molar ratio of 315:1, H_2SO_4 concentration of 0.04 mol and reaction time of 4 h (Ehimen *et al.*, 2010). However, methanol to lipid molar ratio has been observed to reduce if a co-solvent such as hexane, toluene, or chloromethane is introduced to the process (Ruoyu Xu and Mi, 2011). Velasquz-Orta et al. (2012) evaluated different controllable factors of the *in-situ* transesterification process of *C. vulgaris* including catalyst ratio, reaction time, and solvent ratio on FAME yield. The results revealed that a FAME recovery of 77.6% was obtained using alkaline catalyst, NaOH, whereas up to 96.8% conversion was attained using an acidic catalyst, H_2SO_4, but with a longer reaction time (Velasquez-Orta *et al.*, 2012). *In-situ* transesterification for wet-paste microalgae biomass has additional advantages since it avoids drying stage of harvested biomass (Patil *et al.*, 2013). Patil et al. (2013) successfully performed *in-situ* transesterification of wet *Nannochloropsis salina* with the aid of ethanol and microwave radiation and without a catalyst (Patil *et al.*, 2013). Nevertheless, processing wet biomass has adverse influences on the process (Ehimen *et al.*, 2010). Jin et al. (2014) examined several acidic catalysts in direct transesterification of *Chlorella pyrenoidosa* at 350 ˚C and different moisture contents in the presence of ethanol. They demonstrated that moisture content had negative effects on the yield and characteristics of the biodiesel (Jin *et al.*, 2014).

The supercritical extraction process of algal lipids can be combined with the transesterification reaction in a single step. It has some attractive advantages such as short reaction time and avoids the use of chemical catalysts (Raheem *et al.*, 2018). Maira and Conzalo (2018) investigated the supercritical transesterification of *Arthrospira* oil with methanol and ethanol at different

temperatures and co-solvent (CO_2) amounts. They found that biodiesel yield increased from 42 to 65% at 200 °C and from 46 to 72% at 300 °C when the amount of CO_2 increased from 0.0005 to 0.003 g CO_2/g methanol. They also concluded that using CO_2 increased the reaction yield due to a reduction in the critical point of the reaction mixture (Tobar and Núñez, 2018). However, the high operating conditions of this process (usually >240 °C and >8.1 MPa) may degrade the biodiesel produced and promote undesired side reactions.

2.6.3 Biochemical conversion technologies

The biochemical conversion technologies involve the biological processing (degradation) of algal biomass into biofuels (e.g. methane and ethanol) and include anaerobic digestion, alcoholic fermentation and photobiological hydrogen production (Figure 2.9) (Chew *et al.*, 2017). However, thermochemical conversion technologies are preferable over biochemical conversion technologies due to the reasons aforementioned.

2.6.3.1 Anaerobic digestion

Anaerobic digestion (AD) is a biochemical process of converting organic matter into biogas by specialised anaerobic bacteria in an oxygen-free environment. The produced biogas typically contains CH_4 (55–75%), CO_2 (25–45%), traces of H_2, H_2S, CO and other permanent gases (Jankowska *et al.*, 2017; Mohd Udaiyappan *et al.*, 2017). Anaerobic digestion is a low cost conversion technology and capable of processing organic feedstocks with high water content of 80-90% (Raheem *et al.*, 2018). In addition, it can process the whole microalgae cells as well as residuals from other biofuel production technologies (Jankowska *et al.*, 2017). It has been employed in treating industrial wastewater, agricultural wastewater, solid wastes, and sludge from urban wastes and sewage treatment plants (Mohd Udaiyappan *et al.*, 2017). The anaerobic digestion technology consists of multiple processes: hydrolysis, acidogenesis, acetogenesis and methanogenesis. Firstly, biomass (e.g. lipids, carbohydrates, proteins) are decomposed by hydrolysis into their respective soluble oligomers and monomers. After that, hydrolysed oligomers and monomers are converted by acidogenesis into simpler molecules (precursors for methane production), such as H_2, CO_2 and acetate by acetogenic bacteria. Finally, methanogenesis takes place to produce methane by methanogenic bacteria which are highly sensitive to oxygen (Man Kee Lam and Lee, 2011). The operating conditions, main and co-products, and product properties of anaerobic digestion of microalgae are summarised in table 2.6.

Digester design, feedstock characteristics, and the process operational conditions are the main factors affecting the anaerobic digestion process. Temperature and pH are the most important

operational parameters in addition to solid and hydraulic retention time but with less importance. The optimum temperature and pH are 35 °C and 6.8–7.2 respectively (Cioabla *et al.*, 2012). The C:N ratio is a key factor for an efficient and stable anaerobic digestion process. Anaerobic digestion of biomass having low C:N ratio produces high concentrations of dissolved ammonia (NH_4) through the decomposition of protein which in turn inhibits methanogenesis (Hansen *et al.*, 1998). To avoid nutritional imbalance for high biogas production, a C:N ratio within a range of 20:1 and 30:1 is preferable (Hidaka *et al.*, 2014). However, for too low C:N ratio, co-digestion of algal biomass with a carbon rich organic feedstock, such as sewage sludge and paper waste can be adapted to increase production rate (Yen and Brune, 2007). Costa et al. (2012) achieved an increase of 26% in methane production when co-digesting *Ulva* sp. with sewage sludge and manure (Costa *et al.*, 2012).

The complex structural cell wall of microalgae is the main challenge for an efficient biogas production which causes limited accessibility of substrate to micro-organisms, therefore, pre-treatment is often required to deconstruct the structure of the cell wall and increase bacteria activity (Raheem *et al.*, 2018). Passos et al. (2013) obtained higher biogas production yields via microwave pre-treatment. The biogas yield of 307 mL g^{-1} volatile solid was attained in comparison to biogas yield of 172 mL g^{-1} volatile solid without any pre-treatment (Passos *et al.*, 2013). Anaerobic digestion demonstrates many advantages over other technologies such as it is efficient for organic matter removal, applicable at any scale, capable of using a wide variety of substrates as feedstock, less expensive to build and it consumes less energy. Moreover, this technology can generate multi end-products such as biogas and digestate which are easily separated and used as a source of energy and fertilizers respectively. However, the degradation process of microalgae cell walls by extracellular enzymes of hydrolytic bacteria is too slow due to the reason mentioned earlier and consequently a limited hydrolysis rate renders the anaerobic digestion into a lengthy and inefficient bioprocess (Passos *et al.*, 2014; Magdalena *et al.*, 2018).

2.6.3.2 Alcoholic fermentation

Sugar (e.g. glucose and sucrose), starch, and cellulose stored in biomass can be converted via alcoholic fermentation into bioethanol. Initial product contains approximately 10-15% ethanol, consequently, further concentration and purification by distillation and rectification is required to remove water and impurities (C. H. Tan *et al.*, 2015). Residuals from this process are still valuable to be processed by thermal conversion technologies such as HTL, pyrolysis, gasification, and anaerobic digestion into biofuels. Starch and cellulose are the most common carbohydrates exist in the microalgae that can be used to produce bioethanol (Shih-Hsin Ho *et al.*, 2012). Traditional bioethanol production from microalgae typically takes place through

three steps. Firstly, algal biomass is pre-treated with acids or enzymes to deconstruct their cell walls and recover stored fermentable starch. After that, starch is hydrolysed using enzymes (e.g. α-amylases) to produce simple sugars which are then fermented into bioethanol using yeast strains. In the final stage, bioethanol separation and purification is performed (McKendry, 2002). The most common microorganisms used for ethanolic fermentation are yeasts of the genus *Saccharomyces* or bacteria of the genus *Zymomonas* (de Farias Silva and Bertucco, 2016). The operating conditions, main and co-products, and product properties of alcoholic fermentation of microalgae are summarised in table 2.6.

Microalgae such as *C. vulgaris* are good candidates for bioethanol production due to their high starch content approximately 37% (DW), and bioethanol conversion of up to 65% has been reported (Atsushi Hirano *et al.*, 1997). *Scenedesmus obliquus* are also able to accumulate about 50-60% (DW) carbohydrates in normal medium after exhaustion of the nitrogen source (Shih-Hsin Ho *et al.*, 2013; Möllers *et al.*, 2014). However, using nitrogen depletion strategy to increase the accumulation of carbohydrate has a drawback on the viability of the process due to the reduced algal biomass yield. Another route to produce bioethanol from microalgae is the use of metabolic path-ways in dark conditions, redirecting photosynthesis to produce acids, alcohols, and small amounts of hydrogen. Complex organic polymers are hydrolysed by fermentative and hydrolytic microorganisms into monomers, which are subsequently converted into a mixture of organic acids of low molecular weight and alcohols such as acetic acids and ethanol (de Farias Silva and Bertucco, 2016). Ueno et al. (1998) used dark fermentation to produce bioethanol from *Chlorococcum littorale* achieving a maximum ethanol productivity of 450 μmol g^{-1} (DW) at 30 ˚C (Ueno *et al.*, 1998). However, the literature has concluded that dark fermentation of microalgae is not an efficient process to produce bioethanol.

Although the microalgae biomass seems to require mild conditions for hydrolysis and for fermentation in the traditional route of bioethanol production, this route has several drawbacks including the requirement of multistep processes which needs more energy and the use of enzymes and yeasts which accounts for a considerable portion of the costs. Moreover, microalgae are diverse in terms of their cellular structure (different biochemical compositions and type of carbohydrates) and therefore a specific enzyme is required to efficiently saccharify each microalgae species (de Farias Silva and Bertucco, 2016).

2.6.3.3 Hydrogen production via photobiological process

Hydrogen (H_2), which is an efficient and clean energy carrier, can be produced from microalgae and cyanobacteria via a photo-biological process. Some species can produce hydrogen as an

electron donor by direct or indirect photolysis of water using light energy under anaerobic condition (Cantrell *et al.*, 2008; Azwar *et al.*, 2014). In photolytic biological systems, microalgae use sunlight to convert water molecules into hydrogen ions (H^+) and oxygen during photosynthesis. Hydrogenase enzymes convert the hydrogen ions into hydrogen under anaerobic conditions. This technology has a long-term potential to sustainably produce hydrogen with low environmental impact. However, the oxygen formed during the process may represent the main problem due to its ability to inhibit hydrogenase enzymes (Suali and Sarbatly, 2012). Moreover, H_2 production instead of fixing carbon is not the normal function of algal photosynthesis. The enzymes that produces H_2 are not even synthesized under normal growth conditions. Finally, the high cost of photobioreactor materials and operation is also another challenge which may limit the commercial application of this technology (Ghirardi *et al.*, 2008).

2.7 Conclusion

Microalgae are feasible as a biofuel feedstock which can meet the huge global fuel demand in a sustainable manner. However, there are some technical impediments that limit the commercial use of microalgae; especially for low-value products such as biofuels. Selection of suitable microalgae species, cultivation, harvesting, drying and conversion of biomass into biofuel are the main stages in the algal-based fuel production process. Efficient microalgae species should have rapid growth rate, the ability to survive in different environments, high lipid productivity, and high efficiency for the uptake of nutrients under different production conditions. Low biomass yield is the major challenge in current cultivation systems resulting in dilute growth culture. Microalgae harvesting and dewatering are major operational costs that hinder the development and expansion of the large-scale use of microalgae for biofuels. Harvesting represents a substantial process cost, accounting for an estimated 20-30% of the total cost of production. A cost effective and reliable technique for bulk harvesting has yet to be adopted across the microalgae sector. A successful harvesting technique needs have the following characteristics:

- Have high recovery efficiencies and concentration factors;
- Rapid;
- Growth media and species independent;
- Easy to scale up;
- Able to operate continuously with high throughput;
- Does not prevent the spent culture recycling;

- Low cost.

If such a harvesting technique is developed, an economically viable fuel could be achieved. The comparison of available harvesting technologies described in this chapter has shown that foam flotation and bio-flocculation can harvest a wide range of microalgae in an economical way. However, bio-flocculation is not recommended for biofuel production since it is a highly species dependent process and produces biomass of low lipid content. Flotation columns have simple construction, lower capital and operating costs, improved recovery and enrichment, and a smaller footprint.

The drying stage has high energy demands which may result in a negative energy balance when producing microalgae-based biofuels since it broadly contributes up to 59% of the total energy consumption. Therefore, the better option is to process wet microalgae directly into biofuel to substantially reduce the energy consumption associated with dewatering and drying. However, processing wet microalgae has adverse effects on the *in-situ* transesterification process. Hydrothermal liquefaction takes place under high water content and seems to be a very promising technology for algal biofuel production but is at an early stage of development.

Parameter	Conversion Process					
	Transesterification	**Liquefaction**	**Pyrolysis**	**Gasification**	**Fermentation**	**Anaerobic Digestion**
Feedstock conditions	Extracted algal lipid, mainly TAG, blended with alcohol	Algal slurry with moisture content up to 95%	Up to 10% water content algal biomass	Less than 40% water content algal biomass	Carbohydrate rich/pre-treated algae to release starch, sugar, and cellulose	Algal biomass wastes from other conversion process or whole algae
Operating conditions	With methanol Temp.: 35-65 ˚C. With ethanol: Temp.: 35-78 ˚C Press.: 1 atm. For higher reaction temp., a pressure vessel is required.	Sub or super-critical water Temp.: 250-374 ˚C Press.: 39-215 bar	Temp.: 200-700 ˚C Press: 1 atm. absence of oxygen	Temp.: 700-1000 ˚C Press: 1 atm. partial oxidation gasifying agent: air, steam, or steam-O_2 mixture	Temp.: 30-40 ˚C Press.: 1 atm.	Temp.: bacteria working: 0-70 ˚C In literature: 25-37 ˚C Press.: 1 atm.
Main product	Biodiesel (Fatty acid methyl ester (FAME) Fatty acid ethyl ester (FAEE))	Bio-oil (cyclic nitrogenates such as pyrolle, indole, pyrazine, and pyrimidine, cyclic oxygenates like phenols and phenol derivatives with aliphatic side-chains and cyclic nitrogen and oxygen compounds like pyrrolidinedione and piperidinedione, esters, fatty acids, and hydrocarbons)	flash pyrolysis: bio-oil 75% including (aliphatic and aromatic hydrocarbons like Cyclopropene, 1-butyl-2-ethyl- and phenols, acids like Benzoic acids)	Temp.: 700-850 ˚C Co: 9-50% H_2: 5-56%	Ethanol (C_2H_5OH)	55-75%vol CH_4 (productivity of 61-430 cm^3 Total $Solid^{-1}$)
			slow pyrolysis: syngas 25%, major components (CH_4, CO_2)	Temp.: 850-1000 ˚C 64% w/w methanol		
Products properties	Energy content: 41 MJ/kg Density: 864 kg m^{-3} Viscosity: 5.2*10^{-4} Pa s at 40 ˚C flash point: 371 K, pour point: 259 K, Cetane number: 52 min, ash content: 0.21 wt.% Nitrogen content: 0.002-0.007 wt.% water content:0.02 vol.% Acid Number, mg KOH/g: 0.4-0.45. Oxidation stability at 110 °C: 90 min	Energy content: 30-39 MJ/kg Density: 943 kg m^{-3} Viscosity: 0.33382 Pa s at 40 ˚C Wt.%: Carbon content: 79.2t% Hydrogen content: 10% Nitrogen content: 4-8% Oxygen content: 5-18% Sulphur Content: 0.1-1.3% H/C molar ratio: 1.56 water content:2.8 wt.% Acid Number, mg KOH/g: 68	Bio-oil: Energy content: 28-41 MJ/kg Density: 920-980 kg m^{-3} Viscosity: 0.02-0.061 Pa s at 40 ˚C Wt.%, Carbon content: 59% Hydrogen content: 7.9% Nitrogen content: 8% Oxygen content: 25% Sulphur Content: <0.5 % water content:2% Syngas: Energy content: 1.2-4.8 MJ/kg	Syngas: HHV: 3.338 MJ/kg, cold gas efficiency: 44.24% (30% moisture feedstock) HHV: 5.138 MJ/kg, cold gas efficiency: 73.81% (5% moisture feedstock)	Energy content: 30 MJ/kg Density: 772 kg m^{-3} Viscosity: 8.34*10^{-4} Pa s at 40 ˚C	Caloric value: 11 MJ/m^3
Co-products	Glycerol	solid: 16%, gases: 30%, 6-20% methane, H_2, > 90% CO_2, aqueous phase 17% (water + dissolved organics)	Bio-char: 2% with flash pyrolysis : 20% with slow pyrolysis	Methane (2-25%) , CO_2, other hydrocarbon (C_2H_4, C_2H_6, C_2H_2), tar: up to 20%, and ash	CO_2	CO2, traces of H_2, H_2S, CO
Catalysts	Homogenous or heterogeneous Acid: sulphuric acid, $FeCl_3$, $ZnCl_2$ Alkali: NaOH, CaO, KOH, Enzymatic: lipase, Rhizomucor mieher	Homogenous or heterogeneous Na_2CO_3, KOH, CH_3COOH, HCOOH NiO $Co/Mo/Al_2O_3$	Zeolite like HZSM-5 Na_2CO_3 Metal oxide like ZnO, Al_2O_3	K_2CO_3 Ni–Pt/Al_2O_3 Dolomite	Hydrochloric, sulphuric acids Enzymatic catalysts Ethanol yeast	Hydrochloric, sulphuric acids Enzymatic catalysts Acidogenic bacteria Methanogens bacteria
Reference	(Ramachandran *et al.*, 2013) (Vijayaraghavan and Hemanathan, 2009) (Suali and Sarbatly, 2012) (Velasquez-Orta *et al.*, 2012) (Leung *et al.*, 2010) (Nautiyal *et al.*, 2014)	(Suali and Sarbatly, 2012) (Bennion, 2014) (Tian *et al.*, 2014) (Elliott *et al.*, 2014) (Yunhua Zhu *et al.*, 2013) (Elliott *et al.*, 2013)	(Zeng *et al.*, 2013) (Babich *et al.*, 2011) (Campanella and Harold, 2012) (Suali and Sarbatly, 2012) (Belotti *et al.*, 2014) (Brennan and Owende, 2010)	(Brennan and Owende, 2010) (Suali and Sarbatly, 2012) (López-González *et al.*, 2014a) (Díaz-Rey *et al.*, 2014)	(Wu *et al.*, 2014) (Brennan and Owende, 2010) (Suali and Sarbatly, 2012)	(M. Wang *et al.*, 2013a) (Rodriguez *et al.*, 2015) (Kamat *et al.*, 2013) (Astals *et al.*, 2015) (Yuan *et al.*, 2014) (Meng Wang and Park, 2015) (Mohd Udaiyappan *et al.*, 2017)

Table 2.6: Summary of the conversion techniques of microalgae biomass and their products

Chapter 3

Continuous harvesting of microalgae biomass using foam flotation

Abstract

Biomass harvesting and dewatering are major operational costs that constrain the development and expansion of the industrial use of microalgae; particularly low value biofuels. Flotation-based technologies show promise as low cost, energy-efficient harvesters, producing a thickened algae slurry ahead of further dewatering steps. In this study we demonstrate, for the first time, a surfactant-aided foam flotation column that is designed and optimised for the continuous harvest of microalgae. The following operational parameters were optimised; surfactant concentration, air flow rate, feed flow rate, column height, liquid pool depth, and sparger type (i.e. bubble size). The effects of surface characteristics on *Chlorella vulgaris* flotation performance were investigated by quantifying the hydrophobicity, zeta potential, and the contact angle. The hydrophobicity of *C. vulgaris* was enhanced using three surfactants; the cationic cetyltrimethylammonium bromide (CTAB), the anionic sodium dodecyl sulfate (SDS), and the non-ionic TWEEN®20; with CTAB producing the greatest enhancement. Surfactant concentration, column height, and air flow rate had the greatest effect on the algae concentration factor and recovery efficiency. The optimised design (CTAB = 35 mg L^{-1}, air flow rate = 1 L min^{-1}, feed flow rate= 0.1 L min^{-1}, column height = 146 cm, liquid pool depth = 25 cm, with a fine porous sparger) yielded recovery efficiencies of 95, 93, and 89% with 173, 271, and 143-fold biomass enrichments for freshwater *C. vulgaris* and marine *Isochrysis galbana* and *Tetraselmis suecica* microalgae respectively. Achieving high recovery efficiencies for freshwater and in the case of marine microalgae (irrespective of ionic strength) at moderate surfactant dosages, gives foam flotation the advantage of being a growth media independent harvesting process. The process had a very low power consumption (0.052 kWh m^{-3} of algae culture). Our findings demonstrate the potential for continuous, low cost, scalable flotation microalgae harvesting that has particular relevance for the biofuels, water and wastewater treatment industries.

Keywords: Adsorptive bubble separation; Algae biofuels; Biodiesel; Hydrophobicity; Microalgae harvesting

3.1 Introduction

Concerns about the sustainable use of fossil fuels, fluctuating oil prices, environmental pollution, and global climate change are driving moves away from conventional fuels to

biofuels, including those derived from microalgae (Jing Lu *et al.*, 2011; Pragya *et al.*, 2013; Reyes and Labra, 2016). Microalgae are fast growing, photosynthetically efficient oleaginous organisms that can be cultivated in freshwater, brackish, and full-strength seawater, together with a range of nutrient impacted wastewaters. Microalgae have the potential (as yet unrealised due to lack of cost competitiveness) to play a vital role in the biofuels market (Brennan and Owende, 2010; Chinnasamy *et al.*, 2010a; F. Chen *et al.*, 2012; M. K. Lam and Lee, 2012; Farid *et al.*, 2013; Andrew K. Lee *et al.*, 2013; Coons *et al.*, 2014). Biofuels aside, there are established markets for microalgae biomass and extracts in the cosmetics, nutraceuticals, and pharmaceuticals industries. Equally, microalgae are both a problem and an opportunity for water utilities and the wastewater industry.

Harvesting and dewatering of the microalgae biomass represents a substantial process cost, accounting for an estimated 20-30% of the total cost of production (Molina Grima *et al.*, 2003; Greenwell *et al.*, 2010; Milledge and Heaven, 2012). Harvesting from dilute algae suspensions is challenging due to the small cell size translating to a low specific gravity, as well as the cell surface being negatively charged thereby maintaining a stable colloidal suspension. Other impediments stem from the ionic strength of the culture medium due to salinity, hydrophobicity, pH and culture age (Milledge and Heaven, 2012; Udom *et al.*, 2013). Consequently, there are a number of challenges inherent in microalgae harvesting such as a low recovery efficiency and/or high capital and operating costs.

A cost effective and reliable technique for bulk harvesting has yet to be adopted across the microalgae sector (Uduman *et al.*, 2010a; Gouveia, 2011; Laamanen *et al.*, 2016). A wide range of solid-liquid separation techniques have been trialled, both individually or in combination, such as coagulation and flocculation, followed by sedimentation, flotation, centrifugation, or filtration (Figure 3.1). Gravity sedimentation is a very simple solid-liquid separation method and commonly used to separate microalgae from water; however, it is a time-consuming process due to long settling time and needs higher resource efficiency (large land areas) for settling ponds. Moreover, the total suspended solid from sedimentation is low which increases the cost of further downstream processes (T. Coward *et al.*, 2013). Therefore, sedimentation is rarely used alone to harvest algal biomass and it is therefore combined with coagulation and flocculation. However, flocculation is currently uneconomical as the amount, and hence costs, of flocculant necessary for large scale harvesting is prohibitive (Brennan and Owende, 2010). Centrifugation is the most rapid and suitable harvesting technique for a wide range of microalgae species. However, it is an energy-intensive method (requiring as much as 3000 kWh ton^{-1} (Benjamin T. Smith and Davis, 2013)). Filtration is another common harvesting technique

but it is highly dependent on the size of the microalgae, is abrasive to many species and is energy intensive due to pumping. Frequent replacement or backwash of filters are other disadvantages (Bilad *et al.*, 2013). A successful harvesting system needs to be effective, rapid, low cost, species independent, scalable, and should be able to operate continuously if required. An added benefit would be the potential to partially process the biomass *in situ*, e.g. weakening of the cell wall prior to conversion into biofuel (Laamanen *et al.*, 2016; Lananan *et al.*, 2016).

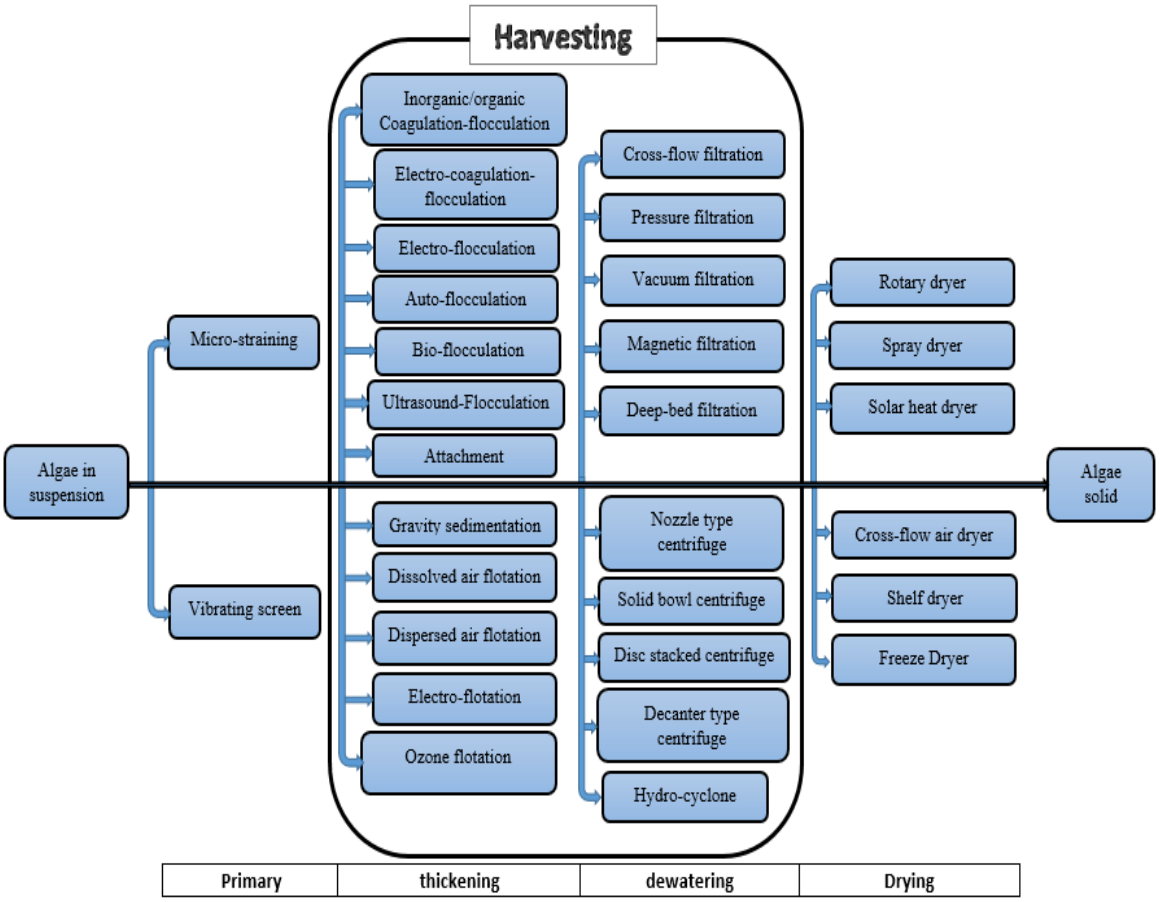

Figure 3.1: A summary of microalgae harvesting and dewatering methods by category; primary harvesting, algae slurry thickening, further dewatering, and drying. Redrawn from Barros et al. (2015) and Pahl et al. (2013) (Pahl *et al.*, 2013; Barros *et al.*, 2015).

Due to its simplicity and low capital and operating costs, adsorptive bubble separation is widely used in industrial and domestic wastewater treatment, and in the mining, pharmaceutical, and food industries (Jenkins *et al.*, 1972; Rubio *et al.*, 2002; Fuerstenau *et al.*, 2007; Schramm and Mikula, 2012). Foam flotation, which is a subclass of adsorptive bubble separation, shows considerable promise as a microalgae biomass harvesting and enrichment method. The flotation column has many advantages over conventional flotation cells including: simple construction, lower capital and operating cost, improved recovery, higher grade products, less wear and tear due to the absence of moving parts, and a smaller footprint (Sastri, 1998). It is energetically

unfavourable for hydrophobic particles to remain wholly within the liquid phase. They will adsorb onto the surface of bubbles which will transport them to the liquid surface for collection and removal (P. Stevenson and Li, 2014). Most microalgae species are weakly hydrophobic, especially those that are algaenan-free like *Chlorella vulgaris* (López Barreiro *et al.*, 2013; Ling Xia *et al.*, 2017b); therefore, surface-active materials (surfactants) are added not only to stabilise the foam in the system but also to enhance the hydrophobicity of the microalgae. The foam flotation process involves generating bubbles by gas flow, either through a porous or jet sparger. Destabilised microalgae and free surfactant will adsorb onto the bubbles and are removed from the column as foam (P. Stevenson and Li, 2012a). Foam is an effective medium to adsorb microalgae as it possesses a high specific surface area which results in a high recovery efficacy whilst only a small volume of interstitial liquid is collected, enabling good biomass enrichment.

Previous surfactant-aided flotation harvesting research has been performed in batch or semi-batch modes, with recovery efficiencies of up to 97% (Y. M. Chen *et al.*, 1998; J. C. Liu *et al.*, 1999; Phoochinda and White, 2003; Phoochinda *et al.*, 2005; Rita K. Henderson *et al.*, 2008; Garg *et al.*, 2013; Kurniawati *et al.*, 2014; Alhattab and Brooks, 2017). When combined with electro-flocculation a recovery efficiency of 98.9% was achieved (Ling Xu *et al.*, 2010). In a forerunner to the present study, Coward et al. (2013) harvested *Chlorella vulgaris* in batch mode, attaining a high concentration factor of almost 230 but at the expense of recovery efficiency (T. Coward *et al.*, 2013). For most bulk harvesting techniques, especially flotation operating in batch or semi-batch modes, it is challenging to realise an effective combination of a high recovery efficiency (for greater biomass removal from the growth medium) and concentration factor (to lower downstream dewatering and drying costs). Very few reported works on bulk harvesting techniques have focused on the recovery efficiency and concentration factor of the harvested microalgae together due to the trade-off between them. For instance, Garg et al. (2013) recovered 85% of *Tetraselmis* sp. using mechanical flotation cells with dodecylammonium hydrochloride (DAH) surfactant but at the expense of enrichment in which only six-times more concentrated microalgae was obtained (Garg *et al.*, 2013). However, this shortcoming may be overcome if a pivotal combination between the factors affecting both the recovery efficiency and concentration factor is achievable in a continuous foam flotation column. Continuous mode harvesters are also more suitable for high throughput applications such as biofuels production, whereas batch or semi-batch modes have more downtimes and typically need higher resource efficiency (i.e. space and energy). Furthermore, commercial

scale algae production is typically continuous or semi-continuous; there is thus a demand for the capability to harvest continuously.

The work presented in this chapter developed and optimised a foam flotation column to continuously harvest *C. vulgaris, Isochrysis galbana* and *Tetraselmis suecica*. This work also aimed to evaluate the effectiveness and economic feasibility of the process. To the best of our knowledge, this is the first study to demonstrate low cost and continuous microalgae harvesting using foam flotation with a focus on both biomass recovery and enrichment.

3.2 Materials and methods

3.2.1 Microalgae culture

Freshwater *C. vulgaris*, and marine *I. galbana* and *T. suecica* were grown using BG-11 and F/2 media in seven polycarbonate carboys (Nalgene 10 L) at 20 ± 2 ºC in a non-sterile environment. Photoperiod was 16L:8D using a combination of cold and warm fluorescent lights with an average illuminance of 2,500 lux. The cultures were agitated by aeration using an aquarium air pump (Koi Air, KA50, 0.032 mPa), and maintained semi-continuously.

3.2.2 Surfactant types

Three surfactants were used; the synthetic anionic foam stabiliser sodium dodecyl sulphate (SDS, $CH_3(CH_2)_{11}OSO_3Na$), (AMRESCO, USA); the non-ionic emulsifier and detergent TWEEN®20 (polysorbate 20, $C_{58}H_{114}O_{26}$) , (Sigma-Aldrich, UK); and the common quaternary ammonium cationic surfactant hexadecyltrimethylammonium bromide (CTAB, $CH_3(CH_2)_{15}N(Br)(CH_3)_3$), (G-Biosciences, USA). CTAB has been demonstrated as the most suitable surface-active material to remove algal biomass from wastewater (T. Coward *et al.*, 2013; Laamanen *et al.*, 2016). It has also been used in wastewater treatment and in the extraction of DNA (Koner *et al.*, 2010; Fu *et al.*, 2017). Even though the cationic surfactant CTAB is harmful, especially to aquatic organisms, it can disrupt algae cell walls and promote cell lysis. Therefore, it may be used for simultaneous harvesting and cell disruption prior to lipid extraction or direct biofuel conversion.

3.2.3 Hydrophobicity tests

Hydrophobicity tests on *C. vulgaris* were carried out using a modified microbial adhesion to hydrocarbons method (Rosenberg *et al.*, 1980; Garg *et al.*, 2012), with or without the addition of 20 and 40 mg L^{-1} of CTAB, 20 and 40 mg L^{-1} of SDS, and 2 and 4 mL of TWEEN 20. Hydrophobicity was also measured after addition of 70 and 100 mg L^{-1} of trivalent aluminium chloride salt, $AlCl_3$ (Sigma-Aldrich, UK) in the presence of 40 mg L^{-1} of SDS. In this method,

8 mL of microalgae culture, 0.46 ± 0.13 g L^{-1} concentration (dry weight equivalent to 9.58 × 10^6 ± 1.1 × 10^6 cells mL^{-1}, which approximates to cell densities within raceway based microalgae production systems (Y. Chisti, 2013)) was placed in a test tube, in duplicate. Two millilitres of n-hexane (95% purity, Sigma-Aldrich, UK) was then added to each tube and shaken vigorously for one minute; the resulting suspension was settled for two minutes. Afterwards, 2 mL was carefully drawn from the aqueous layer at the bottom of each tube, placed in a UV cuvette, and the absorbance read at 620 nm using a spectrophotometer (Jenway, Model 7315, Bibby Scientific Ltd, UK); this allowed the proportion of cells that had moved to the water-hexane interface to be determined. The hydrophobicity (H_{ydro}) of the algal suspension was calculated using equation 3.1:

$$H_{ydro} = \frac{A_o - A_{aq}}{A_o} \times 100\% \quad \cdots (3.1)$$

where: A_o is the absorbance of the microalgae suspension before n-hexane addition and A_{aq} is the absorbance of the aqueous phase after n-hexane addition. Based on the hydrophobicity data, only CTAB was carried forward for optimisation and harvesting trials. The data from the hydrophobicity experiment was compared using an ANOVA test with Dunnett comparison procedure with an alpha level of 0.05.

3.2.4 Adsorption isotherm

The concentration of CTAB adsorbed onto the *C. vulgaris* was determined by surface tension. A calibration curve was created for CTAB in the 0-20 mg L^{-1} range versus surface tension measurements using a microtensiometer (Kibron EZPi^{plus}, Finland) when dissolved in 1 L of water separated from algae culture by centrifugation. Culture medium was used rather than deionised water due to the presence of ions in the medium which may alter surface tension readings. Two different concentrations of algae culture were used here which were 1.2±0.01 and 0.68±0.01 g L^{-1} (equivalent to 24.1 × 10^6±2.6 × 10^4 cells mL^{-1} and 14.2 × 10^6 ±2.2 × 10^4 cells mL^{-1} respectively). The mixture (20 mg of CTAB in 1 L of algae culture) was stirred continuously for 15 min using a magnetic stirrer. Two 10 mL samples were centrifuged for 30 min at 15,000 rpm (25,155 RCF) to separate the algae from the medium. The supernatant was collected and the surface tension was measured to determine the concentration of un-adsorbed surfactant that remained in the medium.

3.2.5 Zeta (ζ) potential experiments

Colloidal systems such as microalgae suspensions consist of highly dispersed particles (discontinuous phase) distributed uniformly throughout a dispersion medium (continuous

phase) (Pahl *et al.*, 2013). The magnitude of the zeta potential (ζ) is a key characteristic in the colloidal system as it gives an indication of the suspension stability. The ζ-potential of *C. vulgaris* was measured herein with or without the addition of CTAB at different pH values (4, 6, 8, and 10) using a Zetasizer Nano ZS ZEN3600 instrument, Malvern Instruments Ltd., UK. In a typical experimental trial with surfactant addition, l L of microalgae culture, 0.46 ± 0.13 g L^{-1} concentration dry weight (equivalent to $9.58 \times 10^6 \pm 1.1 \times 10^6$ cells mL^{-1}), was mixed with approximately 35 mg L^{-1} of CTAB and the mixture was stirred continuously for 15 min using a magnetic stirrer. To study the effect of ions from the culture medium on microalgae zeta potential, more trial sets were performed after resuspension of microalgae in deionised water. Four 50 ml samples were collected from the mixture and the pH adjusted using NaOH and HCl solutions. To study of effect of culture ions on ζ-potential, 1 L of microalgae culture was centrifuged for 10 min at 4,000 rpm and re-suspended in deionised water. The ζ-potential measurements were carried out in triplicate.

3.2.6 Measurement of the contact angle

The contact angle of *C. vulgaris* cells, in the form of algal strata on membrane filters, was measured based on the sessile drop technique by using a goniometer (model 250, Rame-Hart, USA) with DROPimage advanced software. The contact angle measurements were performed with and without CTAB addition. Algae with a concentration of 0.46±0.13 g l^{-1} dry weight (equivalent to $9.58 \times 10^6 \pm 1.1 \times 10^6$ cells mL^{-1}) were deposited on a filter (cellulose nitrate membrane, 1.25 μm pore size, 25 mm diameter, MFS) using a syringe filter. CTAB (20, 30, and 40 mg L^{-1}) was dissolved in a 1 L algae culture and stirred continuously for 15 min using a magnetic stirrer prior to the filtration. The obtained algal mats were placed on an agar plate to prevent them from drying until the measurements were made. Contact angle measurements were performed in triplicate with deionised water as a probe liquid. Deionised water has been successfully employed in the contact angle measurements of various microorganisms including yeasts, bacteria, and algae. For the measurements, the filter papers were taken from the agar plate and fixed to glass slides, then dried in air for 50 min. After air-drying, the filter papers were stored in a desiccator over silica gel until use. Readings were recorded after 0.5 sec of the probe liquid deposition (volume of 5 μm), and each sample was tested ten times within 1 sec (Ozkan and Berberoglu, 2013a; Sirmerova *et al.*, 2013).

3.2.7 Foam column dimensions

A bench scale flotation column was used as shown in figure 3.2. The column was constructed from poly(methyl methacrylate) with a 5.15 cm internal diameter. Column height could be

adjusted between 30-160 cm by attaching different tubular modules of 25, 30 or 50 cm lengths. The inlet mixture consisted of algae culture with added surfactant from a 25 L reservoir. The processed culture was discharged to waste from the outlet stream valve at the base of the column, 1 cm above the sparging media. A magnetic stirrer was used to mix the microalgae culture with the surfactant in the feed tank for 10 mins before and during the harvesting experiments. The feed flow rate was measured and controlled by a valve with an ultrasonic flow meter (Atrato, Titan, UK). Another valve was placed on the discharge stream to control the liquid depth in the column. The foam was collected at the top of the column using an annular trough of 30 cm in diameter and 15 cm deep. Low-flow air was fixed against foam flow at the outlet of the foam column to enhance foam collapse. Air bubbles (dispersed phase) were generated by introducing compressed air through a sparger. Two different spargers made from ultra-high molecular weight polyethylene were used with a thickness of 6.0 mm, a diameter of 51.5 mm, and mean pore sizes of 30 and 158 µm for fine and coarse porosity respectively. The air flow rate for each trial was adjusted before the inlet mixture was fed to the column to prevent liquid weeping into the gas line.

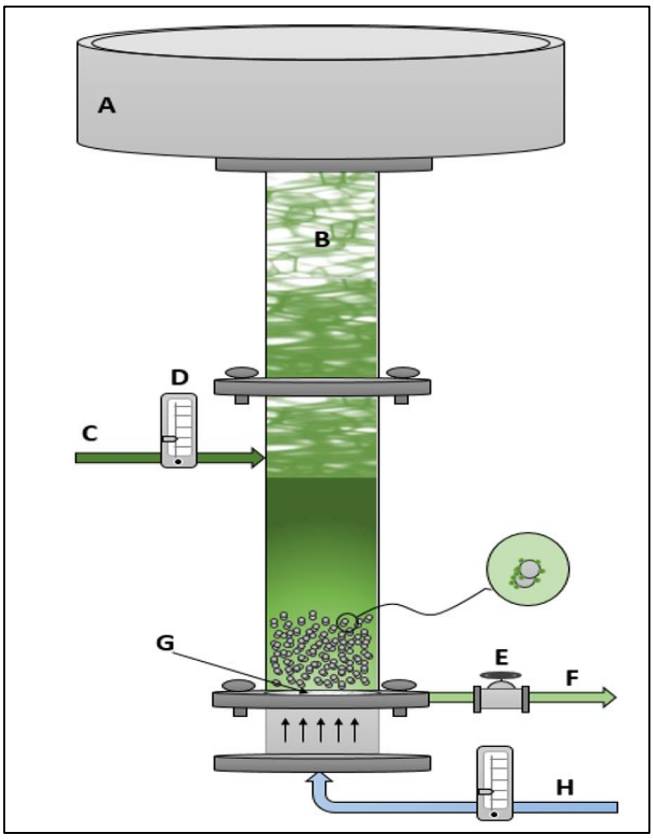

Figure 3.2: Schematic diagram of the continuous foam flotation column. A: Foam collecting cup, B: column tubular module (25, 30 or 50 cm) in height and 5.1 cm in diameter, C: inlet stream, D: inlet flow meter, E: outlet stream valve, F: underflow stream, G: air sparger, H: air input stream.

3.2.8 Harvesting effectiveness criteria

The effectiveness of a solid-liquid separation process is determined by the concentration factor (CF) and the recovery efficiency (RE). The concentration factor is the ratio of the microalgae concentration in the final product to the microalgae concentration in the culture as given in equation 3.2.

$$CF = \frac{Concentration\ of\ algae\ in\ final\ product}{Concentration\ of\ algae\ in\ inlet\ stream} = \frac{\left(\frac{cell}{ml}\right)_{fomate}}{\left(\frac{cells}{ml}\right)_{inlet}} \quad \cdots (3.2)$$

The recovery efficiency is the ratio of the microalgae cells in the final product to the microalgae cells in the culture as given in equation 3.3.

$$Recovery\ efficiency\ (RE) = \frac{cells\ of\ algae\ in\ final\ product}{cells\ of\ algae\ in\ inlet\ stream} 100\% \cdots (3.3)$$

In this work, the effectiveness of the harvesting process was determined by the concentration factor and the recovery efficiency. A calibration curve was constructed correlating cell density and their corresponding absorbance at 750 nm using a spectrophotometer (Jenway, Model 7315, Bibby scientific Ltd, UK), yielding an R^2 of 100% (data not shown). The wavelength of 750 nm was selected as the absorption by chlorophyll and most other pigments is at a minimum (Moheimani *et al.*, 2013). Cell density was measured using an improved Neubauer hemocytometer, with a Leica DM 500 light microscope.

The dry weight concentration of algae culture was measured by the following procedure: Whatman quantitative filter paper, grade 42, was dried at 103 ˚C for 3 hr then left to cool in a desiccator over silica gel until use. A pre-dried paper was weighed using a precision analytical balance (RadWag, model As220/C/2, Poland) to 4 decimal places accuracy. Known culture volume (v), approximately 10 mL, was filtered after placing the pre-weighed paper in the filter unit then dried at the same conditions as above and stored in the desiccator overnight. The dried paper was weighed to 4 decimal places and the dry weight concentration DWC determined according to equation 3.4:

$$DWC = \frac{weight\ of\ dried\ paper\ containing\ algae - weight\ of\ filter\ paper}{Volume\ (v)} \quad \ldots (3.4)$$

3.2.9 Design of experiments

Design of experiments (DOE) is a statistical and mathematical tool used to evaluate and optimise the direct and crossed relations between independent variables and system responses.

It is an advantageous method for minimising the number of experimental trials needed for process optimisation wherein rigorous modelling is intractable to apply due to the complexity of the system being investigated (Montgomery, 2012).

3.2.9.1 Fractional factorial design

A fractional factorial design approach using Minitab software (release 17, Minitab Inc., State College, PA) was applied as a screening tool prior to response surface methodology. The aim of performing the fractional design of experiments was to select the most appropriate sparger for subsequent use in the response surface design. Process variables were; surfactant concentration, airflow rate, column height, feed flow rate, liquid pool depth, and sparger type. Other factors such as pH were not studied, and thus kept constant. The screening trials were conducted on *C. vulgaris* only and the algae concentration in the inlet stream was held at 0.46±0.13 g L^{-1} concentration dry weight (equivalent to $9.58 \times 10^6 \pm 1.1 \times 10^6$ cells mL^{-1}) (Y. Chisti, 2013). A two-level fractional factorial of a resolution IV, ($2^{(6-2)}$), plus two central points was adopted. The lower and higher values of the lower and upper levels for each factor are represented by -1 and +1 in Table 3.1.

Independent variables	Levels	
	-1	+1
Surfactant concentration (mg L^{-1})	30	50
Air flow rate (L min^{-1})	1	2
Column height (cm)	71	122
Inlet flow rate (L min^{-1})	0.2	0.6
Liquid pool depth (cm)	7	20
Sparger type	coarse porous	fine porous

Table 3.1: Values of the independent variables for the fractional factorial design.

3.2.9.2 Response surface design

Once the factorial design evaluation had been completed, a five level half-unblocked Central Composite Design (CCD) with six central points was applied to identify the key process variables, their combinations, and to obtain an optimal higher degree model. CCD was adopted as it provides high quality predictions over the entire design space (Robert, 2012). The factors of interest were surfactant concentration, air flow rate, column height, feed flow rate, and liquid pool depth. CTAB and the fine porous sparger were used in the CCD trials based on results from the previous experiments. Other factors such as pH were kept constant. The harvesting trials were conducted on *C. vulgaris* only and the algae concentration in the inlet stream was held at 0.46±0.13 g L^{-1} concentration dry weight (equivalent to $9.58 \times 10^6 \pm 1.1 \times 10^6$ cells mL^{-}

[1]). Thirty-two experiments were generated and randomised with a repetition of factorial experimental runs i.e. 48 experiments. The five coded levels and their corresponding values of the factors are shown in Table 3.2.

Independent variables	Levels				
	-2	-1	0	+1	+2
Surfactant concentration (mg L^{-1})	20	30	40	50	60
Air flow rate (L min^{-1})	0.5	1	1.5	2	2.5
Column height (cm)	46	71	96	122	146
Inlet flow rate (L min^{-1})	0.05	0.2	0.4	0.6	0.8
Liquid pool depth (cm)	0.5	7	13.5	20	26.5

Table 3.2: Values of the independent variables for the central composite design.

The concentration factor and recovery efficiency responses as a function of the independent variables above were fitted to polynomial quadratic regression models given in equation 3.5 (Sanyano *et al.*, 2013):

$$Y = \beta_o + \sum_{i=1}^{k} \beta_i x_i + \sum_{i=1}^{k} \beta_{ii} x_i^2 + \sum_{i,j=1}^{k} \beta_{ij} x_i x_j \quad \cdots (3.5)$$

where: Y is the predicted response; β_o is the intercept term; β_i is the linear effect coefficient; β_{ii} is the squared effect coefficient; β_{ij} is the interaction effect coefficient; and x_i and x_j are the independent variables.

The goodness of fit of the obtained models was assessed by the lack-of-fit test and the coefficient of determination R^2 and adjusted R^2. Analysis of variance (ANOVA) was performed to determine the statistical significance of each independent variable, their combinations and to exclude insignificant variables at an alpha level of 0.05. A backward stepwise elimination regression was used to build up the quadratic model for the concentration factor and recovery efficiency responses. This technique starts with all candidate factors in the model, i.e. the full model, and then removes the least significant variable for each step based on a Significance Level to Stay (SLS) criterion (Rawlings *et al.*, 1998). Factorial plots were also employed to study the effect of significant variables and their combinations on process responses.

After the analysis of experimental data from the harvesting trials based on CCD design, the flotation process factors were optimised to maximise microalgae recovery at a considerable enrichment. Later, *C. Vulgaris, I. galbana,* and *T. suecica* were harvested continuously, in replicates of two, based on optimised conditions. Algae cell concentrations in the inlet stream

were held at $9.58 \times 10^6 \pm 1.1 \times 10^6$ cells mL^{-1}, $1.01 \times 10^7 \pm 1.29 \times 10^4$ cells mL^{-1} and $1.43 \times 10^6 \pm 7.97 \times 10^4$ cells mL^{-1} for *C. Vulgaris, I. galbana* and *T. suecica* respectively.

3.2.10 Power consumption and harvesting economics

Compression of the gas phase in a flotation column is essential for the sparging process. In other words, the gas should be compressed to overcome the pressure drop across the sparger, hydrostatic pressure of the liquid pool, and pressure drop because of friction due to flowing foam with the column wall. Total power consumption in the flotation column can be directly linked to the required work of the air compressor. The power required W_{comp} for an isentropic compression of an ideal gas was calculated using equation 3.6 (P. Stevenson and Li, 2014):

$$W_{comp} = \frac{RT_o}{\eta_{is}} \frac{\gamma - 1}{\gamma} \left[\left(\frac{P_1}{P_0} \right)^{\frac{\gamma-1}{\gamma}} - 1 \right] \cdots (3.6)$$

where: W_{comp} is the compressor work (J mol^{-1}); R is the universal gas constant (8.314 J mol^{-1} K^{-1}); T_o is the absolute initial temperature (298 ºK); η_{is} is the efficiency of air compressor; γ is the ratio of the isobaric to isochoric heat capacities (1.4 for dry air); P_0 is the pressure upstream of the compressor; and P_1 is the pressure of the compressed gas. A pressure gauge connected to the gas line was employed to measure the compressed gas pressure. The overall compressor efficiencies are within the range of 65-90% (Campbell, 2014). In this work, 70% air compressor efficiency was assumed.

The unit of power consumption according to equation 3.6 is in J mol^{-1} of gas whereas the power consumptions of most harvesting techniques in the literature are reported in kWh m^{-3} of algae culture. Therefore, for ease of comparison with the power consumptions of other techniques, the calculated work value was converted to kWh m^{-3} of algae culture as elucidated later. The associated chemical cost for the foam flotation in US$ m^{-3} of algae culture was also calculated based on the chemical costs and chemical dosage required. Water loss due to evaporation was also determined in the current work by calculating the humidity of air.

3.3 Results and discussion

3.3.1 Hydrophobicity tests

The hydrophobicity assay is a simple and rapid procedure to assess surfactant efficacy prior to foam flotation harvesting. The *C. vulgaris* hydrophobicity data using three surfactant types are shown in figure 3.3. *C. vulgaris* was weakly hydrophobic (24%) but the addition of 20 mg L^{-1} of CTAB increased hydrophobicity to 97% ($p =< 0.001$). Most microalgae species

are negatively charged at typical culture pH; the zeta potential (ζ) of *C. Vulgaris* was -18.02 mV at pH 7. Therefore, CTAB adsorbed onto the algae due to electrostatic interactions between the negatively charged cells and the cationic amphiphilic CTAB with the hydrocarbon tail increasing the alga's hydrophobicity. There was no significant difference in hydrophobicity with 40 mg L^{-1} of CTAB. A slight hydrophobicity increase was observed with 20 ($p = 0.771$) and 40 ($p = 0.734$) mg L^{-1} of SDS. This was due to repulsive forces between the cell and the anionic amphiphilic SDS. The small increase was probably due to some algae cells becoming trapped in the foam generated during shaking of the sample, causing some cells to move away from the sample suspension. Similarly, a small rise in hydrophobicity was found after addition of 2 ($p = 0.255$) and 4 ($p = 0.306$) mL of non-ionic TWEEN 20; likely due to the same reasons as for SDS. The addition of 70 and 100 mg L^{-1} of $AlCl_3$ with 40 mg L^{-1} of SDS increased the hydrophobicity to 50% ($p = 0.001$) and 98% ($p =< 0.001$) respectively (Figure 3.3). This was due to the charge neutralisation of the algal cells induced by Al^{3+} after dissociation of $AlCl_3$ in water, thus enabling SDS to be adsorbed onto the cell surface and therefore increasing the hydrophobicity. However, the need for additional chemical treatment increases the harvesting cost. As such, only CTAB was carried forward for harvesting trials.

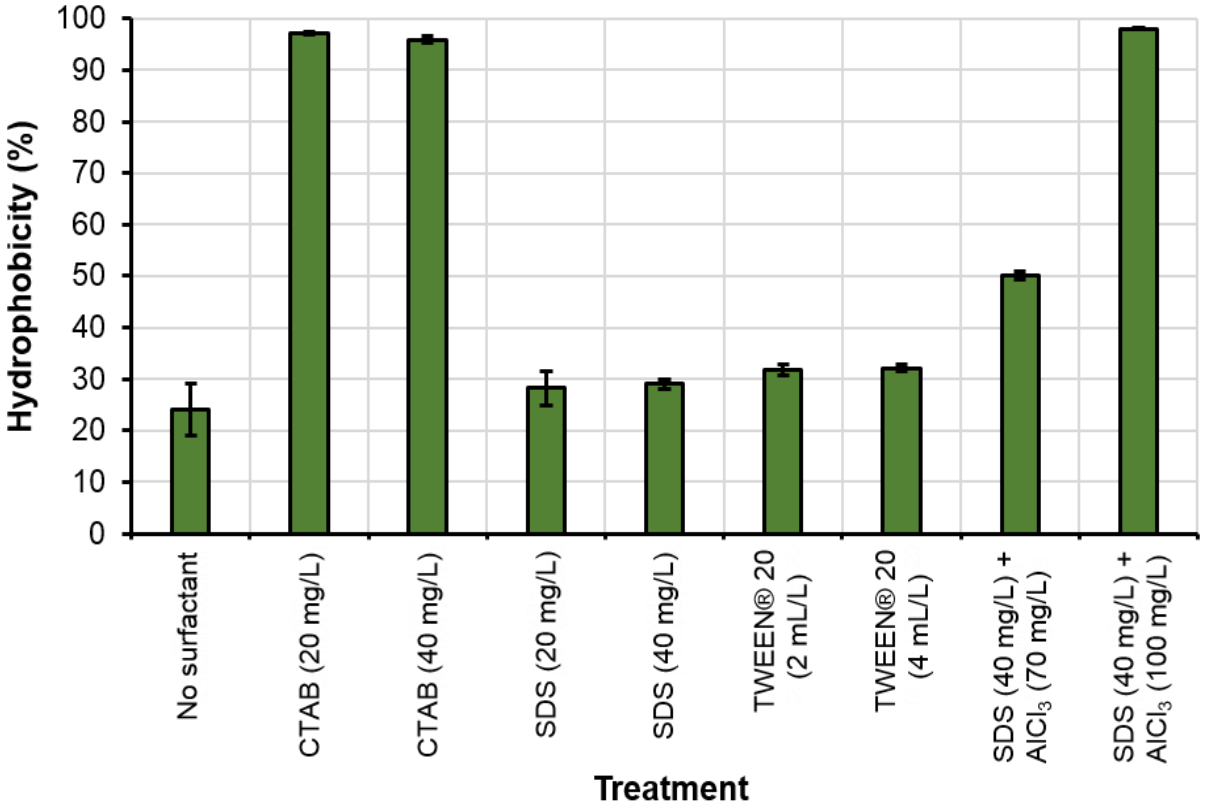

Figure 3.3: The hydrophobicity (%) of *Chlorella vulgaris* with and without added surfactants (CTAB, SDS and TWEEN® 20). $AlCl_3$ was added to two further SDS treatments to modify the surface charge of the algae cells. Means ± standard error, n = 2.

3.2 Adsorption isotherm

Measuring the quantity of surfactant adsorbed onto the algae cells is essential to qualify the electrochemical surfactant adsorption hypothesis and to quantify surfactant adsorbed for further analysis. In froth flotation two chemicals are added to the feed. The first is called a frother which acts to reduce the surface tension of the gas-liquid interface and consequently stabilises the froth. The second is a collector which adsorbs to the particles' surface, enhancing its hydrophobicity (P. Stevenson and Li, 2014). In the foam flotation column, surfactants are used for both purposes, i.e. as a foaming agent since the surfactants tend to adsorb at gas-liquid interfaces and as a collector because the surfactants adsorb onto algae cells due to the electrostatic forces of attraction. Therefore, calculating surfactant use for enhancing hydrophobicity and foam stabilisation is important. The CTAB concentration-surface tension calibration curve with the fitted polynomial model is given in figure 3.4. It can be seen from table 3.3 for the algae culture of 1.2 ± 0.01 g L^{-1} that 32.2 ± 0.2% of the added CTAB was retrieved from the supernatant i.e. adsorbed to the gas-liquid interface. It may therefore be inferred that 67.8 ± 0.2% of the CTAB was adsorbed onto algae cells. When algae biomass density was reduced to 0.68 ± 0.01 g L^{-1}, the percentage of adsorbed CTAB decreased to 39.9 ± 1.3%, predicting a more stable foam.

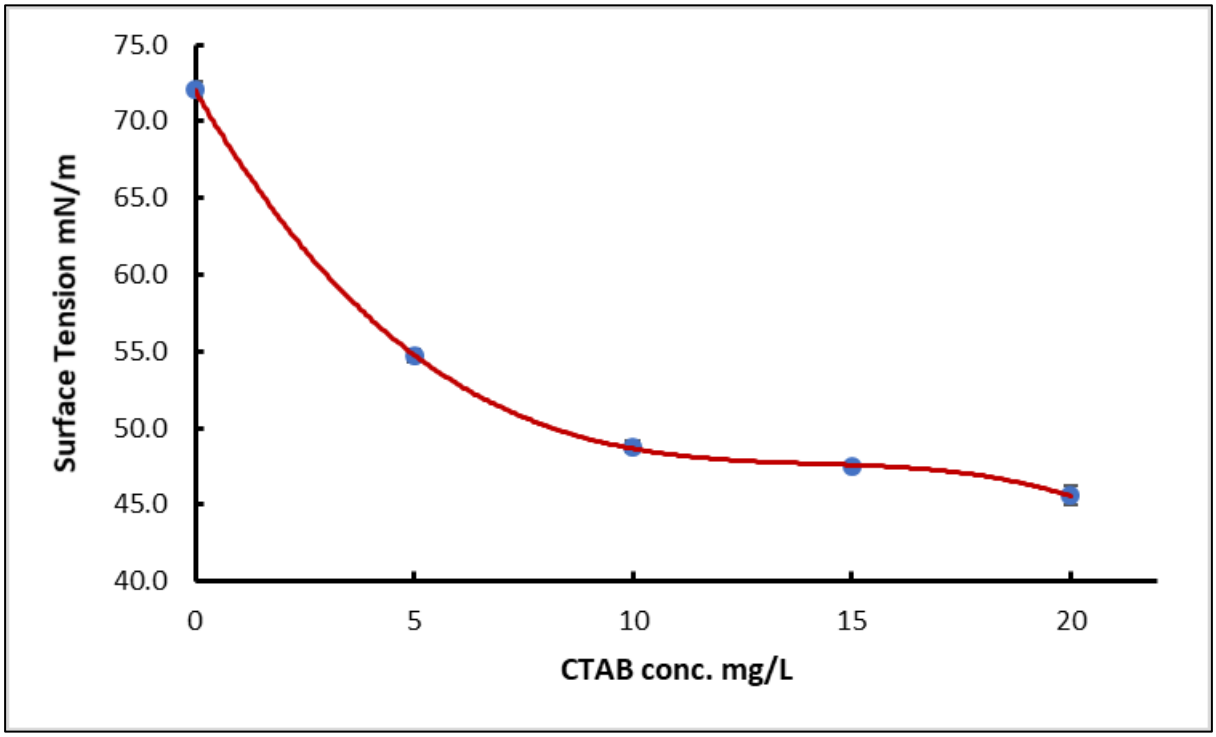

Figure 3.4: The relationship between CTAB concentration and surface tension, showing the calibration curve. Means ± standard error.

It is worth noting that the majority of the remaining free CTAB (non-adsorbed onto algae surfaces) that attached to the air bubbles and generate foam are recovered with the harvested microalgae. Despite the amount of CTAB in the discharge stream not being measured in the current work, this inference was made based on observations from second-stage harvesting trials conducted on samples collected from the discharge stream. A very thin layer of foam was noticed after bubbling air through the samples, indicating that only a small amount of surfactant remained unrecovered in the foamate. The small amount of CTAB in the discharge stream can be easily recovered by a flotation process, consequently, the surfactant-free water can be used for another cultivation cycle.

Algae culture	Cells mL^{-1}	g L^{-1}	Sample	Surface tension (mM m^{-1})	Mean surface tension (mN m^{-1})	CTAB % in supernatant	CTAB % adsorbed to algae
1	$24.1 \times 10^6 \pm 2.6 \times 10^4$	1.2 ± 0.01	1	52.51	52.48 ± 0.04	32.2 ± 0.14	67.8 ± 0.14
			2	52.44			
2	$14.2 \times 10^6 \pm 2.2 \times 10^4$	0.68 ± 0.01	1	48.03	47.96 ± 0.07	60.1 ± 0.92	39.9 ± 0.92
			2	47.89			

Table 3.3: Percentage adsorption of CTAB onto algae cells. Means ± standard error.

3.3.2 Zeta (ζ) potential experiments

The measurements of ζ-potential for *Chlorella* with and without of CTAB addition and after resuspension in deionised water are shown in figure 3.5. The average magnitudes of the ζ-potential were negative and within the range of -13.8 to -18.02 at the tested pH. The highest absolute average ζ-potential was -18.02 at pH ≈ 7. The measurements were in line with those conducted previously by *Hao* et al. (2017) (Hao *et al.*, 2017) in which they reported that the absolute average ζ-potential was -16.88 for *C. vulgaris* at pH 7. CTAB showed an obvious capability to reduce the net charge of the algal cells upon the addition of ≈ 35 mg to the algae culture, therefore it perhaps eliminates their stable suspension. For instance, the average ζ-potential at pH 8 reduced from -17.76 to -8.28 mV. The presence of ions in the microalgae culture had a negative effect on ζ-potential as shown in figure 3.5. The average ζ-potential, absolute value, increased when *C. vulgaris* was re-suspended in deionised water, e.g. at pH 8 ζ-potential changed from -17.76 to -24.12 mV. The centrifugation of *C. vulgaris* and re-suspension in deionised water resulted in the removal of the most positive ions in the BG11 culture medium such as Na^+, Mg^{2+}, Ca^{2+}, Cu^{2+}, and K^+. For the foam flotation process to recover microalgae successfully at higher recovery efficiency, the charge difference between the cell and surfactant should be high. This increases the capability of microalgae to capture surfactant

due to the electrostatic attractive forces between them. This observation was also validated by conducting some batch harvesting trials using the foam column on a microalgae culture that was centrifuged and re-suspended in deionised water. Wang et al. (2014) reported that the surface structures, in addition to extracellular products, are the main factors affecting the net charge of cell surfaces (J. Wang *et al.*, 2014). These factors are directly related to the growth and metabolic level of the algae cells. Therefore, selection of the most suitable culture age in which medium ions are as low as possible is important for an efficient harvesting of microalgae by foam flotation. However, this may increase ash content in the harvested microalgae and thus reduce the biofuel yields.

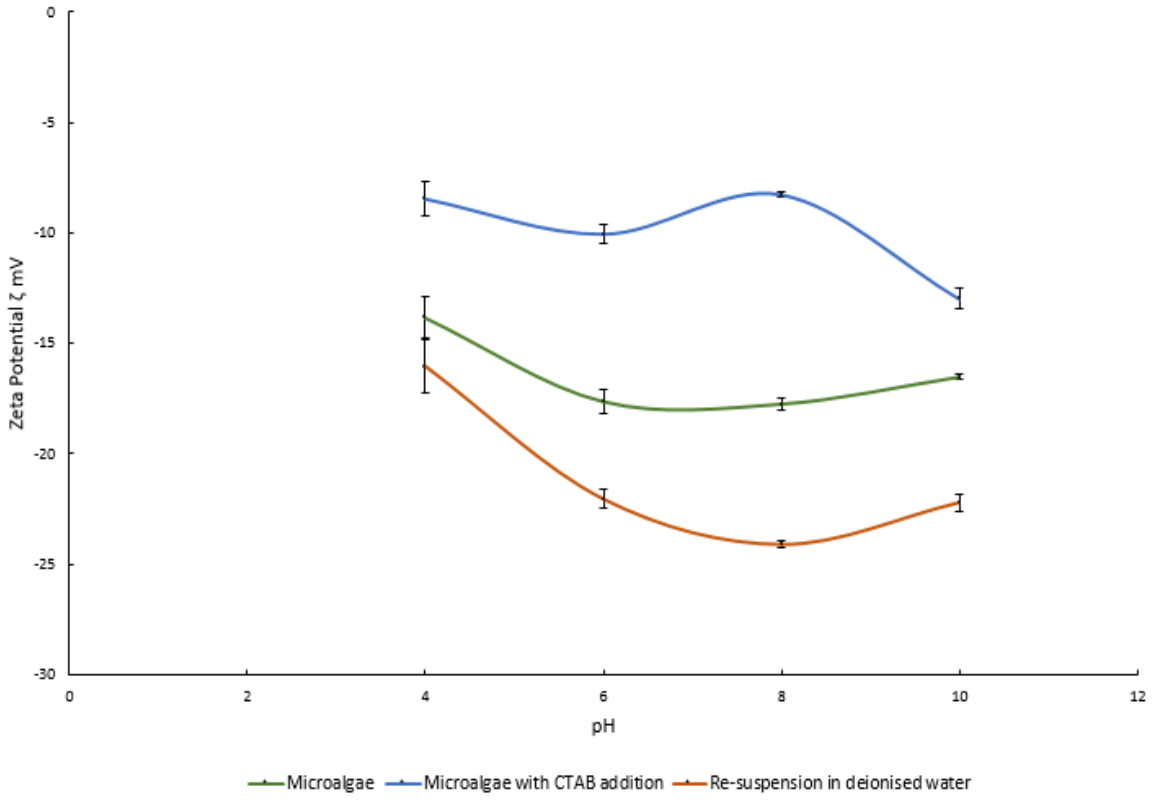

Figure 3.5: Zeta potential (ζ) of *Chlorella vulgaris* at different pH. Means ± standard error.

3.3.3 Measurements of the contact angle

The measured mean contact angles for *C. vulgaris* cells with and without CTAB are shown in figure 3.6. Due to the difficulties in getting an ideal surface because of the size and the shape of microalgae cells, the contact angle was measured over an algal mat according to Ozkan and Berberoglu (Ozkan and Berberoglu, 2013a). As seen from the contact angle measurements (Figure 3.6), *Chlorella* without any surfactant addition had hydrophilic surfaces (contact angle=30.17˚). This hydrophilicity was due to the surface functional groups present on the cell walls. *C. vulgaris* are algaenan-free species and the cell wall contains neutral sugars, proteins,

and uronic acids which have hydrophilic surface functional groups such as hydroxyl, carboxyl, and amine groups (Erbil, 2006; Ozkan and Berberoglu, 2013a). The contact angle value in this work was lower than that reported by Ozkan and Berberoglu (contact angle=42.7˚) which might be due to differences in the biochemical compositions between the algal samples. However, the stabilisation time for the probe liquid on the mats was 0.5 sec, a little longer than that adopted in Ozkan and Berberoglu's work (0.2 to 0.3 sec) which might result in a higher contact angle.

The low hydrophobicity of *C. vulgaris* increased after addition of 20 mg L^{-1} CTAB surfactant as the contact angle increased from 30.17 to 45˚. The increase was likely due to the attachment of long alkyl hydrophobic groups originating from CTAB after dissociation in water. When the CTAB concentrations increased to 30 and 40 mg L^{-1}, the contact angles increased to 49.16 and 53.87˚ respectively, indicating that the hydrophilicities of *C. vulgaris* reduced due to the additional attachments of hydrophobic alkyl groups as shown in figure 3.6. In contrast to the hydrophobicity test by the adhesion to hydrocarbons method, the contact angle method had a better capability to trace the influence of adding more CTAB on microalgae hydrophobicity while no significant increase was observed between 20 and 40 mg L^{-1} CTAB concentrations with the former method.

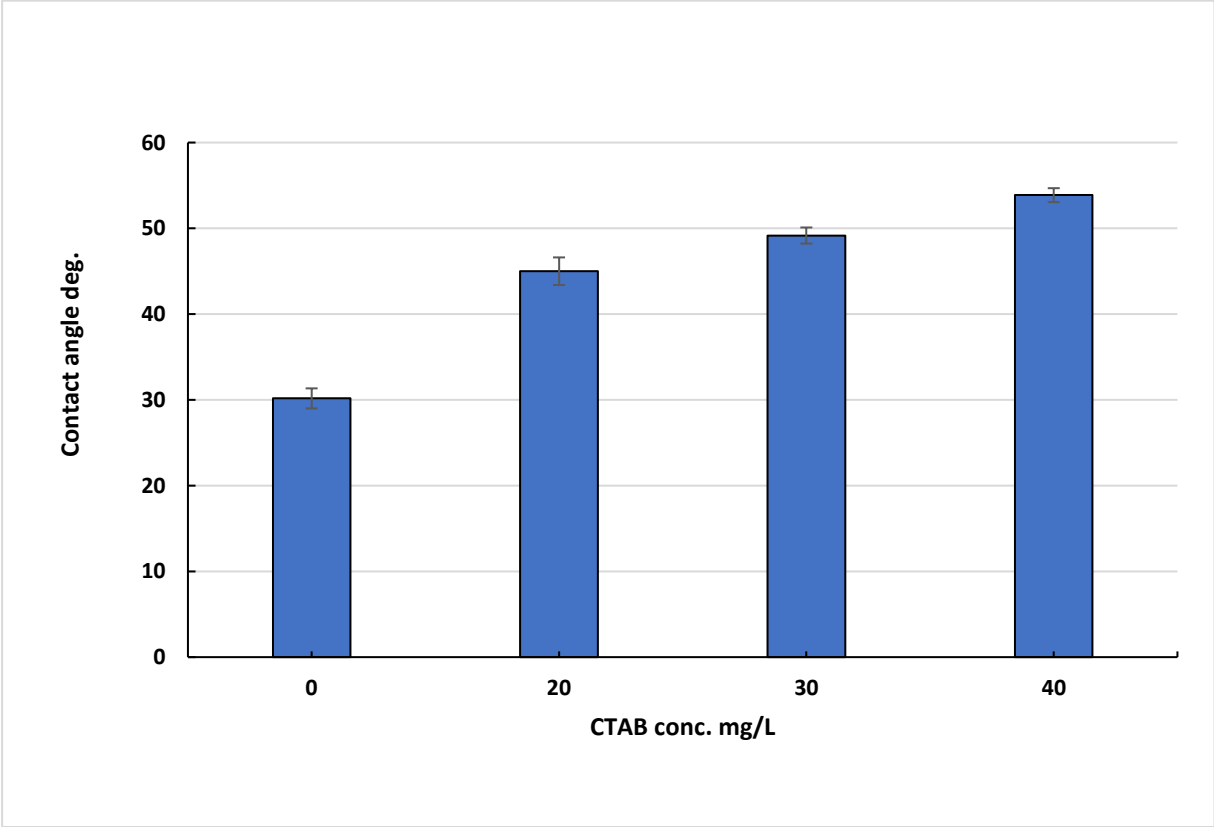

Figure 3.6: Contact angle (degree) of *Chlorella vulgaris* at different CTAB concentrations. Means ± standard error.

3.3.4 Analysis of experimental design

3.3.4.1 Fractional factorial design of experiments

Factorial design of experiments (DOE) is often used as a screening test to differentiate the most significant factors from those of lesser importance (Montgomery, 2012). From the DOE screening trials, higher recovery efficiencies were achieved using the fine porous sparger. When the coarse porous sparger was used, the concentration factor increased; however, the recovery efficiency decreased. An estimation of the bubble size in the liquid pool was made based on Kutateladze and Styrikovich's empirical formula, equation 3.7 (Wallis, 1969):

$$r_b = \left[\frac{\sigma r_o}{g(\rho_f - \rho_g)}\right]^{1/3} \cdots (3.7)$$

where r_b is the bubble radius; r_o is the sparger mean pore size (30 μm for fine porous and 154 μm for coarse porous); σ is the fluid surface tension; g is the acceleration due to gravity; and ρ_f and ρ_g are the fluid and gas densities respectively. A bubble diameter of 1.02 mm is produced using the fine porous sparger at a CTAB concentration of 40 mg L^{-1}, versus 1.76 mm with the coarse porous sparger. Smaller bubbles significantly improved the recovery efficiency ($F = 25.08$, $p=0.001$) but had no significant effect on the concentration factor. The concentration of algae in the foamate increased using the coarse porous sparger. Smaller bubbles provide a larger interfacial area for cell adsorption. They also have a longer residence time within the liquid pool, which increases contact time and adsorption resulting in a higher recovery efficiency. However, a drawback of smaller bubbles is the formation of a wetter foam due to a greater volume of interstitial liquid (of low algae concentration) trapped between the foam lamellae, combined with slower liquid drainage in the rising foam. Based on the DOE outcomes, the fine sparger was employed in all subsequent response surface experiments.

3.3.4.2 Response surface design

The design matrix and results obtained for the CCD are presented in table 3.4. The CCD data were evaluated to determine the statistical significance of each independent variable and the interactions among variables.

The linear effects of all individual factors on concentration factor were significant ($F = 216.18$, $P = < 0.001$; Table 3.5). In addition, the square effects (i.e. square terms in the model) of surfactant concentration, air flow rate, and column height were also significant. The surfactant concentration had the largest effect on the concentration factor followed sequentially by air flow rate, column height, feed flow rate, surfactant concentration^2, column height^2, liquid pool

depth, and air flow rate^2. There were significant interactions between: feed flow rate and surfactant concentration; feed flow rate and air flow rate; feed flow rate and column height; surfactant concentration and air flow rate; surfactant concentration and column height; air flow rate and column height; air flow rate and liquid pool depth; and column height and liquid pool depth (Table 3.5). Feed flow rate and surfactant concentration had the greatest effect on the concentration factor.

Experimental trial number	Variables					Experimental results	
	Feed flow rate	Surfactant conc.	Air flow rate	Column height	Liquid pool depth	Concentration factor	Recovery efficiency
1	0	2	0	0	0	11	78
2	1	1	-1	1	-1	59	23
3	0	0	0	0	0	34	49
4	0	0	0	0	0	37	51
5	0	0	0	0	-2	65	34
6	0	0	0	0	0	51	47
7	0	0	2	0	0	10	59
8	1	1	-1	-1	1	20	67
9	0	0	0	-2	0	41	60
10	0	0	0	0	0	53	37
11	-1	1	1	-1	1	29	89
12	-1	-1	-1	-1	1	63	49
13	0	0	0	0	0	35	33
14	-1	1	1	1	-1	30	63
15	1	1	1	1	1	21	44
16	-1	1	-1	-1	-1	49	56
17	-2	0	0	0	0	23	43
18	1	-1	-1	1	1	263	17
19	1	-1	1	-1	1	30	21
20	0	-2	0	0	0	156	7
21	0	0	0	2	0	102	26
22	0	0	0	0	2	27	90
23	0	0	0	0	0	49	41
24	-1	-1	-1	1	-1	121	23
25	1	-1	1	1	-1	133	13
26	-1	-1	1	1	1	40	43
27	0	0	-2	0	0	90	26
28	1	1	1	-1	-1	25	83
29	1	-1	-1	-1	-1	154	12
30	2	0	0	0	0	47	29
31	-1	-1	1	-1	-1	52	39
32	-1	1	-1	1	1	36	46
33	-1	-1	1	-1	-1	53	41
34	1	1	1	1	1	19	53
35	1	1	1	-1	-1	27	86
36	-1	-1	-1	1	-1	132	19
37	1	1	-1	-1	1	18	68
38	-1	1	-1	-1	-1	56	49
39	1	1	-1	1	-1	43	21
40	1	-1	1	1	-1	127	17
41	-1	1	-1	1	1	35	51

42	1	-1	-1	-1	-1	168	11
43	-1	1	1	1	-1	33	66
44	-1	-1	1	1	1	47	13
45	1	-1	1	-1	1	33	19
46	1	-1	-1	1	1	241	15
47	-1	1	1	-1	1	24	95
48	-1	-1	-1	-1	1	59	28

Table 3.4: Central composite design matrix and experimental results.

All individual factors had a significant linear effect on recovery efficiency (Table 3.6). In addition, the square effect of the liquid pool depth was also significant. Surfactant concentration, column height, air flow rate, feed flow rate, liquid pool depth, and liquid pool depth^2, in that order, most influenced the recovery of algal biomass. There were significant factor interactions between: surfactant concentration and air flow rate; surfactant concentration and column height; and air flow rate and liquid pool depth (Table 3.6), with the interaction between surfactant concentration and air flow rate or column height having the greatest effect on recovery efficiency.

Source of variance	Degree of freedom	Adj. Sum of squares	Adj. Mean square	F-value	P-value
Model	16	148173	9261	101	<0.001
Linear	5	99374	19875	216	<0.001
Feed flow rate	1	8169	8169	89	<0.001
Surfactant conc.	1	54908	54908	597	<0.001
Air flow rate	1	22753	22753	248	<0.001
Column height	1	10304	10304	112	<0.001
Liquid pool depth	1	3240	3240	35	<0.001
Square	3	6845	2282	25	<0.001
Surfactant conc. * Surfactant conc.	1	4416	4416	48	<0.001
Air flow rate * Air flow rate	1	407	407	4	0.044
Column height * Column height	1	2487	2487	27	<0.001
2-way interactions	8	42102	5263	57	<0.001
Feed flow rate * Surfactant conc.	1	12880	12880	140	<0.001
Feed flow rate * Air flow rate	1	2965	2965	32	<0.001
Feed flow rate * Column height	1	3655	3655	40	<0.001
Surfactant Conc. * Air flow rate	1	10440	10440	114	<0.001
Surfactant Conc. * Column height	1	6728	6728	73	<0.001
Air flow rate * Column height	1	861	861	10	0.005
Air flow rate * Liquid pool depth	1	1128	1128	12	0.001
Column height * Liquid pool depth	1	3445	3445	38	<0.001
Error	31	2850	92		
Lack-of-Fit	26	2469	95	1	0.442
Pure Error	5	381	76		
Total	47	151023			

Table 3.5: ANOVA results for the central composite model for the concentration factor.

The plots of the linear, square and interaction effects of the factors for concentration factor and recovery efficiency are shown in figures 3.7 and 3.8 respectively. Lower feed rates resulted in

lower concentration factors and higher recovery efficiencies (Figures 3.7A and 3.8A). This is due to the longer retention time of algae cells in the effervescent liquid which provides more contact time between bubbles and algae. As the feed flow rate increased, the concentration factor increased and the recovery efficiency decreased. According to the adsorption isotherm models for surface active materials such as the Langmuir isotherm model, it is clear that the surface excess, i.e. surface concentration, increases when the surfactant concentration in the bulk liquid increases (Eastoe and Dalton, 2000). Similarly, when the feed flow rate increases, the concentration of algae and free surfactant increases in the liquid pool at the base of the foam column, i.e. the concentration is slowly depleted and the surface concentration is correspondingly high. However, both microalgae and un-adsorbed surfactant concentrations in the liquid pool increase when the feed flow rate is increased. Consequently, the latter influences process responses similar to that of surfactant concentration in the feed stream and leads to a decrease in the influence of feed flow rate.

Source of variance	Degree of freedom	Adj. Sum of squares	Adj. Mean square	F-value	P-value
Model	9	23791	2643	40	<0.001
Linear	5	20757	4151	63	<0.001
Feed flow rate	1	1320	1320	20	<0.001
Surfactant concentration	1	13032	13032	199	<0.001
Air flow rate	1	2190	2190	33	<0.001
Column height	1	3133	3133	48	<0.001
Liquid pool depth	1	1082	1082	17	<0.001
Square	1	521	521	8	0.008
Liquid pool depth* Liquid pool depth	1	521	521	8	0.008
2-way interactions	3	2502	834	13	<0.001
Surfactant Conc.*Air flow rate	1	861	861	13	0.001
Surfactant Conc.*Column height	1	861	861	13	0.001
Air flow rate* Liquid pool depth	1	780	780	12	0.001
Error	38	2491	66		
Lack-of-Fit	33	2235	68	1	0.412
Pure Error	5	256	51		
Total	47	26282			

Table 3.6: ANOVA results for central composite model for the recovery efficiency.

Increasing CTAB concentration reduces the concentration factor, whereas it increases the recovery efficiency (Figures 3.7A and 3.8A). Thus, lower concentration factors and higher recovery efficiencies were obtained at higher CTAB concentrations. The surface tension of the effervescent liquid reduces when the concentration of surface-active materials increases. This causes a reduction in bubble size leading to a wetter foam (T. Coward *et al.*, 2013; P. Stevenson and Li, 2014; T. Coward *et al.*, 2015). Therefore, a wetter foam results in a lower concentration factor and a higher recovery efficiency.

Air flow rate negatively affected the concentration factor but improved the recovery efficiency. Thus, at higher air flow rates lower concentration factors and higher recovery efficiencies were observed. The amount of bubble surface available in a flotation column is crucial in collecting microalgae cells. The effect of air flow rate can be investigated by calculating the bubble surface area flux (S_b) rather than gas hold-up. Bubble surface area flux can be evaluated from the bubble flow rate (n_b), the mean or Sauter mean bubble diameter (d_b), and the column cross sectional area (A_c) as shown in equation 3.8 (Bouchard *et al.*, 2009), where J_g is the superficial gas velocity.

$$S_b = \frac{n_b \pi d_b^2}{A_c} = \frac{6.J_g}{d_b} \quad \ldots (3.8)$$

Increasing the air flow rate will increase the bubble surface area flux resulting in higher recovery efficiencies. Furthermore, Stevenson and Li (Paul Stevenson and Li, 2012b) stated that in a porous medium the generated bubble size decreases with increasing gas flow rate. At lower gas rates, only bigger pores are active and generating mainly big bubbles. When the gas flow rate increases, most of the inactive small pores become active, leading to an increased number of smaller bubbles (L.K. Wang *et al.*, 2010b), and thus a wetter foam. Saleh et al. (2006) stated that, in a foam fractionation column, increasing the volume of a wet foam with the gas flow rate was due to the short residence time for the rising foam to drain the liquid, resulting in a decrease in enrichment and an increase in recovery efficiency (Saleh *et al.*, 2006). It seems possible that such a reason contributed to some extent to decreasing the concentration factor and increasing the recovery efficiency of the harvested algae.

The effect of column height was comparable to that of the feed flow rate. An increasing column height positively influenced the concentration factor but at the expense of the recovery efficiency (Figures 3.7A and 3.8A). The fraction of interstitial liquid trapped between the foam lamellae was negatively related to the column height. This is due to the change in bubble size distribution in the zone beyond that where capillary forces become dominant (de Vries, 1972; Paul Stevenson and Li, 2012b). Also, the foam carrying microalgae dries as it rises up the column, consequently, microalgae cells stick on the column wall at the top resulting in a reduction in the recovery efficiency. This was observed clearly through the harvesting trials especially when low CTAB concentration and air flow rate were used.

An increasing liquid pool depth had a negative effect on the concentration factor but increased the recovery efficiency. This was due to the longer retention time of algae cells and hence a

longer contact time. A deeper liquid pool also increases the gas residence time at the same bubble rise velocity i.e. more time for bubbles to adsorb cells.

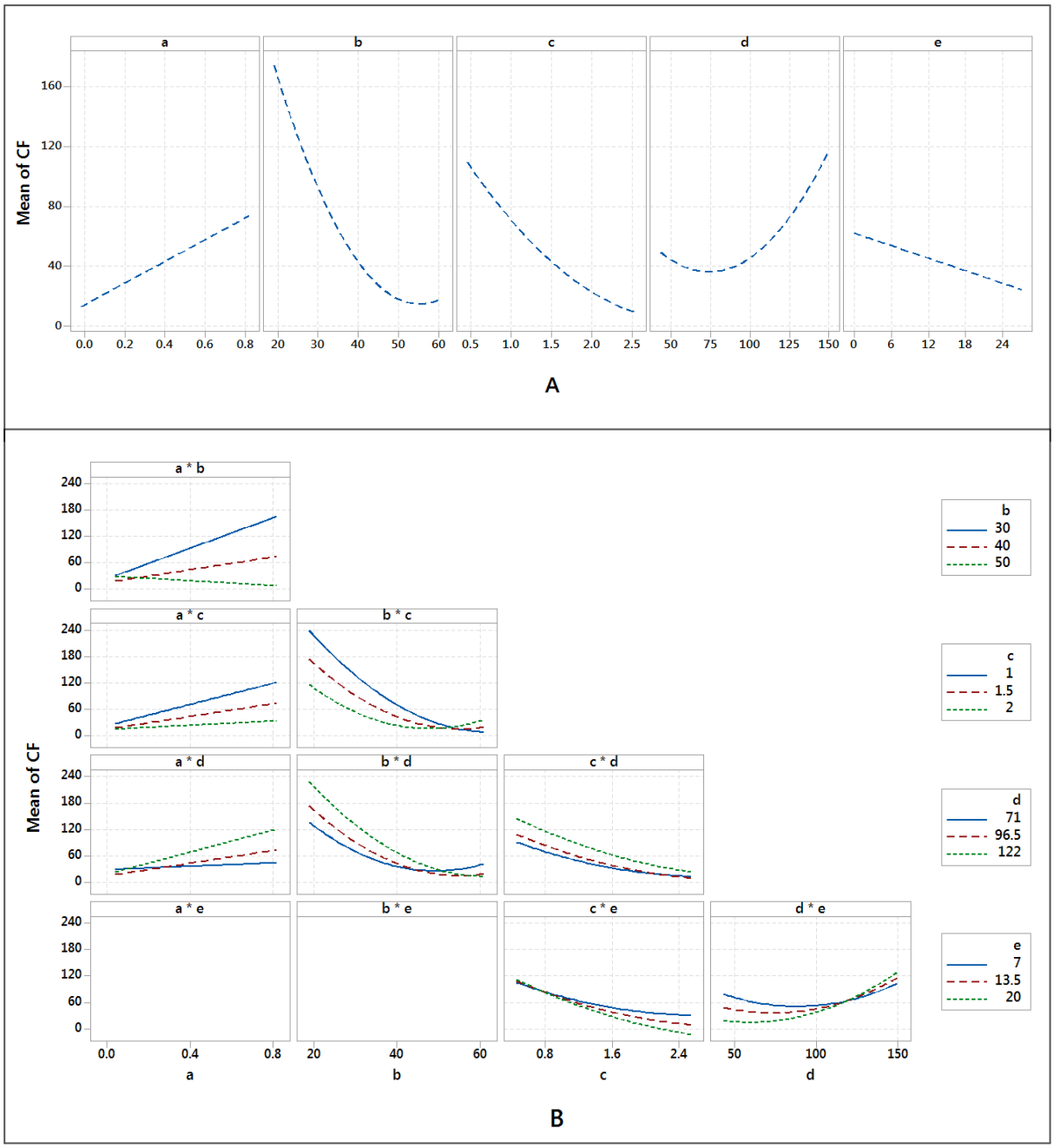

Figure 3.7: The main effects (A) and interaction plots (B) for the mean of concentration factor (CF) ($\alpha = 0.05$). Where (a) is the feed flow rate, (b) is the surfactant concentration, (c) is the air flow rate, (d) is the column height, and (e) is the liquid pool depth.

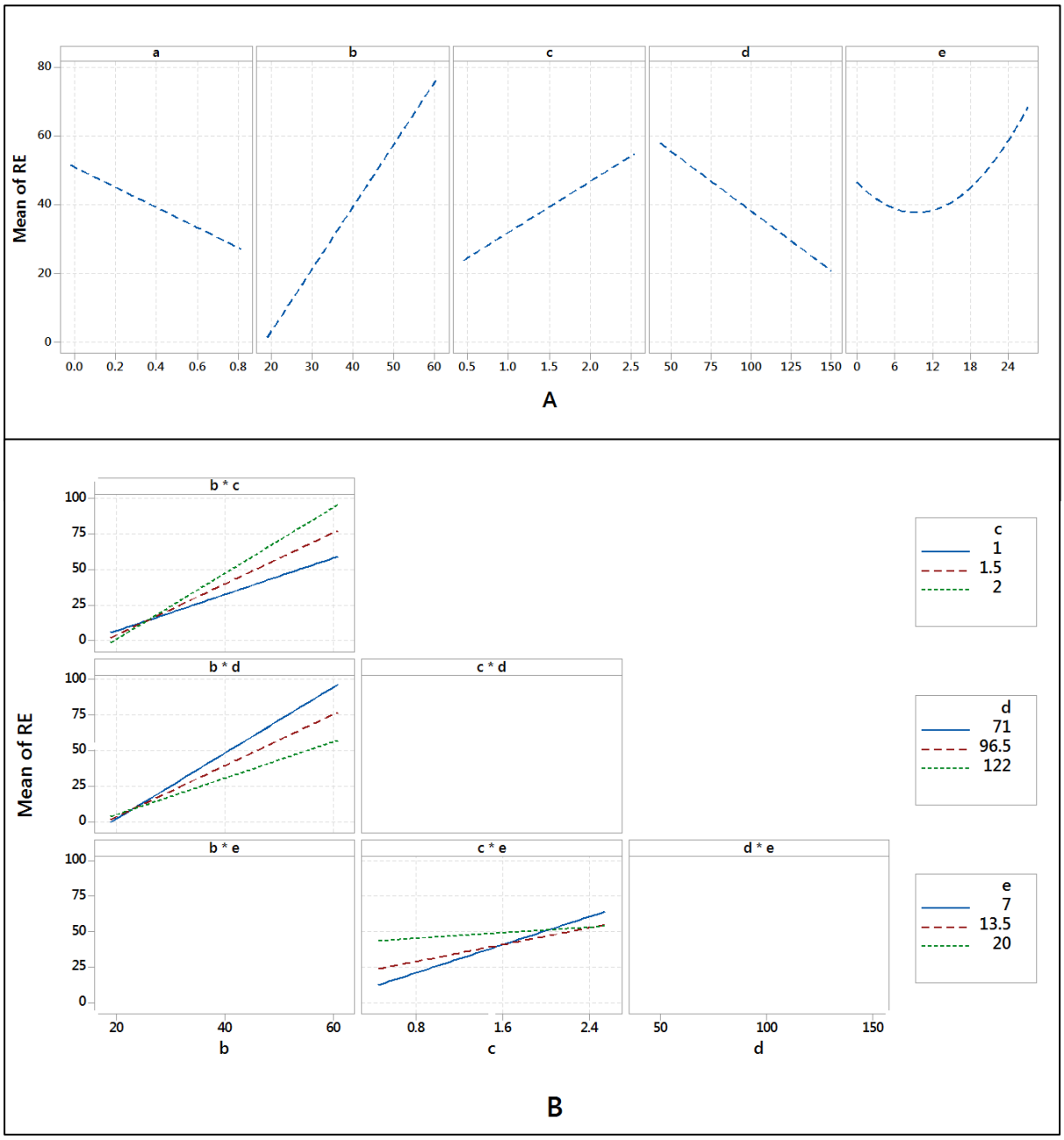

Figure 3.8: The main effects (A) and interaction plots (B) for the mean of the recovery efficiency (RE) (α = 0.05). Where (a) is the feed flow rate, (b) is the surfactant concentration, (c) is the air flow rate, (d) is the column height, and (e) is the liquid pool depth.

The contour plot for significant interactions affecting the concentration factor is shown in figure 3.9 in which any two factors change within the design range while the other three factors are kept constant at their centre values. This reinforces the importance of the interaction between surfactant concentration and the feed flow rate. Concentration factors in the range of 250 to 300 can be achieved by combining a high feed flow rate with a low surfactant concentration. Similarly, higher concentration factors were gained due to the interaction between the surfactant concentration with air flow rate and surfactant concentration with column height (Figures 3.9D

and E). Concentration factors between 150 and 200 can be achieved by combining a high feed flow rate with a low air flow rate and/or high column height (Figures 3.9B and C). Thus, increasing feed flow rate can counteract the negative effects of the high surfactant concentration and air flow rate on the concentration factor response.

The quadratic model (equation 3.9) for concentration factor was significant (p = >0.05; Table 3.5). The lack-of-fit compares the residual error to the pure error that was obtained from the six replicate runs at the centre points. In addition, high R^2 and R^2_{adj} values were achieved for the fitted model, 98.11 and 97.14% respectively, this is to say the model can explain more than 98% of the total variability in the data.

$$CF = 442.1 + 387.3F - 9.83S - 142.4A - 1.07H - 7.83D + 0.13S^2 + 17.55A^2 + 0.02H^2 + 0.08D^2 - 10.03FS - 96.2FA + 2.1FH + 2.45FD + 3.61SA - 0.06SH - 0.41AH - 1.83AD + 0.06HD \quad \cdots (3.9)$$

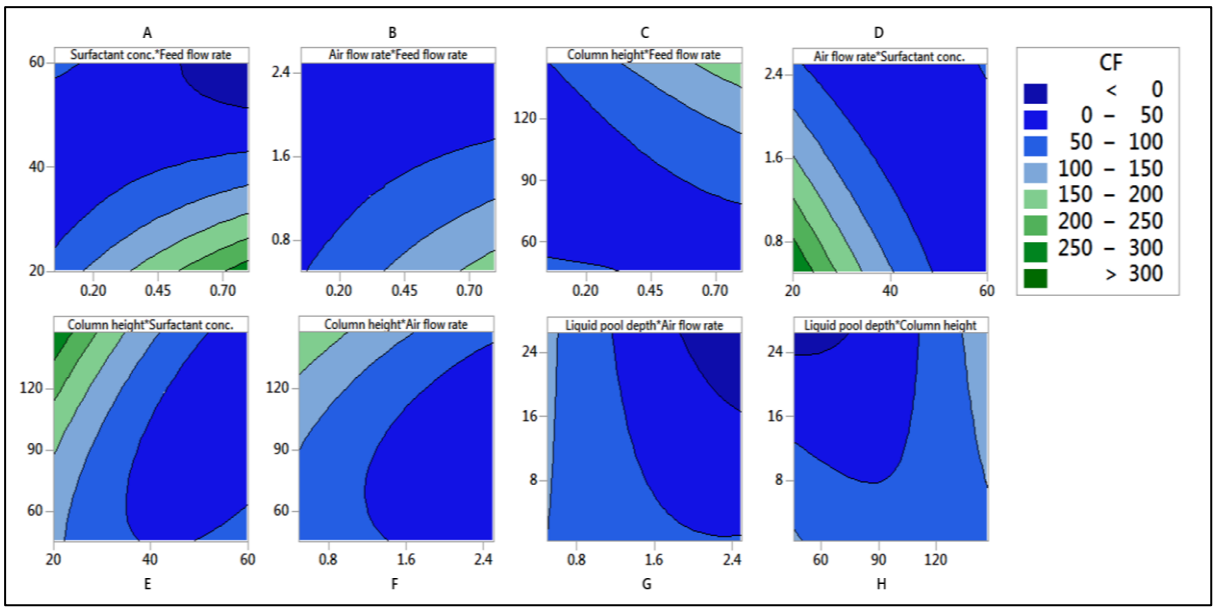

Figure 3.9: Contour plots for the significantly interacting factors in the quadratic model for concentration factor (CF). Hold values: feed flow rate = 0.4 L min^{-1}, surfactant concentration = 40 mg L^{-1}, air flow rate = 1.5 L min^{-1}, column height = 96 cm, liquid pool depth = 13.5 cm.

Where: F is the feed flow rate; S is the surfactant concentration; A is the air flow rate; H is the column height; and D is the effervescent liquid depth.

The recovery efficiency interaction plots (Figures 3.8B and 3.10B) revealed that recovery efficiencies of over 90% can be achieved by combining high surfactant concentration and high air flow rate, due to smaller bubbles produced when the inlet surfactant concentration increases

resulting in a high specific surface area and a longer time for adsorption. On the other hand, increasing column height counteracts the positive effect of the high surfactant concentration (Figures 3.8B and 3.10A) due to the increased residence time and corresponding interstitial liquid drainage opportunities that a taller column provides.

The regression model (equation 3.10) was significant (p = 0.412), explaining up to 90% of the total variability in the data.

$$RE = -50 - 29.07F + 2.21S - 6.2A + 0.47H + 044D + 0.098D^2 + 1.04SA - 0.02SH - 1.52AD \quad \cdots (3.10)$$

Where: F is the feed flow rate; S is the surfactant concentration; A is the air flow rate; H is the column height; and D is the effervescent liquid depth.

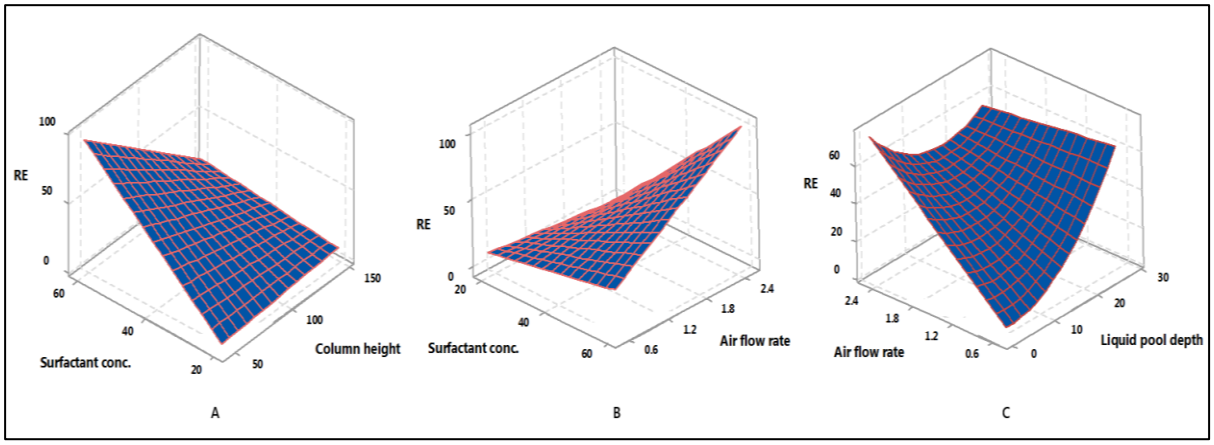

Figure 3.10: Surface plots for the significantly interacting factors in the quadratic model for recovery efficiency (RE). Hold values: feed flow rate = 0.4 L min^{-1}, surfactant concentration = 40 mg L^{-1}, air flow rate = 1.0 L min^{-1}, column height = 110 cm, liquid pool depth = 13.5 cm.

3.3.5 Harvesting of freshwater and marine microalgae based on the optimised flotation factors

The outcomes from the CCD design demonstrated that CTAB concentration, air flow rate, and column height had the strongest effects on biomass recovery. However, using a high CTAB concentration and a high air flow rate does not favor high concentration factor. Instead, prolonging the contact time for adsorption by increasing liquid pool depth and reducing feed flow rate with a moderate CTAB concentration and air flow rate is more desirable to achieve a good combination between recovery and enrichment of microalgae biomass. The factors from the CCD design were optimised by the response optimiser to achieve this objective. The values of factors under the optimised design were CTAB = 35 mg L^{-1}, air flow rate = 1 L min^{-1}, feed flow rate = 0.1 L min^{-1}, column height = 146 cm, and liquid pool depth = 25 cm. *C. vulgaris*, *I.*

galbana, and *T. suecica* were then harvested continuously based on the above values. Results for recovery efficiency and the concentration factor are shown in figure 3.11.

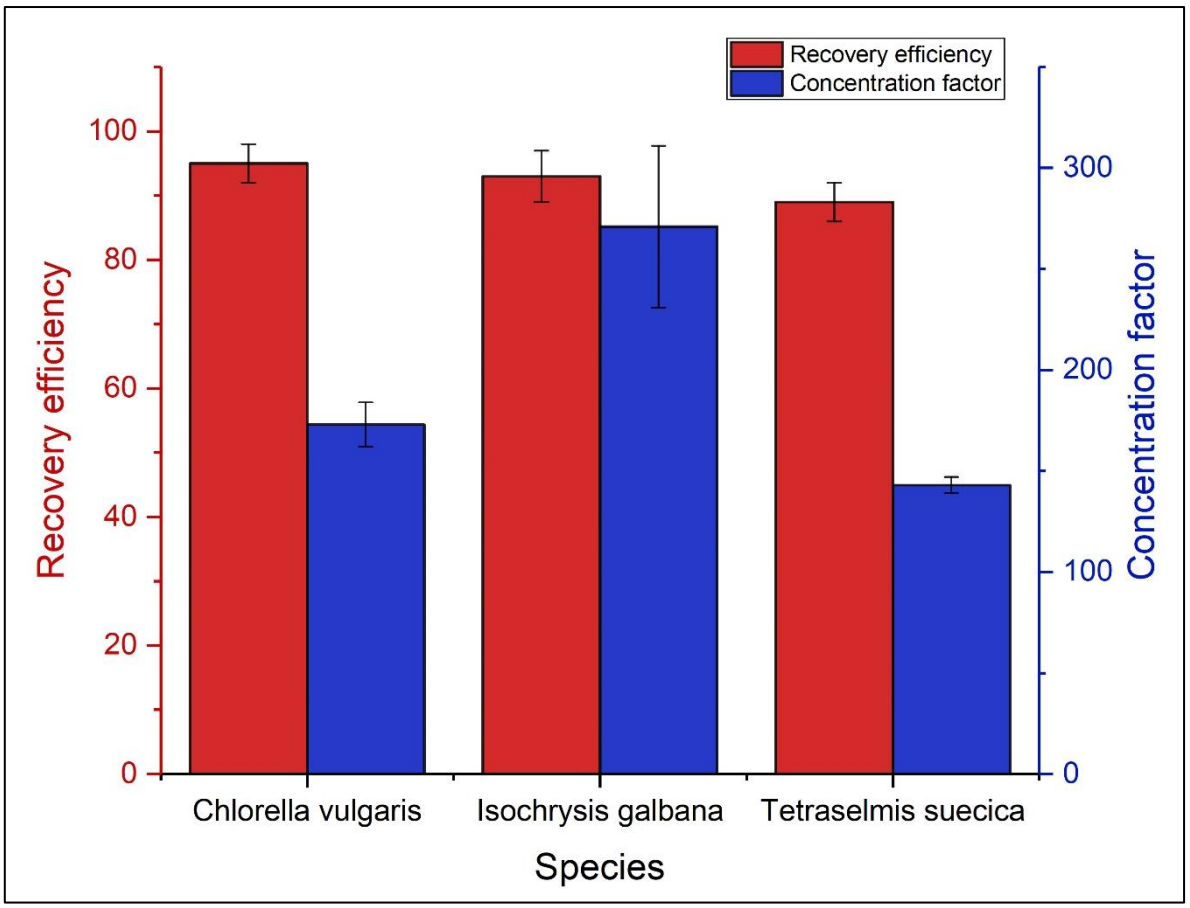

Figure 3.11: The recovery efficiency and the concentration factor plots for *Chlorella vulgaris*, *Isochrysis galbana,* and *Tetraselmis suecica* based on the optimised design. Means ± standard error.

The results showed an excellent recovery efficiency of 95% and a final biomass 173-times more concentrated than the initial *C. vulgaris* culture. For marine microalgae, recovery efficiencies of 93% and 89% at 271 and 143 enrichment factors were obtained for *I. galbana* and *T. suecica* respectively. Even though the concentration factors for all harvested species were not similar, attaining similar recovery efficiencies for both freshwater and marine microalgae increases the potential of foam flotation becoming a media independent harvester as opposed to coagulation and flocculation processes where high amounts of coagulants and flocculants are required for harvesting marine microalgae due to the ionic strength of seawater. More stable foam was also noticed through the harvesting trials of the marine microalgae which is probably due to the ions in the seawater.

Very similar recovery efficiencies of *C. vulgaris* were observed in both the current work and that conducted by Kurniawati et al. (2014) (Kurniawati *et al.*, 2014). They were able to achieve a separation efficiency of 93% using a foam flotation column operated in batch mode with natural saponin surfactant and chitosan flocculants together. Whilst their work has the advantage of using natural biochemicals to harvest microalgae, the need for additional chemical treatment increases the harvesting cost. In comparison to the batch flotation harvesting trials of *C. vulgaris* conducted by Liu et al. (1999), a lower recovery efficiency was gained in their work (90%) which was probably due to the lower air flow rate (0.114 L min^{-1}) even though higher CTAB concentration (40 mg L^{-1}) was used (J. C. Liu *et al.*, 1999). The flotation recovery efficiencies obtained in this work for *Chlorella* and *Tetraselmis* species were close to those obtained previously by Garg et al. (2013) even though the differences between both experimental trials include surfactant types and dosage, the flotation apparatus type, and the operating mode (Garg *et al.*, 2013). They used mechanical flotation cells with the addition of two surfactant types (tetradecyl trimethylammonium bromide, C_{14}TAB and dodecylammonium hydrochloride, DAH). However, the enrichments gained herein for both species were many-folds higher than those obtained by the Garg group. This was probably due to the significant interplay between the process factors, as well as the effect of column height as the foam carrying microalgae dries as it rises up the column. This presents another advantage to column flotation besides the simplicity of construction and low energy consumption. In comparison to other flotation harvesting trials, the percentage recovery obtained in this work for *C. vulgaris* (95%) was similar to that obtained by Henderson et al. (94.8%) (R. K. Henderson *et al.*, 2010). However, they used dissolved air flotation (DAF) in a batch mode (10 min) with aluminium sulphate as a coagulant to harvest a culture of *C. vulgaris* of cell density of $5 \times 10^5 \pm 5 \times 10^4$ cells ml^{-1}. Prior to their work above, Henderson et al. (2008) conducted harvesting trials also using DAF working in a batch mode but with different types of cationic and anionic surfactants instead of coagulants (Rita K. Henderson *et al.*, 2008). The maximum removal efficiency of *C. vulgaris* obtained in their work (54%) was substantially lower than that obtained by the current work. This reduction in the percentage recovery was probably due to the addition of surfactants to the saturator rather than the microalgae culture which has advantages of reducing the bubble size and altering the bubble charge but it did not enhance the hydrophobicity of microalgae or compensate the absence of coagulant role on increasing the cell size due to the aggregation. With the exception of Garg et al.'s work, neither the concentration factors nor the harvesting economics were reported in the other works since their trials were performed for wastewater treatment rather than producing biomass for biofuel production.

On the other side, CTAB, can disrupt the algae cell wall and promote cell lysis. Coward et al. (2014) observed that the presence of CTAB in the harvested microalgae enhanced lipid recovery and profile as well as increased the solubility of some phospholipids in the cell membrane (T. Coward *et al.*, 2014). The disruption of the algal cell wall and the enhancement in lipid recovery and profile due to the CTAB surfactant attached to the harvested microalgae offer additional advantages to the flotation technique to drive down the cost of processing and produce biomass which is more advantageous for liquid hydrocarbon biofuels.

3.3.7 Power consumption and harvesting economics

Selecting the optimal harvesting technique relies on the relationship between the efficiency of algal biomass recovery and the operational energy requirements. The inconsistency between harvesting efficiency and energy consumption is the major drawback in most harvesting techniques. The power consumption associated with bubble generation was calculated based on the pressure of the compressed air through the sparger plus other operating conditions. The compressor work W_{comp} (J mol^{-1}) was calculated according to equation 3.6 after measuring the compressed gas pressure (P_1) using the pressure gauge as shown in Table 3.7. Other work values were determined after converting joule to kilowatt-hour and calculating the number of moles to volume ratio of the gas using the ideal gas law (equation 3.11) at the conditions (T_o, P_1) in table 3.7. Only one calculated value was reported herein even though all compressor works were calculated for both sparger types, liquid pool depths, and air flow rates.

$$\frac{n}{v} = \frac{p}{RT} \quad \ldots (3.11)$$

The power consumptions of most harvesting techniques in the literature were reported in the units of kWh m^{-3} of algae culture. This can be determined if the calculated work value (kWh m^{-3} of gas) is multiplied by the ratio of the volumetric flow rate of the gas inlet to the volumetric flow rate of the medium inlet (feed) in the flotation process. The model values of air flow rate and feed flow rate used to harvest the three species of microalgae were of 1 L min^{-1} and 0.1 L min^{-1} (0.001 and 0.0001 m^3 min^{-1}) respectively; therefore, the ratio of the volumetric flow rate of gas to the volumetric flow rate of microalgae feed was 10.

The calculations of the total cost of the foam flotation column including compressor work and chemicals to harvest 1 m^3 of microalgae culture were also performed as shown in table 3.7. The continuous foam flotation (this work) had a low total harvesting cost of US$ 0.179 in comparison to that calculated by Coward et al. (US$ 0.915) to harvest the same volume of microalgae by dissolved air flotation using ferric chloride flocculants (T. Coward *et al.*, 2015).

Condition	R J/mole.K	T_o K	η_{is}	γ (air)	P_1 Kpa	P_0 Kpa	W_{comp} J/mole of gas	W_{comp} kWh/mole of gas	W_{comp} kWh/m^3 of gas
Fine porous sparger, 1 L min^{-1}, air flow rate, and 25 cm liquid pool depth	8.314	293.15	0.7	1.4	113.4	101.3	399.27	1.11*10^{-4}	5.16*10^{-3}

Condition	W_{comp} kWh/m^3 of algae	Energy cost US$ per kWh	Chemical cost US$ kg^{-1}	Chemical additive g m^{-3}	Chemical cost US$ m^{-3}	Total cost US$ (to harvest 1 m^3 of microalgae)
Fine porous sparger, 1 L min^{-1}, air flow rate, and 25 cm liquid pool depth	0.052[a]	0.004[b]	5[c]	35	0.175	0.179

[a] The value was calculated based on the compressor work kWh per m^3 of gas and the ratio of the inlet gas flow rate and feed flow rate in foam flotation process

[b] Energy cost was calculated from the data prepared by U.S. Deparment of Energy based on average price of electricty to the US industrial sector as of November 2017-US$ 0.0679 per kWh (Hankey, 2018)

[C] Based on a bulk price of US$ (1-5) per kg with a min. order of 1 metric ton (www.alibaba.com)

Table 3.7: The compressor work W_{comp} and the predicated cost of harvesting 1 m^{-3} of algae culture.

Water loss due to evaporation was determined in the current work by calculating the humidity of saturated air and the humidity of air. The humidity of the saturated air (H_s) in kg_{water} per $kg_{dry\ air}$ and the percentage humidity ($H\%$) can be calculated by the equations 3.12 and 3.13.

$$H_s = \left(\frac{M_w}{M_A}\right)\left(\frac{P_s}{P - P_s}\right) \dots (3.12)$$

$$H\% = 100\left(\frac{H}{H_s}\right) \dots (3.13)$$

Where: M_w is the molecular weight of water (18.016 g mol^{-1}); M_A is the molecular weight of air (28.84 g mol^{-1}); P_s is the vapour pressure of the water at system temperature (Pa); P is the system pressure (Pa); and H is the humidity of air in kg_{water} per $kg_{dry\ air}$.

The vapour pressure of water at 18 ˚C is 2.0665 kPa (from steam table). Thus, using equation 3.12, the humidity of saturated air is 0.013 $kg_{water}kg_{dry\ air}^{-1}$.

Assuming 100% relative humidity, the humidity of air is 0.013 $kg_{water}kg_{dry\ air}^{-1}$. During the optimised harvesting trials, the flow rate of air and culture feed were 1000 mL min^{-1} and 100 ml min^{-1} respectively. The volume of water in the air $V_{water\ in\ air}$ is:

$$V_{water\ in\ air} = Q_{air} * \rho_{air} * H * \frac{1}{\rho_{water}}$$

$$V_{water\ in\ air} = 1000\frac{ml}{min} * 1.212 * 10^{-6}\frac{kg}{ml} * 0.013\frac{kg_{water}}{kg_{dryair}} * \frac{1}{0.001\frac{kg}{ml}}$$

$$V_{water\ in\ air} = 0.0158 \text{ ml min}^{-1}$$

Where: Q_{air} is the air flow rate (ml min^{-1}), ρ_{air} and ρ_{water} are the densities of air and water (kg ml^{-1}) respectively. Based on the calculated water fraction in air, it can be concluded that the water loss is negligible and does not affect the enrichment of the harvested microalgae.

3.4 Conclusion

In foam flotation, collectors (surfactants) are important to enhance the hydrophobicity of microalgae cells and create a metastable foam yielding high recovery efficiencies and biomass enrichment (concentration factor). The measurements of the surface characteristics of *C. vulgaris* demonstrated that this species has an electronegative and hydrophilic surface. CTAB was found to be the most appropriate surfactant due to the electrostatic interaction between it and the electronegative microalgae. Moreover, CTAB was able to reduce the net charge as well as the hydrophilicity of *C. vulgaris*, resulting in better harvesting performances. This was due to the attachment of the positive long hydrophobic alkyl groups originating from CTAB after dissociation in water. The harvesting trials demonstrated that the continuous foam flotation process operated at the optimised factors yielded recovery efficiencies of 95, 93, and 89% together with 173, 271 and 143-fold biomass enrichments for freshwater *C. vulgaris* and marine *I. galbana* and *T. suecica* respectively. However, the insignificant reduction in the recovery efficiencies of the marine species was likely due to the salinity of seawater or to some extent, the surface physicochemical properties of these species. Generally, within the flotation process there is a trade-off between attaining a high recovery efficiency and a high concentration factor (Alhattab and Brooks, 2017); however, the current continuous process has circumvented that particular compromise, representing a significant advance in foam flotation harvesting of microalgae biomass. What is more, our continuous foam flotation column demonstrated a very low power consumption, 0.052 kWh m^{-3}, with a low total harvesting cost (including the chemical cost) of US$ 0.179 per 1 m^3 of microalgae. Our findings demonstrate that foam

flotation is a very promising approach for the continuous bulk harvesting of microalgae biomass, whether it be for high-value fine chemicals or low-value biofuels. Indeed, the continuous harvesting approach may be especially relevant for the wastewater industry wherein microalgae are used as nutrient scrubbers, or in environmental management and remediation, e.g. the removal of harmful or toxic microalgae blooms from waterways, including municipal water supplies.

Chapter 4

Continuous harvesting of microalgae by foam flotation: process intensification through enhanced drainage

Abstract

Foam flotation can be utilised as an energy-efficient harvesting and enriching technique for microalgae biomass with the potential to significantly reduce the production cost of algae derived biofuel. The concentration of algae in the foamate from a foam column is determined by a combined effect of interfacial adsorption and foam drainage. In this chapter, three tubular modules with differing smooth-successive contraction and expansion ratios were compared for drainage enhancement. These modules (hereafter called foam risers) had diameter ratios of 0.25, 0.5, and 0.75, a transition section of 60˚ angle on both sides, and a 7 cm long throat section. The impact of the risers on drainage of the liquid fraction in the rising foam was measured according to the pressure profile across the column. Harvesting experiments were performed using *Chlorella vulgaris* at air flow rates of 1.0, 1.5, and 2.0 L min^{-1} and at four concentrations (20, 30, 40, and 50 mg L^{-1}) of the cationic surfactant, hexadecyltrimethylammonium bromide (CTAB, $CH_3(CH_2)_{13}N(CH_3)_3$-Br). Further trials were also conducted under the optimised design for the foam flotation process that delivered the best combination of microalgae recovery efficiency and concentration factor. The microalgae concentration in the foamate increased approximately 1.2 to 3 times using the risers. The highest concentration factors and recovery efficiencies were obtained under process conditions (CTAB = 35 mg L^{-1}, air flow rate = 1 L min^{-1}, feed flow rate = 0.1 L min^{-1}, column height = 146 cm, liquid pool depth = 25 cm, fine porosity sparger). A recovery efficiency of 91% was obtained with a concentration factor of 722, which was approximately 4.2 times greater than that obtained without a riser. The continuous foam flotation column fitted with a foam riser of 0.25 diameter ratio demonstrated a very low power consumption, 0.052 kWh m^{-3} of algae culture, with a total suspended solids yield of 14.6%; this compares favourably with other dewatering techniques such as centrifugation and filtration. The presence of the smooth-successive contraction and expansion risers engenders significant intensification of the foam flotation column and thus the process.

Keywords: Foam flotation, Foam drainage, Algae biofuels, Microalgae harvesting, Process intensification

Chapter four

4.1 Introduction

Global challenges coincident with fossil fuels burning (energy security, environmental pollution, climate change) are some of the main drivers behind the ongoing search for affordable, reliable and environmentally friendly fuels (Pragya *et al.*, 2013). Within the transport industry biofuels play a central role in addressing demand for liquid fuels; however, environmental, economic and ethical problems continue to dog the expansion of biofuels (Muylaert *et al.*, 2017). Microalgae have as yet unrealised potential as a third generation biofuels feedstock (Wenchao Yang *et al.*, 2014). Mass microalgae cultures have low suspended solids content which necessitates extensive dewatering operations prior to downstream processing. The harvesting and dewatering stage can account for approximately one third of the production costs of biofuels from microalgae, and as such represents a logical target for efficiency gains through innovation.

In addition to the dilute nature of algae cultures, the small cell size (the majority of strains being less than 30 μm), combined with a negatively charged cell surface, ensure that most harvesting techniques have a high energy requirement and are consequently not cost-effective (Milledge and Heaven, 2012).

Among the many harvesting techniques that have been reported, flotation, which is an adsorptive bubble separation technique, shows genuine promise as a microalgae biomass harvesting and enrichment method (Ndikubwimana *et al.*, 2016). Foam is highly concentrated dispersions of gas (dispersed phase) in a liquid (continuous phase) (Bhakta and Ruckenstein, 1997). Foam generated by surface-active materials (surfactants) in foam flotation columns represents an effective medium to adsorb microalgae as it presents a high specific surface area, which results in a high recovery efficiency combined with the collection of only a small volume of interstitial liquid, enabling good biomass enrichment. During producing foam, different mechanisms either to form, stabilise, or destroy foam are involved including the formation of liquid films and foams, drainage, coarsening of foams, and rupture of liquid films (Jianlong Wang *et al.*, 2016a).

Although the foam flotation column can achieve a significant combination of high recovery efficiency and concentration factor, further enhancement in the concentration factor of microalgae is pivotal to markedly lower downstream dewatering and drying costs. In adsorptive bubble separation, the enrichment can be increased if the liquid quantity is minimised while maintaining the flux of bubble surfaces (Xueliang Li *et al.*, 2011a). Chapter three demonstrated that the factors of foam flotation had opposing effects on both recovery efficiency and

concentration factor (see 3.3.4 analysis of experimental design). For example, a higher surface area for adsorption of microalgae can be obtained by increasing surfactant concentration, but simultaneously the interstitial liquid volume (of low algae concentration) will concomitantly increase, thus lowering the concentration factor.

Foam drainage is the passage of liquid downward through a foam. It is a complex physicochemical hydrodynamic process governed by several factors including the hydrodynamic parameters of the foam system such as the shape and size of the Plateau borders, liquid hold-up in foam, gas–liquid interface properties, as well as the rate of foam destruction due to the bubble coalescence because of the inter-bubble gas diffusion or the rupture of liquid films between neighbouring bubbles; nevertheless, these simultaneous factors are yet to be fully understood (Kruglyakov *et al.*, 2008).

Several methods have been proposed to reduce the liquid volume within a foam column. The superficial drainage velocity in a vertical foam column (j_d) can be calculated using the empirical equation 4.1:

$$j_d = \frac{\rho_f g r_b^2}{\mu} m\varepsilon^n \ldots (4.1)$$

Where ρ_f and μ are the density and viscosity of the interstitial liquid respectively; g is gravitational acceleration; r_b is an average bubble size; m and n are adjustable parameters which are constants for a given system (they are calculated by a forced drainage method); and ε is the liquid fraction of the foam. It is clear from equation 4.1 that the only way to increase the superficial drainage velocity without changing liquid properties is by increasing the bubble size or liquid fraction (P. Stevenson and Li, 2014).

Smaller bubbles offer a larger interfacial area for cell adsorption. They also have a longer residence time within the liquid pool, which increases contact time and adsorption resulting in a higher recovery efficiency. However, a drawback of smaller bubbles is the formation of a wetter foam due to a greater volume of interstitial liquid trapped between the foam lamellae, combined with slower liquid drainage in the rising foam. Bando et al. (2000) fabricated a flotation column to recover metal ions in a manner similar to that of an air-lift reactor by inserting a draft tube into the liquid pool and sparging gas bubbles through the tube. The smaller bubbles were recirculated to the bottom through the downcomer due to the liquid convection established by the draft tube. This resulted in a foam consisting mainly of large bubbles (Bando *et al.*, 2000). However, even though they managed to gain a drier foam, a lower metal ions recovery rate was obtained. Similar results were obtained in Chapter three when a gas sparger

of a coarse porosity was used except that Bando achieved better adsorption rate when the draft tube was used. Aquayo and Lemlich (1974) succeeded in reducing the liquid fraction within a foam in a foam fractionation column at high superficial gas velocities using perforated plates with circular orifices of 2 mm diameter and a 3% perforation area (Aguayo and Lemlich, 1974). However, Aguayo and Lemlich also reported that a plate-less column running at low gas velocities performed better than the column with perforated plates. Wang et al. (2010) used a vacuum to enlarge the bubble size within the foam layer in a foam fractionation column, obtaining a higher concentration factor but at the expense of a lower recovery efficiency (Jianlong Wang *et al.*, 2010a).

Alternative approaches to enhance foam drainage by manipulating the foam flow through inclined plates have been proposed (Dickinson *et al.*, 2010; Yong Wang *et al.*, 2013b), as well as spiral internal structures (Q. W. Yang *et al.*, 2011b), and via sudden contraction and expansion using a foam riser (Xueliang Li *et al.*, 2011a). Wang et al. (2013) trialled an inclined foam channel to enhance foam drainage for protein recovery from wastewater. Under the best conditions, they achieved an enrichment of 10.2, which was 1.93 times that gained using a conventional vertical column (Yong Wang *et al.*, 2013b). Using internal spirals in the foam fractionation column increased the enrichment of sodium dodecyl sulphate to 15.7, which was 2.5 times that obtained with a conventional column (Q. W. Yang *et al.*, 2011b). However, both the inclined and spiral approaches suffered from reduced recovery efficiencies.

In this Chapter, the drainage enhancement of foam carrying microalgae is investigated in a continuous foam column using sections with smooth-successive contraction and expansion. We offer a simple design foam riser that can easily be fitted into a foam column unlike other more complex drainage improvement methods such as spiral internal or inclined channels. To the best of our knowledge, this is the first study to attempt to intensify the foam flotation harvesting of microalgae biomass for biofuel production.

4.2 Materials and methods

4.2.1 Microalgae culture

Non-axenic *Chlorella vulgaris* was grown in three 10 L Nalgene polycarbonate carboys using BG11 medium at 20 ± 2 ˚C with a 16L:8D photoperiod using a mix of cold and warm fluorescent lights with an average illuminance of 2,500 lux. The cultures were agitated by aeration using an aquarium air pump (Koi Air, KA50, 0.032 mPa), and maintained semi-continuously.

4.2.2 Foam column dimensions

A bench scale poly(methyl methacrylate) flotation column was used (Figure 4.1), of 51.5 mm internal diameter and a column height that could be adjusted between 30-160 cm by attaching additional tubular modules of 25, 30 or 50 cm lengths. The inlet mixture consisted of algae culture with added surfactant (CTAB: hexadecyltrimethylammonium bromide (CTAB, $CH_3(CH_2)_{13}N(CH_3)_3$-Br)) from a 25 L reservoir. The processed culture was discharged to waste from the outlet stream valve at the base of the column, 1 cm above the sparging media. The microalgae culture and surfactant were mixed in the feed tank for 10 mins using a magnetic stirrer before and during the harvesting experiments. The feed flow rate was measured and controlled by a valve with an ultrasonic flowmeter (Atrato, Titan, UK). Another valve was placed on the discharge stream to control the liquid depth in the column. The foam was collected at the top of the column using an annular trough of 30 cm in diameter and 15 cm deep. Air bubbles (dispersed phase) were generated by introducing compressed air through a sparger. The sparger was made from ultra-high molecular weight polyethylene with a thickness of 6.0 mm, a diameter of 51.5 mm, and a mean pore size of 30 μm. The air flow rate for each trial was adjusted before the inlet mixture was fed to the column to prevent liquid weeping into the gas line.

4.2.3 Drainage enhancer module

The column described in figure 4.1 is a conventional foam flotation column. In this work, three foam risers of different smooth-successive contraction and expansion ratios were developed with a structure similar to a Venturi tube (Figure 4.2). These modules had 0.25, 0.5, and 0.75 diameter ratios, a transition section of 60˚ angle on both sides, and a 7 cm long throat section. The risers were drawn in Google SketchUp 2015 and printed using a 3D printer (Stratasys, model uPrint SE Plus, USA). Each riser was individually inserted between two column tubular modules during harvesting trials.

A smooth-successive rather than a sudden-successive contraction and expansion riser design was chosen as in preliminary trials we failed to obtain a sufficiently high algae recovery efficiency with the latter design whereupon the microalgae in the rising foam adhered to the clearance around the riser orifice. The position of the foam riser within the column was not studied as this was beyond the scope of this work plus the foam is wetter in the zone adjacent to the bubbly liquid-foam layer whereas it is drier at the top of the column. Therefore, as a compromise the riser was fitted to the middle of the column, 60 cm above the sparger.

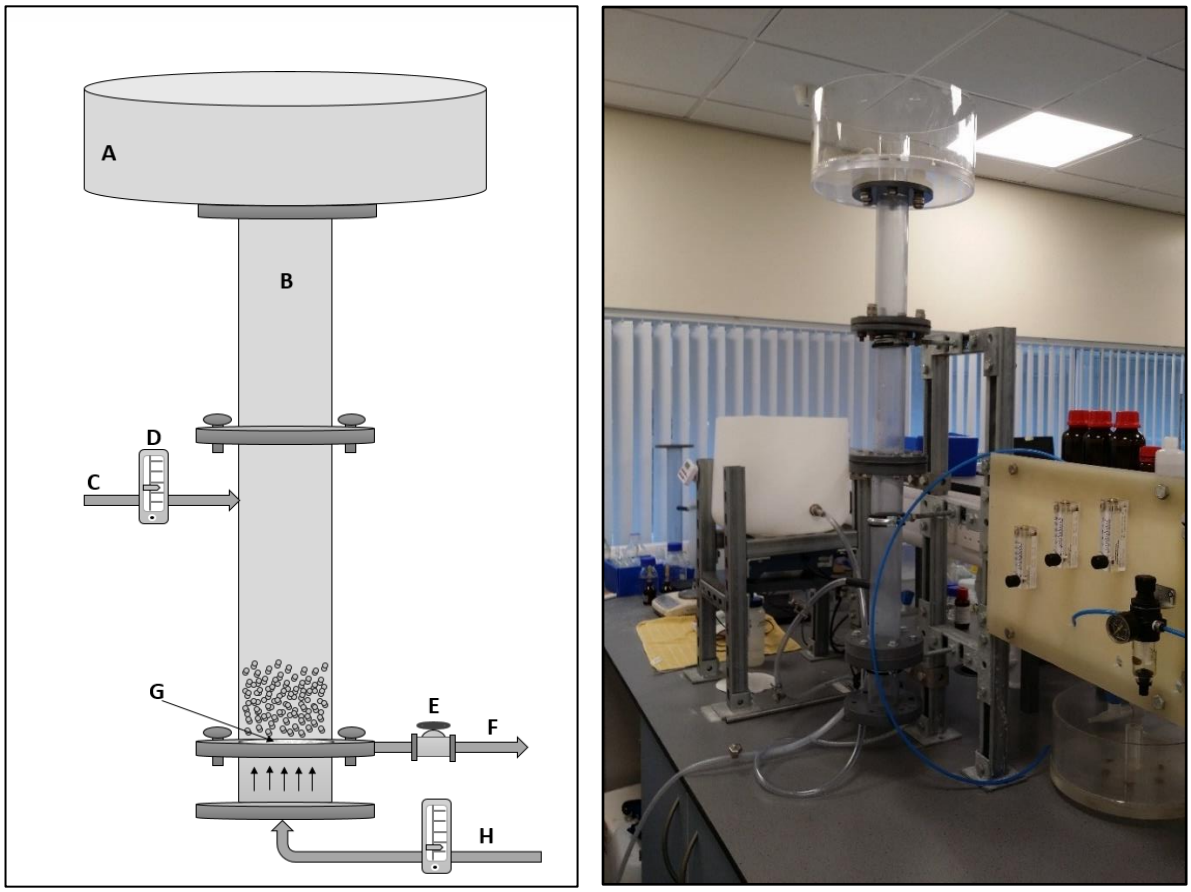

Figure 4.1: Schematic and photo of the continuous foam flotation column. A: Foam-collecting cup, B: column tubular module (25, 30 or 50 cm) in height and 5.1 cm in diameter, C: inlet stream, D: inlet flow meter, E: outlet stream valve, F: underflow stream, G: air sparger, H: air input stream.

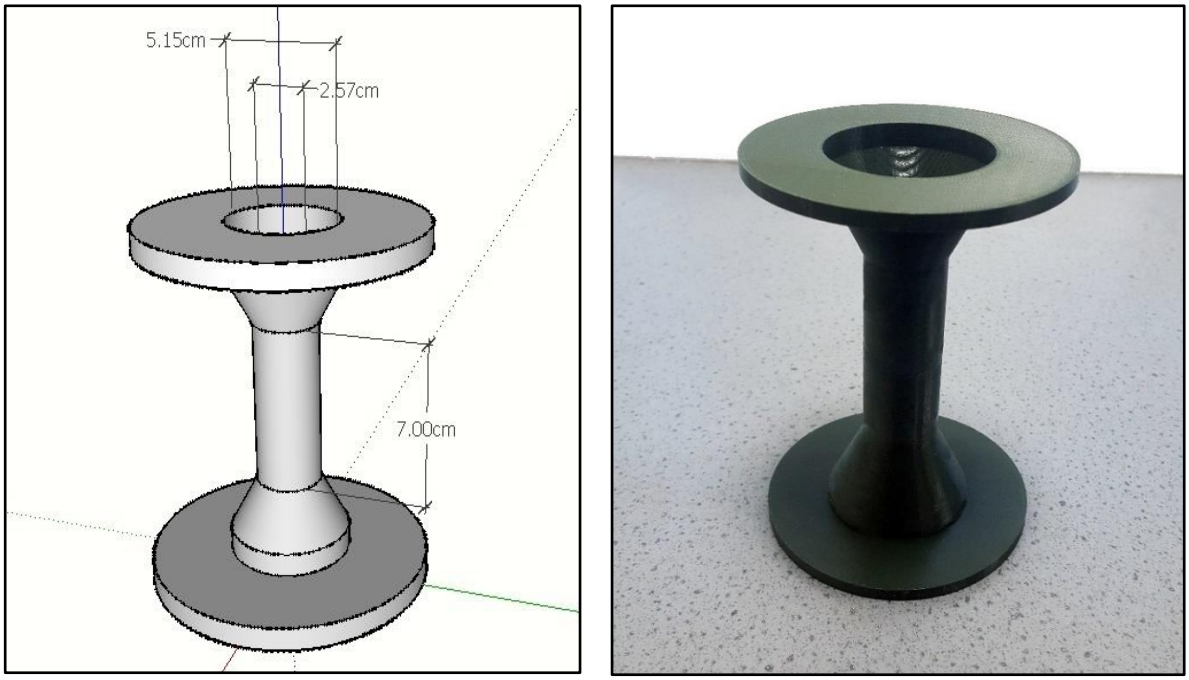

Figure 4.2: A foam riser with smooth-successive contraction and expansion diameter ratio of 0.5 and photo of the continuous foam flotation column with the foam riser.

4.2.4 Harvesting experiments

The *C. vulgaris* harvesting trials were conducted at air flow rates of 1.0, 1.5, and 2.0 L min^{-1} and different CTAB concentrations (20, 30, 40, and 50 mg L^{-1}). These variables were chosen as we had previously shown that they had the greatest effects on both microalgae recovery and enrichment (see 3.3.4 analysis of experimental design). Other foam flotation variables were standardised during harvesting trials as following: column height = 122 cm, liquid pool depth = 20 cm, and inlet feed flow rate = 0.2 L min^{-1}. The algae concentration in the inlet stream was 0.46 ± 0.13 mg mL^{-1} (equivalent to $9.58 \times 10^6 \pm 1.1 \times 10^6$ cells mL^{-1}). In Chapter three, CTAB produced the greatest enhancement in microalgae hydrophobicity, thus it was used again here. Each harvest experiment had two replicate runs. The effectiveness of the harvesting trials was determined by the concentration factor (CF) and the recovery efficiency (RE) as given in equations 4.2 and 4.3.

$$CF = \frac{Concentration\ of\ algae\ in\ final\ product}{Concentration\ of\ algae\ in\ inlet\ stream} = \frac{\left(\frac{cell}{ml}\right)_{fomate}}{\left(\frac{cells}{ml}\right)_{inlet}} \quad \cdots (4.2)$$

$$RE = \frac{cells\ of\ algae\ in\ final\ product\ (fomate)}{cells\ of\ algae\ in\ inlet\ stream} 100\% \cdots (4.3)$$

A calibration curve was constructed correlating cell density and their corresponding absorbance at 750 nm using a spectrophotometer (Jenway, Model 7315, Bibby scientific Ltd, UK), yielding an R^2 of 100% (data not shown). Cell density was measured using an improved Neubauer hemocytometer, with a Leica DM 500 light microscope.

4.2.5 Harvesting of microalgae based on optimised flotation factors

Before being able to compare the effectiveness of our harvesting technique with those that have been reported previously (see Table 4.1 and references therein), extra harvesting trials with the foam riser were conducted under flotation factors optimised for a higher biomass recovery and concentration factor (CTAB = 35 mg L^{-1}, air flow rate = 1 L min^{-1}, feed flow rate = 0.1 L min^{-1}, column height = 146 cm, and liquid pool depth = 25 cm). Total suspended solids (TSS) were also measured for comparison with other methods. The harvested algae were placed in an aluminium dish and dried between 103 to 105 ºC for 24 hours. TSS was calculated using equation 4.4 (Patrick E. Wiley *et al.*, 2009):

$$TSS = \frac{Wt_3 - Wt_1}{Wt_2 - Wt_1} 100\% \cdots (4.4)$$

Where: Wt_1 is the aluminium dish weight (g); Wt_2 is the wet sample and dish weight (g); and Wt_3 is the dry sample and dish weight (g).

4.2.6 Liquid holdup profile in the foam

In addition to the investigation of the foam riser impact on drainage of the liquid fraction in the pneumatic foam, liquid profile is of paramount importance to understand the liquid transport in the foam column (Jianlong Wang *et al.*, 2016a). The pressure gradient in a vertical circular section foam column is due to the weight of the fluid in the column and the wall shear stress as described by equation 4.5 (P. Stevenson and Li, 2014):

$$\frac{dp}{dy} = \rho_L g \varepsilon_L + \rho_g g (1 - \varepsilon_L) - \frac{4\tau_w}{D} \approx \rho_L g \varepsilon_L \ \ldots (4.5)$$

Where: p is the pressure ($N.m^{-2}$); y is the positive upward length (m); ρ_L, ρ_g are liquid and gas densities respectively ($kg.m^{-3}$); g is the acceleration due to gravity ($m.s^{-2}$); ε_L is the liquid

fraction in the foam; τ_w is the wall shear stress (N.m^{-2}); and, D is the diameter of the foam column (m). However, the wall shear stress is insignificant in comparison to the hydrostatic pressure generated by the weight of water. Thus, the liquid fraction profile in the foam column can be determined by measuring the pressure gradient of the foam according to equation 4.6. As *C. vulgaris* has a density close to that of water, the density of *C. vulgaris* in the foam was assumed to be the same as that of water.

$$\varepsilon_L = \frac{1}{\rho_L g}\frac{dp}{dy} \quad \ldots (4.6)$$

In this work at steady state conditions, the pressure gradient was measured at 5 cm intervals up the column using a high accuracy digital pressure meter (Kane 3500, UK) connected to a 0.9 cm internal diameter glass tube. The tube was inserted into the foam to the desired depth during harvesting experiments at different CTAB concentrations (30, 60, and 80 mg L^{-1}) and air flow rates (1 and 2 L min^{-1}). The column height was held at 96 cm, the liquid pool depth was 20 cm, the feed flow rate was 0.2 L min^{-1} and the fine sparger was used. To examine the proposed foam risers for drainage enhancement, additional trials were performed in the presence of those risers at a CTAB concentration of 80 mg L^{-1} and an air flow rate of 1 L min^{-1}. The foam risers were placed at the middle of the column and the pressure profile measurements were conducted in duplicate for each harvest trial.

4.3 Results and discussion

4.3.1 Effect of the foam riser on the concentration factor of the harvested microalgae

4.3.1.1 Effect of the surfactant concentration

CTAB, a quaternary ammonium cationic surfactant, has been widely used in wastewater treatment and in the extraction of DNA (Xinwei Cheng *et al.*, 2014; T. Coward *et al.*, 2014). In Chapter three, CTAB beneficially modified the surface physicochemical properties of *C. vulgaris* by increasing the hydrophobicity and reducing the net charge of the algae cells, resulting in improved flotation performance.

The effect of CTAB concentration on concentration factor with and without a foam riser present under a stable continuous process is shown in figure 4.3 under operating conditions of air flow rate of 2 L min^{-1}; column height of 122 cm; liquid pool depth of 20 cm; and feed flow rate of 0.2 L min^{-1}. Four CTAB concentrations were used in these trials and ranged from 20 to 50 mg L^{-1}. The microalgae concentration factor decreased as CTAB concentration increased, regardless of whether the riser was present or not. This was studied during the screening of the foam flotation factors. Both creation and deformation of gas-liquid interfaces are involved

during bubble generation. The effect of surfactants on either bubble breakup or bubble coalescence rates can change the bubble size (Prince and Blanch, 1990). Bubble breakup can be assessed using Weber number (W_e) which is a dimensionless ratio of the inertial force that causes the bubble deformation such as shear stress and pressure of turbulence to the surface tension that restores the bubble sphericity (equation 4.7). The surface tension of the bubbly liquid reduces when CTAB concentration increases. Larger inertial forces applied to the bubbles and/or lower surface tension makes this criterion number exceed its critical value, which exists at the point where inertial (disruptive) force balance surface tension (cohesive) force; consequently, promoting the bubble breakup process causing a reduction in bubble size which produces a wetter foam (Prince and Blanch, 1990; Jianlong Wang *et al.*, 2016a). Also, higher CTAB concentration produces more stable bubbles and impedes bubble coalescence as well, resulting in a higher recovery efficiency and a lower concentration factor (Gupta *et al.*, 2007).

$$W_e = \frac{u^2 d_b \rho_f}{\sigma} \quad \ldots (4.7)$$

Where: d_b is the bubble diameter; u is the velocity; ρ_f is the density of liquid; and σ is the surface tension. With each foam riser, the microalgae concentration factor in the foamate increased but at differing ratios. The concentration factor was 228 under 20 mg L^{-1} CTAB without a riser. The 0.75 diameter ratio riser increased the concentration factor to 319, which was 1.4 times that obtained with the bare column. The concentration factor increased to 417 and 444 with the 0.5 and 0.25 diameter ratio risers respectively, i.e. 1.8 and 1.9 times that obtained without a riser. When the CTAB concentration was increased to 30 mg L^{-1}, the concentration factor decreased to 51 due to the increase in the wetness of the foam; however, when the 0.75, 0.5, and 0.25 diameter ratio risers were used, the concentration factor increased to 60, 88, and 153 respectively (1.2, 1.7, and 3 times that obtained without a riser). At CTAB concentrations of 40 and 50 mg L^{-1}, the concentration factors of harvested microalgae were 30 and 19 respectively, again increasing as smaller diameter ratio risers were used (Figure 4.3).

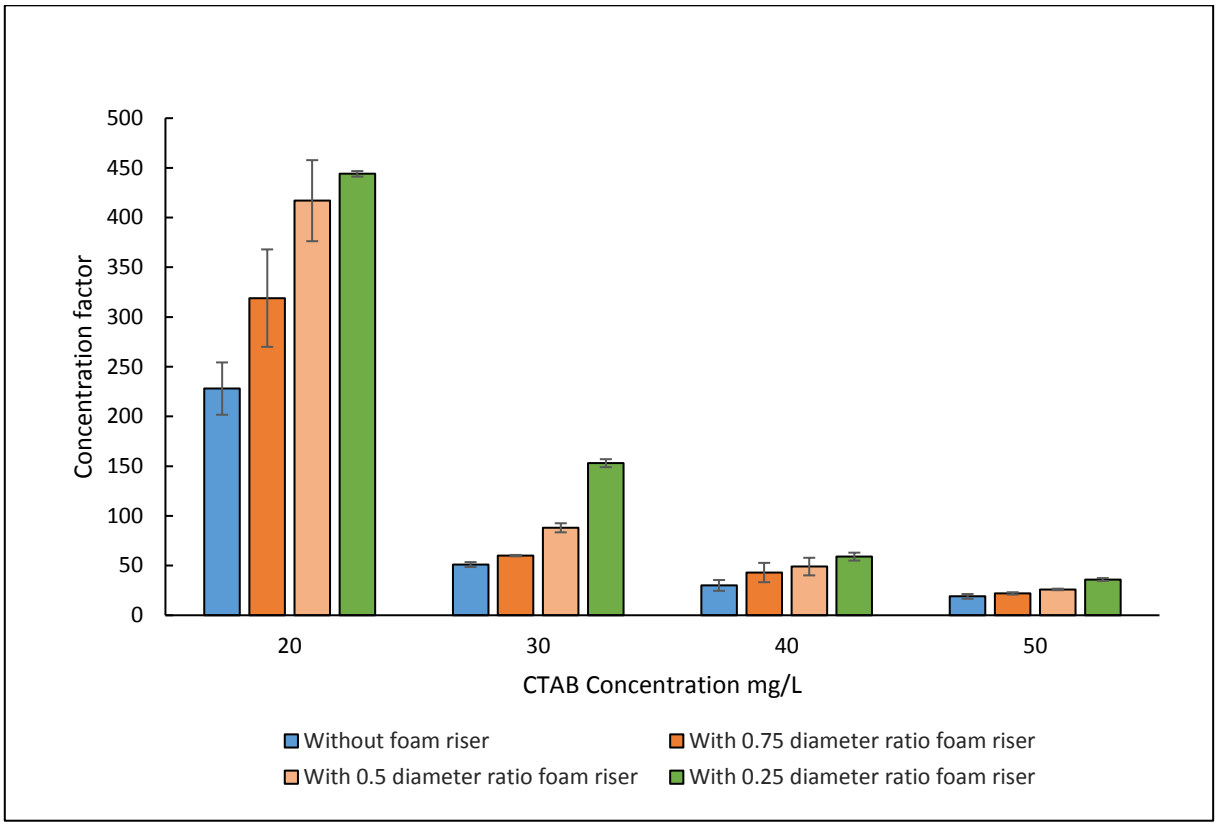

Figure 4.3: The concentration factor of the harvested microalgae under different CTAB concentrations and 2 L min^{-1} air flow rate with/without foam risers, error bars represent standard error.

According to equation 4.1, the bubble size or liquid fraction within the foam layer needs to be increased to increase the superficial drainage velocity in the vertical foam column. Foam flow through the contraction and expansion may lead to changes in the bubble size distribution due to coalescence of bubbles because of the inter-bubble gas diffusion or the rupture of the foam lamella. A small increase in mean bubble size was observed by Li et al. (2011) when they used a foam riser with a sudden contraction and expansion in a foam fractionation column to concentrate a solution of SDS (Xueliang Li *et al.*, 2011a). Measuring the bubble size distribution within the foam with or without the riser can provide evidence of any significant changes in bubble size; however, Stevenson stated that bubble size distribution measured through the column wall may not be representative of the distribution within the foam bulk because of bubble deformation by the column wall and also that smaller bubbles tend to thrust larger bubbles away from the column wall (P. Stevenson and Li, 2014). Lu et al. (2013) observed that the drainage velocity between the bubbles and the column was higher than that between the adjacent bubbles when they investigated the wall effect on drainage of SDS stabilised foam. This is another plausible explanation as the foam flow through the contraction of the riser increases the contact area between the wall and foam (Ke Lu *et al.*, 2013).

The effect of bubble coarsening rate on the foam liquid fraction was observed by Vera and Durian (Vera and Durian, 2002). They dispersed nitrogen gas bubbles in an aqueous solution of alpha olefinsulfonate and measured the volume of liquid that seeped out from the foam against time. They concluded that the rate of foam drainage was significantly increased due to the evolution of foam structure by gas diffusion from high to low pressure (smaller to larger) bubbles. In other words, as the average bubble size becomes larger due to coarsening, the rate of drainage increases. Conversely, the foam drainage process is governed by the laminar flow driven by gravity and capillarity. Foam drainage causes a reduction in the liquid volume fraction through the column which leads to an increase in the capillary pressure. The latter in turn induces bubble coarsening and accelerates the coalescence (i.e. foam drainage is a key factor for coarsening and bubble coalescence) (Arnaud and Dominique, 2002; Saint-Jalmes, 2006; Kruglyakov *et al.*, 2008). Both latter mechanisms (i.e. coarsening and bubble coalescence) govern the average bubble size within foam as well as its life. However, some previous studies have reported that adsorbed hydrophobic particles to the gas-liquid interface act as a barrier to impede coarsening and prevent bubble coalescence (Binks, 2002; Abkarian *et al.*, 2007).

In addition, when the foam containing microalgae flows upward through the contraction of the foam riser, the superficial gas and liquid velocities increase and consequently the liquid fraction within the foam increases as well. Again, the superficial drainage velocity will increase as the liquid fraction increases. Thus, as the mean bubble size and liquid fraction within the foam increased with the presence of the foam risers, the concentration factor for the harvested microalgae increased.

Figure 4.3 shows that the microalgae enrichment ratios with the riser setups differ with CTAB concentration. For example, the 0.25 diameter ratio riser increased the concentration factor by a factor of 3 over that without a riser at 30 mg L^{-1} CTAB whereas the concentration factor increased about 1.9 times at 20 mg L^{-1}. As the liquid fraction increased with CTAB concentration, the foam riser appeared to be more efficient at higher liquid fractions. This observation is in accord with the empirical equation 4.1, as the drainage velocity increases with higher liquid fractions, resulting in greater enrichment ratios. It is worth noting that with the structure of our foam riser, there is a path for interstitial liquid to be released downwards to the foam under the riser; this may engender internal reflux which promotes adsorption of more microalgae in the interstitial liquid onto bubbles even though that liquid has a low microalgae concentration.

4.3.1.2 Effect of the air flow rate

The effect of air flow rate on concentration factor was investigated with and without foam riser present, as shown in figure 4.4 under operating conditions of cationic CTAB concentration of 30 mg L^{-1}; column height of 122 cm; liquid pool depth of 20 cm; and feed flow rate of 0.2 L min^{-1}. Three air flow rates (1, 1.5, and 2 L min^{-1}) were investigated in tandem with the risers.

The microalgae concentration factor decreased as the air flow rate increased irrespective of foam riser usage (Figure 4.4). Increasing the air flow rate will increase the bubble surface area flux resulting in wet foam which has lower concentration factors. The microalgae concentration factor was 189 at air flow rate of 1 L min^{-1} without a riser, increasing to 347 with the 0.75 diameter ratio riser and to 533 and 752 when the 0.5 and 0.25 diameter ratio risers were used. When the air flow rate was increased to 1.5 L min^{-1}, the concentration factor without a riser fell from 189 to 89. The concentration factor increased to 134 with the 0.75 diameter ratio riser and further increased to 230 and 383 with the 0.5 and 0.25 diameter ratio risers, respectively. At 2 L min^{-1} the concentration factor reduced further; 51 without a riser and 60, 88 and 153 with the 0.75, 0.5 and 0.25 diameter ratio risers, respectively.

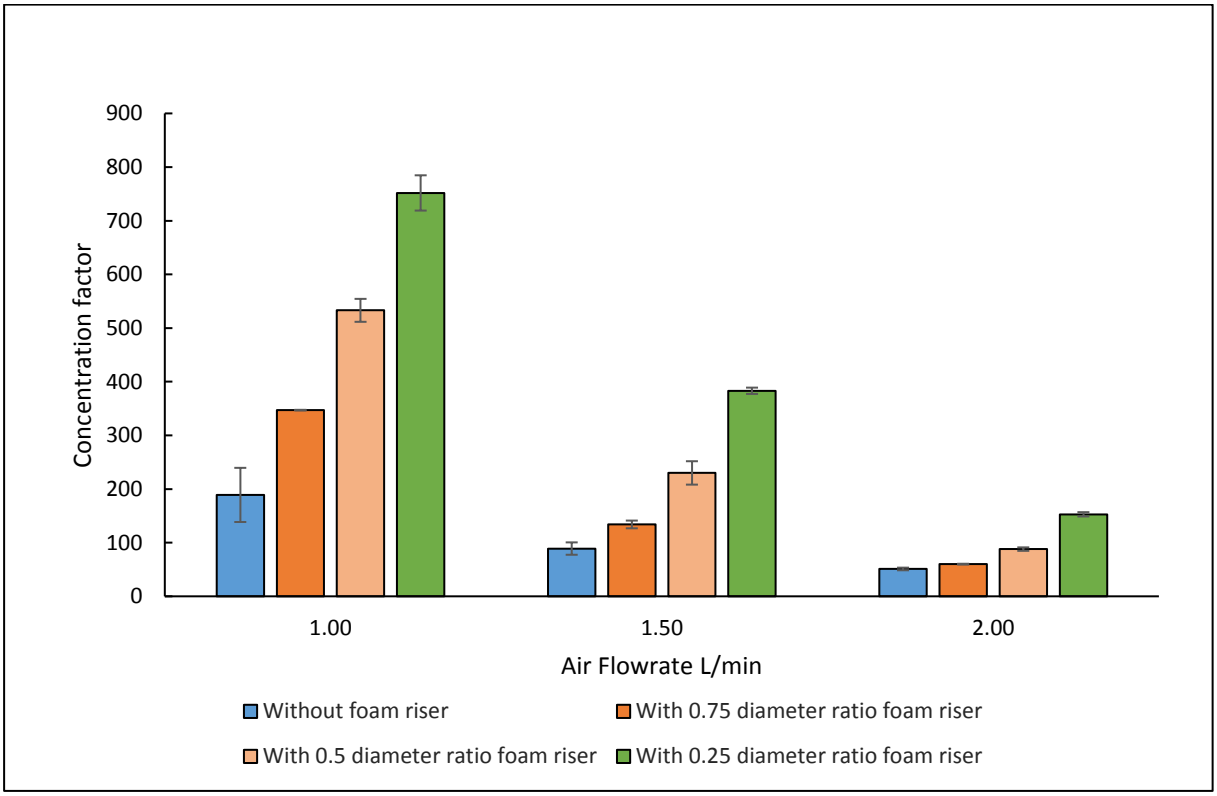

Figure 4.4: The concentration factor of the harvested microalgae under different air flow rates and 30 mg L^{-1} CTAB concentration with/without foam risers, error bars represent standard error.

4.3.2 Harvesting of microalgae based on optimised flotation factors

The greatest enhancement in algae concentration factor was achieved using the 0.25 contraction and expansion diameter ratio riser. Thus, *C. vulgaris* was harvested continuously based on the optimised process (CTAB = 35 mg L^{-1}, air flow rate = 1 L min^{-1}, feed flow rate = 0.1 L min^{-1}, column height = 146 cm, and liquid pool depth = 25 cm) with and without the 0.25 diameter ratio riser (Figure 4.5). The purpose of harvesting microalgae under those conditions was to achieve an effective combination of a high recovery efficiency (for greater biomass removal from the growth medium) and concentration factor (to lower downstream dewatering and drying costs) which is pivotal for driving down the cost of handling and processing bulk quantities of microalgae.

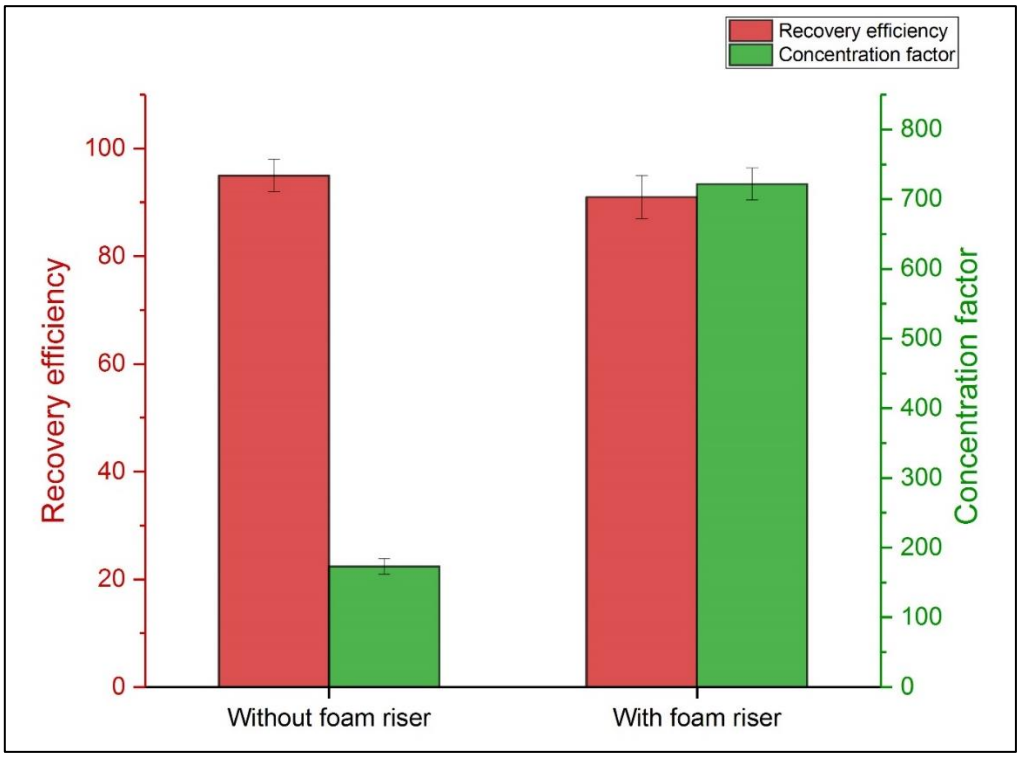

Figure 4.5: The concentration factor and recovery efficiency of the harvested microalgae under the most advantageous conditions with and without foam risers, error bars represent standard errors.

The concentration of harvested microalgae was considerably enhanced under optimised conditions with the foam riser (Figure 4.5). The initial culture was concentrated by approximately 722-times when the foam riser was used compared with 173 without a riser. However, a small reduction in biomass recovery efficiency was observed (Figure 4.5), reducing to 91 from 95%. This was almost certainly a consequence of the adhesion of microalgae biomass to the riser wall (Figure 4.6). Relative to the improvement in overall biomass

enrichment, this minor reduction in biomass recovery is an acceptable trade-off. Furthermore, the recovery efficiencies in both columns (with and without risers) were similar when determined based on microalgae concentration in the discharge stream. Total suspended solids were also measured in the presence and absence of the riser. A total suspended solids yield of 5.6% was obtained for the conventional foam column while it increased to 14.6% with the riser that compares favourably with other dewatering harvesting techniques. For example, a Nozzle discharge centrifuge was reported to yield a total suspended solids of 2-15% with power consumption of 0.9 kWh m^{-3} of microalgae, *Scenedesmus* (Molina Grima *et al.*, 2003). Such a considerable increase in total suspended solids without additional costs is vital to lower downstream dewatering and drying costs.

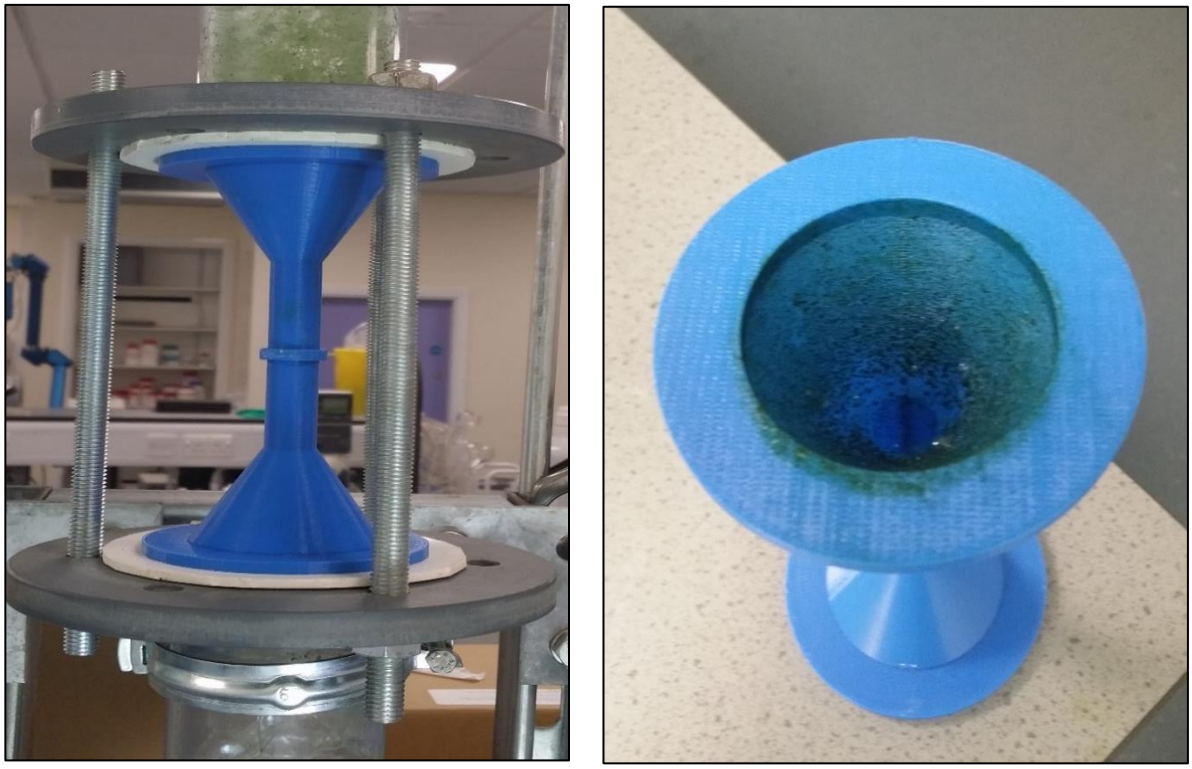

Figure 4.6: Foam riser of 0.25 successive contraction and expansion inserted in the foam column (left), algae biomass adhered to the inner wall of the foam riser (right).

Energy consumption, total suspended solids, recovery efficiency, and concentration factor for various harvesting methods including the current method are presented in table 4.1. The concentration factor obtained with the 0.25 contraction and expansion ratio riser in the continuous foam column outperformed all those achieved by other harvesting techniques. A considerable gain in TSS was also achieved (14.6%), which was comparable to most dewatering techniques such as Nozzle discharge centrifuge even though the latter might be used to harvest and concentrate microalgae cultures of concentration several times higher than our initial

culture concentration. The process demonstrated a very low power consumption (0.052 kWh m^{-3} of algae culture) with no extra costs after applying the riser. Therefore, the continuous foam column fitted with a riser can eradicate some key challenges associated with the most commonly used bulk harvesting techniques.

Harvest method	Operational mode	Microalgae	Energy consumption (kWh m^{-3})	TSS (%)	CF and RE
Chamber filter (Molina Grima *et al.*, 2003)	Discontinuous	*Coelastrum proboscideum*	0.88	22-27	245
Vacuum filter; non-pre-coat vacuum drum filter (Molina Grima *et al.*, 2003)	Continuous	*C. proboscideum*	5.9	18	180
Vacuum filter; suction filter (Molina Grima *et al.*, 2003)	Discontinuous	*C. proboscideum*	0.1	8	80
Tangential flow filtration (Danquah *et al.*, 2009)	Continuous	Multi-strain *Tetraselmis suecica/ Chlorococcum* sp.	0.38	N/A	48
Vibrating screens (Uduman *et al.*, 2010a)	N/A	N/A	0.4	1-6	15-60
Nozzle discharge centrifuge (Molina Grima *et al.*, 2003)	Continuous	*Scenedesmus*, *C. proboscideum*	0.9	2-15	20-150
Decanter bowl centrifuge (Molina Grima *et al.*, 2003)	Continuous	*Scenedesmus*, *C. proboscideum*	8	22	11
Hydro-cyclone (Molina Grima *et al.*, 2003)	Continuous	*C. proboscideum*	0.3	0.4	4
Electrolytic flocculation	Batch	Multi-strain algae/ diatoms	0.33	N/A	N/A
Electrocoagulation (Uduman *et al.*, 2011)	Batch, 15 min, 10V	*Tetraselmis*	2.75	N/A	N/A
Sedimentation					
Lamella separators (Shelef *et al.*, 1984; Uduman *et al.*, 2010a)	Discontinuous	Multi-strain *Chlorella/ Coelastrum*	0.1	0.1-1.5	16
Dissolved air flotation (Patrick E. Wiley *et al.*, 2009)	Batch	Multi-strain *Chlorella/ Scenedesmus*	7.6	5	N/A (85)
Suspended air flotation (Patrick E. Wiley *et al.*, 2009)	Batch		0.003	4.8	N/A (77)

Electro-flotation (Shelef *et al.*, 1984)	Batch	Multi-strain *Chlorella/ Coelastrum*	Very high, N/A	3-5	N/A
Foam flotation by Jameson cell (Garg *et al.*, 2015)	N/A	*Tetraselmis* sp. *M8*	N/A	N/A	23 (99)
Foam flotation based on optimised factors without a foam riser	Continuous	*Chlorella vulgaris*	0.052	5.6	173 (95)
Foam flotation (this study) based on optimised factors with a foam riser	Continuous	*Chlorella vulgaris*	0.052	14.6	722 (91)

Table 4.1: Energy consumption, total suspended solids (TSS) and concentration factor (CF) of different microalgae harvesting techniques. Where reported, the recovery efficiency (RE %) is given in parentheses.

4.3.3 Liquid holdup profile

The liquid holdup is a relevant factor affecting the rate of foam drainage and can characterise the foam as well. It is the total liquid fraction existent in the foam per unit volume. In this work, the liquid holdup profiles in the foam were determined by measuring the pressure profile of the foam in the column. The harvesting trials were performed at different CTAB concentrations and air flow rates as those factors, in addition to the column height, had the greatest effect on the foam flotation efficiency as Chapter three revealed (see 3.3.4 analysis of experimental design). However, a taller column was not tested here as it proved logistically difficult to insert the glass tube from the column apex.

The measured pressures and calculated liquid fraction profiles at different CTAB concentrations and air flow rates are shown in figure 4.7. The pressure gradients demonstrated sharper transitions at the pool/foam interface. Similarly, the liquid holdup profiles showed sharp transitions not only at the pool/foam interface but also in the onset zone of the wet foam. A previous hypothesis stated that the liquid fraction in the effervescent liquid phase and in the wet foam would be around 0.8 and 0.1 respectively (Kamalanathan, 2015). The liquid fraction for the wet foam beyond its beginning zone and the drier foam at the top of the column remained relatively constant; this was expected as the foam dries as it rises up the column. The initial liquid fraction for the generated foam were obviously much larger than that in the foam at the top of the column, demonstrating that foam is an effective medium for considerably concentrating the recovered microalgae biomass and this represents another advantage added to the foam flotation column over other flotation techniques. Moreover, when the foam becomes

drier at the top of the column, it will possess some preferable characteristics including more fragile structure with thinner liquid films which improve the foam collapse and will recover microalgae easily for further downstream processing.

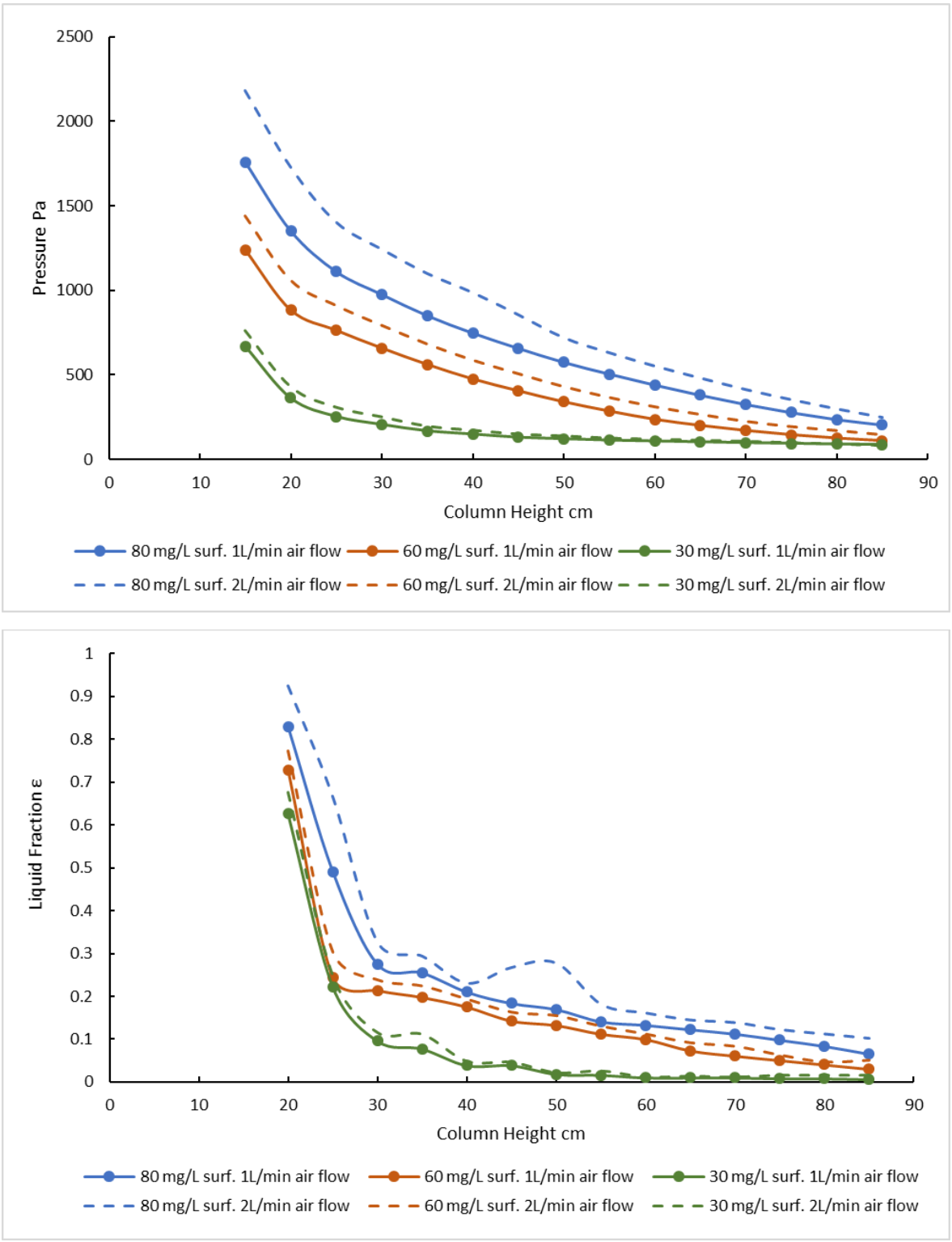

Figure 4.7: Pressure (top) and liquid holdup (bottom) profiles of the foam in the column when using CTAB (30, 60, and 80 mg/L) at two air flow rates (1 and 2 L/min). The liquid pool/foam interface occurs at 20 cm.

The pressure and liquid profiles were shown to increase with increasing CTAB concentration. The surface tension of the effervescent liquid reduced as the CTAB concentration increased. This caused a reduction in bubble size, leading to a wetter foam. Moreover, the rising foam comprising smaller bubbles had a slower liquid drainage when the liquid holdup profile of the foam made from 80 mg L^{-1} CTAB was compared to 30 mg L^{-1} (Figure 4.7). The pressure and liquid holdup profiles also increased with increasing air flow rate. This is probably due to the short residence time and drainage opportunity for the rising foam with a higher air flow rate or due to the reduction in bubble size distribution as Stevenson and Li (Paul Stevenson and Li, 2012b) previously stated.

Additional trials to determine the liquid holdup profiles in the foam were performed to examine the efficacy of the foam riser modules for drainage enhancement. These harvesting trials were conducted at a CTAB concentration of 80 mg L^{-1} and an air flow rate of 1 L min^{-1} as shown in figure 4.8. The values of the above factors were chosen to guarantee a stable continuous foam i.e. to obtain higher water content in the foam. Similar to the previous observations, all liquid fraction profiles in figure 4.8 showed a sharp transition not only at the pool/foam interface but also at the onset zone of the wet foam. The liquid fraction of the foam in all zones underneath the risers were a little higher than that in the column without a riser. This was probably due to the liquid drainage caused by the risers, leading to small increases in the water content of the foam. However, as the foam left the risers, the water content began to reduce (Figure 4.8), with the water content of the foam passing through the 0.25 contraction and expansion ratio riser being the lowest. This agreed with all previous outcomes that showed that the best drainage enhancement could be obtained with a riser of lower diameter ratio.

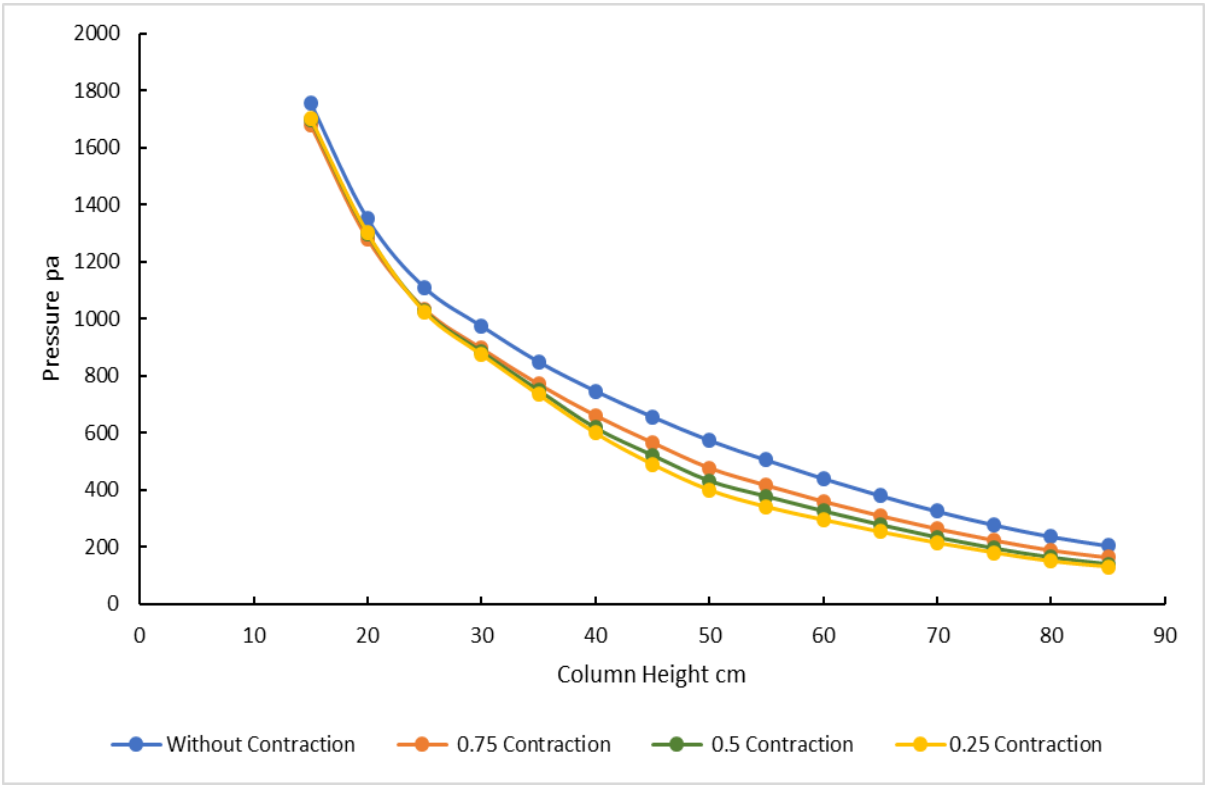

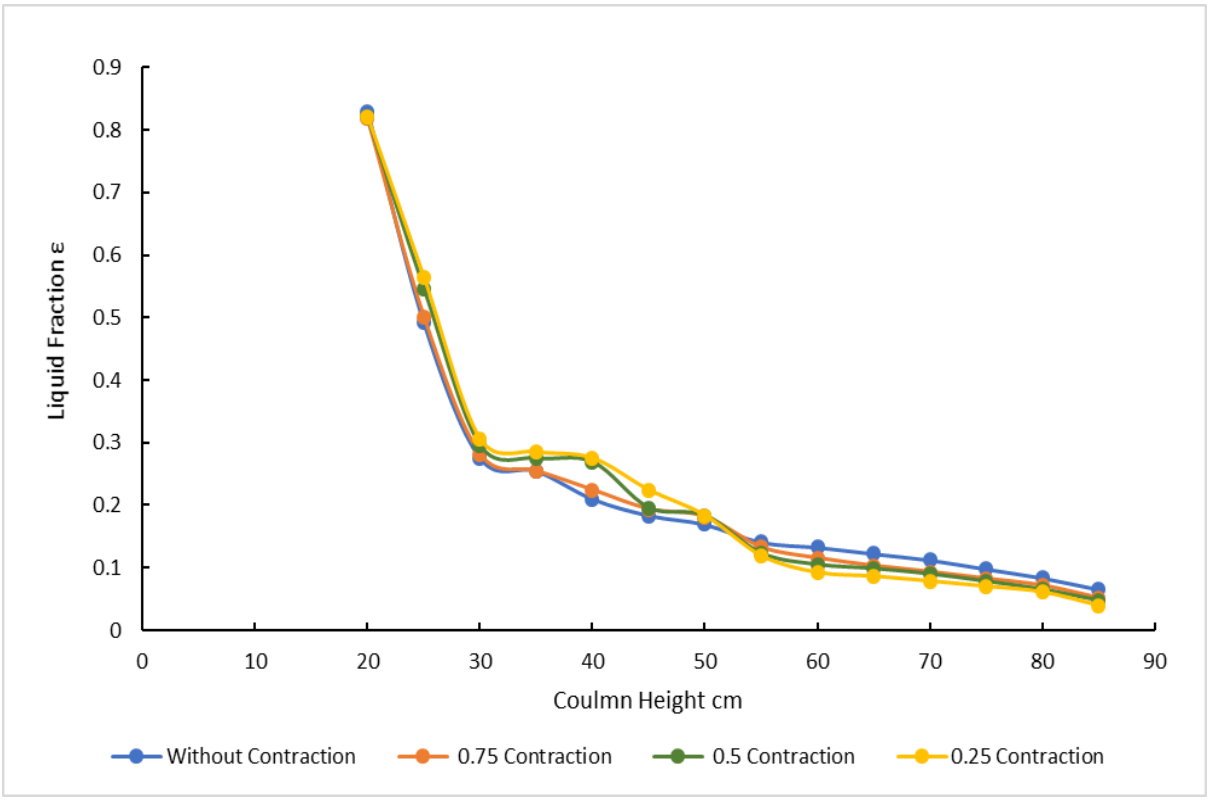

Figure 4.8: Pressure (top) and liquid holdup (bottom) profiles of the foam in the column with and without a foam riser under set CTAB (80 mg/L) and air flow rate (1 L/min) conditions. The liquid pool/foam interface occurs at 20 cm.

4.4 Conclusion

In this chapter, the effect on the drainage of rising foam containing microalgae was investigated using three risers of different smooth-successive contraction and expansion ratios (0.25, 0.5, and 0.75), with different CTAB concentrations and air flow rates. Each riser enhanced the drainage due to the increase in the liquid fraction and likely by changing the bubble size distribution as the foam passed through contraction and expansion. A microalgae concentration factor (444) was achieved under the conditions of: air flow rate 2 L min^{-1}; column height 122 cm; liquid pool depth 20 cm; feed flow rate 0.2 L min^{-1}; and 20 mg L^{-1} CTAB, with the 0.25 contraction and expansion ratio riser - approximately double that attained without the riser. The highest microalgae concentration factor was attained with a CTAB concentration of 30 mg L^{-1} and an air flow rate of 1 L min^{-1} - nearly four times higher than without the riser. Trials performed under the conditions for the best combination of microalgae recovery efficiency and concentration factor (CTAB = 35 mg L^{-1}, air flow rate = 1 L min^{-1}, feed flow rate = 0.1 L min^{-1}, column height = 146 cm, and liquid pool depth = 25 cm) revealed a recovery efficiency of 91% and a final biomass 722-times more concentrated than the initial *C. vulgaris* culture. The liquid holdup of the foam for all risers was lower than that of the bare column, whereas it was higher before passing through the foam risers, which was probably due to the higher drainage velocity of the interstitial liquid. What is more, our continuous foam flotation column demonstrated a very low power consumption, 0.052 kWh m^{-3} of algae culture, with a total suspended solids yield (14.6%). Our findings demonstrate that foam flotation is a very promising approach for the continuous harvesting of microalgae biomass.

Chapter 5

Modeling of a continuous foam flotation column used for algal biomass recovery based on flotation kinetic and probability models

Abstract

Foam flotation, which is a subclass of adsorptive bubble separation, is a selective separation process which shows notable promise as a microalgae biomass harvesting and enrichment method. A good mathematical model is a substantial tool for systematic and consistent process analysis. A wide range of flotation models have been developed based on the processes and sub-processes occurring in flotation. Therefore, to better characterise the harvesting process by flotation, the recovery rate of *Chlorella vulgaris* in continuous foam flotation was studied in this chapter based on the available phenomenological models (i.e. kinetics and probabilistic models). The available literature has concluded that the classical first order kinetic model is better than other flotation kinetic models. The effects of CTAB concentration and air flow rate on the flotation rate constant were investigated. The results demonstrated that the flotation rate constant increased with CTAB concentration and air flow rate. The efficiencies of collision, attachment, and detachment between microalgae cells and air bubbles in the flotation column were investigated based on experimental measurements of bubble size, bubble rise velocity and microalgae cell size. A wide bubble size distribution was generated within a size range of 204 to 2909 μm and Sauter mean diameters ranging from 811 to 1713 μm under different surfactant concentrations and air flow rates. The collision, attachment, and collection efficiencies of microalgae were calculated for intermediate and potential flow conditions based on the bubble Reynolds number. The maximum collision, attachment, and collection efficiencies were 2.75, 99.87, and 2.74% respectively. The low collection efficiency caused by the low collision efficiency of microalgae cell and bubble was largely attributed to the small cell size (*C. vulgaris*: 7.44 ± 0.42 μm). However, the recovery efficiencies obtained theoretically were not in agreement with the experimental recovery efficiencies, indicating that there are probably other mechanisms for interactions between microalgae particles and air bubbles that are not considered in the commonly used collision models.

Keywords

Kinetic order; foam flotation; ultimate recovery; collision efficiency; attachment efficiency; contact angle; *Chlorella vulgaris*

Chapter five

5.1 Introduction

Adsorptive bubble separation is a process of separation and concentration based on differences in the physicochemical properties of interfaces such as hydrophobicity. Due to its simplicity and low capital and operating costs, it is widely used in industrial and domestic wastewater treatment, and in the mining, pharmaceutical, rubber, glass, plastics, and food industries, and removing radioactive contaminants from soil (Jenkins *et al.*, 1972; Rubio *et al.*, 2002; Fuerstenau *et al.*, 2007; Schramm and Mikula, 2012; Bu X, 2016; Gharai and Venugopal, 2016). Foam flotation, which is a subclass of adsorptive bubble separation, is a selective separation process which shows notable promise as a microalgae biomass harvesting and enrichment method. In a foam flotation process, surfactant is added to stabilise the foam and enhance the hydrophobicity of microalgae. Small bubbles are generated which attach to the microalgae cells and cause them to rise to the surface where they are removed from the column in the foam.

Unlike other separation processes foam flotation is a complex process involving the interactions between three phases (solid, gas, and liquid) in the presence of surfactant chemicals. Therefore, the development of mathematical models for the flotation process has proven difficult (Bu X, 2016). Nevertheless, a remarkable number of empirical, probability, and kinetic models have been developed to better understand the flotation process. Most empirical models use a trial and error feedback approach for optimisation and they are very specific to their environment. Using statistical techniques to determine the empirical model parameters does not give them any physical significance and they do not provide any deep intuitive understanding of the flotation process. It is also difficult for the empirical models to offer more predictive capacity outside the conditions adopted in their calculations (A. V. Nguyen and Schulze, 2004). For instance, Li et al. (2016) developed an empirical model to relate the froth rheology to the process variables, however, their empirical model is only valid for the froth with a local shear rate of 2 s^{-1} (Chao Li *et al.*, 2016). The authors also highlighted that the established empirical model is not applicable to other systems having different ore properties or flotation cell designs. Consequently, phenomenological models (i.e. probability and kinetic models) are only considered in this work.

The efficient capture between a bubble and a hydrophobic particle occurs when they first undergo an adequately close encounter (within the range of attractive surface forces). This process is governed by the hydrodynamics controlling their approach in the bubbly liquid zone. Then, the intervening liquid film between the particle and bubble becomes thinner due to the surface forces between the particle and bubble leading to a critical thickness at which film

rupture takes place. This is followed by the establishment of a stable three-phase contact line (the boundary between the receding liquid phase, solid particle surface, and advancing gas phase). This sequence (drainage of intervening liquid, film rupture, and the formation of a stable three-phase contact line) represents the second process of collection (i.e. attachment). However, the particle can be forced out from that stable bubble-particle aggregate when sufficient kinetic energy (shear and gravitational forces) equal or exceeding the detachment energy is supplied to the particle and this represents the third part of collection (i.e. detachment). However, shear forces are lower in a foam flotation column than in mechanical flotation cells due to the absence of an impeller which is an advantage for the flotation column. The gravitational forces are also low for microalgae recovery owing to the small cell size of most microalgae species. This dissection of a bubble-particle capture efficiency into three process efficiencies was published by Derjaguin and Dukhin in 1961 (Derjaguin and Dukhin, 1961) and included the effect of hydrodynamics, surface forces, and diffusiophoresis. They proposed that the collection efficiency or probability (E_{col}) of a particle and a bubble was equal to the product of three efficiencies or probabilities as presented in equation 5.1 (Ralston *et al.,* 1999; Miettinen *et al.*, 2010):

$$E_{col} = E_c . E_a . E_s \ldots (5.1)$$

Where: E_c is the collision efficiency; E_a is the attachment efficiency; and E_s is the stability efficiency of the particle-bubble aggregate.

Kinetic models of particles capture by bubbles are based on the analogy between collision of molecules in a chemical reaction and collision of hydrophobic or hydrophilic particles with gas bubbles in the bubbly liquid zone of a flotation process. Various differential equations of chemical reaction kinetics have been applied to describe the flotation process. Zuniga in 1935 proposed a first-order differential equation to represent results obtained from laboratory batch flotation tests (Zuniga, 1935). The first order flotation kinetic model is based on theory and experiment which indicate that the collision rate between the bubbles and particles is first order with respect to the number of particles and that the bubble concentration remains constant (bubble concentration >>> number of particles) (Sutherland, 1948). Fifteen years later, Arbiter proposed a second order differential equation to correlate the published flotation recovery data as well as his own results (Arbiter, 1952). In contrast to the first order model, the bubble concentration in the second order kinetic model changes with time. The generalised form of the equations used by Zuniga and Arbiter can be written as in equation 5.2.

$$\frac{dC}{dt} = -kC^n \ldots (5.2)$$

Where: C is the concentration of particles in the bubbly liquid zone; k is the flotation rate constant; t is the flotation time; and n is the order of flotation kinetics.

Particle recovery in the foamate (R) at flotation time (t) is defined as:

$$R(t) = \frac{C_i - C(t)}{C_i} = 1 - \frac{C(t)}{C_i} \ldots (5.3)$$

where: C_i is the initial concentration of particles in the bubbly liquid. The maximum recovery, R_∞ after infinite time can be calculated from equation 5.3 at C_∞ (i.e. the concentration of particles remaining in the bubbly liquid after infinite time) as set out below:

$$R_\infty = 1 - \frac{C_\infty}{C_i} \ldots (5.4)$$

Substituting from equations 5.3 and 5.4 into equation 5.2 gives:

$$\frac{dR}{dt} = k(R_\infty - R)^n \ldots (5.5)$$

The distribution of values for the rate constant ($f(k)$) is often used instead of a single value for k to represent the distribution of floatability for particles in a bubbly liquid (Yianatos, 2007). The floatability of particles is the percentage of floating particles (Corona-Arroyo *et al.*, 2018) or the tendency of particles to float (Runge *et al.*, 2003). It is a function of particle characteristics that influence the flotation rate constant such as particle geometry (shape and size), surface energy, hydrophobicity, and liberation properties of particles as well as liquid surface tension and pH (Leroy *et al.*, 2011; Guerrero-Pérez and Barraza-Burgos, 2017; Wencheng Xia, 2017; Corona-Arroyo *et al.*, 2018). Therefore, this concept was introduced to extend the applicability of kinetic models for the heterogeneity of particles (Bu X, 2016) and equation 5.5 can be written as below:

$$\frac{dR}{dt} = f(k)(R_\infty - R)^n \ldots (5.6)$$

The available literature has concluded that the classical first order kinetic model is better than other flotation kinetic models and can be used to optimize the process since it can be applied to both batch and continuous flotation processes with high confidence level (Gharai and Venugopal, 2016). Moreover, Nguyen and Schulze (2004) stated that the flotation kinetic is first order for dilute pulp or flotation of single minerals (A. V. Nguyen and Schulze, 2004).

The first order recovery of microalgae in a batch flotation process can be described by general equation 5.7 (Bu X, 2016). Some first-order models and their continuous and discrete distribution functions are summarized in Table A.1 (appendix 1).

$$R(t) = R_\infty \left[1 - \int_0^\infty e^{-kt} f(k) dk\right] \ldots (5.7)$$

Where $f(k)$ is the continuous distribution of the rate constant or k spectrum, which is normalized $\int_0^k f(k)dk = 1$. For continuous flotation, the recovery of microalgae can be described by the following equation (Yianatos, 2007):

$$R = R_\infty \int_0^\infty \int_0^\infty (1 - e^{-kt}) f(k) E(t) dk dt \ldots (5.8)$$

where: $E(t)$ is the residence time distribution function for continuous flotation process with different mixing characteristics. The continuous recovery of microalgae from the growth culture depends on the flotation rate distribution of microalgae, the actual mean residence time, and the mixing region in the collection zone.

To better characterise the harvesting process, the recovery rate of *Chlorella vulgaris* in continuous foam flotation was studied in this chapter based on the available phenomenological models (i.e. kinetics and probabilistic models) with the aid of experimental measurements of the recovery efficiency, bubble size, gas holdup, bubble rise velocity and microalgae cell size.

5.2 Materials and methods

5.2.1 Microalgae culture

The growth conditions for *C. vulgaris* used herein have been described previously (see 3.2 materials and methods).

5.2.2 Flotation tests for kinetic study

The schematic diagram of the foam flotation column is shown in figure 5.1. The column was constructed from poly(methyl methacrylate) cylindrical sections with a 5.15 cm internal diameter. The column height was adjusted by bolting together cylindrical sections of different lengths. The inlet mixture consisted of algae culture mixed with surfactant in a 25 L reservoir. The spent culture was discharged to the tailing tank from the outlet stream valve at the base of the column, 1 cm above the sparging media. A magnetic stirrer was used to mix the microalgae culture with the surfactant in the feed tank for 10 mins prior to and during the flotation tests.

The feed was pumped to the column by a peristaltic pump (Masterflex L/S, model 07554-95, Cole-Parmer, UK). A valve was placed on the culture discharge stream to control the liquid depth in the column. Air bubbles (dispersed phase) were generated by introducing compressed air through a sparger made from ultra-high molecular weight polyethylene with a thickness of 6.0 mm, a diameter of 51.5 mm, and mean pore sizes of 30 µm. The flotation tests were conducted using *C. vulgaris* and the algae concentration in the inlet stream was held at 0.46±0.13 g L^{-1} concentration dry weight (equivalent to $9.58 \times 10^6 \pm 1.1 \times 10^6$ cells mL^{-1}). Cationic hexadecyltrimethylammonium bromide (CTAB, $CH_3(CH_2)_{13}N(CH_3)_3$-Br), G-bioscience, USA, was used as a foaming agent at three different concentrations (20, 30, and 40) mg L^{-1}. Evaluation of the most important factors in the foam flotation process (see 3.3 results and discussion) had shown that surfactant concentration and air flow rate had the largest effects on the process performance, therefore, the flotation kinetics were also studied at different air flow rate magnitudes (1 and 2) L min^{-1}. The other process factors (column height, inlet stream flow rate, and liquid pool depth) were held constant at 96 cm, 0.15 L min^{-1}, and 25 cm respectively. The foam and the processed culture from the discharge stream were collected over time until reaching steady-state. Then, feed and discharge streams valves were turned off simultaneously. The microalgae remaining in the column was collected and counted to determine the cell residence times. Each continuous flotation test was conducted with three replicates.

In this work, the recovery of *C. vulgaris* was determined using equation 5.3. A calibration curve was constructed correlating cell density and their corresponding absorbance at 750 nm using a spectrophotometer (Jenway, Model 7315, Bibby scientific Ltd, UK), yielding an R^2 of 100% (data not shown). Cells density was measured using an improved Neubauer hemocytometer, with a Leica DM 500 light microscope.

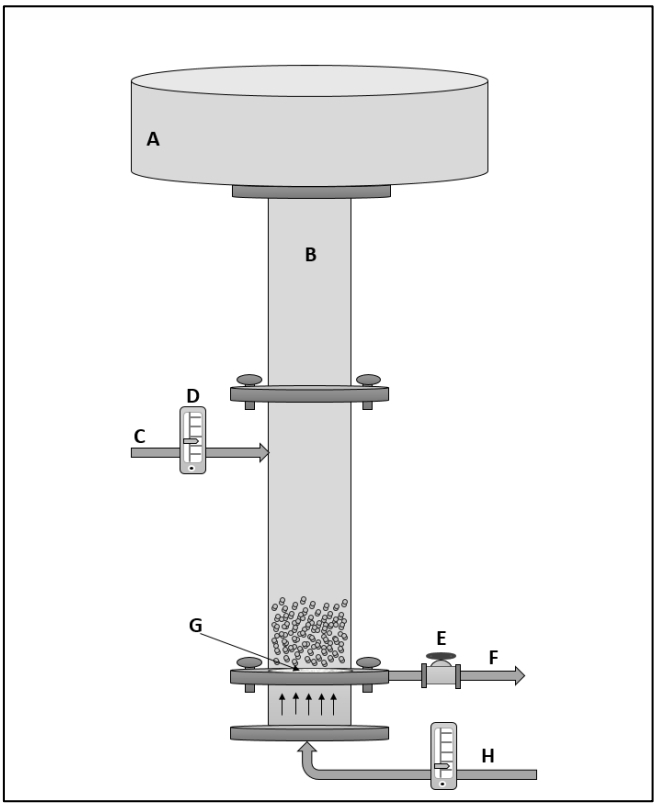

Figure 5.1: Schematic diagram of the continuous foam flotation column. A: Foam-collecting cup, B: column tubular module (25, 30 or 50 cm) in height and 5.1 cm in diameter, C: inlet stream, D: inlet flow meter, E: outlet stream valve, F: underflow stream, G: air sparger, H: air input stream.

5.2.3 Analytical methods (algal cell size, bubble size and rising velocity).

Bubble size distribution (BSD) and rising velocity in the bubble swarm were measured in the liquid pool of the foam flotation column (Figure 5.1) at three CTAB concentrations (20, 30, and 40) mg L^{-1} and four air flow rates (0.5, 1, 1.5, and 2) L min^{-1}. During all the experiments, the liquid pool depth, column height, and inlet stream flow rate were held constant at 25 cm, 96 cm, and 0.15 L min^{-1} respectively. To avoid the presence of additional surfactants from previous tests, the system was flushed before each trial. The most common methods adopted to measure the bubble size distribution are optical and acoustical techniques. Bubble characterisation by photography has been described as a tiresome and time-consuming method; however, it is able to measure both bubble size and distribution in addition to track individual bubbles through a sequence of photographs to determine the bubble rise velocity (T. Coward *et al.*, 2015), therefore it was employed in this work.

A high-speed camera (Photron FASTCAM SA3) connected to a computer were used to photograph the bubbles generated in the foam column. The images were calibrated (pixels to millimetres) by placing one ruler on the outside wall and one inside the flotation column and

focusing the camera on them. Besagni et al. (2016) evaluated the conversion factor by placing a ruler in the centre of a bubble column for different radial positions (Besagni *et al.*, 2016). They found that the maximum difference in the conversion factor was 0.5 pixel/mm and the influence of optical distortion was negligible. In this work, the conversion factors at different radial positions were determined by a method similar to that adopted by Besagni's group. The maximum difference in the conversion factor was 0.64 pixel/mm in this work. The high-speed camera was run at 2000 frames per second (fps) and a minimum of 250 high quality images were taken for each experimental trial. The back-light method was employed to illuminate the experimental trials using (Nebula4) hydroponic plant lights which were fitted with four Philips 55W florescent lamps.

The open source image analysis software, ImageJ, version 1.51j (National Institutes of Health, Bethesda, Maryland, USA) was used to determine the bubble size distribution. To achieve a reliable BSD, between 300-350 bubbles were analysed for each experimental trial. Bubble rise velocity was determined by tracking individual bubbles over a sequence of photographs. Several bubble rise velocities obtained by the above method were also validated using Photron FASTCAM Analysis software (PFA-Demo version).

Microalgae size (minimum of 10 readings) was measured microscopically using a Leica DM 500 light microscope with ImageJ.

Lastly, the gas holdup in the bubbly liquid pool at different air flow rates was measured according to Besagani and Inzoli's method (Besagni and Inzoli, 2016). The procedure involves measuring the height of the liquid free surface before and after air aeration. The gas holdup was then determined using equation 5.9:

$$\varepsilon_G = \frac{H_D - H_o}{H_D} \ldots (5.9)$$

where: H_o and H_D are the heights of the liquid free surface before and after air aeration respectively.

5.3 Results and discussion

5.3.1 Bubble size distribution and rise velocity

Bubble size distribution (BSD) and bubble rise velocity were measured optically in the liquid pool of the foam flotation column. During these experimental trials, only tap water with CTAB were fed into the foam column due to the high optical density of microalgae cultures. However, slightly larger bubble sizes with a slower rise velocity are expected in the presence of

microalgae cells. Vazirizadeh et al. (2016) studied the impact of introducing 4% (w/w) (40% talc and 60% quartz solid) on the bubble size distribution in a flotation column. They found that the presence of solids increased the bubble size (Vazirizadeh *et al.*, 2016). Similar observations were reported by Kuan and Finch (2010) when they studied the effect of talc on pulp and froth properties. They suggested that the coalescence between bubbles due to the presence of particles was responsible for this phenomenon. In froth flotation, frother is present to stabilize bubbles against coalescence and the adsorption of frother by talc would drive the system back to the water only case. However, the reduction in frother concentration due to adsorption did not offer a complete explanation since the frother remaining in the pulp exceeded the critical coalescence concentration. Therefore, they suggested that talc can remove frother directly from the bubble surface and increase coalescence rate (Kuan and Finch, 2010). Like the retardation of bubbles by the presence of surface active materials, the rise velocity of bubbles is more likely reduced owing to the presence of microalgae cells. The Sauter mean bubble diameter (d_{32}) has been widely used with the superficial gas rate (J_g) to describe the dispersion efficiency of the gas phase in flotation machines (Leiva *et al.*, 2010); therefore, Sauter mean bubble diameter was adopted in this work as the mean bubble diameter and calculated by equation 5.10. The bubble Reynolds number (Re_b) was calculated using equation 5.11:

$$d_{32} = \frac{\sum n_i d_i^3}{\sum n_i d_i^2} \dots (5.10)$$

$$Re_b = \frac{V_b d_{32} \rho_f}{\mu} \dots (5.11)$$

In equations 5.10 and 5.11, n is the number of bubbles; d is the bubble diameter; V_b is the bubble rise velocity; ρ_f is the fluid density (= 998.2 kg m^{-3} at 18 ˚C); and μ is the fluid viscosity (= 1.053 mPa.s at 18 ˚C). Contour plots for Sauter mean bubble diameter, bubble rise velocity, and bubble Reynolds number within the liquid pool for different CTAB concentrations and air flow rates are presented in Figure 5.2. Surfactant concentration and air flow rate are the most important factors in foam flotation as our previous investigations have demonstrated (see 3.3 results and discussion), therefore, evaluating their effects on bubble size distribution and bubble rise velocity and consequently the hydrodynamic condition of foam is essential to improve flotation performance. A wide range of bubble sizes were generated with Sauter mean diameters ranging from 811 to 1713 µm under different CTAB concentrations and air flow rates as shown in figure 5.2a. Nearly all bubbles generated in this work were spherical as shown in figure 5.3. With increasing CTAB concentration, the Sauter mean bubble diameter decreased for all air

flow rates, dropping from 1713 to 1210 µm; 1238 to 924 µm; 1111 to 816 µm; and 876 to 811 µm when CTAB concentration was increased from 20 to 40 mg L^{-1} at air flow rates of 2, 1.5, 1, and 0.5 respectively.

a

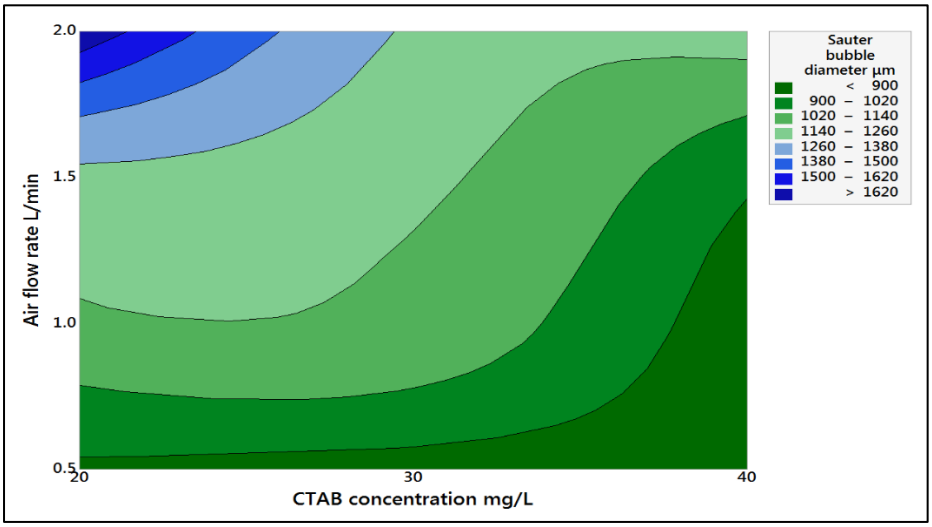

b

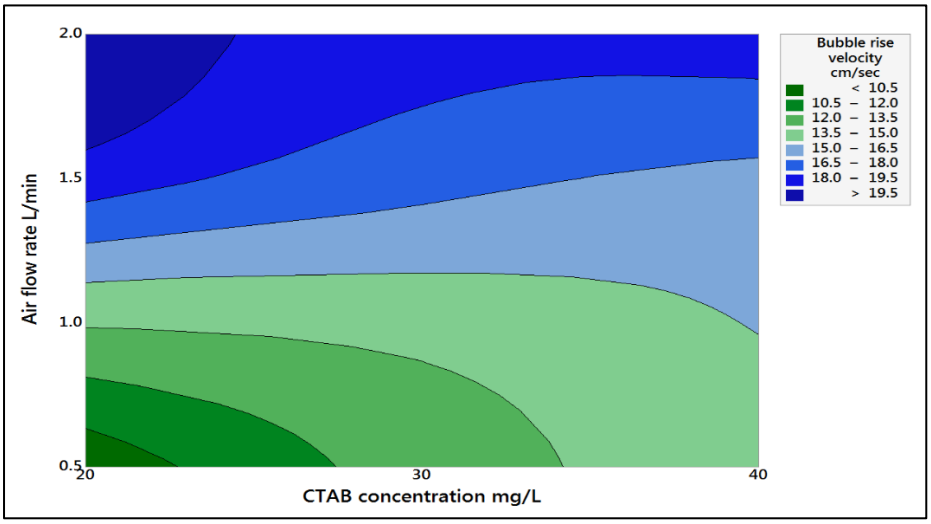

c

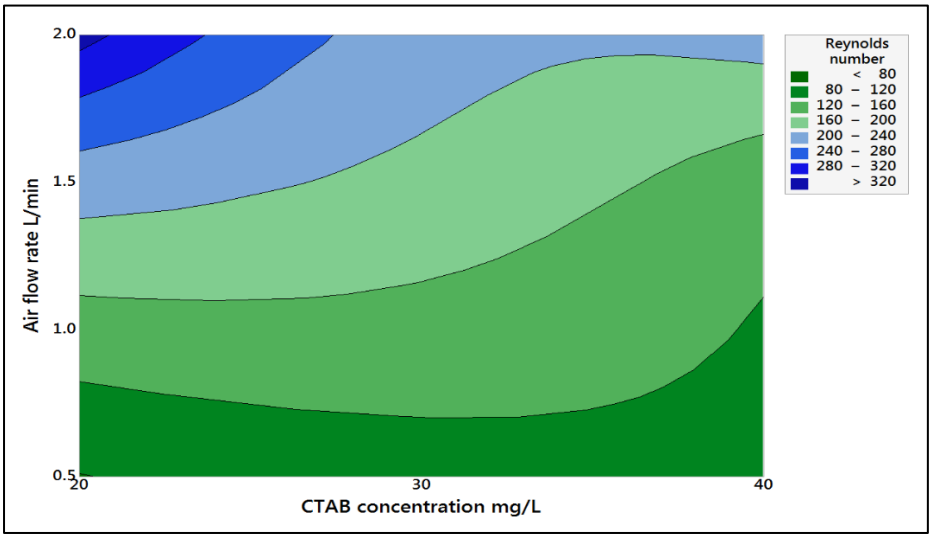

Figure 5.2: Contour plots for the (**a**) Sauter mean bubble diameter, (**b**) bubble rise velocity, and (**c**) bubble Reynolds number within the liquid pool of the foam flotation column under 20, 30, and 40 mg L^{-1} CTAB concentrations and 0.5, 1, 1.5, and 2 L min^{-1} air flow rates.

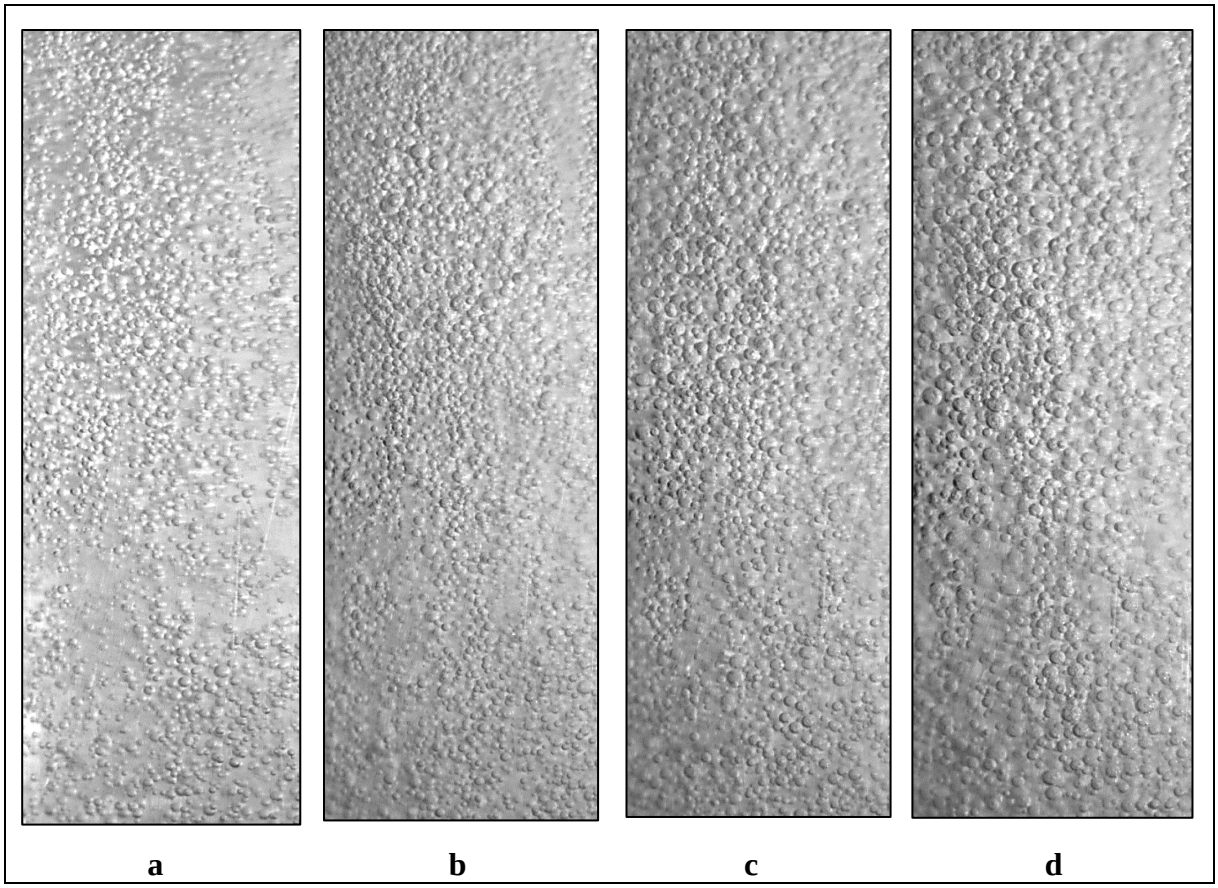

Figure 5.3: Clouds of spherical bubbles generated using a sparger made from ultra-high molecular weight polyethylene with a thickness of 6.0 mm, a diameter of 51.5 mm, and mean pore sizes of 30 µm at 30 mg L^{-1} CTAB concentration and different air flow rates **(a**) 0.5 L min^{-1} with Sauter mean bubble diameter of 849 µm, (**b**) 1 L min^{-1} with Sauter mean bubble diameter of 1097 µm, (**c**) 1.5 L min^{-1} with Sauter mean bubble diameter of 1166 µm, and (**d)** 2 L min^{-1} with Sauter mean bubble diameter of 1245 µm.

The surface tension between the gas and liquid reduces when the concentration of CTAB increases and therefore causes a reduction in the mean bubble size. However, increasing the air flow rate led to an increase in the Sauter bubble size under all surfactant concentrations, increasing from 876 to 1713 µm; 849 to 1245 µm; and 811 to 1210 µm when air flow rate was increased from 0.5 to 2 L min^{-1} at CTAB concentrations of 20, 30, and 40 mg L^{-1} respectively. In contrast, Stevenson and Li (Paul Stevenson and Li, 2012b) stated that in a porous medium the generated bubble size decreases with increasing gas flow rate. At lower gas rates, only bigger pores are active and generating mainly big bubbles. When the gas flow rate increases, most of the inactive small pores become active, leading to an increased number of smaller

bubbles (L.K. Wang *et al.*, 2010b). However, many other operating parameters beside air flow rate govern the process of bubble formation and subsequently affect the bubble size including static/flow condition of the liquid phase, physicochemical properties such as liquid density, viscosity, surface tension, and the polar or non-polar nature of the liquid phase. In addition, the dimensions of the pores, pore configuration, and material (Kulkarni and Joshi, 2005) will affect the size. Smaller bubbles have a longer residence time in the bubbly liquid due to its slower rise velocity which leads to a longer contact time between gas and solid phases and consequently enhances the collection efficiency of microalgae particles. Moreover, the rise velocity of a spherical bubble in a liquid is retarded by the existence of surface active materials in which small amounts are enough to render the bubble surface more rigid (Manica *et al.*, 2016). The smallest average bubble size produced had a Sauter mean diameter of 811 µm at 0.5 L min^{-1} air flow rate and 40 mg L^{-1} CTAB concentration, while the largest had a Sauter mean diameter of 1713 µm at 2 L min^{-1} air flow rate and 20 mg L^{-1} CTAB concentration.

The effect of both surfactant concentration and air flow rate on the bubble rise velocity is shown in figure 5.2b. Higher bubble rise velocity was observed at higher air flow rate and lower surfactant concentration. This was due to the larger superficial gas velocity and bubble size produced at these operating conditions which also increased the Reynolds number as shown in figure 5.5c. A range of Reynolds number between 79 and 334 was determined in this work which allowed for different flow regimes of liquid flow around the rising bubbles. The minimum bubble Reynolds number was 79 at a bubble rise velocity of 9.5 cm sec^{-1}, surfactant concentration of 20 mg L^{-1}, and air flow rate of 0.5 L min^{-1} whereas the maximum bubble Reynolds number was 334 at a bubble rise velocity of 20.6 cm sec^{-1}, surfactant concentration of 20 mg L^{-1}, and air flow rate of 2 L min^{-1}.

The recovery of microalgae by bubbles depends greatly on the amount of bubble surface available. Therefore, the effect of air flow rate on the particle collection rate can be assessed based on the specific bubble surface which is similar to the specific area used in heat and mass transfer studies. The ratio between the superficial gas velocity (J_g) and the Sauter mean bubble diameter (d_{32}) is known as the bubble surface area flux (S_b) and can be calculated according to equation 5.12 (Bouchard *et al.*, 2009). S_b has been widely used for describing the dispersion efficiency of the gas phase in flotation machines and advocated as a key process factor (Leiva *et al.*, 2010).

$$S_b = \frac{6.J_g}{d_{32}} \quad \ldots (5.12)$$

The contour plot for the bubble surface area flux at different CTAB concentrations and air flow rates is shown in figure 5.4. From this figure, it can be seen that both higher air flow rate and CTAB concentration produce larger bubble surface area fluxes.

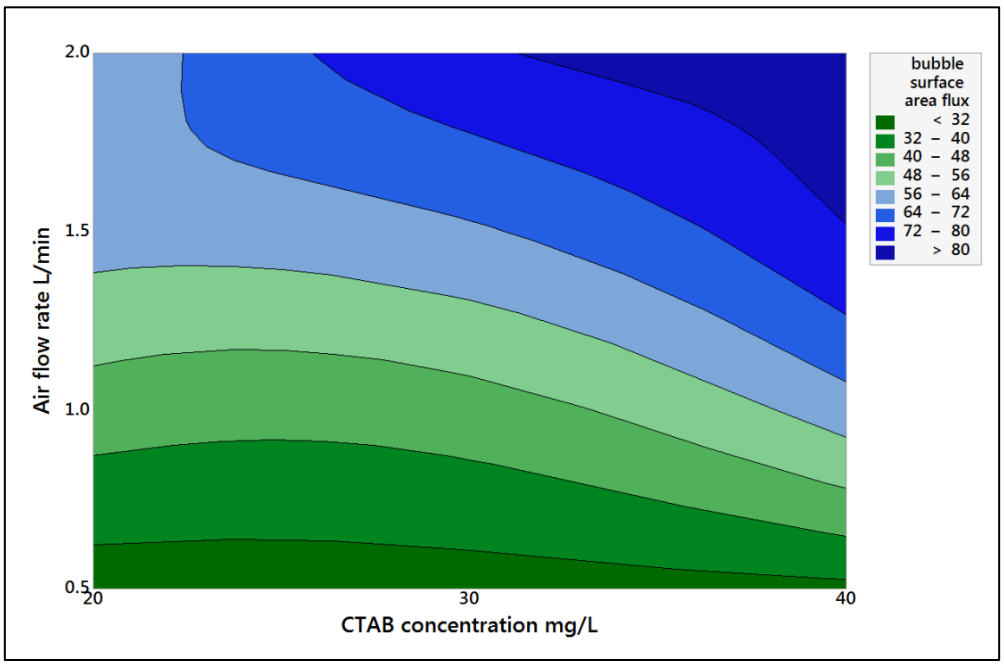

Figure 5.4: Contour plots for the bubble surface area flux within the liquid pool of the foam flotation column under 20, 30, and 40 mg L^{-1} CTAB concentrations and 0.5, 1, 1.5, and 2 L min^{-1} air flow rates

5.3.2 Collection efficiency of microalgal strains in foam flotation column

It was proposed by Derjaguin and Dukhin in 1961 that the collection or capture efficiency (E_{col}) of a particle by a gas bubble in the collection zone of a flotation machine was equal to the product of bubble-particle collision (E_c), attachment (E_a), and the stability of particle-bubble aggregate (E_s) efficiencies as given previously by equation 5.1 (Derjaguin and Dukhin, 1961). The collection efficiency of microalgae cells by air bubbles was studied theoretically in this chapter based on experimental measurements of bubble size, bubble rise velocity and microalgae cell size for better understanding of the flotation process and to compare the experimental and theoretical recovery efficiencies.

5.3.2.1 Bubble-particle collision efficiency

Before particle and bubble attachment can occur, they first should undergo an adequately close encounter (within the range of attractive surface forces). This process is governed by the hydrodynamics controlling their approach in the bubbly liquid zone. Inertial, gravitational, and hydrodynamic drag forces are the main forces in addition to Brownian diffusion that influence

the motion of particles in their trajectories and may deviate them from fluid streamlines. Figure 5.5 shows four particle-bubble collision mechanisms including gravity, inertia, interception, and Brownian diffusion. For coarse particles which have densities greater than that of the fluid surrounding the rising bubbles, particles have a certain settling velocity and cannot follow fluid streamlines. Therefore, the trajectory of particles deviates from fluid streamlines as in the inertia collision mechanism or after a very short time as in the gravity collision mechanism and collide directly with the bubble surface. On the other hand, the collision mechanism by interception occurs when a flow of liquid surrounding the rising bubbles carries the fine particles along the fluid streamlines and causes the collision between particles and bubbles due to the former finite size. The last mechanism, Brownian diffusion, is only significant for particles with sizes smaller than several microns that move randomly in the bubbly liquid (Ralston *et al.*, 1999; Dai *et al.*, 2000; Miettinen *et al.*, 2010).

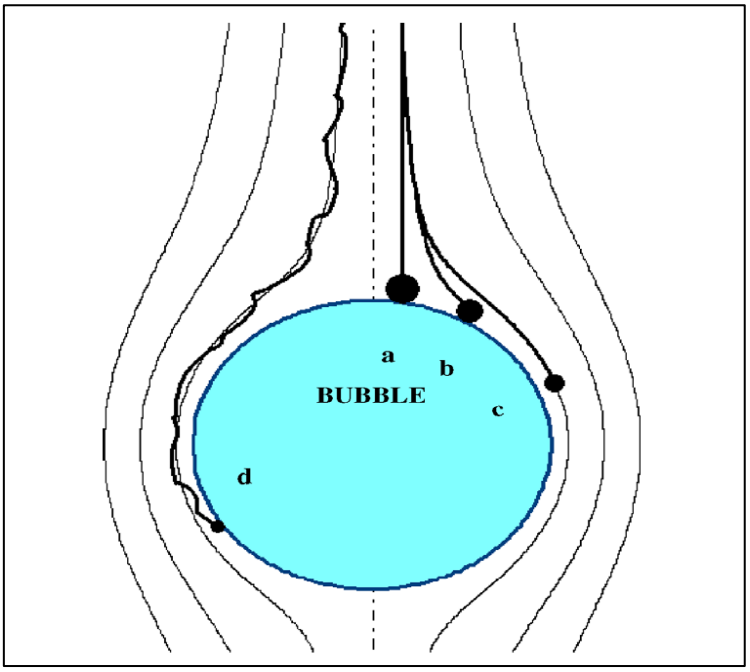

Figure 5.5: Schematic representation of four particle-bubble collision mechanisms, (a) inertia, (b) gravity, (c) interception, and (d) Brownian diffusion. The particle trajectories are in thick lines whereas the fluid streamlines are in thin lines

Derjaquin et al. (1984) stated that the inertial forces and the long-range hydrodynamic interaction i.e. hydrodynamic drag forces, mainly govern the transfer of small particles to the bubble surface (Derjaguin *et al.*, 1984). However, the inertial forces, as described earlier, dominate in the case of large and dense particles. The dimensionless Stokes number (St) which is calculated according to equation 5.13, can be used to illustrate the shape of the particle trajectory in the fluid flow and discriminate between collision mechanisms.

$$St = \frac{\rho_p u_b d_p^2}{9 d_b \mu} \ldots (5.13)$$

In equation 5.13, ρ_p and d_p are the density and diameter of the particle; u_b and d_b are the velocity and diameter of the bubble respectively; and μ_f is the viscosity of the fluid. As *C. vulgaris* has a small average particle size (7.44 ± 0.42 μm), the calculated Stokes number for all bubble sizes and rise velocities was in the range of 6.3×10^{-4} to 1.1×10^{-3} (i.e. $St << 1$) and consequently it was concluded that inertial forces had no effect on the motion of microalgae particles and interception was the dominant collision mechanism.

Inside flotation cells, the process of collecting particles by bubbles occurs under a complex flow and in an intensively agitated environment. However, the efficiency of particle-bubble collision can be calculated using stream functions when the fluid streamlines around the bubble are considered to be at more quiescent conditions, for example potential flow, rather than highly turbulent conditions. The turbulent flow makes the motion of particles and bubbles inside the flotation machine more complicated and hence difficult to analyse. Moreover, such quiescent conditions are more acceptable in column flotation since no external mixing is used. The streamlines are the trajectories that fine particles follow through encounter with bubbles. The stream functions under different flow conditions including Stokes, intermediate or potential flow conditions can be determined by solving the Navier-Stokes equation analytically. The general bubble-particle collision efficiency model (E_c) is shown in equation 5.14, where d_p is the particle diameter; d_b is the bubble diameter; n and A are parameters that depend on the flow conditions which can be evaluated by the bubble Reynolds number as given in table 5.1 (Miettinen *et al.*, 2010; Shahbazi *et al.*, 2010).

$$E_c = A\left(\frac{d_p}{d_b}\right)^n \ldots (5.14)$$

No.	Flow regime	Flow condition	A	n
1.	Stokes	$Re_b << 1$	$\frac{3}{2}$	2
2.	Intermediate	$1 < Re_b < 100$	$\frac{3}{2} + \frac{4Re_b^{0.75}}{15}$	2
3.	Potential	$100 < Re_b < 500$	3	1

Table 5.1: A and n values for different flow regimes.

The bubble-particle collision efficiency was calculated at different CTAB concentrations (20, 30, and 40 mg L^{-1}) and air flow rates (0.5, 1, 1.5, and 2 L min^{-1}) using equation 5.14 with the

values of parameters n and A from table 5.1. The bubble Reynolds number obtained previously had a range from 79 to 334, therefore, the flow regimes of liquid around a rising bubble were of the intermediate and potential types. The contour plot of the bubble-particle collision efficiency is shown in figure 5.6 for different CTAB concentrations and air flow rates. The smallest collision efficiency was 0.062% and was observed under intermediate flow conditions with a bubble Reynolds number of 79, CTAB concentration of 20 mg L^{-1}, and air flow rate of 0.5 L min^{-1}, whereas the largest collision efficiency was 2.75% and was observed under potential flow conditions with a bubble Reynolds number of 109, CTAB concentration of 40 mg L^{-1}, and air flow rate of 0.5 L min^{-1}.

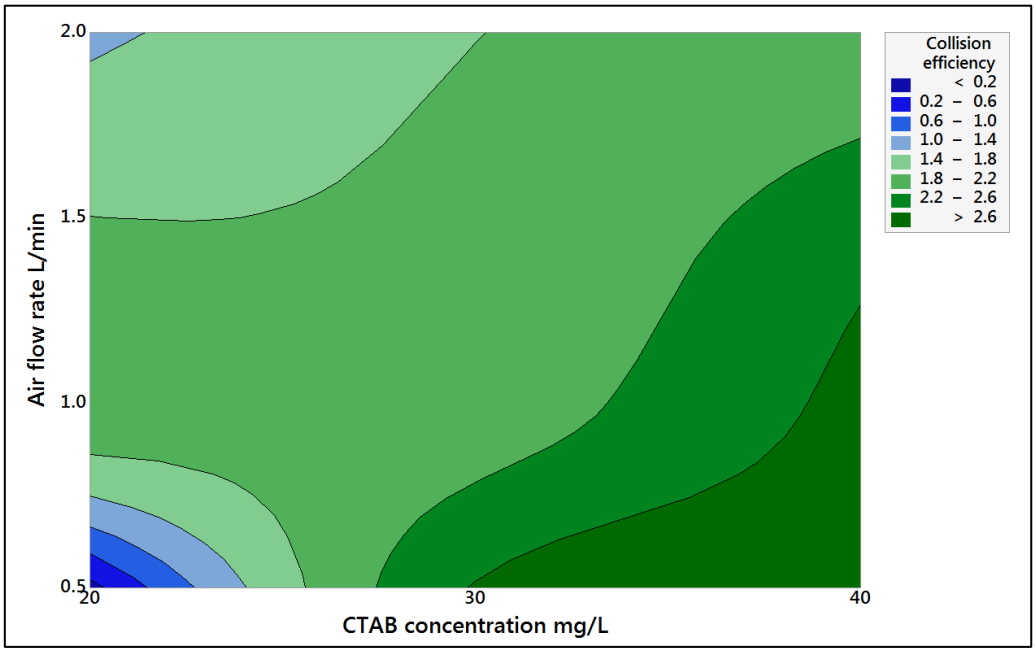

Figure 5.6: Contour plots for the bubble-particle collision efficiency within the liquid pool of the foam flotation column under 20, 30, and 40 mg L^{-1} CTAB concentrations and 0.5, 1, 1.5, and 2 L min^{-1} air flow rates

From equations 5.11, 5.13 and 5.14, it is obvious that both particle and bubble sizes are the main factors affecting the collision efficiency in addition to the particle density as well as bubble rising velocity. Higher collision efficiency favours smaller bubble sizes and higher particle sizes. Therefore, the largest collision efficiency herein was obtained at higher CTAB concentration and lower air flow rate as both variables at these conditions produced smaller bubble sizes (Figure 5.6). Potential flow, with a collision efficiency of 2.75%, appears to be more advantageous over the intermediate flow in which collision efficiency is 0.062%. Particle density and bubble rise velocity increase the Stokes number and consequently will change the dominant collision mechanism from interception to inertia or gravity. Bubble rise velocity also

has the ability to change the liquid flow conditions at the bubble surface. The present work did not illustrate the effect of microalgae cell size on the collision efficiency since only the average value of microalgae cell size was used. However, some aggregations among microalgae cells were noticed under the microscope after CTAB addition. This might be due to the charge neutralisation of the algal cells induced by the cationic surfactant. Nevertheless, the effect of the microalgae cell aggregations did not significantly increase the bubble-particle collision efficiency.

5.3.2.2 Bubble-particle attachment efficiency

Bubble-particle attachment efficiency has generally been studied and modelled regarding contact and induction times in which the attachment of a bubble to a particle takes place when the contact time between the bubble and particle is longer than the induction time. In comparison with the available collision models, the number of bubble-particle attachment models is very limited owing to the difficulties in measuring the quantities used in attachment models such as the induction time. In the flotation process, when a particle and a bubble are in close vicinity, an intervening liquid film is formed between them. This film is usually unstable when the particle is hydrophobic and therefore it tends to become thinner until a stable three-phase contact line is formed. The contact time (t_{con}) is defined as the time when both the particle and the bubble are in contact after their collision, whereas the induction time (t_{ind}) is defined as the time required for the thinning of the liquid film between the bubble and particle, film rupture, and the formation of the equilibrium three-phase contact line (A. V. Nguyen *et al.*, 1997; Dai *et al.*, 1999; Miettinen *et al.*, 2010). Yoon and Luttrell in 1989 reported that the formation of the stable three-phase line of contact is very short for hydrophobic and fine particles. They also assumed that the time for liquid film rupture is of 10^{-9} s order (Yoon and Luttrell, 1989). Therefore, only the first part in the above sequence that is the time for the liquid film to thin is the most important component of time induction

Previous studies have demonstrated that induction time decreases with decreasing particle size and increasing surface hydrophobicity of the particle. Experimental as well as theoretical studies showed that the induction time (sec) varied with particle size according to a power function relationship as shown in equation 5.15 (Ye and Miller, 1988; Dai *et al.*, 1999).

$$t_{ind} = Ad_p^B \ldots (5.15)$$

Where: A is a parameter that depends inversely on the particle contact angle; and B is a parameter, with a value of 0.6, independent of bubble size, particle size and contact angle. Based on the results from Dai et al. (Dai *et al.*, 1999), the parameter A was considered by the present

researchers to have the following relation with the particle contact angle ($A = 6/\theta_{ca}$), where: θ_{ca} is the contact angle of *C. vulgaris* in degrees. The contact angle of *C. vulgaris*, in the form of algal strata on membrane filters, was measured based on the sessile drop technique as described previously (see 3.2 materials and methods). The contact angle value was used to calculate the induction time. The measured contact angles of *C. vulgaris* cells and the calculated induction times at different CTAB concentrations are shown in figure 5.7.

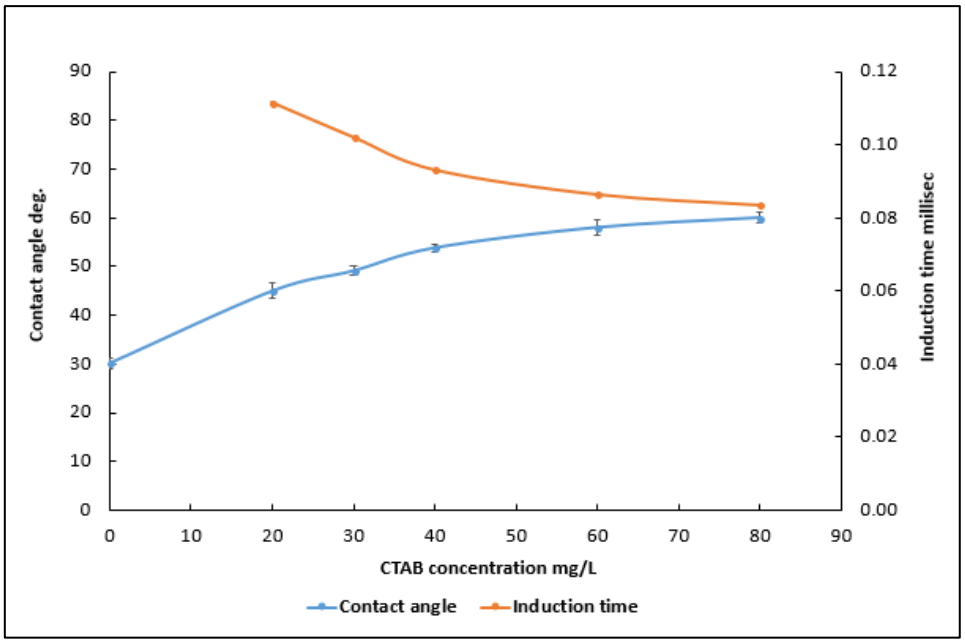

Figure 5.7: The contact angle of *Chlorella vulgaris* and induction time at different CTAB concentrations.

On the other hand, the contact time is linked to the bubble-particle collision. When a particle with high kinetic energy impacts a bubble surface, it may cause a significant distortion on the bubble surface and consequently the particle may rebound from the bubble surface because of the elastic energy of the deformed part of the surface. However, it has been suggested that the rebound of particle from bubble surface was negligible for small particles (< 100 µm) due to their very small kinetic energy (Dobby and Finch, 1987). After impact, the particle slides along the bubble surface. In essence, the contact time is the sum of the impact time and sliding time. However, the impact time for small sized particles is smaller than the sliding time (Schulze and Gottschalk, 1981; Schulze, 1989), thus this work suggested that the effects of bubble surface distortion and rebound of particle from the bubble surface was small, therefore, the contact time was equal to the sliding time. The sliding time (t_{sl}) in seconds can be determined according to the model derived by Dobby and Finch in 1986 (Dobby and Finch, 1986).

$$t_{sl} = -\frac{d_p + d_b}{2(u_p + u_b) + u_b\left(\frac{d_b}{d_p + d_b}\right)^3} \ln\left(tan\frac{\theta_c}{2}\right) \ldots (5.16)$$

Where: u_p is the particle settling velocity, calculated using Stokes' law (equation 5.17); θ_c is the angle of collision, calculated using equation 5.18 (Nguyen-Van, 1994; Anh V. Nguyen *et al.*, 1998).

$$u_p = \frac{(\rho_p - \rho_f) g d_p^2}{18\mu} \ldots (5.17)$$

$$\theta_c = cos^{-1}\left(\frac{\sqrt{(X + C)^2 + 3Y^2} - (X + C)}{3Y}\right) \ldots (5.18)$$

Where: X, Y, C are dimensionless parameters and only dependent on the bubble Reynolds number; g is the acceleration due to gravity. X, Y, C are calculated using the following relationships:

$$X = \frac{3}{2} + \frac{9Re}{32 + 9.888Re^{0.694}}$$

$$Y = \frac{3Re}{8 + 1.736Re^{0.518}}$$

$$C = \frac{u_p}{u_b}\left(\frac{d_b}{d_p}\right)^2$$

Another model can be used to determine the bubble-particle collision angle for bubble Reynolds number range between 20 and 400 as shown in equation 5.19.

$$\theta_c = 78.1 - 7.37 \log(Re_b) \ldots (5.19)$$

The collision angle between bubbles and particles varies between 60 and 64. It increased as the air flow rate and bubble Reynolds number decreased. The maximum collision angle was 64˚, obtained under intermediate flow conditions with bubble Reynolds number of 79, CTAB concentration of 20 mg L^{-1}, and air flow rate of 0.5 L min^{-1} whereas the minimum collision angle was 60˚, obtained under potential flow conditions with bubble Reynolds number of 334, CTAB concentration of 20 mg L^{-1}, and air flow rate of 2 L min^{-1}.

According to equation 5.16, the calculated sliding times or contact times for all CTAB concentrations and air flow rates were longer than the corresponding induction times indicating that the attachment of bubble-particle would take place under all operating conditions, that is

to say the thin film would rupture and the stable three-phase contact line would form between the microalgae particle and air bubble. The shortest sliding time of 0.9 millisecond was obtained at a CTAB concentration of 40 mg L^{-1} and air flow rate of 1 L min^{-1} whereas the longest sliding time of 1.5 millisecond was obtained at a CTAB concentration of 20 mg L^{-1} and air flow rate of 0.5 L min^{-1}.

Bubble-particle attachment efficiency (E_a) can be approximated using the generalised model proposed by Nguyen et al. (1998) (Anh V. Nguyen *et al.*, 1998) as presented in equation 5.20.

$$E_a = sech^2\left(\frac{2u_b A t_{ind}}{d_p + d_b}\right) \dots (5.20)$$

Where:

$$A = \frac{u_p}{u_b} + 1 + \frac{1}{2}\left(1 + \frac{d_p}{d_b}\right)^{-3}$$

Attachment efficiencies close to unity were obtained under all experimental conditions demonstrating that microalgae-bubble attachment would occur as the comparison between the contact time and induction time had showed. The maximum attachment efficiency occurred under intermediate flow conditions with a bubble Reynolds number of 79, CTAB concentration of 20 mg L^{-1}, and air flow rate of 0.5 L min^{-1}.

5.3.2.3 Bubble-particle stability efficiency

Particle size, particle hydrophobicity, and external detaching forces such as inertial and gravitational forces are the main factors that affect the stability of bubble-particle aggregates. For flotation of fine particles in flotation machines, the stability efficiency of bubble-particle aggregate is often considered as negligible (Miettinen *et al.*, 2010). Therefore, for the flotation of *C. vulgaris* in a foam column, the stability efficiency of bubble-particle aggregate was neglected, i.e. $E_s = 1$ as *Chlorella* species have small cell sizes and no intensive turbulent agitation existed in the foam column.

After calculating the collision and attachment efficiencies between microalgae particles and air bubbles, the collection efficiencies of microalgae particles by air bubbles at different experimental conditions were calculated using equation 5.1. According to figure 5.8, the collection efficiencies demonstrated that it was difficult to float microalgae particles due to the low collision efficiencies between microalgae particles and bubbles. The largest collection efficiency was 2.74% and obtained under potential flow conditions with a bubble Reynolds number of 109, CTAB concentration of 40 mg L^{-1}, and air flow rate of 0.5 L min^{-1} whereas the

smallest collection efficiency was 0.06% and obtained under intermediate flow conditions with a bubble Reynolds number of 78, CTAB concentration of 20 mg L^{-1}, and air flow rate of 0.5 L min^{-1}. These results showed that the effect of surfactant concentration on the microalgae recovery was higher than the effect of air flow rate. CTAB has a pronounced influence on the air bubble size as well as particle surface forces i.e. hydrophobic and electrostatic forces (see 3.3 results and discussion) and consequently it affects both the collision and attachment efficiencies.

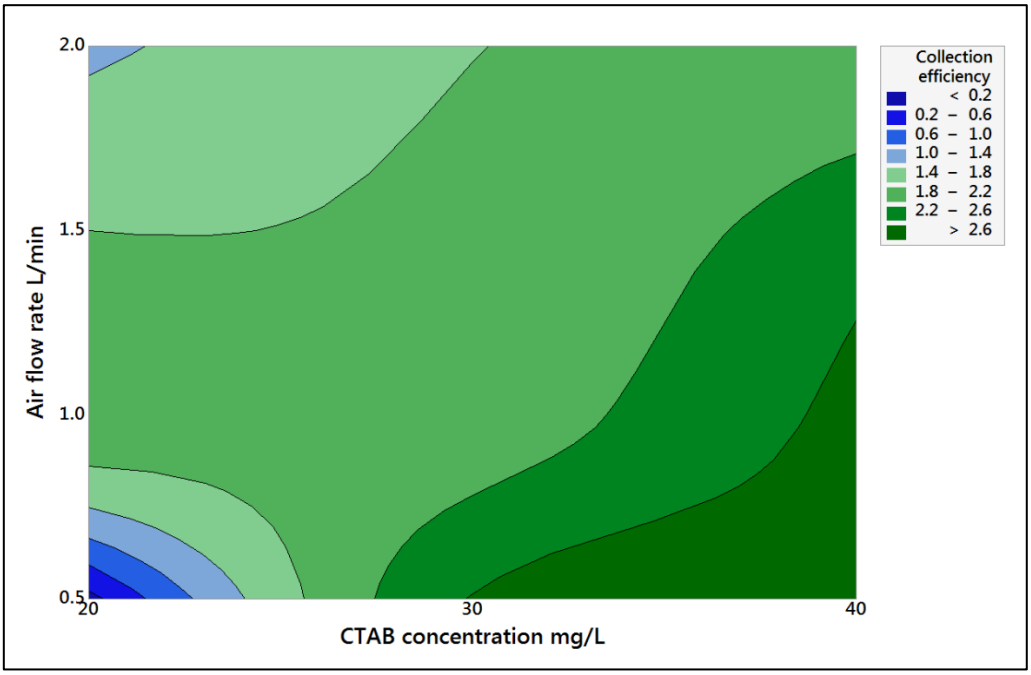

Figure 5.8: The contour plot for the collection efficiency of microalgae particle by air bubble within the liquid pool of the foam flotation column under 20, 30, and 40 mg L^{-1} CTAB concentrations and 0.5, 1, 1.5, and 2 L min^{-1} air flow rates

5.3.3 Calculation of the flotation rate constant for continuous flotation of microalgae

As mentioned in section 5.1, kinetic models for flotation processes are based on analogy with chemical reaction kinetics. In this work, the recovery of microalgae in the bubbly liquid zone is modelled by a first-order rate process using previous empirical correlations. It is a function of three parameters: flotation rate constant (k), microalgae particle retention time, and degree of axial mixing; that is to say, it generally takes the form of equation 5.21 (Dobby, 1984).

$$R = R_{\infty} f\left(k, \tau_p, Pe_p\right) \dots (5.21)$$

Where: τ_p is the particle residence time (s) and Pe_p is the equivalent particle Peclet number (S. Dobby and A. Finch, 1986).

$$Pe_p = \frac{(J_l + u_p)h}{Di} \dots (5.22)$$

Where: J_l is the liquid superficial velocity (cm s^{-1}), h is the liquid pool depth (cm), and Di is the axial dispersion coefficient (cm^2 s^{-1}). The particle settling-velocity (u_p) can be calculated using Masliyah's relationship (Masliyah, 1979).

$$u_p = \frac{g d_p^2 (1 - \varepsilon_G)^{2.7} (\rho_p - \rho_l)}{18\mu(1 + 0.15 Re_p^{0.687})} \dots (5.23)$$

The particle Reynolds' number (Re_p) can be calculated using equation 5.24:

$$Re_p = d_p u_p \varepsilon_l \frac{\rho_p - \rho_l}{\mu} \dots (5.24)$$

Where: ε_l, ε_G are the liquid and gas holdup in the liquid pool. The gas holdup measurements are shown in figure 5.9.

The flotation rate for the microalgae cells since they have, to a certain extent, a narrow size distribution, and similar shape and maybe surface properties, is expected to remain constant during the tests and a single value for k can be used instead of the distribution function of k. The particle residence time is dependent on the operation mode. If flotation operates in a continuous mode, it is the average retention time of the particle in the flotation environment. In this work, it is calculated according to equation 5.25 as well as 5.26 (Dobby, 1984; Kaya and Laplante, 1986).

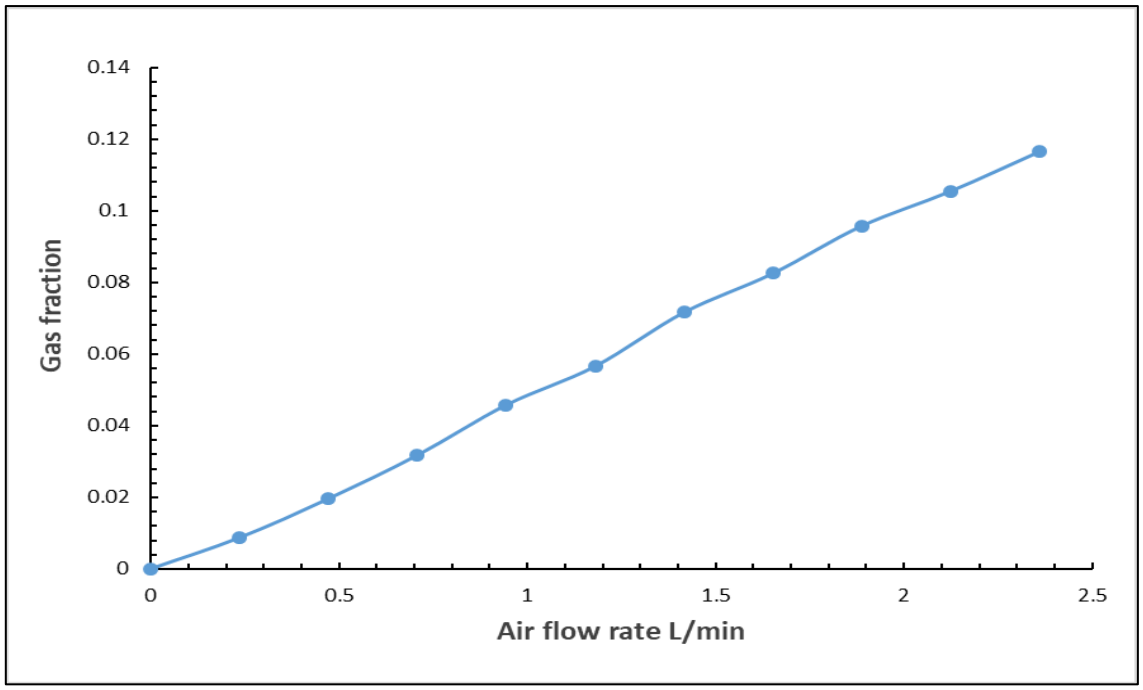

Figure 5.9: Gas holdup measurements

$$\tau_p = \frac{microalgae\ cells\ in\ the\ liquid\ pool\ (cells)}{discharge\ cell\ flow\ rate\ (cells/min)} \ldots (5.25)$$

$$\frac{\tau_p}{\tau_l} = \frac{J_l}{J_l + u_p} \ldots (5.26)$$

Where: τ_l is the liquid residence time and equal:

$$\tau_l = \frac{h(1 - \varepsilon_G)}{J_l}$$

However, both residence times (i.e. for particle and liquid) can be determined from residence time distribution experiments using particle and liquid tracers (Dobby and Finch, 1991). From equation 5.26, the particle residence time increases with decreasing particle size, to come close the liquid phase residence time.

The mixing characteristics within a flotation column are crucial in predicating recovery. There are two extremes of mixing which are plug flow and perfect mixing or fully mixed reactor. In plug flow, particles pass unmixed through the column meaning that the residence time of all elements of the fluid including the particles is the same. Therefore, a concentration gradient of floatable particles along the axis of the column exists (Dobby, 1984; Mills and O'Connor, 1990; Dobby and Finch, 1991; Mankosa *et al.*, 1992).

For a first order rate flotation system exhibiting plug flow and a retention time τ_p, the recovery is given by equation 5.27:

$$R = 1 - e^{-k\tau_p} \ldots (5.27)$$

In the other extreme (perfect mixing), there is a distribution of retention time (commencing with time zero) and the concentration is the same throughout the reactor. The recovery of a first order rate flotation system exhibiting perfect mixing is described by equation 5.28:

$$R = \frac{k\tau_p}{1 + k\tau_p} \ldots (5.28)$$

In the continuous mechanical flotation cells, the flow condition approximates perfect mixing where the discharge stream is considered to have the same concentration as the cell itself. In a laboratory flotation column, the flow condition would approximate plug flow while the liquid and solids in plant columns are transported under conditions between plug flow and perfectly mixed (Dobby, 1984). However, the difference in recovery between the two flow conditions is significant. For example, when $k\tau_p$ = 2.5, a recovery of 92% was obtained under plug flow

condition compared to 71% for perfectly mixed. Using a recovery model that comprises the liquid or particle degree of mixing is more precise. Therefore, the recovery model by Wehner and Wilhelm (1956) (equation 5.29), which is the analytical solution of the axial dispersion model was used in this work to calculate the flotation kinetic constants (Wehner and Wilhelm, 1956; Satterfield, 1973).

$$R = 1 - \frac{4ae^{\frac{Pe_p}{2}}}{(1+a)^2 e^{\frac{aPe_p}{2}} - (1-a)^2 e^{\frac{-aPe_p}{2}}} \dots (5.29)$$

Where:

$$a = \sqrt{1 + \frac{4k\tau_p}{Pe_p}} \dots (5.30)$$

Equation 5.29 can be simplified to 7.25 and 7.28 when the Peclet number approaches infinity (plug flow) and zero (perfect mixing) respectively. It is clear from equation 5.29 that both the kinetic rate constant and the mixing conditions are crucial factors to be considered to scale up flotation columns.

Dobby and Finch's model (1986) (equation 5.31) was used in this work for calculating Peclet number (S. Dobby and A. Finch, 1986). This model was used rather than conducting experiments to obtain our own model because it can estimate the Peclet number for a wide range of column diameters, column heights, superficial gas and liquid velocities. It is typical for the current column dimensions and operating conditions.

$$Pe = 18.28\frac{h}{D}\left[\frac{J_l}{1-\varepsilon_g} + u_p\right] J_g^{-0.3} \dots (5.31)$$

Where: D is the column diameter (cm). The equation 5.29 was then solved to determine flotation rate constants at different air flow rates and CTAB concentrations. The relationships between the air flow rate and CTAB concentration with the recovery efficiency and flotation rate constant are shown in figures 5.10 and 5.11 respectively. As the previous results have shown, the recovery efficiency of microalgae cells increases with increasing air flow rate and CTAB concentration. The positive effect of the air flow rate and CTAB concentration on the recovery of microalgae (Figure 5.10) is due to higher bubble surface area flux (S_b) for adsorption rather than bubble size as discussed earlier.

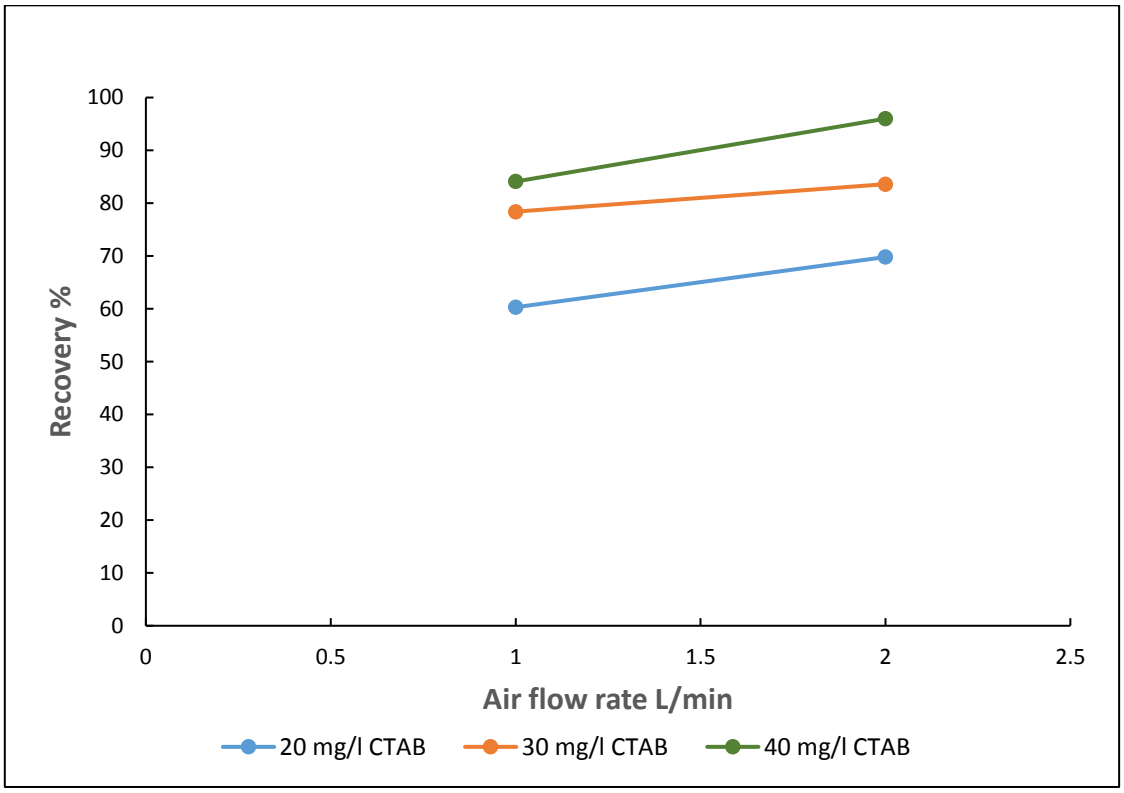

Figure 5.10: The recovery efficiency of microalgae particle by air bubbles under 20, 30, and 40 mg L^{-1} CTAB concentrations and 1 and 2 L min^{-1} air flow rates.

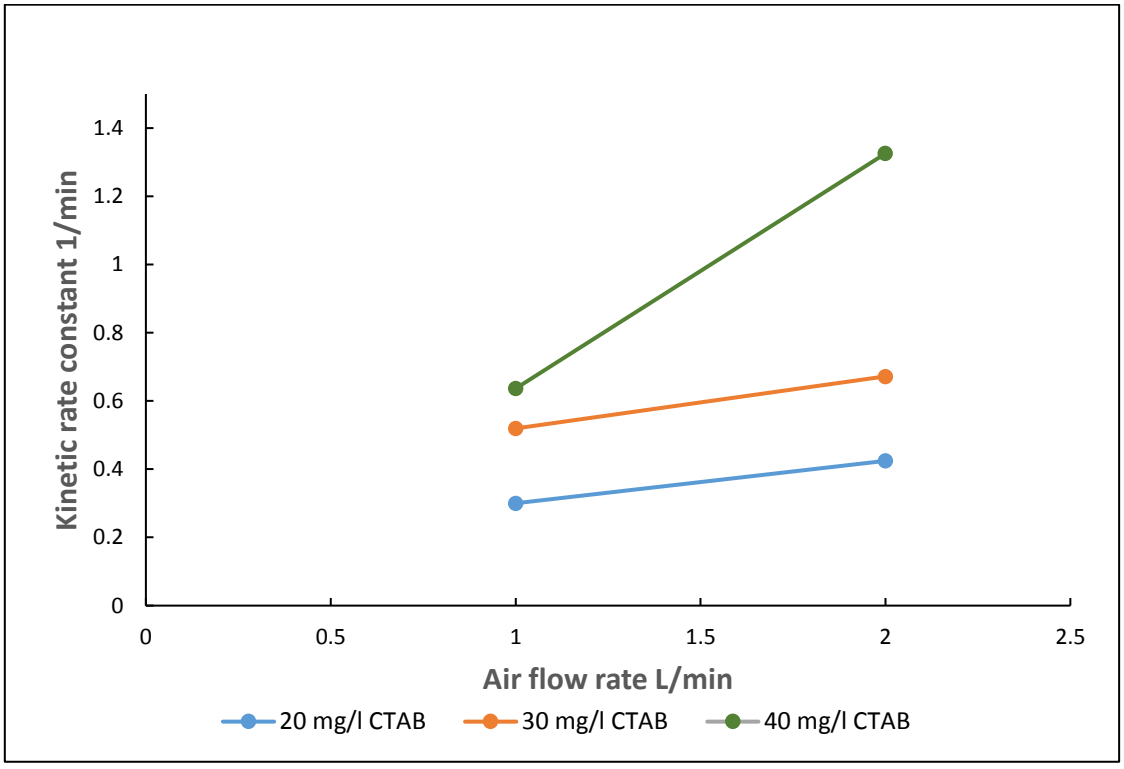

Figure 5.11: flotation rate constant in continuous flotation under 20, 30, and 40 mg L^{-1} CTAB concentrations and 1 and 2 L min^{-1} air flow rates.

The flotation rate constant also increases as air flow rate and CTAB concentration increases. The increase in the flotation kinetic rate constant is probably due to the same reason above (i.e. the increase in the total bubble surface area flux).

To compare between the recovery efficiencies obtained experimentally and theoretically, the calculated collection efficiencies were converted to recovery efficiencies using Nguyen's model (equation 5.32) (A. V. Nguyen and Schulze, 2004).

$$R = 1 - \exp\left[-E_{col} * \left(1 + \frac{u_p}{u_b}\right)\right] \dots (5.32)$$

The obtained theoretical recovery efficiencies were not in agreement with the experimental data for the recovery efficiencies as set out in table 5.2. High cell recovery efficiencies were obtained indicating that there may be other forces between microalgae particles and air bubbles such as electrostatic forces not considered in the published collision models used in this work. For example, the collision model proposed by Reay and Ratcliff in 1973 and 1975 (Reay and Ratcliff, 1973; Reay and Ratcliff, 1975) which is similar to the general collision model presented in equation 5.14 only worked well for electrically uncharged particles such as glass beads. The model has n and A values of 1.9 and 1.25 when both particle and liquid densities are similar and n and A values of 2.05 and 3.6 when particle to liquid density ratio is of 2.5. Therefore, long-range interaction forces between particle and bubble surfaces may need to be taken into account in the collision models for algae cells with bubble surfaces. Moreover, microalgae are deformable and can also support mobile surface charge distribution. Therefore, the nature of the interaction between microalgae and gas-liquid interfaces is distinctly different from hard spheres with uniform charge distribution. Furthermore, the measurements of the liquid holdup in the rising foam (see chapter 4.3 results and discussion) demonstrated that the onset zone of the foam (10 cm above the pool/foam interface) was very wet with a liquid holdup range of 0.9 to 0.1. Consequently, and owing to more quiescent conditions at that foam zone than those in the bubbly liquid, the trajectories that microalgae cells in the liquid accompanying the rising foam (i.e. hydraulically entrained cells) follow through encounter with foam bubbles are probably different and lead to improved collision efficiencies. This is another possible explanation to elucidate the distinction between experimental and theoretical recovery efficiencies (Table 5.2).

Another evidence that supports the experimental recovery efficiencies achieved in this work can be introduced through calculating bubble coverage by particles. The gas holdup in the bubbly liquid at an air flow rate of 2 L min^{-1} was 0.1. The number of gas bubbles (N_b) at an air

flow rate of 2 L min^{-1} can be then calculated based on the total gas volume (V_g) and the volume of a gas bubble (V_b).

Experimental trial conditions		Experimental recovery efficiency %	theoretical recovery efficiency %
CTAB Conc. mg/L	Air flow rate L/min		
20	1	60.3	2
20	2	69.8	1.3
30	1	78.4	2.2
30	2	83.6	1.9
40	1	84.1	2.4
40	2	96	1.9

Table 5.2: Comparison between the experimental and theoretical recovery efficiencies at different experimental conditions.

$$V_g = N_b * V_b \ldots . (5.33)$$

$$\pi r_c^2 h_g = N_b * \frac{4}{3} \pi r_b^3$$

Where: r_c is the radius of the flotation column (2.58 cm); $h_g$is the gas height in the flotation column (2.78 cm) and it was calculated from the gas holdup (ε_G = 0.1); and r_b is the average radius of bubbles generated at an air flow rate of 2 L min^{-1} and a CTAB concentration of 40 mg L^{-1} (0.12 cm).

$$N_b = 8.03 * 10^3 \; bubbles$$

Total surface area of gas bubbles (A_g) can be calculated using equation 5.34

$$A_g = N_b * 4 * \pi * r_b^2 \ldots (5.34)$$

$$A_g = 1.45 * 10^3 \; cm^2$$

During the foam flotation process, the total number of microalgae cells entering the column (N_{mf}) is equivalent to the summation of cells attached to gas bubbles (N_{mg}) and cells dispersed in liquid (N_{ml}) as presented in equation 5.35.

$$N_{mf} = N_{mg} + N_{ml} \ldots (5.35)$$

At an air flow rate of 2 L min^{-1} and a CTAB concentration of 40 mg L^{-1}, a recovery efficiency of 96% was obtained which means 9.2×10^8 cells were in touch with the gas bubbles compared to 3.82×10^7 cells dispersed in liquid. The total cross-sectional area of microalgae cells of average radius of 3.72*10^{-4} cm (r_m) can be written using the bubble coverage (B_c) as follows:

$$N_{mg} * \pi * r_m^2 = B_c * A_g$$

$$B_c = \frac{9.2 * 10^8 * \pi * (3.72 * 10^{-4})^2}{1.45 * 10^3} = 0.28$$

The maximum theoretical bubble coverage of a flat surface by particles of equal sizes is 0.906 and it is considerably larger than the calculated bubble coverage by microalgae cells (0.28), indicating that the gas bubbles produced at the operating conditions of air flow rate of 2 L min^{-1} and CTAB concentration of 40 mg L^{-1} can recover that percentage of microalgae cells (96%).

5.4 Conclusion

Foam flotation is an attractive technique for recovering and concentrating algal biomass from culture medium. However, the development of mathematical models for the flotation process has proven difficult due to interactions between solid, gas, and liquid phases within the process. Therefore, kinetic models and probability models were adopted in this work to get a better insight into the events in the flotation process of microalgae. A wide range of bubble sizes were generated with Sauter mean dimeters ranging from 811 to 1713 µm under different CTAB concentrations and air flow rates. The smallest bubble size of 811 µm was obtained at a CTAB concentration of 40 mg L^{-1} and an air flow rate of 0.5 L min^{-1} whereas the largest bubble size of 1713 µm was obtained at a CTAB concentration of 20 mg L^{-1} and an air flow rate of 2 L min^{-1}. The Sauter mean bubble diameter decreased with increasing CTAB concentration whereas it increased with increasing air flow rate. Based on the calculated bubble Reynolds number under different operating conditions, the flow of liquid around the rising bubble surface either obeyed intermediate or potential flow conditions. The calculations for collision, attachment, and detachment efficiencies between *C. vulgaris* and air bubbles demonstrated that microalgae cells had low collision efficiencies due to the small cell size resulting in low collection efficiencies. The bubble-microalgae particle attachment and stability efficiencies were at or close to unity due to the surface forces between air bubbles and cells, including electrostatic and hydrophobicity forces as well as small cell size. High attachment efficiencies were also predicted based on comparison between the contact time and induction time in which the latter was longer under all experimental trials. The recovery of microalgae and the flotation rate constant increased with air flow rate and CTAB concentration. This was probably due to the increase in the total bubble surface area flux. Good agreement between the theoretical and the experimental recovery efficiencies was not obtained in this work indicating that there may be other forces between microalgae particles and air bubbles not considered in the commonly used collision models.

Chapter 6

Direct hydrothermal liquefaction of microalgae *Chlorella vulgaris* harvested by foam flotation

Abstract

Direct hydrothermal liquefaction (HTL) of algal biomass without extra stages for dewatering and drying or intermediate storage can yield detailed information about the feasibility of this process as it represents a more realistic scenario for the application of HTL. Therefore, HTL of *C. vulgaris* recovered by the foam flotation process with solid loading of approximately 15% was accomplished directly at different temperatures and holding times. The fate of the cationic surfactant (CTAB) as well as its influence on the HTL product yield and distribution were also investigated and compared to those from the HTL of *C. vulgaris* recovered by centrifugation, which was adopted as a benchmark. CTAB in addition to three model compounds (starch, bovine serum albumin (BSA), and rapeseed oil) representative of the three macronutrients present in *C. vulgaris* (carbohydrate, protein, and lipid) were also liquefied individually to support interpretation of the results. CTAB was almost entirely converted into bio-oil by the HTL with a maximum yield of 98.97% at 320˚C.

Generally, higher bio-oil yields and lower water-soluble organics, solid residue, and gas product yields were obtained from the HTL of microalgae harvested by foam flotation compared to the centrifugation control. A maximum bio-oil yield of 50.54% was obtained at 300˚C reaction temperature and 10 min holding time. Direct HTL of harvested microalgae rather than pulverised or freeze-dried microalgae enhanced the conversion of biomass and increased the bio-oil yield at mild conditions when compared to literature values. Elemental CHN analysis, GC-MS identification, and FTIR spectra indicated that there was a reduction in nitrogen content in the bio-oil from the HTL of algal biomass recovered by foam flotation whereas hydrogen content was increased. Identified compounds included esters, fatty acids, hydrocarbons, ketones, aldehyde, and N-containing compounds. The recovery energy in the bio-oil from the HTL of microalgae harvested by foam flotation (73.5%) was higher than that for the centrifugation control (51.4%). Finally, different reaction pathways were also proposed and discussed in this work based on compounds and their chemical classes identified by the GC-MS analysis.

Chapter six

Keywords

Hydrothermal liquefaction; microalgae; foam flotation; bio-oil; biofuel

6.1 Introduction

The growing demand for and non-sustainability of conventional transportation fuels are major issues of global concern affecting energy security and the environment. Replacing petroleum fuels and products with similar products generated from renewable sources should eliminate most of these issues. Among several types of renewable energy resources such as solar energy, hydro and wind energy, biomass such as microalgae is plentiful, diverse, and considered a unique renewable source of energy that can be processed into liquid hydrocarbons. It can be converted chemically, thermo-chemically, and biologically into a wide range of biofuel products such as biodiesel and bioethanol (Pragya *et al.*, 2013; Shakya *et al.*, 2017). Microalgae have been branded as a third-generation source of biofuels and are considered a valuable biomass. Microalgae can play a vital role in the biofuel market due to their simple structures, fast growth rate, and higher lipid content. Microalgae do not occupy arable land and do not compete with food crops. They can be cultivated in freshwater, brackish, and seawater all year round (Wenchao Yang *et al.*, 2014; Golzary *et al.*, 2015). Obtaining an economic extraction of the lipid from the wet microalgae is one of the main challenges for microalgae-based biodiesel. The conventional approach for producing biofuels from algal biomass has been to select high-lipid yielding microalgae strains, which are subjected to an energy intensive drying, solvent extraction, and transesterification process to produce biodiesel. These steps are expensive and use organic solvents that are potentially toxic and which are produced using non-sustainable resources. The transesterification process requires high-lipid microalgae strains, which are slower growing than other strains, thus limiting the potential productivity of algal biomass and biofuels. Thermochemical conversions like hydrothermal liquefaction (HTL) are faster than the biochemical conversions (P. Biller and Ross, 2011a; López Barreiro *et al.*, 2013).

Amongst all processes for converting biomass into biofuels, HTL appears a promising technique that offers the advantage of being able to convert the entire biomass into a range of biofuels with oil productivity of a desirable quantity, compared to transesterification which only converts the lipids. For example, a bio-oil yield of 64% (DW) was obtained from the HTL of *Botryococcus braunii* at 300 ˚C (Dote *et al.*, 1994). HTL can be used to process biomass with a high water content, thus microalgae recovered by most dewatering harvesting techniques can be processed directly or only partial drying of the algal biomass may be required unlike

traditional thermochemical processes such as gasification and pyrolysis. This removes the major energy consumption associated with drying the biomass. This process is a synonym of hydrous pyrolysis; however, HTL is performed at lower temperatures and heating rates than pyrolysis. Low oxygen content and tar yield, and high-energy efficacy are other advantages of HTL over pyrolysis. On the other hand, bio-oils from HTL cannot be treated using conventional fossil fuel refineries due to their high nitrogen content and a hydro-treating process is necessary to upgrade the bio-oil and remove the nitrogen (Patrick Biller *et al.*, 2013; Wagner *et al.*, 2016; Gollakota *et al.*, 2018).

HTL is a biomass-to-liquid conversion process conducted in water temperatures typically in the range of 250-374 ˚C and high pressures in the range of 39-215 bar with or without the presence of a catalyst. HTL can also be performed at temperatures higher than the critical point of water (374 ˚C) but it has been found that the oil yield is reduced above the critical temperature (López Barreiro *et al.*, 2013). The density and dielectric constant of water changes when it is heated under pressure as shown in figure 6.1 (data was adopted from the steam table). As the water approaches its critical point, it acts more like a non-polar solvent with lower density, resulting in different properties that make the water more affinitive to organic compounds. The products from HTL are an energy-dense bio-oil, some gas which consists mainly of CO_2, a nutrient-rich aqueous phase, and residual solid. The bio-oil is of high energy density similar to that of fossil petroleum but it cannot be treated directly within a conventional oil refinery as mentioned earlier (Garcia Alba *et al.*, 2011; López Barreiro *et al.*, 2013; Anastasakis and Ross, 2015).

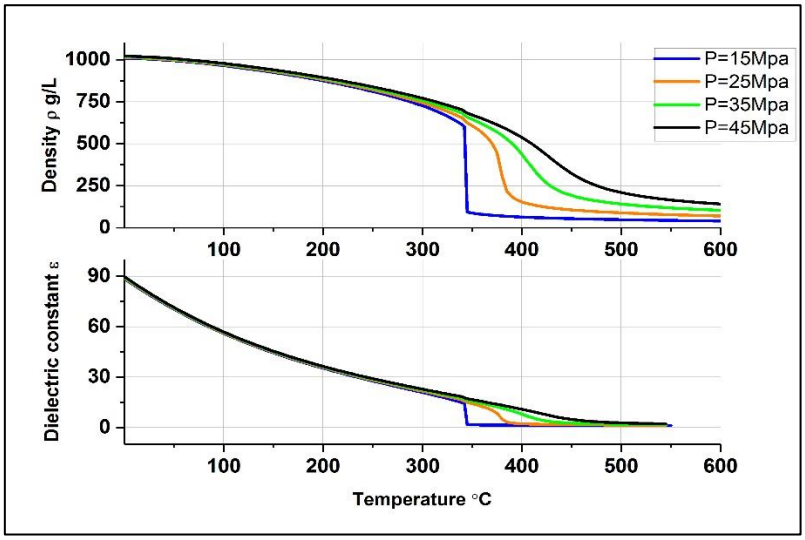

Figure 6.1: Water properties (density and dielectric constant) under different temperatures and pressures

In the last decade, interest in HTL of microalgae has increased significantly. A substantial number of papers have investigated the technology parameters such as temperature and reaction time on bio-oil yields and the other phases produced. Temperatures covering the entire HTL range and holding times in the range of 5-120 min have been investigated for different microalgae species including *Nannochloropsis* sp*, Botryococcus brabunii, and C. vulgaris*. The use of catalyst in this thermochemical process (including homogenous and heterogeneous catalysts) has also been studied (P. Biller *et al.*, 2011a; Duan and Savage, 2011).

Other researchers have studied the relationship between bio-oil yields from HTL of microalgae and the biochemical composition of the microalgae by studying and comparing HTL of various model compounds that represent the carbohydrate, protein, and lipid fractions of microalgae and HTL of three microalgae strains (*N. Oculata, C. Vulgaris, and P. Cruentum*). The authors proposed that the conversion efficiencies of different biochemical fractions to bio-oil were 55 to 80% for lipids, 11 to 18% for protein, and 6 to 15% for carbohydrate (P. Biller and Ross, 2011a). However, these outcomes were contradicted by the results from other researchers who obtained high bio-oil yields when low-lipid strains were used (Yu *et al.*, 2011). Vardon et al. (2011) investigated the relationship between bio-oil yields and the biochemical composition of *Arthrospira* (*Spirulina*). Again, the results confirmed the strong relationship between bio-oil yield and microalgae lipid content (Vardon *et al.*, 2011).

The majority of the previous HTL work, even if not stated explicitly, has been performed using pulverised-dried or freeze-dried microalgae mixed with deionised water (Shuping *et al.*, 2010; P. Biller *et al.*, 2011a; P. Biller and Ross, 2011a). Very few HTL trials were conducted with intact algal biomass as obtained from the culture medium (Valdez *et al.*, 2011; Vardon *et al.*, 2011; López Barreiro *et al.*, 2013). However, some have stored the wet algae as frozen slurry until it was used. Using microalgae in different physical states will probably affect the bio-oil composition and yield since the extractability of some constituents might change due to the pulverising and freeze-drying. Therefore, bio-oil yield and composition obtained from direct HTL of algae paste recovered by any harvesting technique without drying and storing is more meaningful.

Foam flotation, which is a subclass of adsorptive bubble separation, shows considerable promise as a microalgae biomass harvesting and enrichment method. Foam generated by surface-active materials (surfactants) represents an effective medium to adsorb microalgae as it possesses a high specific surface area, which results in a high recovery efficiency whilst only a

small volume of interstitial liquid is collected, enabling good biomass enrichment. In Chapter four, an average total suspended solid (TSS) of approximately 14.6% has been achieved by developing a continuous and low cost foam flotation harvester. Cationic hexadecyltrimethylammonium bromide (CTAB) was used as a surfactant during the harvesting trials (see 4.3 results and discussion).

Coward et al. (2014) investigated the effect of CTAB on the lipid content and fatty acid profiles of *C. vulgaris* harvested by a batch foam flotation column. They observed an increase in the total extractable lipid due to the solubilisation of the phospholipid bilayer by CTAB (T. Coward *et al.*, 2014). Borges et al. (2011) noticed higher percentages of C16:0, C16:1, and C20:5 fatty acids were recovered from both *N. oculata* and *T. weissflogii* after harvesting using anionic and cationic flocculants. They also noticed an increase of C14:0 and a decrease of C20:5 in the lipid recovered from *N. oculata* when an anionic flocculant was used (Lucelia Borges *et al.*, 2011).

The aims of this study are to investigate, for the first time, the direct HTL of microalgae harvested by foam flotation without extra stages for dewatering or drying and without biomass storage. This provides detailed information about the feasibility of the process and it represents a more realistic scenario for the application of HTL. An additional advantage of this work is that it will investigate the influence of CTAB, which is attached to microalgae biomass, on the bio-oil product yield and composition. HTL of microalgae recovered by centrifugation was performed as a benchmark (control). Model compounds (starch, bovine serum albumin (BSA), and rapeseed oil) representative of the three categories of biochemical compounds present in microalgae (carbohydrate, protein, and lipid) were processed individually by HTL to support interpretation of the results. Due to the absence of algaenan in *C. vulgaris* (an insoluble macro-polymer of hydrocarbons), the HTL processing of this compound in isolation was not performed in this study.

6.2 Materials and methodology

6.2.1 Microalgae culture

The growth conditions used for *C. vulgaris* have been described previously (see 4.2 materials and methods).

6.2.2 Harvesting experiments

The harvesting experiments for *C. vulgaris* have been described previously (see 4.2 materials and methods).

6.2.3 Materials and chemicals

The model lipid (rapeseed oil) was purchased from Henry Colbeck, UK. All other materials including starch, bovine serum albumin (BSA), CTAB, lab solvents, and chemicals for measuring total carbohydrate, protein, and lipids contents were purchased from Sigma-Aldrich, UK and used as received.

6.2.4 Characterisation methods

Higher Heating Values (HHV) of the biomass feedstock and bio-oils were measured by a Parr bomb calorimeter. Microalgae feedstock and bio-oils were also analysed for CHN content using an elemental analyser (Vario MACRO cube, UK). Sulphur content was assumed negligible due to its relatively small amount and oxygen content was calculated by difference. The ash content of the feedstock, model compounds, and bio-oils was measured as the residual fraction after combustion at 575 ˚C using a muffle furnace with a ramping program.

Total carbohydrate content for the microalgae feedstock was determined by the phenol-sulfuric acid method optimised by Mercz (1994) (Mercz, 1994). Total protein content for the microalgae was determined using the Lowery method and the total lipid content was determined gravimetrically using the Bligh and Dyer method (Moheimani *et al.*, 2013).

Total suspended solids (TSS) were measured for *C. vulgaris* harvested by both techniques to adjust the feed concentration (≈15%) before loading to the reactor. The harvested microalgae were placed in an aluminium dish and dried between 103 to 105 ºC for 24 hours. TSS was calculated using equation 6.1:

$$TSS = \frac{Wt_3 - Wt_1}{Wt_2 - Wt_1}\ 100\% \quad \cdots (6.1)$$

Where: Wt_1 is the aluminium dish weight (g); Wt_2 is the wet sample and dish weight (g); and Wt_3 is the dry sample and dish weight (g).

6.2.5 Apparatus and experimental procedure

HTL experiments were performed in a batch tubular reactor of 75 ml internal volume similar to those reported in the literature (Wagner *et al.*, 2016). The reactor was fabricated from

Swagelok stainless tubing and fitted with a pro K-type thermocouple (RS, UK), a vent valve, a pressure gauge, and a pressure relief valve as shown in figure 6.2; all were purchased from Swagelok, UK. In a typical HTL experiment, 20 ml of harvested microalgae slurry, approximately 15% total solid content, was charged to the reactor. Then, the reactor was securely sealed and inserted into a vertical tube furnace (Carbolite Gero, EVT 1200, UK), which was already preheated to 800 ˚C to achieve high heating rate. For the HTL of the model compounds and CTAB, 3 g of compound was mixed with 17 g of deionised water giving a mass fraction of 15%. Three different reaction temperatures (280, 300, and 320 ˚C), two holding times (0 and 10 min), and a heating rate of 32 ˚C/min were used to investigate the effect of reaction temperature and holding time on product yields. However, for the HTL of the model compounds and CTAB, only two reaction temperatures (300 and 320 ˚C) with no holding time were used. Previous work on the HTL of model compounds representative of those found in microalgae was performed at different batch holding times ranging from 10 to 60 mins. Therefore, in this work, the model compounds were processed with no holding time. All HTL reactions for the harvested microalgae and model compounds were carried out in duplicate. Mean values were reported in the results and the standard deviation was used as the uncertainty of the experimental trial. Batch holding time in the work (10 min) did not include the heating or cooling periods.

Figure 6.2: The batch HTL reactor (left) and the reactor inside the vertical tube furnace (right)

During the process, the pressure was autogenous due to the partial vaporisation of water and was monitored using the pressure gauge. According to the steam table of the saturated liquid water and pressure gauge readings, the maximum pressure was in the range of 63-112 bar under various trial sets. Following each trial, the reactor was washed and then further cleaned by heating 25 ml of deionised water to 230˚C and venting the produced steam through the vent valve. After completion of the HTL reaction, the reactor was removed from the furnace and allowed to cool to room temperature. The gas fraction was vented through the vent valve into a Tedlar gas sampling bag (Sigma-Aldrich, UK). Then, the reactor contents were poured through filter paper (Whatman, grade 42, Sigma-Aldrich, UK) using a vacuum filtration unit to recover water-soluble organics (can pass through the filter). The oil phase product was then separated by repeatedly washing out the reactor and solid residue with dichloromethane until the solvent remained clear. The oil-solvent mixture was decanted into a pre-weighed round bottom flask. Thereafter, the solvent was evaporated in a rotary evaporator and the flask was left overnight in a fume cupboard to eliminate any remaining solvent within the purified bio-oil. Filter paper with the solid residue was dried overnight in an oven (Memmert, Germany) and then stored in a desiccator over a desiccant (Silica Gel) until it was weighed.

6.2.6 Product yields and analysis

The chemical composition of the bio-oil fraction was analysed by gas chromatography-mass spectrometry (GC-MS, PerkinElemer Clarus500-560D) using an Elite-5MS capillary column, 30m length and 0.25mm inner diameter, and 0.25µm film thickness. The carrier gas was helium with flow rate set at 1.0 ml/min. The oven temperature was set at 40 ˚C, maintained for 5 min, and then increased at a rate of 5 ˚C min^{-1} to 250 ˚C with a final hold of 5 min. Mass detector inlet line and ion source temperatures were set to 150 and 180 ˚C respectively. The mass spectrometer was run in positive ionisation mode at 70 electron energy in m/z scan range of 30-600. Compounds were identified by comparing chromatogram spectra peaks with a mass-spectral library using NIST (National Institute of Standards and Technology).

The gas fraction composition was analysed in a gas chromatograph Varian 450-GC equipped with an Alltech Hayesep column (1.5m length and 2mm inner diameter), a thermal conductivity detector (TCD), and a flame ionisation detector (FID). Argon gas (mobile phase) was used as carrier gas through the column. Gas compositions were normalised after gas analysis to subtract oxygen and nitrogen gases that were not generated during the HTL reaction but likely introduced during feedstock loading to the reactor and/or when the gas products were sampled.

Fourier-transform infrared (FTIR) spectroscopic analysis was performed on model compounds (starch, BSA, and rapeseed oil), all microalgae feedstocks harvested by centrifugation and foam flotation, and bio-oils produced by the HTL of *C. vulgaris* harvested as above, as well to characterise their chemical functional groups. FTIR spectra herein were used as supporting data to the GC-MS analysis of HTL bio-oils. A FT-IR spectrophotometer (Agilent, Cary 630, UK) was used in absorbance mode over a range of 4000-650 cm^{-1} wavelengths. Each spectrum was collected after 50 scans at a resolution of 4 cm^{-1} in two replicates for each sample.

The product yields of the hydrothermal reaction were calculated using equation 6.2 except for water-soluble organic yield, which was calculated instead by difference. This was because of the difficulty in obtaining an accurate overall mass balance closure due to the design of the reactor (figure 6.2) when the water-soluble compound fraction was measured. The water phase yield was only determined with the HTL trials for starch due to difficulty in recovering all solid residue from the reactor. All product yields were determined on an ash-free dry basis (daf). HTL conversion was calculated according to equation 6.3, where M_{SR}, M_{Ash}, and M_{algae} are the masses of solid residue, ash in microalgae, and algal feedstock respectively.

$$Yields\ (wt.\%) = \frac{weight\ of\ the\ products\ (dry\ basis)}{weight\ of\ microalgae\ (Ash\ free\ dry\ basis)} \ldots (6.2)$$

$$Liquefaction\ conversion\ (\%) = \left(1 - \frac{(M_{SR} + M_{Ash})}{M_{algae}}\right) * 100\% \ldots (6.3)$$

6.3 Results and discussion

6.3.1 HTL of the model compounds and cationic surfactant (CTAB)

The product yields (bio-oil, water-soluble organics, solid residue, and gas) from the HTL of starch, BSA, rapeseed oil, and CTAB are shown in figure 6.3 in term of weight percentage. The ash content for the three model compounds were 0, 0.84, and 0.27% for starch, BSA, and rapeseed oil respectively compared to 8.56% for the microalgae biomass (see table 6.1).

The product distributions from the HTL of the model compounds (Figure 6.3) were not in accord with those from previous works conducted by Biller and Ross (2011) (P. Biller and Ross, 2011a) and Teri et al. (2014) (Teri *et al.*, 2014). This is likely due to differences in the operational conditions (temperatures and holding times) among these studies. The bio-oil, water-soluble organic, solid, and gas yields from the HTL of starch were 3.17, 3.61, 63.03, and 6.57% respectively at 300 ˚C. When the temperature increased to 320 ˚C, the bio-oil, water-

soluble organic, and gas yields increased to 3.79, 4.35, and 7.71% while solid yield reduced to 61.9%. However, the actual values of solid yield from starch were higher than the values measured. This was due to difficulties in recovering all solids from the reactor wall. Thus, the mass balance closures from the HTL of starch were not 100% as the yields of the water-soluble organic were not calculated by difference but measured directly instead. From the HTL of rapeseed oil, the bio-oil, water-soluble organic, solid, and gas yields were 94.67, 4.13, 1.2, and 0% respectively at 300 ˚C. The yields of bio-oil and gas fractions increased to 95.3 and 0.9% while the yields for water-soluble organic and solid fractions reduced to 2.79 and 1.01% respectively at 320 ˚C. Hydrothermal treatment of BSA at 300 ˚C showed that bio-oil, water-soluble organic, solid, and gas yields were 17.73, 68.32, 6.63, and 7.31% respectively. When BSA was treated hydrothermally at 320 ˚C, the yields of bio-oil and gas fractions increased to 23.4 and 9.1% while the yields of water-soluble organic and solid fractions reduced to 62.61 and 4.89%. It is clear from the hydrothermal processing of the model compounds that starch favours the formation of solids, rapeseed oil favours the formation of bio-oil, and BSA favours the formation of water-soluble organics. These outcomes were in line with those obtained previously despite the differences in the operating conditions of the trial sets such as temperature, holding time, and heating rate (P. Biller and Ross, 2011a; Teri *et al.*, 2014; Wagner *et al.*, 2016).

Figure 6.3 shows that bio-oil yield is in the order of lipid > protein >carbohydrate for the HTL of the model compounds at both 300 and 320 ˚C without holding time. This order was consistent with those of Biller and Ross (2011) and Teri et al. (2014). However, the bio-oil yields gained in this work, except for rapeseed oil, were lower than those obtained by the above researchers for starch and BSA. This is likely due to differences in the experimental operating conditions. Biller and Ross (2011) and Teri et al. (2014) performed their HTL trials at 350 ˚C and holding time ranged from 10 to 60 min.

The HTL of CTAB demonstrated that it is almost entirely converted into bio-oil with a very little solid fraction (Figure 6.3). Neither water-soluble organics nor gas fractions were obtained at either HTL temperatures. The bio-oil yields were 98.53 and 98.97% at 300 and 320 ˚C while the solid residues were 1.43 and 1.2% at 300 and 320 ˚C respectively. CTAB is a quaternary ammonium salt with a long tail of alkyl, hexadecyl $C_{16}H_{33}$, derived from natural fatty acid. Thus, as the hydrothermal treatment of vegetable oil produces mainly bio-oil, hydrothermal treatment of CTAB does too. It is essential in this work to identify the main compounds of bio-oil from the HTL of CTAB to understand the contributions that it makes to the bio-oil produced

by the HTL of microalgae harvested by foam flotation, therefore the identification of bio-oil from HTL of CTAB was pursued.

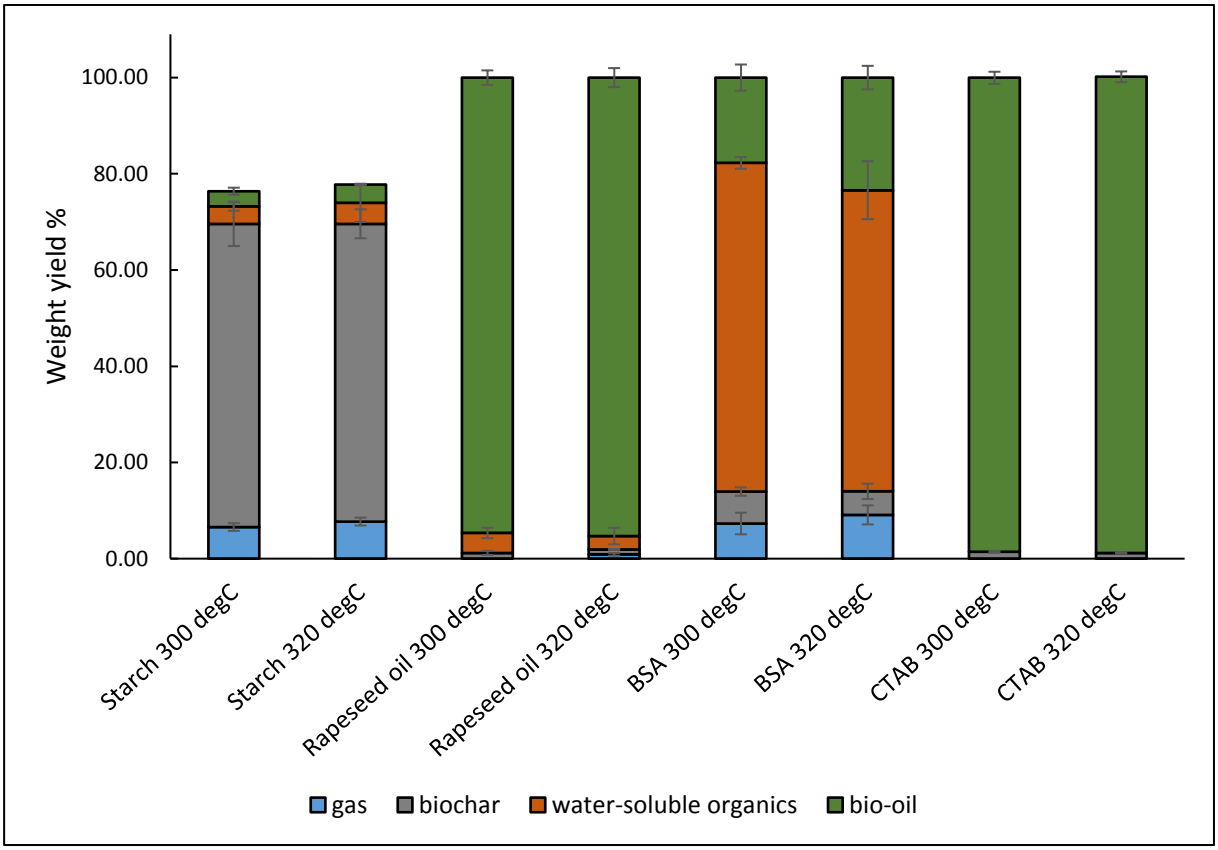

Figure 6.3: Product distribution from the HTL of three model compounds and CTAB at two temperatures; 300 and 320 ˚C, 32 ˚C/min heating rate, and no holding time.

The identification of the main compounds in the bio-oils from the HTL of the model compounds was not performed herein since the results of this work have already been published by other researchers even though the operational conditions including temperature, holding time, and heating rate in their work are different from those in our experimental trials. Therefore, the bio-oil from the HTL of CTAB at 320˚C was only analysed by GC-MS to identify the most abundant compounds. N, N-dimethyl-1-hexadecanamine; 2-methyl-1-hexadecanol; 2-hexadecanol; 2 methyl-2-heptanamine; 1-hexadecene; and N, N-dimethyl-1-heptadecanamine in this order were the main compounds identified. The dissociation constant of water (k_w) increases from 10^{-14} to 10^{-11} under HTL conditions which promotes the splitting of water molecules into hydrogen and hydroxide ions (H^+ and OH^-). These ions can help catalyse different reactions (like hydrolysis, base-catalysed, and acid-catalysed reactions) during the process (J. Zhang *et al.*, 2013; Gai *et al.*, 2014). However, Teri et al. (2014) observed interactions between different model compounds during the HTL reaction at 350 ˚C for 60 min

(Teri *et al.*, 2014). In other words, various compounds may be obtained due to the reactions between the hydrolysed components of CTAB, protein, lipid, and carbohydrate. The identified compounds demonstrated that a C16 amine is likely to be a good identifier for the contribution of CTAB to the bio-oil.

The reaction temperature affected all product yields from the HTL of model compounds. When the temperature increased, bio-oil and gas fraction yields increased while water-soluble organics and solid residue yields decreased. The temperature influence on the bio-oil yield from the BSA was higher than other model compounds in which the bio-oil yield increased by about 7% when the temperature increased only 20 degrees, while no higher than a 1% raise were observed for starch or rapeseed oil. This is likely due to the higher temperature promoting protein degradation thereby increasing bio-oil yield at the expense of water-soluble organics and solid residue.

6.3.2 Microalgae characterisation

The characterisation of the *C. vulgaris* used in this work is presented in table 6.1. The proximate analysis demonstrated that the ash content was 8.56% (daf). *C. vulgaris* were cultivated at high growth rate leading to high protein and carbohydrate and low lipid content (table 6.1). Such a biochemical composition is advantageous for investigating the influence of the type of flotation process and CTAB presence on the HTL product distribution especially after the observations of Coward et al. (2014). The elemental composition (daf) of the biomass was 52.21±0.1% carbon, 7.65±0.04% hydrogen, 9.01±0.07% nitrogen, and 31.17±0.21% oxygen. The empirical formula of *C. vulgaris* was $C_{6.76}H_{11.88}NO_{3.02}$. The H/C and O/C molar element ratios (daf) were determined from the elemental composition as 1.76 and 0.45 respectively.

Properties		*C. vulgaris*
Higher heating value (HHV) MJ/kg		24.31
Empirical formula (daf)		$C_{6.76}H_{11.88}NO_{3.02}$
Molar element ratio (daf)	H/C	1.76
	O/C	0.45
Elemental analysis wt.% (daf)	Carbon	52.21±0.1
	Hydrogen	7.65±0.04
	Nitrogen	9.01±0.07
	Oxygen (by difference)	31.17±0.21
Proximate analysis wt.%	Moisture	-
	Ash	8.56±0.53
Biochemical composition (daf)	Carbohydrate	28.3±1.6
	Protein	55.7±2.2
	Lipid	11.9±1.1

Table 6.1: Characterisation of the *C. vulgaris* feedstock.

6.3.3 HTL of C. vulgaris harvested by centrifugation and foam flotation

6.3.3.1 Temperature effect on product distribution and process conversion

The product yields (bio-oil, water-soluble organics, solid residue, and gas) from the HTL treatment of *C. vulgaris* harvested by foam flotation and centrifugation techniques at three different reaction temperatures (280, 300 and 320 ˚C), a heating rate of 32 ˚C/min, and no holding time are shown in figure 6.4. HTL at high heating rates and no holding time is an opportunity to study the process at circumstances near to continuous processing mode with low residence time. This will provide information that may aid subsequent intensification of the process. The bio-oil, water-soluble organic, solid, and gas yields from the HTL of *C. vulgaris* recovered by centrifugation were 13.11, 43.41, 41.39, and 2.09% respectively at 280 ˚C. When the temperature increased to 300 ˚C, the bio-oil and gas yields increased to 23.15 and 3.75% while the water-soluble organic and solid residue yields dropped to 35.99 and 37.29%. Torri et al. (2012) reported that HTL of microalgae species which accumulate algaenan at temperatures beyond 300˚C, boosts full extraction of the algaenan and its derivatives into the bio-oil phase (Torri *et al.*, 2012). However, *C. vulgaris* is an algaenan-free species and the increase in bio-oil yield with temperature was most likely due to the increasing conversion of intermediate water-soluble organics into the bio-oil fraction and thermal cracking of more protein and carbohydrate compounds at higher temperatures. In microalgae, triglycerides (TGA) are the main constituent of lipids and can be converted hydrothermally to fatty acids and glycerol. In general, fatty acids contribute to the bio-oil fraction while the glycerol contributes to the water-soluble organic fraction. A previous study observed that the maximum glycerol yield by HTL of microalgae was 4-6 wt. % at 260 ˚C and this amount decreased as reaction temperature increased. This observation may support the reduction in water-soluble organic yield at higher temperature due to the conversion of intermediate water-soluble organics into a bio-oil product (Shakya *et al.*, 2017).

Again, when the HTL treatment temperature increased to 320˚C, the bio-oil and gas yields increased to 26.73 and 4.89% whereas the water-soluble organic and solid residue yields reduced to 35.24 and 33.14%. The measurements of *C. vulgaris* biochemical compositions harvested by centrifugation demonstrated that protein, carbohydrate, and lipid contents were 55.7±2.2, 28.3±1.6, and 11.9±1.1%. The higher water-soluble organic and solid residue yields from the HTL of microalgae harvested by centrifugation, especially at a lower reaction temperature (280 ˚C), were due to the high protein and carbohydrate contents before water-

soluble organics and solid residue were converted into bio-oil or degraded at higher temperatures. Ross et al. (2010) reported that the HTL of protein produced amino acids and peptides, thus the increase in water-soluble product yield at lower temperature was likely due to the presence of high amounts of amino acids and peptides before they undergo further decomposing and repolymerising into bio-oil at higher temperatures (Ross *et al.*, 2010). The HTL of starch (as model carbohydrate compound) produced approximately 4 wt.% water-soluble organic yield, thus this might contribute to the water-soluble organic fraction as *C. vulgaris* has high carbohydrate content. The low bio-oil yields, especially at lower reaction temperature (280 ˚C), were due to the low lipid content of *C. vulgaris* recovered by centrifugation.

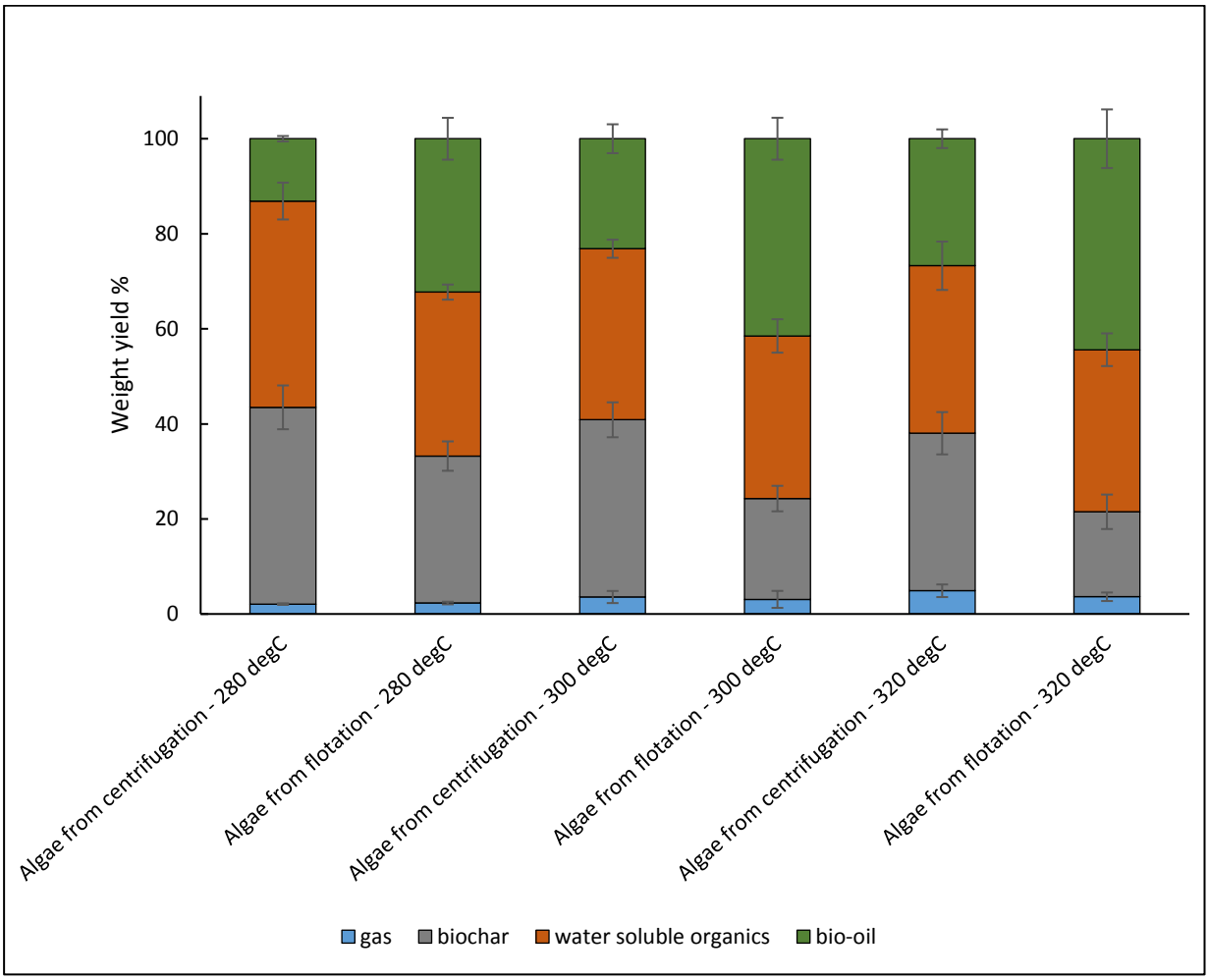

Figure 6.4: Product distribution from the HTL of microalgae harvested by foam flotation and centrifugation at three temperatures (280, 300, and 320 ˚C), a heating rate 32 ˚C/min, and no holding time.

When *C. vulgaris* harvested by foam flotation was treated by hydrothermal processing at 280 ˚C, the bio-oil yield increased to 32.27% while it was 13.11% for the centrifugation control. The biochemical composition of *C. vulgaris* harvested by foam flotation was 55.9±1.9, 23.9, and 19.6±2.2% for protein, carbohydrate, and lipid respectively. The increase in lipid content was 7.7% compared to centrifugation. The increase in bio-oil yield from the foam flotation treatment was 19.16% which is not explained even if complete conversion of lipid into bio-oil is considered. It is worth noting that not only CTAB adsorbed onto the microalgae cells are recovered with the harvested microalgae but also the remaining free CTAB that attaches to the air bubbles and generates the foam as well, resulting in an increase in the long chain hydrocarbon content. However, the amount of free CTAB which accompanies the harvested microalgae slurry was not enough to increase the bio-oil product to the obtained yield.

On the other hand, the yields of water-soluble organics, solid residue, and gas products dropped to 34.51, 30.92, and 2.31% compared to the centrifugation control (Figure 6.4). The reduction in the water-soluble organic yield might be linked to the higher yield of the bio-oil product and could be explained by the hydrolysed proteins and amino acids being converted into bio-oil at lower temperatures (Torri *et al.*, 2012). CTAB can disrupt the cell wall and promote cell lysis especially when it is used in high concentration. This enhances the recovery of internal cell contents like DNA and lipid and increase the solubility of some phospholipids in the cell membrane as well (T. Coward *et al.*, 2014), thereby enhancing bio-oil yield.

The lower solid residue yield from the foam flotation harvested *C. vulgaris* compared to the centrifugation treatment at 280 ˚C was undoubtedly due to the reduction in the carbohydrate content of the former microalgae feedstock. The presence of CTAB with the harvested *C. vulgaris* did not likely promote more carbohydrate degradation resulting in lower gas yield. Teri et al. (2014) observed that the interactions between biochemical components of microalgae (protein, carbohydrate, and lipid) might also be responsible for higher bio-oil yield and not the sole influence of each biochemical component in isolation (Teri *et al.*, 2014).

The trends in the yield for all products from the HTL of *C. vulgaris* with CTAB were similar to those without CTAB (i.e. the bio-oil and gas yields increased while the water-soluble organic and solid residue yields decreased) as the reaction temperature increased to 300 and 320˚C (Figure 6.4). It is worth noting that the enhancement in the bio-oil yield when temperature increased from 280 to 300 ˚C was more than twice as large as the increase in bio-oil yields

when temperature increased from 300 to 320 ˚C for both feedstocks. However, the bio-oil yields at 320 ˚C were higher than those at lower temperatures.

The conversions from the HTL of both *C. vulgaris* harvested by centrifugation and foam flotation at 32 ˚C/min heating rate and no holding time are shown as a function of temperature in figure 6.5. The reaction temperature showed a remarkable effect on the process conversion for both feedstocks. For the HTL of *C. vulgaris* harvested by centrifugation, the process conversion increased from 58.5 to 66.8% as the temperature rose from 280 to 320 ˚C while the process conversion increased from 69 to 82% for *C. vulgaris* harvested by foam flotation across the same temperature range. In general, increasing reaction temperature offers higher energy for cracking more carbohydrate, protein, and lipid into small fragments, resulting in higher conversions. However, the liquefaction conversions of *C. vulgaris* harvested by foam flotation were higher than those for the liquefaction of *C. vulgaris* harvested by centrifugation (Figure 6.5). This was likely due to the capability of CTAB in enhancing the decomposition of microalgae and consequently promoting the depolymerisation of long chain and high molecular weight polysaccharides, hemicellulose and protein into small fragments even at lower temperatures. The capability of CTAB to enhance the depolymerisation reaction was observed by Vanini *et al.* (2013) when they investigated the influence of CTAB on the depolymerisation reaction of post-consumption bottle-grade polyethylene terephthalate (PET) in alkaline solution. They reported that the presence of CTAB increased the reaction performance by 85%, while the reaction time was decreased from 6 to 2h (Vanini *et al.*, 2013).

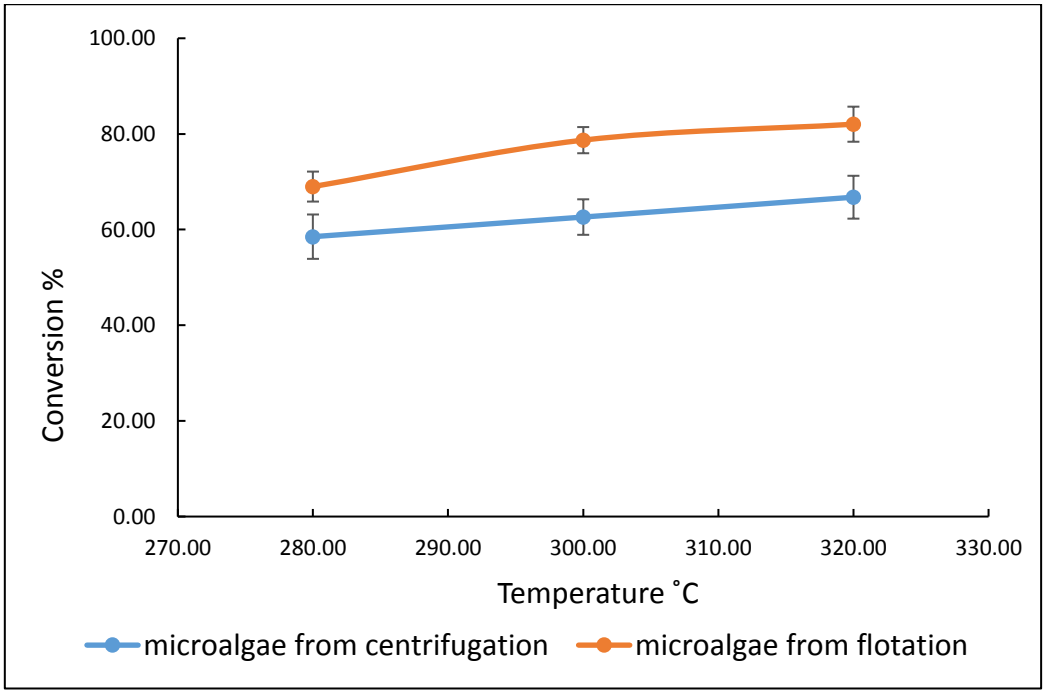

Figure 6.5: HTL conversions of *C. vulgaris* harvested by foam flotation and centrifugation at three temperatures (280, 300, and 320 ˚C), a heating rate of 32 ˚C/min, and no holding time.

6.3.3.2 Holding time effect on product distribution

The yields of bio-oil, water-soluble organics, solid residue, and gas products from the HTL treatment of *C. vulgaris* harvested by foam flotation and centrifugation at two holding times of 0 and 10 min, reaction temperature of 300 ˚C, and heating rate of 32 ˚C/min are shown in figure 6.6. Batch holding time in the current work did not include the heating or cooling periods. For the HTL of *C. vulgaris* harvested by centrifugation at 300 ˚C with no holding time, the bio-oil, water-soluble organics, solid residue, and gas yields were of 23.15, 35.99, 37.29, and 3.57% respectively. When the batch holding time changed to 10 min at the same temperature, the bio-oil and gas yields increased to 36.52 and 5.5% respectively whereas water-soluble organics and solid residue yields reduced to 34.88 and 23.1%. The effect of holding time on the bio-oil and solid residue yields were higher than its effect on the yields of water-soluble organic and gas fractions. Teri et al. (2014) observed that the holding time parameter in the hydrothermal liquefaction of soy protein, cornstarch, and sunflower oil at 350 ˚C had little effect on both bio-oil and solid residue yields (Teri *et al.*, 2014). However, the yield results in this work demonstrated that the increase in batch holding time at mild temperature favored the conversion of algal biomass into the bio-oil fraction. The increase in the batch holding time likely promotes more carbohydrate and protein degradation and converts more intermediate water-soluble organics into bio-oil. This explanation can be concluded from the increase in gas fraction yield when a longer residence time was adopted.

Biller and Ross (2011) conducted HTL on freeze-dried *C. vulgaris* strains at a reaction temperature of 350˚C, holding time of 60 min, and two heating rates of 10 and 25 ˚C/min (P. Biller and Ross, 2011a). The maximum bio-oil yield obtained in their trials was 36%, which was comparable to the yield gained here but at lower reaction temperature and holding time. It is worth noting that the biochemical composition of *C. vulgaris* liquefied by Biller and Ross was 55% protein, 9% carbohydrate, and 25% lipid (P. Biller *et al.*, 2011b) whereas the *C. vulgaris* used in this work had 55.7±2.2% protein, 28.3±1.6% carbohydrate, and 11.9±1.1% lipid (daf). Although the heating rate used in this work (32 ˚C/min) might increase the bio-oil yield slightly, the researchers believed that direct HTL of harvested microalgae rather than pulverised or freeze-dried microalgae enhanced the conversion of biomass and increased the

bio-oil yield at mild conditions. This is undoubtedly an advantage of direct HTL of algal biomass as it can minimise the cost of the process.

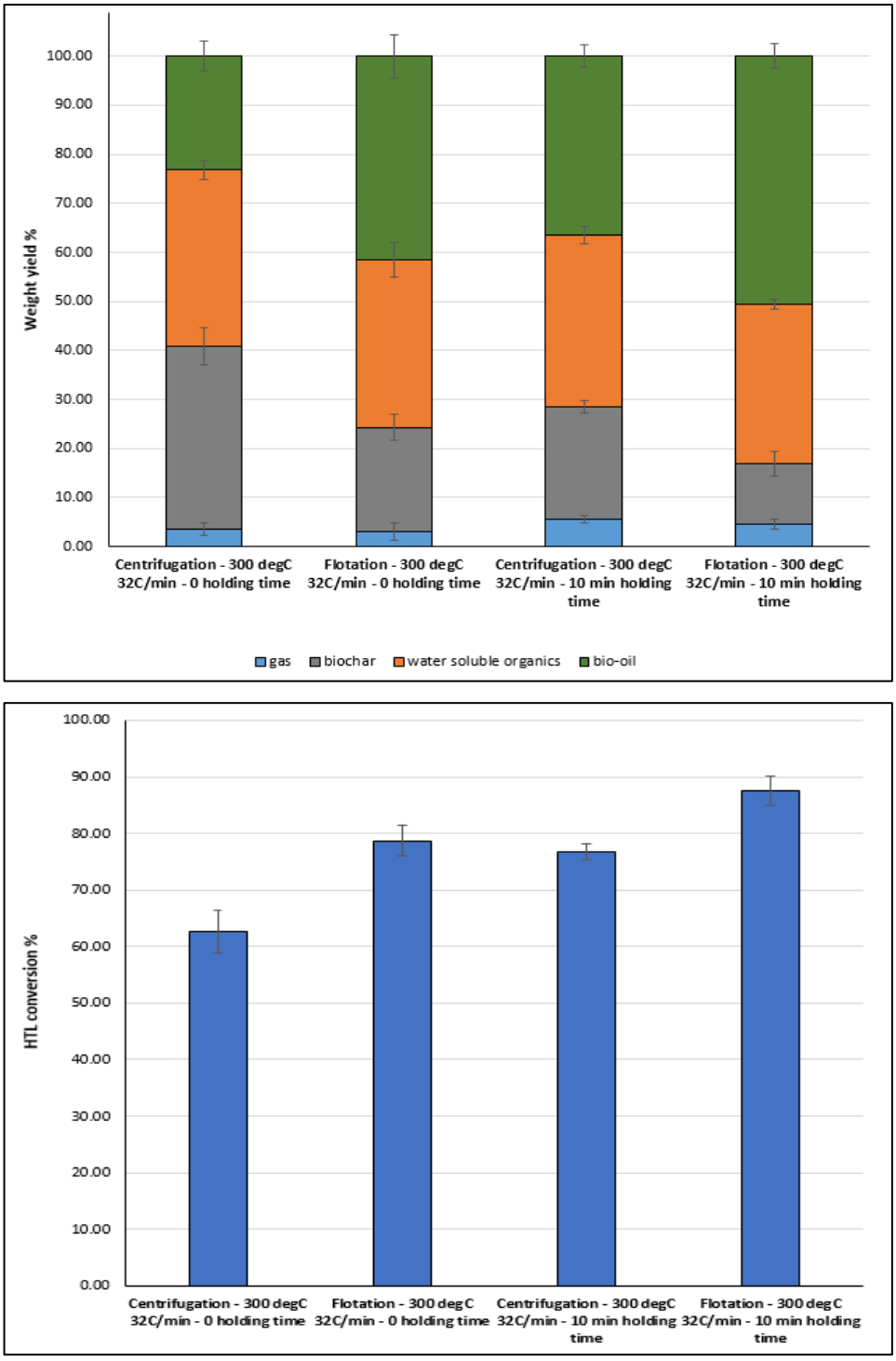

Figure 6.6: Product distribution (top) and process conversion (bottom) from the HTL of *C. vulgaris* harvested by foam flotation and centrifugation at two holding times (0 and 10) min, a reaction temperature of 300˚C, and a heating rate of 32 ˚C/min.

For the HTL of *C. vulgaris* harvested by foam flotation at 300 ˚C with no holding time, the bio-oil, water-soluble organic, solid residue, and gas yields were 41.5, 34.21, 21.21, and 3.08% (Figure 6.6). The yields of bio-oil and gas fractions increased to 50.54 and 4.64% while the yields of water-soluble organics and solid residue dropped to 32.5 and 12.32% when the holding time changed to 10 min at the same reaction temperature. Like the HTL of *C. vulgaris* without CTAB, the effect of the batch holding time on the bio-oil and solid residue yields were higher than its effect on the yields of water-soluble organic and gas fractions. The lower solid residue yield from the HTL of *C. vulgaris* with CTAB compared to that from the HTL of *C. vulgaris* without CTAB was probably because of the reduction in the carbohydrate content of the former feedstock and cell lysis due to the presence of CTAB which made the breaking of carbohydrate easier at mild HTL conditions.

The conversions for the HTL of both feedstocks were also determined at different holding time trials. With longer reaction times increasing the liquefaction conversion (Figure 6.6). Similarly, the prolongation of the reaction time led to higher bio-oil yields due to the promotion in converting more intermediate water-soluble organics; it also enhanced thermal cracking of protein and carbohydrate compounds, resulting in higher HTL conversions.

6.3.4 Energy recovery

Higher heating values (HHV) for the bio-oils from the HTL of *C. vulgaris* harvested by centrifugation and flotation at 300 ˚C and 10 min holding time were determined using an oxygen bomb calorimeter. HHV were then used to calculate the energy recovery which is an important parameter to assess the feasibility of a biomass to biofuel conversion process. However, it does not include any processing energy used during the conversion reaction (P. Biller and Ross, 2011a). Energy recovery (ER) is the ratio of the bio-oil HHV multiplied by its mass to the feedstock HHV multiplied by its mass; it is calculated according to equation 6.4:

$$\text{ER } \% = \frac{HHV_{bio\ oil}\ x\ mass_{bio\ oil}}{HHV_{algal\ feed}\ x\ mass_{algal\ feed}} x100\% \ldots (6.4)$$

Few previous studies have included the energy content of the gas product as well (Brown *et al.*, 2010), however, the energy stored in the bio-oil fraction was only considered in this work.

The measurement results showed that HHVs for the bio-oils from the HTL of *C. vulgaris* harvested by centrifugation and flotation were 33.99 and 35.07 MJ/kg respectively, whereas the HHV for the algal feedstock was 24.13 MJ/kg (daf). This is another advantage for the bio-oil

produced by the HTL of *C. vulgaris* recovered by foam flotation. Higher heating of combustion was probably due to higher amounts of hydrocarbons originating from CTAB. The energy recovery was calculated by substituting the HHV and the bio-oil yield in equation 6.4. Higher energy (73.45%) was recovered from the HTL of *C. vulgaris* harvested by foam flotation compared to that from the HTL of *C. vulgaris* harvested by centrifugation (51.41%). Higher energy recovery was undoubtedly due to the higher yield and heating value for the bio-oil of microalgae from flotation. Moreover, *C. vulgaris* harvested by foam flotation had a HHV of 26.88 MJ/kg compared to 24.13 MJ/kg for *C. vulgaris* harvested by centrifugation due to the higher lipid content which had a HHV of 42.83 MJ/kg (measured in the current work) resulted in higher energy recovery. These outcomes also indicated that HTL of microalgae harvested by foam flotation produced fuel which had a stored energy closer to that of dry algal feedstock than the fuel produced from microalgae harvested by centrifugation.

6.3.5 Gas fraction analysis

The analysis of the gas produced by the HTL of *C. vulgaris* showed that CO_2 was the main gas product and, in most cases, represented more than 90% wt. of the gas. CO was also present but in low amounts. This is an indication that the removal of O_2 in the HTL reaction mainly occurs by decarboxylation rather than decarbonylation. The rest of the gas fraction consisted of small quantities of CH_4, H_2, N_2, C_2H_4, C_2H_6, C_3H_6, and C_3H_8 as shown in figure 6.7 as an example. The gas analysis also demonstrated that the composition of CO_2 increased when increasing the reaction temperature and holding time. This might be due to the gas-water shift reaction between CO and water to produce H_2 and CO_2. This reaction might occur since little increase in the H_2 composition was observed. The concentration of small hydrocarbons increased slightly with higher reaction temperature and longer residence time.

The gaseous products from the HTL of *C. vulgaris* harvested by foam flotation contained less CO_2 and more CO, H_2, and smaller hydrocarbons (Figure 6.7). This is another advantage for the foam flotation harvesting technique in producing biomass more valuable for the biofuel sector. The increase in the compositions of hydrocarbon gases is probably due to disruption of the algae cell wall by CTAB which enhances the thermal cracking of hydrocarbons without the need to increase the reaction temperature or residence time.

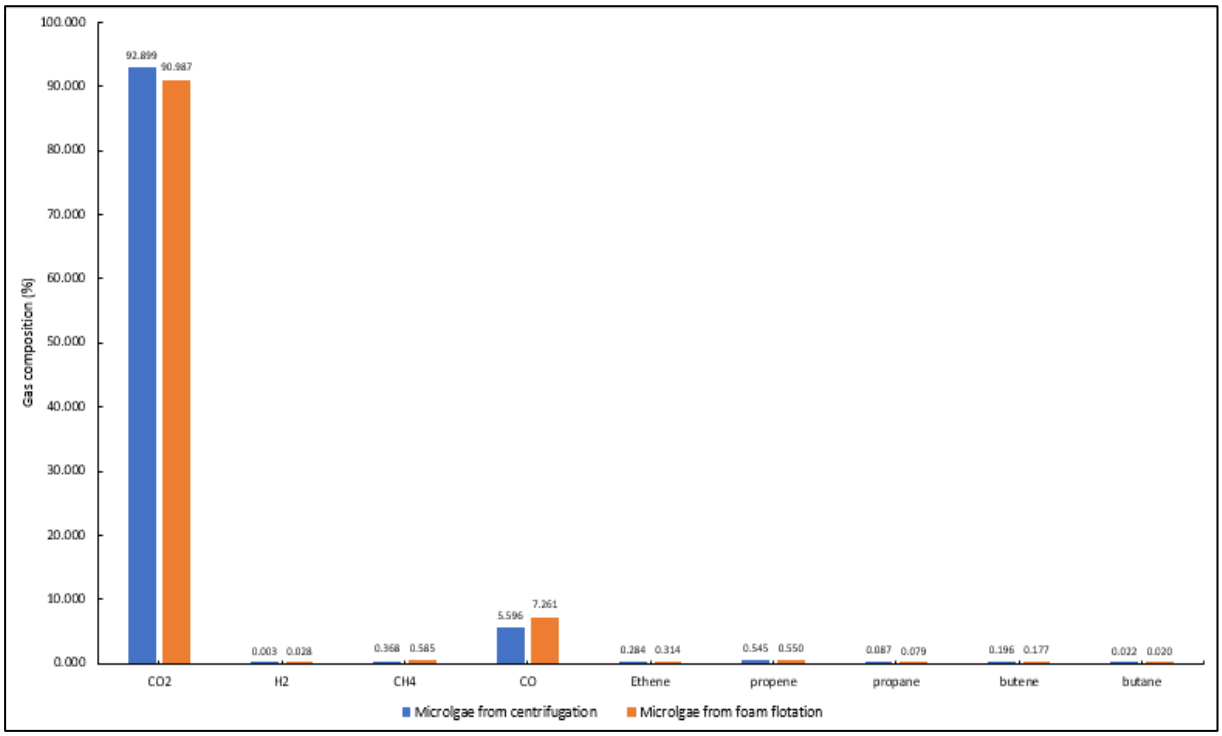

Figure 6.7: Gaseous product compositions from the HTL of *C. vulgaris* harvested by foam flotation and centrifugation at 320 ˚C, a heating rate 32 ˚C/min, and no holding time.

6.3.6 Analysis of bio-oil fraction

6.3.6.1 Elemental analysis and composition of bio-oils

The proximate and ultimate analysis of *C. vulgaris* and the bio-oils from the HTL technology at a reaction temperature of 320 ˚C with no holding time are presented in table 6.2. In this work, sulphur content was assumed negligible and oxygen content was calculated by difference. Compared with the microalgae feedstock, both carbon and hydrogen content of the bio-oils increased while the nitrogen and oxygen content decreased; demonstrating the effectiveness of the hydrothermal process to increase the carbon and hydrogen content in the bio-oil fraction. Maximum increase was observed in the carbon content whereas oxygen content was significantly reduced. Oxygen was probably removed during the HTL of microalgae by dehydration, deoxygenation, and decarboxylation reactions. Both bio-oils had lower nitrogen content compared to the microalgae with the minimum average content for the bio-oil from the HTL of *C. vulgaris* with CTAB. This is another advantage added to the foam flotation harvesting technique over centrifugation as the nitrogen content dropped from 7.37 to 5.46%. The study of temperature effect on the bio-oil yield demonstrated that the production of bio-oils increased with the temperatures while the water-soluble organic yields reduced. However,

the reduction in water-soluble organic amount with increasing temperature in the HTL of *C. vulgaris* recovered by foam flotation was small compared to centrifugation. This indicated that the contribution of carbohydrate into bio-oil at higher temperature was greater than protein in the presence of CTAB with the harvested microalgae, resulting in higher hydrogen and oxygen contents and lower nitrogen content. This was probably due to the efficiency of CTAB in enhancing the cellulose and hemicellulose decomposition. The slightly higher oxygen content in the bio-oil produced by the HTL of *C. vulgaris* with CTAB was expected based on the analysis of gaseous products as the CO_2 reduced while CO increased. This is further evidence that the removal of O_2 in the HTL reaction mainly occurs by decarboxylation rather than decarbonylation. A higher H/C ratio of the bio-oil from *C. vulgaris* harvested by foam flotation compared to centrifugation might indicate that the latter bio-oil contains slightly higher amounts of unsaturated compounds.

Condition	Moisture	Ash	Elemental distribution (daf)				Element ratio		HHV MJ/kg
			C %	H %	N %	O[a] %	H/C	O/C	
Bio-oil from HTL of microalgae harvested by centrifugation	0	≈ 0	69.94±0.16	8.27±0.08	7.37±0.09	14.43±0.17	1.42	0.15	36.31
Bio-oil from HTL of microalgae harvested by flotation	0	≈ 0	69.68±0.35	9.22±0.48	5.46±0.09	15.65±0.76	1.59	0.17	37.73

a: calculated by difference.

Table 6.2: Proximate, ultimate analyses, and energy content of microalgae and HTL bio-oils.

6.3.6.2 Composition of bio-oil fraction

Bio-oil from the HTL of biomass is a complex mixture of compounds and its composition is strongly influenced by the feedstock biochemical composition and the HTL operating conditions (Torri *et al.*, 2012). The precise pathways or mechanisms for the HTL of microalgae are still ambiguous due to the complexity of both feedstock and HTL products. In general, microalgae are first depolymerised into small active fragments such as amino acids and monosaccharides by hydrolysis, these fragments are then further decomposed into smaller compounds by different reactions like dehydration and decarboxylation (decomposition). Most these compounds are highly soluble in water. Lastly, these compounds are often repolymerised until the process is stopped, resulting in more complex compounds including hydrocarbon, ester, ketone, and N-containing compounds (Gollakota *et al.*, 2018). The bio-oils produced by the HTL of microalgae were analysed using GC-MS with the maximum oven temperature set

to 250 ˚C. The identified compounds were then grouped into their chemical classes as shown in table 6.3 (chromatograms not shown). The previous analyses of HTL bio-oils by thermogravimetric analysis (TGA) have indicated that the bio-oil from the HTL of microalgae has a high molecular weight, thus around 50% of the bio-oil fraction (higher boiling compounds) cannot be analysed by GC-MS due to their incapability of elution from the GC column (Anastasakis and Ross, 2011; P. Biller and Ross, 2011a). The original GC-MS spectra identified more than 100 compounds but the majority had low abundance, therefore only peaks with very low abundance (area% < 0.1) were excluded during qualitative analysis.

Bio-oil produced by the HTL of microalgae harvested by centrifugation			Bio-oil produced by the HTL of microalgae harvested by flotation		
Chemical class	Area%	Identified compounds	Chemical class	Area%	Identified compounds
Esters	**3.51**		**Esters**	**11.43**	
C13H24O2	0.44	3-Cyclopentylpropionic acid, 3-methylbutyl ester	C26H50O2	0.81	Cyclopropanetetradecanoic acid, 2-octyl-, methyl ester
C11H18O3	0.46	4-Hydroxy-non-2-ynoic acid, ethyl ester	C21H38O2	0.73	[1,1'-Bicyclopropyl]-2-octanoic acid, 2'-hexyl-, methyl ester
C22H36O2	0.16	Benzeneacetic acid, 4-tetradecyl ester	C12H22O2	0.54	10-Undecenoic acid, methyl ester
C12H24O2	0.92	Heptanoic acid, 3-methylbutyl ester	C17H30O2	3.44	7,10-Hexadecadienoic acid, methyl ester
C17H34O2	1.16	Hexadecanoic acid, methyl ester	C19H34O2	4.00	9,12-Octadecadienoic acid, methyl ester, (E,E)-
C11H22O2	0.38	Hexanoic acid, 1,1-dimethylpropyl ester	C11H22O2	0.22	Hexanoic acid, 1,1-dimethylpropyl ester
Fatty acids	**6.24**		C21H40O2	0.10	Octadecanoic acid, 2-propenyl ester
C12H24O2	6.24	Undecanoic acid, 2-methyl-	C16H32O2	1.13	Pentadecanoic acid, methyl ester
Hydrocarbons	**10.83**		C15H30O2	0.46	Methyl tetradecanoate
C18H28	2.60	1H-Indene, 2,3-dihydro-1,1-dimethyl-	**Fatty acids**	**6.87**	
C26H48	0.51	Anthracene, 9-dodecyltetradecahydro-	C18H34O2	0.88	trans-13-Octadecenoic acid
C26H46	0.13	Benzene, (1-hexylheptyl)-	C9H14O3	0.53	2,4-Octadienoic acid, 7-hydroxy-6-methyl-, [r-[r*,s*-(E,E)]]-
C13H16	0.19	Naphthalene, 1,2-dihydro-1,1,6-trimethyl-	C10H18O2	0.20	3-Decenoic acid, (E)-
C11H22	7.40	Cyclohexane, (1,1-dimethylpropyl)-	C12H24O3	4.43	Dodecanoic acid, 3-hydroxy-
ketones	**25.28**		C14H26O2	0.32	E-9-Tetradecenoic acid
C8H12O2	0.42	1,3-Cyclobutanedione, 2,2,4,4-tetramethyl-	C18H34O4	0.27	Octadecanedioic acid
C9H14O	19.48	2-Cyclohexen-1-one, 3,5,5-trimethyl-	C14H28O3	0.23	Tetradecanoic acid, 2-hydroxy-
C11H18O	5.28	2-Cyclohexen-1-one, 3,6-dimethyl-6-(1-methylethyl)-	**Hydrocarbons**	**20.43**	
C12H22O2	0.11	2H-Pyran-2-one, 6-heptyltetrahydro-	C16H32	4.00	1-Hexadecene
Aldehydes	0.16		C11H22	0.16	3-Undecene, (E)-
C10H20O2	0.16	Octanal, 7-hydroxy-3,7-dimethyl-	C14H28	0.71	7-Tetradecene
Alcohols	**4.28**		C16H34	3.97	Hexadecane
C20H40O	3.69	Isophytol	C15H32	2.86	Pentadecane
C10H20O	0.59	2-Octen-1-ol, 3,7-dimethyl-	C15H30	1.90	Cyclohexane, 1,1,3-trimethyl-2-(3-methylpentyl)-
Nitrogenous compounds	**43.37**		C14H30	6.83	Dodecane, 4,6-dimethyl-
C17H22N4O2	2.35	N-(3-Imidazol-1-yl-propyl)-N'-(4-isopropyl-phenyl)-oxalamide	**ketones**	**9.60**	
C18H37NO	3.75	Octadecanamide	C8H16O	0.16	2-Heptanone, 5-methyl-
C12H25NO	7.03	Dodecanamide	C15H30O	0.71	2-Pentadecanone
C4H7N	0.27	Butanenitrile	C18H36O	4.00	2-Pentadecanone, 6,10,14-trimethyl-
C12H11N	0.10	[1,1'-Biphenyl]-4-amine	C8H12O2	0.18	3-Ethoxy-2-cyclohexen-1-one
C10H17NO3	2.02	1,2-Pyrrolidinedicarboxylic acid, 1-(1,1-dimethylethyl) ester, (S)-	C16H30O2	0.40	Oxacycloheptadecan-2-one
C12H29N3	0.16	1,4-Butanediamine, N'-[4-(dimethylamino)butyl]-N,N-dimethyl-	C13H24O2	0.14	Oxacyclotetradecan-2-one
C11H23N	13.63	1-Butanamine, N-(1-propylbutylidene)-	C19H38O	4.00	2-Nonadecanone
C6H12N2O	1.55	1H-Azepine, hexahydro-1-nitroso-	**Aldehydes**	**3.33**	
C4H6N2	0.13	1H-Imidazole, 1-methyl-	C18H34O	0.90	10-Octadecenal
C9H9N	0.16	1H-Indole, 6-methyl-	C5H8O	0.44	2-Butenal, 2-methyl-
C11H12N2O2	2.46	2,5-Piperazinedione, 3-(phenylmethyl)-	C8H14O	0.27	2-Hexenal, 2-ethyl-
C12H22N2O2	0.28	2,5-Piperazinedione, 3,6-bis(2-methylpropyl)-	C7H12O	0.58	2-Hexenal, 2-methyl-
C15H17NO5	0.17	2H-Pyran-2,4(3H)-dione, dihydro-3,3,5,5-tetramethyl-6-(4-nitrophenyl)-	C5H10O	1.01	Butanal, 3-methyl-
C11H22N2	0.38	3-(t-Octylamino)propionitrile	C10H14O2	0.12	Cyclopentaneacetaldehyde, 2-formyl-3-methyl-α-methylene-
C5H5NO2	0.19	3-Hydroxypyridine-N-oxide	**Alcohols**	**10.10**	
C4H5N3	0.25	4-Aminopyrimidine	C20H40O	9.39	Isophytol

C14H19NO5	0.28	4-Benzyloxy-3-nitromethyl-pentanoic acid, methyl ester	C8H18O	0.22	4-Heptanol, 2-methyl-
C8H14N2O	1.03	5-Pyrrolidino-2-pyrrolidone	C8H14O	0.49	3-Octyn-1-ol
C16H21NO6	0.16	6-Benzyloxy-5-nitromethyl-3-oxoheptanoic acid, methyl ester	**Nitrogenous compounds**	**30.55**	
C9H18N2O3	0.11	dl-Alanyl-l-leucine	C18H37NO	4.00	Octadecanamide
C14H11N3O2	0.66	Furan-2-carbohydrazide, N2-(3-indolylmethylene)-	C14H24N2O8	0.34	1,6-Diaminohexane-N,N,N',N'-tetraacetic acid
C12H27N	0.18	N,3-Diethyl-3-octanamine	C18H39N	0.83	1-Octadecanamine
C9H20N2	1.01	N,N-Diethyl-N'-propylacetamidine	C19H41N	0.28	1-Octadecanamine, N-methyl-
C13H21N	0.51	p-Heptylaniline	C17H37N	18.62	1-Pentadecanamine, N,N-dimethyl-
C3H5NO	0.21	Propanenitrile, 3-hydroxy-	C19H32N2O3	0.63	2H-Benzo[f]oxireno[2,3-E]benzofuran-8(9H)-one, 9-[[[2-(dimethylamino)ethyl]amino]methyl]octahydro-2,5a-dimethyl-
C12H19N3O4	0.41	Pyrimidin-2,4-dione, 1,2,3,4-tetrahydro-5-methyl-1-[[2-hydroxymethyl-3-	C9H15NO	0.34	2H-Inden-2-one, octahydro-, oxime
C22H39NO	0.19	Pyrrolidine, 1-(1-oxo-9,15-octadecadienyl)-	C12H11N	0.16	4-(4-Methylphenyl)pyridine
C19H37NO	1.28	Pyrrolidine, 1-(1-oxooctadecyl)-	C20H26N2O2	1.69	Dasycarpidan-1-methanol, acetate (ester)
C9H16N2O	1.06	Pyrrolidine, 2α-[1-pyrrolidinoformyl]-	C19H41N	3.67	Ethylamine, N-methyl-N-hexadecyl-
C11H18N2O2	0.42	Pyrrolo[1,2-a]pyrazine-1,4-dione, hexahydro-3-(2-methylpropyl)-	**Others**	**0.78**	
C14H16N2O2	0.86	Pyrrolo[1,2-a]pyrazine-1,4-dione, hexahydro-3-(phenylmethyl)-	C8H16O	0.78	Furan, 2-butyltetrahydro-
C9H11NO4	0.15	Pyrrolizin-1,7-dione-6-carboxylic acid, methyl(ester)			
Others	**2.30**				
C14H22O	0.54	Phenol, 2,6-bis(1,1-dimethylethyl)-			
C12H14O2	1.33	1-Naphthalenol, 1,2,3,4-tetrahydro-, acetate			
C8H16O	0.42	Furan, 2-butyltetrahydro-			
total	95.97			93.09	

Table 6.3: Identified compounds in the bio-oils produced by the HTL of *C. vulgaris* at 320 ˚C.

The identification of compounds in the bio-oil product revealed that it is a complex mixture of various compounds including fatty acids, esters, hydrocarbons, ketones, aldehydes, alcohols, and nitrogenous compounds.

Table 6.3 includes six ester compounds with a total peak area of 3.51% for bio-oil from *C. vulgaris* without CTAB whereas it includes nine compounds grouped under the ester chemical class with a total peak area of 11.43% for bio-oil from *C. vulgaris* with CTAB. In the HTL of microalgae, ester formation is likely due to the condensation (dehydration) reaction on the lipid precursors (Ahmed and Bernd, 2004). The greater amount of ester compounds in the bio-oil from microalgae harvested using the foam column is in accordance with the higher lipid content in its microalgae feedstock as explained earlier. GC-MS spectra detected different hydrocarbons in both bio-oils. The bio-oil from the HTL of *C. vulgaris* harvested by foam flotation having the higher percentage area. Different aliphatic hydrocarbons (alkanes and alkenes) were observed in the bio-oil from the HTL of *C. vulgaris* with CTAB while aromatic hydrocarbons were most abundant in the bio-oil from the HTL of *C. Vulgaris* without CTAB, which is favorable. Aliphatic hydrocarbons would likely arise from the decarboxylation or pyrolysis of the corresponding fatty acid with the possibility that the reaction was catalysed by the minerals available in the algal biomass (López-González *et al.*, 2014b). If the proposed pathway was true, this indicated that the bio-oil from *C. vulgaris* with CTAB had higher fatty

acid amounts before they underwent further reactions. However, Wang et al. (2008) observed some long-chain alkanes in the bio-oils from sawdust and stalks which means the possibility of other pathways for formation of alkanes during the HTL reaction as these biomass feedstocks do not contain appreciable amount of fatty acids (Chao Wang *et al.*, 2008). Another likely reaction pathway for the aliphatic hydrocarbons present in the bio-oil is the hydrolysis of CTAB, especially the portion adsorbed onto the air bubbles and recovered with microalgae.

Only one fatty acid compound was identified in the bio-oil produced by the HTL of *C. vulgaris* without CTAB in comparison to seven fatty acid compounds in the bio-oil with CTAB. However, total peak areas for the fatty acid compounds of both bio-oils were very close. Fatty acids are likely produced from the hydrolysis of lipids. For instance, triglyceride is hydrolysed to produce three fatty acid molecules and one glycerol molecule. Generally, fatty acids contribute to the bio-oil fraction whereas glycerol contributes to the water-soluble organic fraction. A recent study observed that maximum glycerol yield by the HTL of microalgae was 4-6 wt.% at 260˚C and this amount decreased as reaction temperature increasd (Shakya *et al.*, 2017). Some microalgae species such as *C. vulgaris* contain sporopollenin, a refractory component in the cell wall, which is extremely resistant to chemicals. Sporopollenin is a chain of related biopolymers derived from highly saturated precursors like fatty acids. Various quantities of oxygenated compounds such as ester, ketone, hydroxyl, ether, and carboxylic acid groups are present in the biopolymers. Therefore, some fatty acid compounds in the bio-oil from the HTL of algae of a low lipid content are likely due to the decomposition of this refractory biopolymer at high temperatures (Guilford *et al.*, 1988).

Ketones were also present in both bio-oils but in different amounts. Total peak area of the ketone compounds in the bio-oil from the HTL of *C. vulgaris* without CTAB was 25.28% compared to only 9.6% for that with CTAB. Biller and Ross (2011) identified four ketone compounds from the hydrothermal liquefaction of a carbohydrate model compound (glucose) at 350 ˚C for 60 min while no ketones were identified from protein and lipid model compounds (P. Biller and Ross, 2011a). Teri et al. (2014) also identified one ketone compound from the HTL of corn starch at 350 ˚C for 60 min (Teri *et al.*, 2014). Carbohydrates are polyhydroxy ketones or aldehydes or substances that produce such compounds upon hydrolysis (David and Michael, 2000). Therefore, ketone compounds are likely to be produced by the decomposition of carbohydrates although the exact pathway is still unclear. The ketone amounts in the bio-oils were consistent with the carbohydrate contents of both microalgae feedstocks. In other words, lower ketone amount in the bio-oil from *C. vulgaris* with CTAB was probably due to the

reduction in carbohydrate content after harvesting using the foam column. Lower ketone quantity in the bio-oil from the HTL of microalgae is more desirable due to the high reactivity of ketone oxygenated groups which increase the oil instability (Su-Ping, 2003).

Because of their higher reactivity compared to ketones, very small amounts of aldehyde compounds are rarely detected by GC-MS analysis of the bio-oil fraction. Nevertheless, small amounts of aldehydes were identified in this work due to the low retention time (zero or 10 minutes). The Maillard reaction, for instance the reaction between aldehyde and amino acid, is favoured by longer residence times which lead to the formation of complex compounds that make up the bio-oil by repolymerisation. Table 6.3 shows that the relative amount of aldehyde compounds in the bio-oil from the HTL with CTAB is a little higher than that in the bio-oil without CTAB.

The qualitative analysis also identified isophytol in both bio-oils, more so from the HTL of *C. vulgaris* with CTAB. Phytol and its derivatives are generally accepted to be derived from the carotenoids (organic pigments) at lower HTL temperatures or from sporopollenin at higher HTL temperatures (Torri *et al.*, 2012). Regardless of the exact source, even though the researchers are satisfied that the derivation from carotenoids was more fortunate, the presence of CTAB with the liquefied biomass enhanced the cell wall lysis, facilitated the extraction of such compounds, and consequently increased the amount of the acyclic diterpene alcohol, isophytol. Other alcoholic compounds were also observed in both bio-oils; however, the relative amount was a bit higher in the bio-oil without CTAB due to their higher content of carbohydrate.

The elemental analysis of both bio-oils demonstrated previously the advantage of using algal biomass recovered by the foam flotation column as an HTL feedstock for lowering the nitrogen content. These outcomes were consistent with the relative amounts of nitrogenous compounds identified from the GC-MS spectra as shown in table 6.3. A wide range of N-containing compounds including pyrazines, amines, pyrroles, pyridines, fatty amides, and indoles were observed from both bio-oils with total peak areas of 30.55 and 43.37% for *C. vulgaris* harvested by foam flotation and centrifugation respectively. However, the bio-oil from algae harvested by foam flotation mostly contained amides and amines with very small amounts of amino acids. The identified nitrogenous compounds were categorised into groups and the possible reaction pathway for each group was elucidated as following (Chiavari and Galletti, 1992; Yaylayan and Kaminsky, 1998; Torri *et al.*, 2012):

1- **Fatty amide and nitriles**: these compounds are produced by the condensation/amination reaction between fatty acids as electrophile and ammonia as nucleophile.
2- **Amine**: these products are formed by the decomposition of amino acids.
3- **Pyrroles and pyrroles derivatives:** formed by the decomposition of proteins.
4- **Pyrazines compounds:** these compounds are the hydrothermal products from the Maillard reaction, the chemical reaction between the reducing sugars and amino acids. The reactive group of the reducing sugars, the carbonyl, and the nucleophilic amino group of the amino acids react to form such compounds.
5- **Pyridines and pyrimidine:** they are in general products from the pyrolysis of proteins; however, pyrimidine is produced particularly by the pyrolysis of DNA and RNA. The latter was not seen in the bio-oil from the HTL of *C. vulgaris* with CTAB.
6- **Piperazine derivatives:** they are most likely produced by the Maillard reaction.
7- **Indoles and aromatic amides (e.g. imidazole):** they are the products from the decomposition of side chain amino acids.
8- **Alkyl aniline:** they are possibly produced by the reaction of ammonia and phenol.

More generally, the N-containing heterocyclic compounds might be also formed by the cyclisation reaction between amino acids (W. Wang *et al.*, 2017). The reduction in nitrogen content in the bio-oil produced by the HTL of *C. vulgaris* with CTAB was probably due to the superior activity of CTAB in promoting cell wall lysis and enhanced the temperature effect to pyrolyse more of the protein fraction into smaller fragments which favour the water-soluble phase rather than bio-oil phase. Obtaining more N atoms in the water-soluble organic fraction would be beneficial as an efficient nutrient source for microalgae growth. Additionally, hydrogen gas, which had higher yield in the HTL of microalgae harvested by foam flotation, may also contribute to a certain extent in capping some free radicals to form more stable compounds of low nitrogen content.

6.3.7 Characterisations by Fourier transform infrared (FTIR) spectroscopy

6.3.7.1 Composition of the model compounds by FTIR

FTIR spectra of the model compounds (starch, bovine serum albumin (BSA), and rapeseed oil) were carried out to characterise functional groups for the carbohydrate, protein, and lipid present in microalgae in isolation which, in conjunction with literature (Gai *et al.*, 2014; Feng Cheng *et al.*, 2017; Shakya *et al.*, 2017; Song *et al.*, 2017), can improve band assignments and interpretation of microalgae and bio-oil spectra. FTIR spectra for the model compounds are

shown in figure 6.8. In the starch spectrum, the main peaks include O-H stretching (3305 cm^{-1}) which is much broader than N-H stretching (3280 cm^{-1}) in protein, C-O-C stretching (1147, 989, and 926 cm^{-1}) and C-H bending vibration (1076 cm^{-1}). The BSA spectrum shows five main bands which are N-H stretching (3280 cm^{-1}), C=O stretching (amide I band, 1636 cm^{-1}), N-H bending/C-N stretching (amide II band, 1508 cm^{-1}), N-O_2 stretching (1398 cm^{-1}) and C-N stretching/N-H bending (amide III band, 1239 cm^{-1}). In the rapeseed FTIR spectrum, the main peaks include C-H stretching (3006, 2922, and 2853 cm^{-1}), C=O stretching (1744 cm^{-1}), C-H bending (1458 and 1376cm^{-1}), C(O)-O stretching (1235 cm^{-1}), and C-O stretching (1159 cm^{-1}).

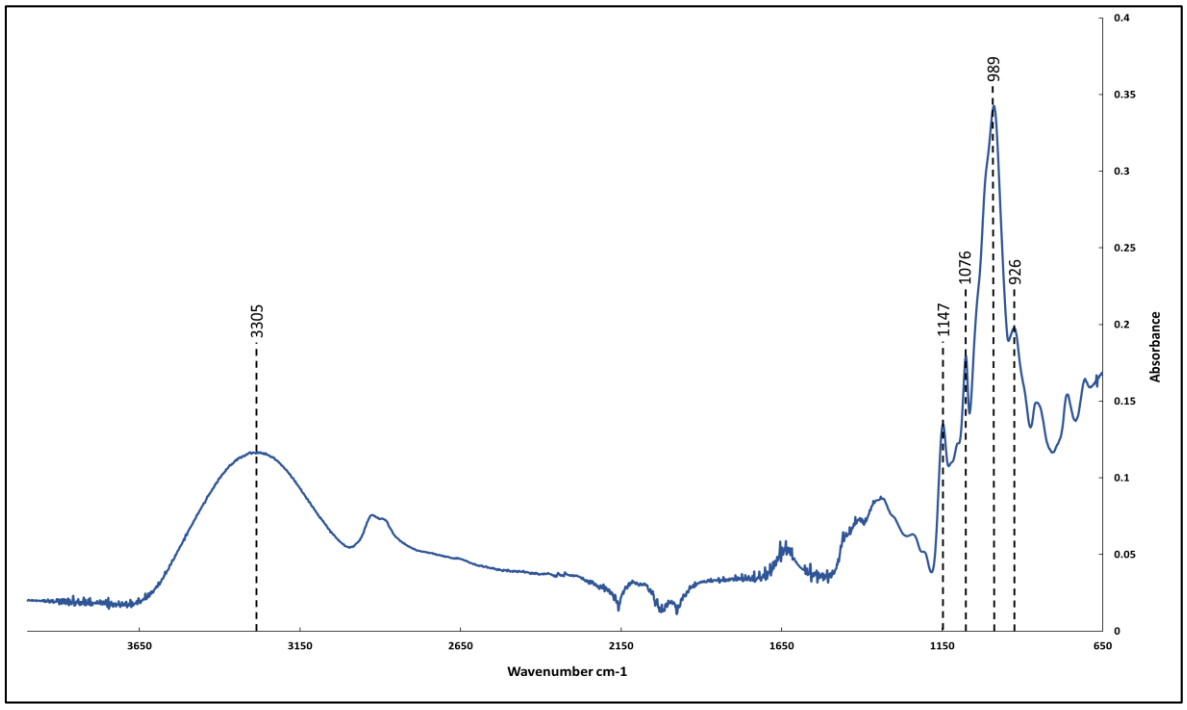

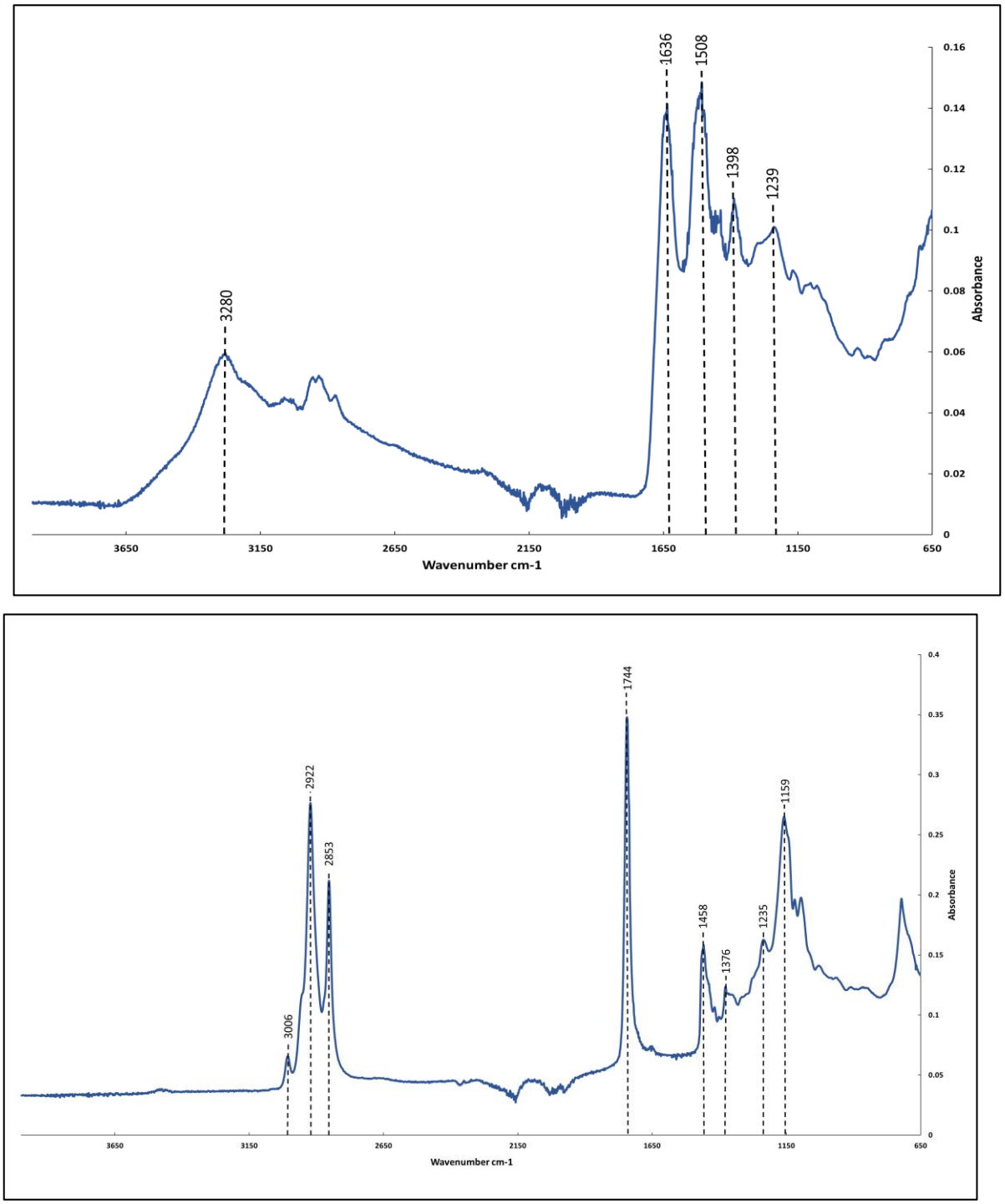

Figure 6.8: FTIR spectra of starch, BSA, and rapeseed oil respectively from top to bottom

6.3.7.2 Composition of algal biomass by FTIR

FTIR spectra for *C. vulgaris* harvested by the centrifugation and foam flotation techniques are shown and compared in figure 6.9. FTIR analysis of the harvested microalgae was carried out to study their functional group characteristics and follow any potential structural change in algal biomass because of the presence of CTAB with the microalgae harvested by foam flotation.

CTAB has been used in the extraction of DNA and found to promote algae cell lysis and enhance lipid recovery and profile as demonstrated earlier (T. Coward *et al.*, 2014).

For *C. vulgaris* harvested by centrifugation, the main peak distributions which indicate the presence of protein are N-H stretching vibration (3280 cm^{-1}), C=O stretching (amide I band, 1636 cm^{-1}), and N-H bending (amide II band, 1524 cm^{-1}). The C-H stretching (2922 and 2851 cm^{-1}), C-H bending (1450 and 1398 cm^{-1}) and C(O)-O/P=O stretching (1238 cm^{-1}) indicate the presence of lipid, and finally, the C-O-C stretching (1144 cm^{-1}) and C-H bending vibration in sugar (1033 cm^{-1}) which indicate the presence of carbohydrate. The P=O stretching (1341-1188 cm^{-1}) is ascribed to the phosphodiester in the algal nucleic acid and phospholipids.

Significant differences were observed in the relative intensity of some peaks in addition to some peak shifting for *C. vulgaris* harvested by flotation (Figure 6.9) particularly within the lipid peaks which was validated hereafter by quantifying the biochemical composition of *C. vulgaris* harvested by centrifugation and flotation. These differences were likely due to the attachment of long alkyl groups originated from CTAB after dissociation in water. The FTIR spectra of both *C. vulgaris* feedstocks (harvested by centrifugation and flotation) also demonstrated that the adsorption of CTAB onto microalgae was a chemisorption process since some changes were observed, indicating that new chemical groups were introduced on the surface of *C. vulgaris*. Small increase in the intensity of C(O)-O/P=O stretching (1238 cm^{-1}) was observed as well and it would be due to the capability of CTAB to promote algae cell lysis and hence enhance recovery of the phospholipids.

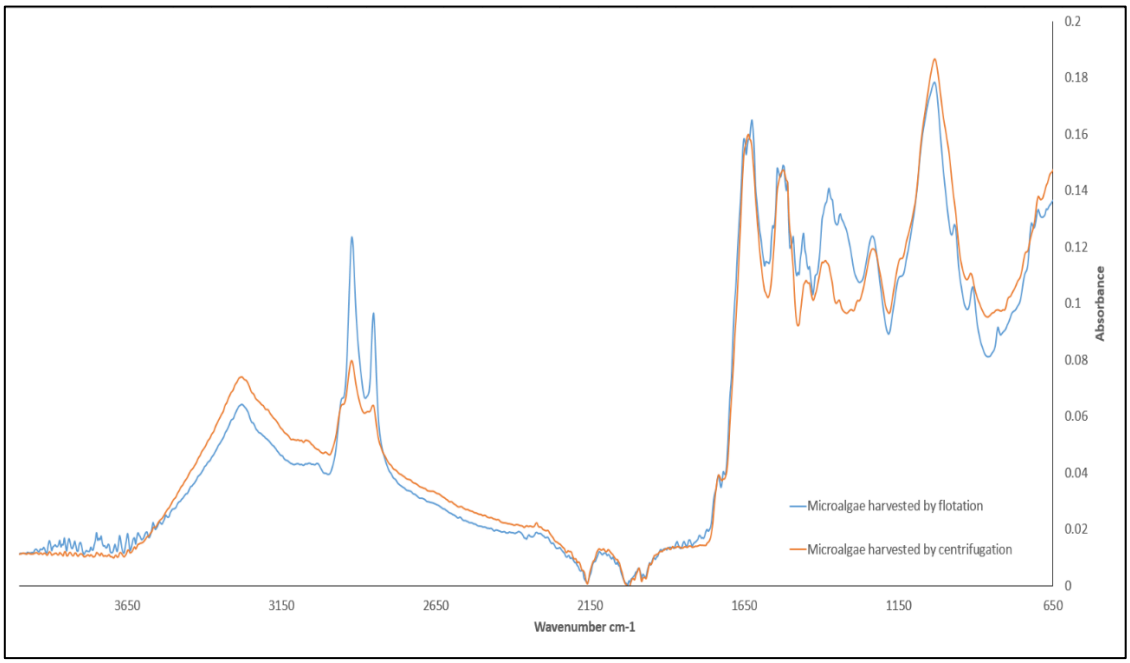

Figure 6.9: FTIR spectra of *C. vulgaris* harvested by centrifugation and flotation under a CTAB concentration of 35 mg L^{-1} of algae culture.

The biochemical composition of *C. vulgaris* harvested by centrifugation was of 55.7±2.2% protein, 28.3±1.6% carbohydrate, and 11.9±1.1% lipid. However, measuring the carbohydrate content for *C. vulgaris* harvested by foam flotation using the conventional method did not give an accurate value due to the alteration in the sugar-extract colour after treatment with the H_2SO_4 solution which might occur because of CTAB presence on the microalgae cell wall whereas no problem was noticed with lipid and protein content measurements. The lipid content of *C. vulgaris* harvested by foam flotation was found to be increased, 19.6±2.2%, while no significant change was observed for the protein content, 55.9±1.9%. The carbohydrate content was solely calculated by difference and was found to be 20.4%.

It is obvious that there was a reduction of the carbohydrate content in *C. vulgaris* harvested by foam flotation while the lipid content increased. The increase in the lipid content can be explained based on two points: firstly, CTAB can disrupt algae cell wall and promote cell lysis. Thus, it enhances the recovery of internal cell contents like lipid and increases the solubility of some phospholipids as well (T. Coward *et al.*, 2014). Secondly, CTAB is a fatty amine salt and quaternary ammonium with one long chain of the alkyl type and is often produced from natural fatty acids (Salager J. L., 2002); this is seen in the FTIR spectrum for CTAB (Figure 6.10), therefore, adsorbed CTAB on the algae cell wall increases the lipid content in *C. vulgaris* harvested by foam flotation. It is worth noting that not only the CTAB adsorbed onto microalgae cell wall is recovered with the harvested microalgae but also the remaining free CTAB used to generate the foam. Both sources will increase the long chain hydrocarbon content.

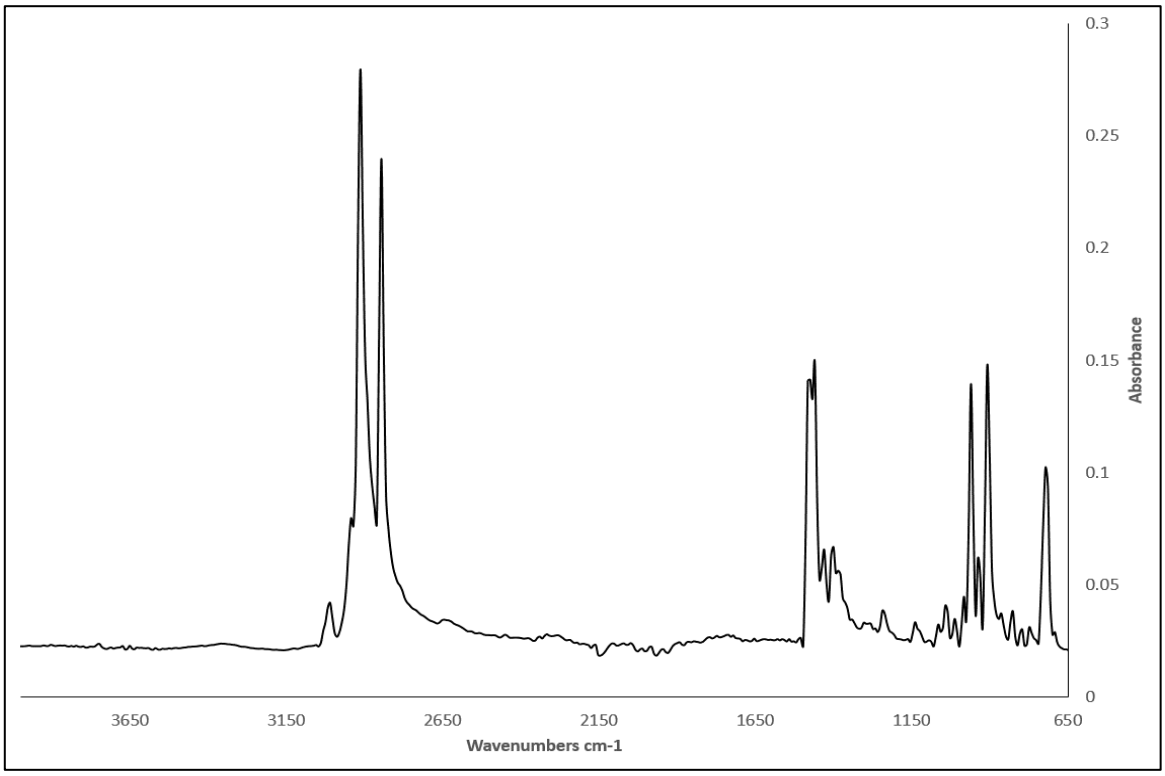

Figure 6.10: FTIR spectrum of cetyltrimethylammonium bromide (CTAB).

Polyanionic polysaccharides (carbohydrates), like those found in microalgae biomass, complex with CTAB due to the electrostatic interaction between them and the reduction in carbohydrate content may be due to the cell wall lysis caused by CTAB or because of the impediments in detecting the stretching vibration of carbohydrate by the FTIR spectrum due to the carbohydrate complexing with the surfactant.

6.3.7.3 Composition of algal biomass and bio-oils by FTIR

The FTIR spectra for the bio-oil produced by the HTL of *C. vulgaris* harvested by centrifugation and the *C. vulgaris* feedstock are shown in figure 6.11. It can be seen from the figure for the bio-oil that N-H stretch (3280 cm^{-1}), C=O stretching (amide I band, 1636 cm^{-1}), and N-H bending (amide II band, 1525 cm^{-1}), C(O)-O/P=O stretching (1238 cm^{-1}), and C-O-C stretching (1144 cm^{-1}) disappear as most groups comprising heteroatoms are processed and eliminated. Simultaneously, a broad band O-H stretching/N-H stretching (3400-3200 cm^{-1}), C-H stretching (2954, 2922, and 2852 cm^{-1}), C=O stretching (1702, 1697, 1670, 1663, and 1624 cm^{-1}), C-H bending (1457 cm^{-1}), C=C stretching (aromatic with amine group, 1654, 1618, and 1438 cm^{-1}), C=C stretching (1570 and 1577 cm^{-1}), and C-H bending (1457, 1376 cm^{-1}) appear to increase. The band (3400-3200 cm^{-1}) is more likely from O-H stretching rather than N-H stretching

vibration since the former is very broad than the latter which is usually less broad and sharper. Some peaks with small intensities with N(O)-O and N=N stretching (1566-1535 cm^{-1}), C-N stretching (amide III in aromatic, 1272 cm^{-1}), C-O stretching (1169 cm^{-1}), =C-H bending (1406, 1413, and 1420 cm^{-1}), and C-H bending (1400 cm^{-1}) appear to grow as well. The FTIR spectrum for the bio-oil reveals the formation of fatty acids and heteroatoms containing saturated and unsaturated aliphatic and cyclic compounds. This inference is strongly supported by the previously described possible HTL pathways which involve hydrolysis, dehydration, decarboxylation, decarbonylation, deamination, amination, rearrangement, and aromatisation (Feng Cheng *et al.*, 2017).

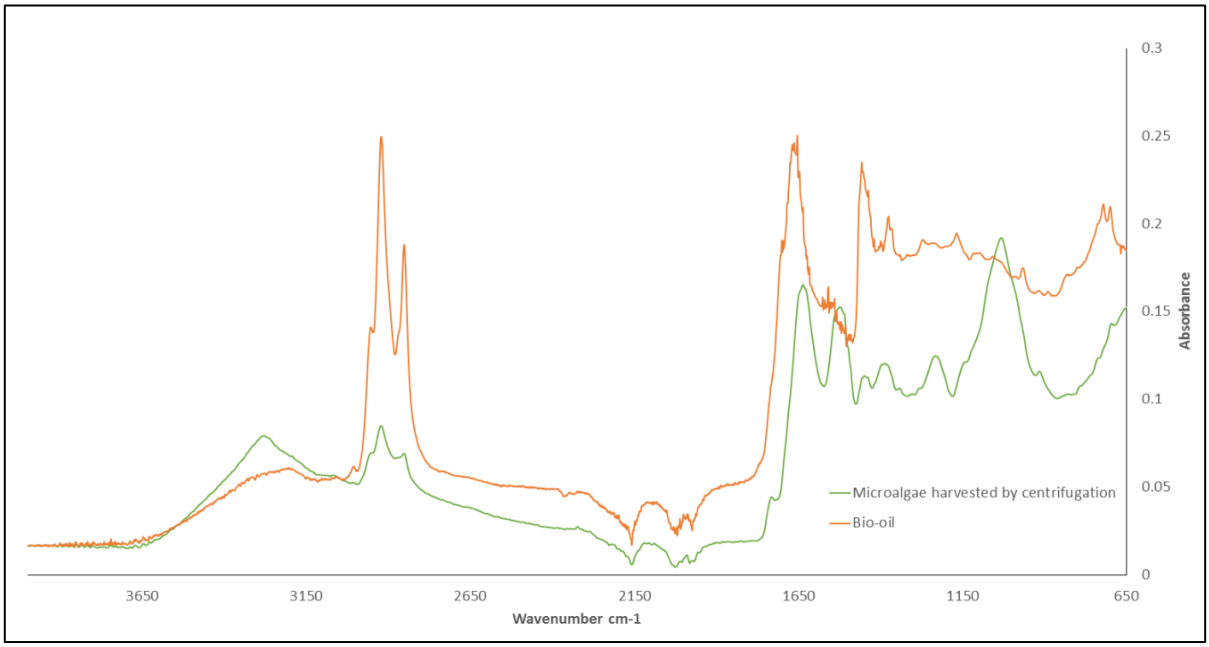

Figure 6.11: FTIR spectra of microalgae (*C. vulgaris*) harvested by centrifugation and bio-oil produced under 320 ˚C, 32 ˚C/min heating rate, and no holding time.

The FTIR spectra for the bio-oil produced by the HTL of *C. vulgaris* harvested by foam flotation and the *C. vulgaris* feedstock are shown in figure 6.12. Small differences in the peak distribution were found in the FTIR spectra for the bio-oils produced from the HTL of *C. vulgaris* harvested by foam flotation and centrifugation. Peaks include N(O)-O and N=N stretching (from 1535 to 1566 cm^{-1}), C-N stretching (amide III in aromatic, 1272 cm^{-1}), C-O stretching (1169 cm^{-1}), =C-H bending (1406, 1413, and 1420 cm^{-1}), and C-H bending (1400 cm^{-1}) look to have disappeared. Moreover, some peaks of low intensities including C=O stretching (1701 and 1629 cm^{-1}), aromatic ring vibration (1591 cm^{-1}) appear to grow, which again reveals the formation of more carboxylic acid and aromatic hydrocarbons. It is worth

mentioning that C=O stretching in 1701 cm^{-1} region may be attributed to the presence of other compounds having C=O stretching such as aldehydes and ketones.

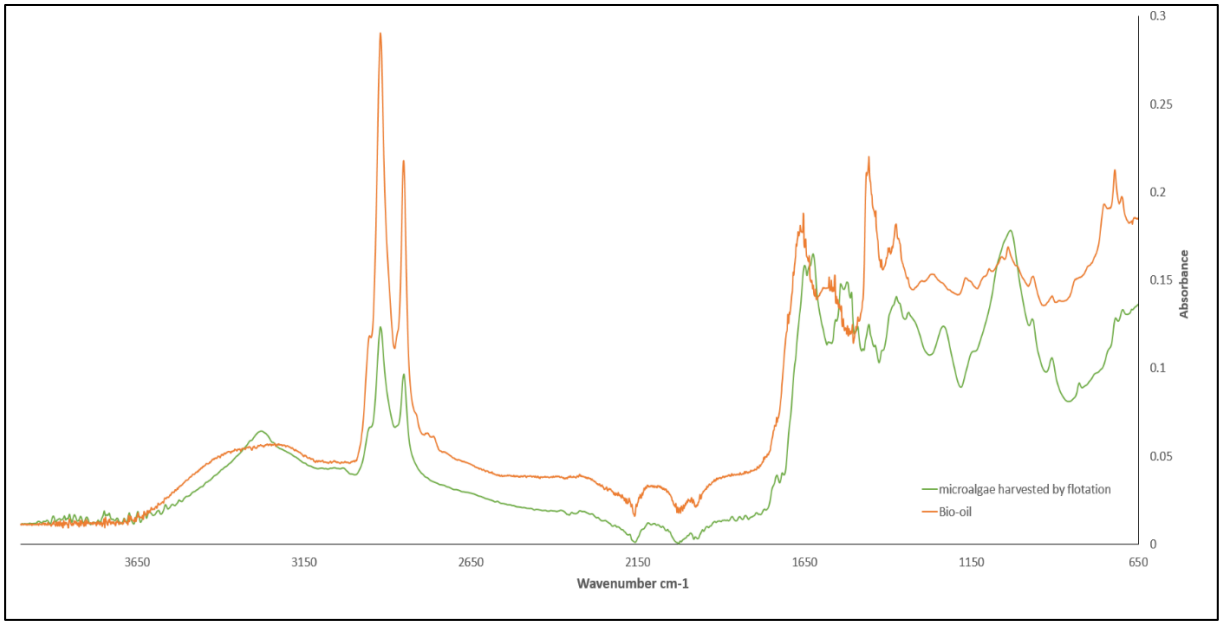

Figure 6.12: FTIR spectra of *C. vulgaris* harvested by flotation and bio-oil produced under 320 ˚C, heating rate 32 ˚C/min, and no holding time.

The FTIR spectra for the bio-oil produced by the HTL of *C. vulgaris* harvested by foam flotation and centrifugation are shown in figure 6.13. The intensities and areas of the FTIR spectra revealed that the bio-oil from the HTL of *C. vulgaris* harvested by flotation had little stronger C-H stretching (2954, 2921, and 2851 cm^{-1}) than the bio-oil from the HTL of *C. vulgaris* harvested by centrifugation. This was probably due to the higher number of alkyl groups in the fatty acid and/or more aliphatic hydrocarbons in the bio-oil from the HTL of *C. vulgaris* harvested by foam flotation.

Figure 6.13 also shows that C=O stretching (amide I band, 1636 cm^{-1}) and C=C stretching (aromatic with amine group, 1654, 1618, and 1438 cm^{-1}) in the bio-oil from the HTL of *C. vulgaris* harvested by centrifugation are larger than the peaks of the same wavenumber in the bio-oil from the HTL of *C. vulgaris* harvested by foam flotation. This outcome suggests more abundance of amides, amine and unsaturated cyclic structure in the former bio-oil. Both bio-oils had obvious C-H bending peaks (1457 and 1376 cm^{-1}) which are sharper for the bio-oil from the HTL of *C. vulgaris* harvested by flotation. The bands in the region from 1100-1040 cm^{-1} were larger in the bio-oil from the HTL of *C. vulgaris* harvested by flotation and they were likely attributed to C-O stretching vibration, indicating the possible presence of alcohol or acid

in the bio-oil. For both bio-oils, some peaks were observed at (739, 721, and 700 cm^{-1}) as well, possibly attributed to the C-H bending from alkene and aromatic and their derivatives. The out-plane C-H vibration of peak at 721 cm^{-1} was slightly stronger in the bio-oil from the HTL of *C. vulgaris* recovered by flotation, showing more alkenes in this oil relative to that from the HTL of *C. vulgaris* harvested by centrifugation. The FT-IR spectra for both bio-oils were consistent with the outcomes from the GC-MS analysis.

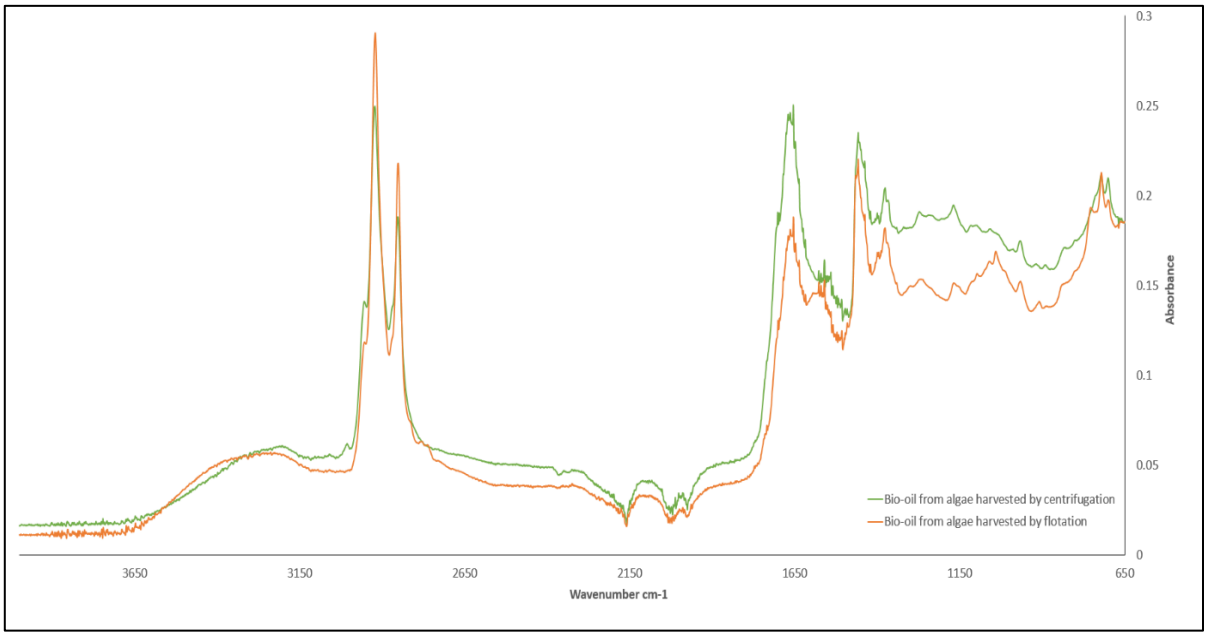

Figure 6.13: FTIR spectra of the bio-oils produced by the HTL of *C. vulgaris* harvested by flotation and centrifugation under reaction temperature of 320 ˚C, heating rate of 32 ˚C/min, and no holding time.

6.4 Conclusion

This work explored the direct hydrothermal liquefaction of microalgae (*C. vulgaris*) harvested by foam flotation and centrifugation. The HTL of *C. vulgaris* harvested by flotation yielded a larger amount of bio-oil than that from the HTL of *C. vulgaris* harvested by centrifugation. This is probably due to the ability of CTAB to disrupt the algae cell wall and promote cell lysis that in turn enhances the recovery of internal cell contents such as lipid, and increases the solubility of the phospholipids bilayer in the cell membrane. Additionally, CTAB that adsorbs onto microalgae cells and the remaining free CTAB that attaches to the air bubbles is recovered with the harvested microalgae resulting in an increase in the long chain hydrocarbon content and consequently greater bio-oil quantities. However, the amount of non-adsorbed CTAB

accompanying the algal slurry was not enough to increase the bio-oil in the products to the yield observed in these experiments. Approximately, seven litres of microalgae culture were harvested to produce the required biomass (3 g) for each HTL experiment and if the total amount of CTAB used to harvest the microalgae culture (0.035×7 = 0.245 g) was considered to accompany the algal slurry, it only represented 8% of the total biomass. Nevertheless, it will contribute to increasing the bio-oil yield to some extent. The increase in the bio-oil yield is likely due to the capability of CTAB in enhancing the disruption of the algal cell wall and promoting cell lysis. This enhances the recovery of internal cell contents like DNA and lipid and increase the solubility of some phospholipids in the cell membrane as well, thereby enhancing bio-oil yield.

Beside higher bio-oil yields, lower amounts of water-soluble organic, solid residue, and gas products were observed. Use of *C. vulgaris* recovered by foam flotation as a feedstock for HTL technology reduced the nitrogen content in the bio-oil fraction as shown by CHN elemental analysis, and GC-MS and FTIR spectra. Analysis by GC-MS indicated higher relative amounts of esters and hydrocarbons in contrast to lower amounts of ketones in the bio-oil from the HTL of *C. vulgaris* with CTAB in comparison to that from the HTL of *C. vulgaris* without. Using *C. vulgaris* harvested by foam flotation as a feedstock for HTL enhanced the bio-oil quality by promoting the yield of light-fraction and hence reduced the viscosity. It also increased the conversion of the liquefaction reaction from 76.8 to 87.6%. However, a slight increase in acidity occurred due to the increase of oxygen content. The outcomes from the energy recovery measurements indicated that the HTL of *C. vulgaris* harvested by the foam flotation column produced fuel which had a stored energy closer to that of dry algal feedstock than the fuel produced from *C. vulgaris* harvested by centrifugation.

Chapter 7

Conclusions and recommendations for future work

7.1 Conclusions

A successful harvesting technique for microalgae needs to be: **effective**, **rapid**, **low cost**, **species independent**, **scalable**, and should be able to **operate continuously** if required. Although a wide range of microalgae culture separation technologies are available, none of them have shown any economic feasibility to recover microalgae for biofuel production. Foam flotation has been branded a promising low-cost technique for physical separation of microalgae from its culture medium. Therefore, in this thesis, the feasibility of using a continuous foam flotation column as a unique harvesting technology that possesses most of the characteristics expected of a successful harvester, was investigated for the first time. Low cost and readily available materials were used to construct the flotation column, with a configuration that could be easily cleaned and changed to fulfil various experimental requirements.

The most important conclusion is that the continuous foam flotation column delivers advantages in terms of both cost and efficiency compared to other commonly used harvesting techniques, as it harvests both freshwater and marine species at low capital and operating costs as well as eliminates the trade-off between high recovery efficiency (for greater biomass removal) and concentration factor (to lower downstream dewatering and drying costs).

The effects of cell surface characteristics were investigated on *Chlorella vulgaris* flotation performance by quantifying the hydrophobicity, zeta potential, and contact angle. The cationic hexadecyltrimethylammonium bromide (CTAB) enhanced the low hydrophobicity and reduced the net charge of the cells; likely due to the attachment of positive long alkyl hydrophobic groups originating from CTAB after dissociation in water. The amount of surfactant adsorbed onto the cells was determined by surface tension to calculate the surfactant quantity remaining for foam induction in the column. Foam stability was influenced by the algal biomass concentration due to the adsorption of surfactant onto the cells. Fractional factorial and central composite design experiments showed that surfactant concentration, column height, and air flow rate had the greatest effect on harvesting effectiveness criteria (recovery efficiency and concentration factor); the process variables were then optimised to achieve an effective combination of a high recovery efficiency and a high concentration factor – a pivotal step forward in flotation harvesting of microalgae. The optimised variables (CTAB = 35 mg L^{-1}, air

flow rate = 1 L min^{-1}, feed flow rate = 0.1 L min^{-1}, column height = 146 cm, liquid pool depth = 25 cm, with a fine porous sparger) were subsequently used to harvest freshwater *C. vulgaris* and marine *Isochrysis galbana* and *Tetraselmis suecica* microalgae, yielding high recovery efficiencies of 95, 93, and 89% together with 173, 271 and 143-fold biomass enrichments, respectively (the improvement in harvesting performance of marine species in particular is noteworthy). Compared to commonly used harvesting techniques, the continuous foam flotation column had a very low power consumption, 0.052 kWh m^{-3}, with a low total harvesting cost (including the chemical cost) of US$ 0.179 per 1 m^3 of microalgae culture.

Besides the bulk harvesting of microalgae, further dewatering and drying are other impediments to producing algal biofuel at competitive prices. Therefore, the possibility of intensifying the continuous foam flotation column by enhancing the foam drainage (i.e. increasing the enrichment of the harvested microalgae) was also evaluated. Drainage enhancement was facilitated by inserting three foam risers with 0.25, 0.5, and 0.75 smooth-successive contraction and expansion diameter ratios into the foam column. Each riser increased the drainage of interstitial water from the foam and increased the concentration of the harvested microalgae. A high concentration factor (722) and total suspended solid yield (14.6%) were achieved with the 0.25 riser, delivering a highly concentrated slurry with a total suspended solid comparable to or better than that achieved by other dewatering techniques such as centrifugation and filtration at lower cost. However, a minor reduction in the recovery efficiency of *C. vulgaris* was observed, from 95 to 91%, potentially due to the adhesion of dry microalgae biomass onto the foam riser wall.

The development of mathematical models for foam flotation has proven difficult due to the interactions between solid, gas, and liquid phases within the process. Instead, kinetic and efficiency models were adopted to better understand the process for microalgae. Bubble size is a crucial factor in foam flotation as it determines the final performance of the process in terms of recovery efficiency and concentration factor. A wide bubble size distribution was generated (204 to 2909 µm) and Sauter mean dimeters ranging from 811 to 1713 µm under different experimental conditions. The Sauter bubble diameter decreased with increasing CTAB concentration but increased with air flow rate. Smaller bubbles have longer residence times in the liquid due to their slower rise velocity, leading to a larger contact time between gas and solid phases and consequently enhancing microalgae collection efficiency. The slower bubble rise velocity at high CTAB concentrations was due to the retardation that occurred when the

CTAB and microalgae adsorbed onto the bubble surface. Theoretically, low microalgae collection efficiencies were observed which were undoubtedly due to the low collision efficiencies between microalgae and bubbles. The theoretical recovery efficiencies did not agree with the corresponding experimental recovery efficiencies. The obtained high experimental recovery efficiencies indicate that there are other forces acting between microalgae and bubbles not considered in the commonly used collision models. The bubble-microalgae attachment and stability efficiencies were at, or close to unity due to the surface forces between bubbles and cells such as electrostatic forces, hydrophobicity, and the small algal cell size.

Hydrothermal liquefaction (HTL) of model compounds (starch, bovine serum albumin (BSA), and rapeseed oil) in isolation showed that the bio-oil yield was in the order of lipid > protein > carbohydrate. CTAB was almost entirely converted into bio-oil with very little solid fraction. The direct HTL of *C. vulgaris* recovered by foam flotation and centrifugation (control) were performed. HTL at high reaction temperatures (> 370 ˚C) produced a high gas yield whereas low temperatures (< 250 ˚C) were not sufficient; therefore, a mild temperature range (between 280 and 320 ˚C) was adopted. The HTL of *C. vulgaris* harvested by foam flotation yielded more bio-oil than cells harvested by centrifugation; likely due to CTAB disrupting the cell wall and promoting cell lysis thereby increasing the solubility of the cell membrane phospholipids bilayer; a further advantageous feature for CTAB aided foam flotation. Moreover, the increases in bio-oil yield might occur in part due to the selective separation of higher lipid content cells which are floated more easily due to their low density. The HTL of *C. vulgaris* harvested by foam flotation also offered lower water-soluble organic, solid residue, and gas product yields, with a lower bio-oil nitrogen content, and higher relative amounts of esters and hydrocarbons and lower amounts of ketones, with an overall increased conversion efficiency of 87.6% versus 76.8% in the control. The energy recovery calculations indicated that HTL of *C. vulgaris* harvested using the foam column produced fuel with a stored energy closer to that of dry algal feedstock than the fuel produced from *C. vulgaris* harvested using centrifugation.

Overall, this piece of work adds several contributions to the literature:

Firstly, it demonstrates that the continuous foam flotation column is a **low cost**, **rapid**, and an **effective** harvesting technology for recovering microalgae with high recovery efficiency and concentration factor. In comparison to centrifugation and filtration, the continuous foam flotation column offers lower construction, energy, and maintenance costs with comparable or

better biomass yield. It also offers a shorter harvesting time and a lower floor space compared to coagulation and/or flocculation followed by sedimentation, therefore lending itself to be **scalable**. What is more, other characteristics of the successful harvester were noticed in our foam flotation column such as it is growth media and apparently **species independent** (harvesting freshwater and marine species) and able to **operate continuously**. Apart from the microalgae harvesting for biofuel production, the continuous foam flotation (this work) has other applications (e.g. in water and wastewater treatment industries). If the foam column is used as a separation and purification technology for wastewater instead of dissolved air flotation, it will remove microalgae as well as their excreted EPS (comprising mainly carbohydrates and proteins) and reduce the operating cost by about US$ 0.736 m^{-3} with a remarkable reduction in capital and maintenance costs due to its simplicity. Moreover, foam flotation can potentially improve water and chemical recycling since it can recover nearly whole chemicals (i.e. surfactant) from the processed water.

Secondly, compared to the dissolved air flotation and electro-flotation techniques, the foam flotation column with foam riser (this work) can lower the energy consumption required for drying 1 kg of microalgae to produce biomass suitable for syngas (approx. 15% saving) and pyrolytic oil (approx. 10% saving) production. Whereas it can lower the energy consumption required for drying the same quantity of microalgae by approximately 20 and 13% to produce the same products when compared to lamella separators.

Thirdly, foam flotation yields algal biomass suitable to produce larger quantities of HTL oil (about 8-14% larger than what has been reported in the literature) at lower temperatures and holding times. By subtracting the energy required to heat the reactor to the desired temperature, this will reduce the energy consumption for converting microalgae into bio-oil by approximately 83-100% if only the difference between holding times is considered (this work had 0 - 10 min holding time and the work reported in the literature had 60 min). Also, foam flotation yields algal biomass typical of that needed to produce higher HTL oil quality. It has a lower nitrogen content, higher relative amounts of esters and hydrocarbons and lower amounts of ketones. Consequently, this will reduce the costs of downstream processes required for upgrading the bio-oil.

Fourth, achieving high bio-oil yields at low holding times with the HTL of microalgae recovered by foam flotation can engender significant intensification of the HTL process. In other words, to hydrothermally liquefy algal biomass not harvested by foam flotation in a

continuous mode at high bio-oil productivity and yield, high feed flow rates and residence times are required, therefore reactors with large volumes would be required. This increases the constructional costs as well as energy consumption for heating the reactor. Moreover, high pressure reactors are not easy to scale up since the allowable operating pressure reduces as the reactor diameter increases and consequently the reactor wall thickness should be increased to compensate the reduction in the allowable operating pressure. These drawbacks will make the continuous HTL process unfavourable for processing microalgae harvested by the available harvesting techniques except for foam flotation.

Fifth, delivering a highly concentrated slurry with a total suspended solids content of 14.6% (besides the capability of CTAB to influence the cell wall and facilitate the extraction of lipids from microalgal biomass, i.e. coupling of dewatering and cell disruption) can undoubtedly advance the other techniques for converting wet biomass into biofuel such as *in-situ* transesterification, especially that microalgae phospholipids can also be converted into FAME. Such a total suspended solids content should reduce, to some extent, the extra volumes of solvent and homogenous catalyst used to overcome the low biodiesel yields due to high moisture content.

Sixth, HTL of microalgae has a lower environmental impact than that of pyrolysis. Firstly, a rough estimate of a reduction of 48% in the total energy needed for bio-oil production was made; this is due to avoiding the need to dry the feedstock and operating at a lower reaction temperature. Secondly, it has been reported that the greenhouse gas (CO_2) emissions are less than 221.4 g CO_{2eq} per MJ biodiesel when the HTL technique is used instead of pyrolysis. Higher CO_2 emission associated with pyrolysis is attributed to combustion of co-products to reduce process energetics. However, HTL of microalgae does not yet have net energy ratio (energy consumed to energy produced) close to that of diesel (0.2) but it has the potential to become a viable process if the energy required by the other microalgae production phases (e.g. cultivation) is reduced.

7.2 Recommendations for future work

Although the current study has attempted to consider the continuous foam flotation column and direct HTL conversion of harvested microalgae into bio-oils from different aspects, further research projects on the continuous foam flotation and direct HTL are still required. Microalgae are very diverse. To date, around 35,000 species have been described and the real number will be considerably higher. This work only investigated the harvesting of three species; freshwater

Chlorella vulgaris and marine *Isochrysis galbana* and *Tetraselmis suecica*. To examine the extent of its species independence will require a broader approach to harvesting, covering a range of taxa and growth forms (unicells, chains, and colonies). Moreover, foam flotation is highly dependent on the physicochemical properties of interfaces. Therefore, the physicochemical surface properties of each chosen species must be studied based on the surface free energy and zeta potential with and without the presence of surface active materials prior to the harvesting trials. This will provide crucial information regarding algal cell-to-cell and algal cell-to-bubble interactions and enable the best selection of surfactant even though surface charge can significantly determine their interactions.

The effects of growth phase and growth medium are of high importance, not only on the biochemical composition of microalgae but also on their surface characteristics. Therefore, investigations on these factors need to be considered for a wide range of microalgae species including those with resistant hydrophobic biomacromolecules in their cell walls (e.g. algaenan, such as *Nannochloropsis gaditana*, *Dunaliella tertiolecta* and *Scenedesmus* sp.). Separate to harvesting from defined media, continuous harvesting of species cultivated in wastewater is strongly recommended.

Attempts to develop a collision model for the microalgae particle-air bubble system in both liquid and foam zones is crucially important. Some assumptions must be considered such as the microalgae particle inertia is negligible due to its small cell size and the bubble surface is completely retarded i.e. an immobile surface, due to the presence of surfactants. Also, the number of bubble-particle attachment models is very limited due to the difficulties in measuring some quantities in attachment models such as induction time. Therefore, developing an attachment model for microalgae particles and bubbles as well as empirical correlation for induction time calculation is recommended.

Direct conversion of the harvested microalgae into HTL oils must be considered for a wide range of species with differing biochemical compositions (both freshwater and marine). The mechanisms and kinetics of the HTL reaction are still unclear and much research is required by hydrothermally liquefying various model compounds in isolation and in mixture under different operating conditions. Research into upgrading the produced microalgae bio-oils is also needed to evaluate the upgrading process with the enhancements occurred on the bio-oil from the HTL of microalgae with CTAB. Trials on upgrading the HTL oils using the vis-breaking process are also required. Research on the utilisation of microalgae harvested by foam flotation should not

be limited to biofuels, but should expand to include producing high-value products like those used in the health food and pharmaceutical industries.

Conferences attended and publication submitted

Conferences

Muayad A.S. Al-karawi, Abbas A. Umar, Gary S. Caldwell, and Jonathan G.M. Lee. Continuous harvesting of microalgae using dispersed foam flotation. Oral Presentation at the 3rd European congress of applied biotechnology. September 27 – October 1st, 2015 – Nice, France.

Muayad A.S. Al-karawi, Gary S. Caldwell, and Jonathan G.M. Lee. Foam flotation as an energy-efficient harvesting technique of microalgae biomass. Oral Presentation at the 7th UK algae conference. July 6th –7th, 2017 – Swansea, UK.

Muayad A.S. Al-karawi, Olivia G., Salihu D. Musa, Gary S. Caldwell, and Jonathan G.M. Lee. Drainage enhancement in the continuous foam flotation column used for algae biomass recovery. Oral Presentation at the 10th world congress of chemical engineering. October 1st – 5th, 2017 – Barcelona, Spain.

Publications

Muayad A.S. Al-karawi, Gary S. Caldwell, and Jonathan G.M. Lee. (2018) "Continuous harvesting of microalgae biomass using foam flotation", Algal Research, 36, pp. 125-138.

References

Abdel-Raouf, N., Al-Homaidan, A. A. and Ibraheem, I. B. M. (2012) 'Microalgae and wastewater treatment', *Saudi Journal of Biological Sciences*, 19(3), pp. 257-275.

Abdelaziz, A. E., Leite, G. B., Belhaj, M. A. and Hallenbeck, P. C. (2014) 'Screening microalgae native to Quebec for wastewater treatment and biodiesel production', *Bioresour Technol*, 157, pp. 140-8.

Abkarian, M., Subramaniam, A. B., Kim, S.-H., Larsen, R. J., Yang, S.-M. and Stone, H. A. (2007) 'Dissolution Arrest and Stability of Particle-Covered Bubbles', *Physical Review Letters*, 99(18), p. 188301.

Acién, F. G., Molina, E., Reis, A., Torzillo, G., Zittelli, G. C., Sepúlveda, C. and Masojídek, J. (2017) '1 - Photobioreactors for the production of microalgae A2 - Gonzalez-Fernandez, Cristina', in Muñoz, R. (ed.) *Microalgae-Based Biofuels and Bioproducts*. Woodhead Publishing, pp. 1-44.

Aguayo, G. A. and Lemlich, R. (1974) 'Countercurrent Foam Fractionation at High Rates of Throughput by Means of Perforated Plate Columns', *Industrial & Engineering Chemistry Process Design and Development*, 13(2), pp. 153-159.

Agwa, O. K. and Abu, G. O. (2014) 'Utilization of poultry waste for the cultivation of Chlorella sp. for biomass and lipid production', *Int. J. Curr. Microbiol. Appl. Sci.*, 3(8), pp. 1036-1047.

Ahmad, A. L., Mat Yasin, N. H., Derek, C. J. C. and Lim, J. K. (2011) 'Optimization of microalgae coagulation process using chitosan', *Chemical Engineering Journal*, 173(3), pp. 879-882.

Ahmed, I. R. and Bernd, R. T. (2004) 'Condensation Reactions and Formation of Amides, Esters, and Nitriles Under Hydrothermal Conditions', *Astrobiology*, 4(2), pp. 211-224.

Aitken, D. (2014) *An assessment of the sustainability of bioenergy production from algal feedstock*. University of Edinburgh.

Alam, M. A., Wan, C., Guo, S. L., Zhao, X. Q., Huang, Z. Y., Yang, Y. L., Chang, J. S. and Bai, F. W. (2014) 'Characterization of the flocculating agent from the spontaneously flocculating microalga Chlorella vulgaris JSC-7', *J Biosci Bioeng*, 118(1), pp. 29-33.

Alfafara Catalino, G., Nakano, K., Nomura, N., Igarashi, T. and Matsumura, M. (2002) 'Operating and scale- up factors for the electrolytic removal of algae from eutrophied lakewater', *Journal of Chemical Technology & Biotechnology*, 77(8), pp. 871-876.

Alhattab, M. and Brooks, M. S. (2017) 'Dispersed air flotation and foam fractionation for the recovery of microalgae in the production of biodiesel', *Separation Science and Technology*.

Anastasakis, K. and Ross, A. B. (2011) 'Hydrothermal liquefaction of the brown macro-alga Laminaria saccharina: effect of reaction conditions on product distribution and composition', *Bioresour Technol*, 102(7), pp. 4876-83.

Anastasakis, K. and Ross, A. B. (2015) 'Hydrothermal liquefaction of four brown macro-algae commonly found on the UK coasts: An energetic analysis of the process and comparison with bio-chemical conversion methods', *Fuel*, 139, pp. 546-553.

Anthony, R. J., Ellis, J. T., Sathish, A., Rahman, A., Miller, C. D. and Sims, R. C. (2013) 'Effect of coagulant/flocculants on bioproducts from microalgae', *Bioresour Technol*, 149, pp. 65-70.

Arbiter, N. (1952) 'Minerals Beneficiation - Flotation Rates and Flotation Efficiency', *Trans. AIME. Sept.*, pp. 791-796.

Arnaud, S.-J. and Dominique, L. (2002) 'Time evolution of aqueous foams: drainage and coarsening', *Journal of Physics: Condensed Matter*, 14(40), p. 9397.

Asadullah, M., Ito, S.-i., Kunimori, K., Yamada, M. and Tomishige, K. (2002) 'Energy Efficient Production of Hydrogen and Syngas from Biomass: Development of Low-Temperature Catalytic Process for Cellulose Gasification', *Environmental Science & Technology*, 36(20), pp. 4476-4481.

Aslan, S. and Kapdan, I. K. (2006) 'Batch kinetics of nitrogen and phosphorus removal from synthetic wastewater by algae', *Ecological Engineering*, 28(1), pp. 64-70.

Astals, S., Musenze, R. S., Bai, X., Tannock, S., Tait, S., Pratt, S. and Jensen, P. D. (2015) 'Anaerobic co-digestion of pig manure and algae: Impact of intracellular algal products recovery on co-digestion performance', *Bioresource Technology*, 181, pp. 97-104.

Azadi, P., Brownbridge, G., Mosbach, S., Smallbone, A., Bhave, A., Inderwildi, O. and Kraft, M. (2014) 'The carbon footprint and non-renewable energy demand of algae-derived biodiesel', *Applied Energy*, 113, pp. 1632-1644.

Azwar, M. Y., Hussain, M. A. and Abdul-Wahab, A. K. (2014) 'Development of biohydrogen production by photobiological, fermentation and electrochemical processes: A review', *Renewable and Sustainable Energy Reviews*, 31, pp. 158-173.

Babich, I. V., van der Hulst, M., Lefferts, L., Moulijn, J. A., O'Connor, P. and Seshan, K. (2011) 'Catalytic pyrolysis of microalgae to high-quality liquid bio-fuels', *Biomass and Bioenergy*, 35(7), pp. 3199-3207.

Bando, Y., Kuze, T., Sugimoto, T., Yasuda, K. and Nakamura, M. (2000) 'Development of bubble column for foam separation', *Korean Journal of Chemical Engineering*, 17(5), pp. 597-599.

Barros, A. I., Gonçalves, A. L., Simões, M. and Pires, J. C. M. (2015) 'Harvesting techniques applied to microalgae: A review', *Renewable and Sustainable Energy Reviews*, 41, pp. 1489-1500.

Beach, E. S., Eckelman, M. J., Cui, Z., Brentner, L. and Zimmerman, J. B. (2012) 'Preferential technological and life cycle environmental performance of chitosan flocculation for harvesting of the green algae Neochloris oleoabundans', *Bioresource Technology*, 121(0), pp. 445-449.

Belotti, G., de Caprariis, B., De Filippis, P., Scarsella, M. and Verdone, N. (2014) 'Effect of Chlorella vulgaris growing conditions on bio-oil production via fast pyrolysis', *Biomass and Bioenergy*, 61, pp. 187-195.

Bennion, E. P. (2014) *LIFE CYCLE ASSESSMENT OF MICROALGAE TO BIOFUEL: THERMOCHEMICAL PROCESSING THROUGH HYDROTHERMAL LIQUEFACTION OR PYROLYSIS*. Utah State University.

Besagni, G., Brazzale, P., Fiocca, A. and Inzoli, F. (2016) 'Estimation of bubble size distributions and shapes in two-phase bubble column using image analysis and optical probes', *Flow Measurement and Instrumentation*, 52, pp. 190-207.

Besagni, G. and Inzoli, F. (2016) 'Influence of internals on counter-current bubble column hydrodynamics: Holdup, flow regime transition and local flow properties', *Chemical Engineering Science*, 145, pp. 162-180.

Bhakta, A. and Ruckenstein, E. (1997) 'Decay of standing foams: drainage, coalescence and collapse', *Advances in Colloid and Interface Science*, 70, pp. 1-124.

Bhave, R., Kuritz, T., Powell, L. and Adcock, D. (2012) 'Membrane-Based Energy Efficient Dewatering of Microalgae in Biofuels Production and Recovery of Value Added Co-Products', *Environmental Science & Technology*, 46(10), pp. 5599-5606.

Bilad, M. R., Discart, V., Vandamme, D., Foubert, I., Muylaert, K. and Vankelecom, I. F. (2013) 'Harvesting microalgal biomass using a magnetically induced membrane vibration (MMV) system: filtration performance and energy consumption', *Bioresour Technol*, 138, pp. 329-38.

Bilad, M. R., Discart, V., Vandamme, D., Foubert, I., Muylaert, K. and Vankelecom, I. F. J. (2014) 'Coupled cultivation and pre-harvesting of microalgae in a membrane photobioreactor (MPBR)', *Bioresource Technology*, 155, pp. 410-417.

Biller, P., Friedman, C. and Ross, A. B. (2013) 'Hydrothermal microwave processing of microalgae as a pre-treatment and extraction technique for bio-fuels and bio-products', *Bioresource Technology*, 136(Supplement C), pp. 188-195.

Biller, P., Riley, R. and Ross, A. B. (2011a) 'Catalytic hydrothermal processing of microalgae: Decomposition and upgrading of lipids', *Bioresource Technology*, 102(7), pp. 4841-4848.

Biller, P., Riley, R. and Ross, A. B. (2011b) 'Catalytic hydrothermal processing of microalgae: decomposition and upgrading of lipids', *Bioresour Technol*, 102(7), pp. 4841-8.

Biller, P. and Ross, A. B. (2011a) 'Potential yields and properties of oil from the hydrothermal liquefaction of microalgae with different biochemical content', *Bioresour Technol*, 102(1), pp. 215-25.

Biller, P. and Ross, A. B. (2011b) 'Potential yields and properties of oil from the hydrothermal liquefaction of microalgae with different biochemical content', *Bioresource Technology*, 102(1), pp. 215-225.

Binks, B. P. (2002) 'Particles as surfactants—similarities and differences', *Current Opinion in Colloid & Interface Science*, 7(1), pp. 21-41.

Borges, F. C., Xie, Q., Min, M., Muniz, L. A. R., Farenzena, M., Trierweiler, J. O., Chen, P. and Ruan, R. (2014) 'Fast microwave-assisted pyrolysis of microalgae using microwave absorbent and HZSM-5 catalyst', *Bioresource Technology*, 166, pp. 518-526.

Borges, L., Morón-Villarreyes, J. A., D'Oca, M. G. M. and Abreu, P. C. (2011) 'Effects of flocculants on lipid extraction and fatty acid composition of the microalgae Nannochloropsis oculata and Thalassiosira weissflogii', *Biomass and Bioenergy*, 35(10), pp. 4449-4454.

Borrego, A. G., Hagemann, H. W., Prado, J. G., Guillén, M. D. and Blanco, C. G. (1996) 'Comparative petrographic and geochemical study of the Puertollano oil shale kerogens', *Organic Geochemistry*, 24(3), pp. 309-321.

Bosma, R., van, S. W., Tramper, J. and Wijffels, R. (2003) 'Ultrasound, a new separation technique to harvest microalgae', *J. Appl. Phycol.*, 15, pp. 143-153.

Bouchard, J., Desbiens, A., del Villar, R. and Nunez, E. (2009) 'Column flotation simulation and control: An overview', *Minerals Engineering*, 22(6), pp. 519-529.

Brady, P. V., Pohl, P. I. and Hewson, J. C. (2014) 'A coordination chemistry model of algal autoflocculation', *Algal Research*, 5, pp. 226-230.

Breil, C., Abert Vian, M., Zemb, T., Kunz, W. and Chemat, F. (2017) '"Bligh and Dyer" and Folch Methods for Solid–Liquid–Liquid Extraction of Lipids from Microorganisms. Comprehension of Solvatation Mechanisms and towards Substitution with Alternative Solvents', *International Journal of Molecular Sciences*, 18(4), p. 708.

Brennan, L. and Owende, P. (2010) 'Biofuels from microalgae—A review of technologies for production, processing, and extractions of biofuels and co-products', *Renewable and Sustainable Energy Reviews*, 14(2), pp. 557-577.

Brown, T. M., Duan, P. and Savage, P. E. (2010) 'Hydrothermal Liquefaction and Gasification of Nannochloropsis sp', *Energy & Fuels*, 24(6), pp. 3639-3646.

Brown Tristan, R. and Brown Robert, C. (2013) 'A review of cellulosic biofuel commercial-scale projects in the United States', *Biofuels, Bioproducts and Biorefining*, 7(3), pp. 235-245.

Bu X, X. G., Peng Y, Ge L, Ni C. (2016) 'Kinetics of flotation. Order of process, rate constant distribution and ultimate recovery', *Physicochemical Problems of Mineral Processing*, 53(1), pp. 342-365.

Buga, L. A. (2005) *Enantioselective Enrichment of Selected Pesticides by Adsorptive Bubble Separation*. TECHNICAL UNIVERSITY OF MUNICH.

Bui, T. T., Nam, S.-N. and Han, M. (2015) 'Micro-Bubble Flotation of Freshwater Algae: A Comparative Study of Differing Shapes and Sizes', *Separation Science and Technology*, 50(7), pp. 1066-1072.

Campanella, A. and Harold, M. P. (2012) 'Fast pyrolysis of microalgae in a falling solids reactor: Effects of process variables and zeolite catalysts', *Biomass and Bioenergy*, 46, pp. 218-232.

Campanella, A., Muncrief, R., Harold, M. P., Griffith, D. C., Whitton, N. M. and Weber, R. S. (2012) 'Thermolysis of microalgae and duckweed in a CO2-swept fixed-bed reactor: Bio-oil yield and compositional effects', *Bioresource Technology*, 109, pp. 154-162.

Campbell, J. M. (2014) *Gas Conditioning and Processing Volume 2:The Equipment Modules*. 9th edn. Norman, Oklahoma: Campbell Petroleum

Caniaz, R. O., Simsek, S., Arca, S., Sarayloo, E., Kavakli, I. H. and Erkey, C. (2018) 'Upgrading blends of microalgae feedstocks and heavy oils in supercritical water', *The Journal of Supercritical Fluids*, 133, pp. 674-682.

Cantrell, K. B., Ducey, T., Ro, K. S. and Hunt, P. G. (2008) 'Livestock waste-to-bioenergy generation opportunities', *Bioresource Technology*, 99(17), pp. 7941-7953.

Cerff, M., Morweiser, M., Dillschneider, R., Michel, A., Menzel, K. and Posten, C. (2012) 'Harvesting fresh water and marine algae by magnetic separation: Screening of separation parameters and high gradient magnetic filtration', *Bioresource Technology*, 118, pp. 289-295.

Chaiwong, K., Kiatsiriroat, T., Vorayos, N. and Thararax, C. (2013) 'Study of bio-oil and bio-char production from algae by slow pyrolysis', *Biomass and Bioenergy*, 56, pp. 600-606.

Chakinala, A. G., Brilman, D. W. F., van Swaaij, W. P. M. and Kersten, S. R. A. (2010) 'Catalytic and Non-catalytic Supercritical Water Gasification of Microalgae and Glycerol', *Industrial & Engineering Chemistry Research*, 49(3), pp. 1113-1122.

Chen, F., Liu, Z., Li, D., Liu, C., Zheng, P. and Chen, S. (2012) 'Using ammonia for algae harvesting and as nutrient in subsequent cultures', *Bioresour Technol*, 121, pp. 298-303.

Chen, L., Wang, C., Wang, W. and Wei, J. (2013) 'Optimal conditions of different flocculation methods for harvesting Scenedesmus sp. cultivated in an open-pond system', *Bioresour Technol*, 133, pp. 9-15.

Chen, W.-H., Lin, B.-J., Huang, M.-Y. and Chang, J.-S. (2015) 'Thermochemical conversion of microalgal biomass into biofuels: A review', *Bioresource Technology*, 184, pp. 314-327.

Chen, Y. M., Liu, J. C. and Ju, Y.-H. (1998) 'Flotation removal of algae from water', *Colloids and Surfaces B: Biointerfaces*, 12(1), pp. 49-55.

Cheng, F., Cui, Z., Chen, L., Jarvis, J., Paz, N., Schaub, T., Nirmalakhandan, N. and Brewer, C. E. (2017) 'Hydrothermal liquefaction of high- and low-lipid algae: Bio-crude oil chemistry', *Applied Energy*, 206, pp. 278-292.

Cheng, X., Chen, X., Su, X., Zhao, H., Han, M., Bo, C., Xu, J., Bai, H. and Ning, K. (2014) 'DNA Extraction Protocol for Biological Ingredient Analysis of Liuwei Dihuang Wan', *Genomics, Proteomics & Bioinformatics*, 12(3), pp. 137-143.

Cheng, Y. L., Juang, Y. C., Liao, G. Y., Ho, S. H., Yeh, K. L., Chen, C. Y., Chang, J. S., Liu, J. C. and Lee, D. J. (2010) 'Dispersed ozone flotation of Chlorella vulgaris', *Bioresour Technol*, 101(23), pp. 9092-6.

Cheng, Y. L., Juang, Y. C., Liao, G. Y., Tsai, P. W., Ho, S. H., Yeh, K. L., Chen, C. Y., Chang, J. S., Liu, J. C., Chen, W. M. and Lee, D. J. (2011) 'Harvesting of Scenedesmus obliquus FSP-3 using dispersed ozone flotation', *Bioresour Technol*, 102(1), pp. 82-7.

Chew, K. W., Yap, J. Y., Show, P. L., Suan, N. H., Juan, J. C., Ling, T. C., Lee, D. J. and Chang, J. S. (2017) 'Microalgae biorefinery: High value products perspectives', *Bioresour Technol*, 229, pp. 53-62.

Chiaramonti, D., Prussi, M., Buffi, M., Rizzo, A. M. and Pari, L. (2017) 'Review and experimental study on pyrolysis and hydrothermal liquefaction of microalgae for biofuel production', *Applied Energy*, 185, pp. 963-972.

Chiavari, G. and Galletti, G. C. (1992) 'Pyrolysis-gas chromatography/mass. spectrometry of amino acids', *Analytical and Applied Pyrolysis*, 24, pp. 123- 137.

Chinnasamy, S., Bhatnagar, A., Claxton, R. and Das, K. C. (2010a) 'Biomass and bioenergy production potential of microalgae consortium in open and closed bioreactors using untreated carpet industry effluent as growth medium', *Bioresour Technol*, 101(17), pp. 6751-60.

Chinnasamy, S., Bhatnagar, A., Hunt, R. W. and Das, K. C. (2010b) 'Microalgae cultivation in a wastewater dominated by carpet mill effluents for biofuel applications', *Bioresource Technology*, 101(9), pp. 3097-3105.

Chisti, Y. (2007) 'Biodiesel from microalgae', *Biotechnology Advances*, 25(3), pp. 294-306.

Chisti, Y. (2012) 'Raceways-based production of algal crude oil', *Microalgal Biotechnology: Potential and Production*, pp. 113-146.

Chisti, Y. (2013) 'Constraints to commercialization of algal fuels', *Journal of Biotechnology*, 167(3), pp. 201-214.

Christenson, L. and Sims, R. (2011) 'Production and harvesting of microalgae for wastewater treatment, biofuels, and bioproducts', *Biotechnol Adv*, 29(6), pp. 686-702.

Cioabla, A. E., Ionel, I., Dumitrel, G.-A. and Popescu, F. (2012) 'Comparative study on factors affecting anaerobic digestion of agricultural vegetal residues', *Biotechnology for Biofuels*, 5(1), p. 39.

Converti, A., Casazza, A. A., Ortiz, E. Y., Perego, P. and Del Borghi, M. (2009) 'Effect of temperature and nitrogen concentration on the growth and lipid content of Nannochloropsis oculata and Chlorella vulgaris for biodiesel production', *Chemical Engineering and Processing: Process Intensification*, 48(6), pp. 1146-1151.

Coons, J. E., Kalb, D. M., Dale, T. and Marrone, B. L. (2014) 'Getting to low-cost algal biofuels: A monograph on conventional and cutting-edge harvesting and extraction technologies', *Algal Research*.

Corona-Arroyo, M. A., López-Valdivieso, A. and Song, S. (2018) 'Contact angle and vacuum floatability of ultrafine size particles', *Separation Science and Technology*, 53(6), pp. 999-1005.

Costa, J. C., Gonçalves, P. R., Nobre, A. and Alves, M. M. (2012) 'Biomethanation potential of macroalgae Ulva spp. and Gracilaria spp. and in co-digestion with waste activated sludge', *Bioresource Technology*, 114, pp. 320-326.

Coward, T. (2012) *Foam Fractionation: An Effective Technology for Harvesting Microalgae Biomass*. Newcastle University.

Coward, T., Lee, J. G. M. and Caldwell, G. S. (2013) 'Development of a foam flotation system for harvesting microalgae biomass', *Algal Research*, 2(2), pp. 135-144.

Coward, T., Lee, J. G. M. and Caldwell, G. S. (2014) 'Harvesting microalgae by CTAB-aided foam flotation increases lipid recovery and improves fatty acid methyl ester characteristics', *Biomass and Bioenergy*, 67, pp. 354-362.

Coward, T., Lee, J. G. M. and Caldwell, G. S. (2015) 'The effect of bubble size on the efficiency and economics of harvesting microalgae by foam flotation', *Journal of Applied Phycology*, 27(2), pp. 733-742.

Craggs, R., Sutherland, D. and Campbell, H. (2012) 'Hectare-scale demonstration of high rate algal ponds for enhanced wastewater treatment and biofuel production', *Journal of Applied Phycology*, 24(3), pp. 329-337.

Crittenden, J. C., Trussell, R. R., Hand, D. W., Howe, K. J. and Tchobanoglous, G. (2012) 'Coagulation and Flocculation', in J. C. Crittenden, R. R. T., D. W. Hand, K. J. Howe and G. Tchobanoglous (ed.) *MWH's Water Treatment: Principles and Design, Third Edition*.

Csordas, A. and Wang, J.-K. (2004) 'An integrated photobioreactor and foam fractionation unit for the growth and harvest of Chaetoceros spp. in open systems', *Aquacultural Engineering*, 30(1), pp. 15-30.

Cui, Y. (2013) *Fundamentals in Microalgae Harvesting: From Flocculation to Self-attachment*. North Carolina.

D'Hondt, E., Martín-Juárez, J., Bolado, S., Kasperoviciene, J., Koreiviene, J., Sulcius, S., Elst, K. and Bastiaens, L. (2017) '6 - Cell disruption technologies A2 - Gonzalez-Fernandez, Cristina', in Muñoz, R. (ed.) *Microalgae-Based Biofuels and Bioproducts*. Woodhead Publishing, pp. 133-154.

Dai, Z., Fornasiero, D. and Ralston, J. (1999) 'Particle–Bubble Attachment in Mineral Flotation', *Journal of Colloid and Interface Science*, 217(1), pp. 70-76.

Dai, Z., Fornasiero, D. and Ralston, J. (2000) 'Particle–bubble collision models — a review', *Advances in Colloid and Interface Science*, 85(2), pp. 231-256.

Danquah Michael, K., Ang, L., Uduman, N., Moheimani, N. and Forde Gareth, M. (2009) 'Dewatering of microalgal culture for biodiesel production: exploring polymer flocculation and tangential flow filtration', *Journal of Chemical Technology & Biotechnology*, 84(7), pp. 1078-1083.

Danquah, M. K., Gladman, B., Moheimani, N. and Forde, G. M. (2009) 'Microalgal growth characteristics and subsequent influence on dewatering efficiency', *Chemical Engineering Journal*, 151(1-3), pp. 73-78.

Dassey, A. J. (2013) *DESIGNING A COST EFFECTIVE MICROALGAE HARVESTING STRATEGY FOR BIODIESEL PRODUCTION WITH ELECTROCOAGULATION AND DISSOLVED AIR FLOTATION*. Louisiana State University.

Dassey, A. J. and Theegala, C. S. (2013) 'Harvesting economics and strategies using centrifugation for cost effective separation of microalgae cells for biodiesel applications', *Bioresource Technology*, 128, pp. 241-245.

David, L. N. and Michael, M. C. (2000) *Lehninger Principles of Biochemistry*. 3rd. edition edn.

Davudov, D. and Moghanloo, R. G. (2017) 'A systematic comparison of various upgrading techniques for heavy oil', *Journal of Petroleum Science and Engineering*, 156, pp. 623-632.

de Farias Silva, C. E. and Bertucco, A. (2016) 'Bioethanol from microalgae and cyanobacteria: A review and technological outlook', *Process Biochemistry*, 51(11), pp. 1833-1842.

de Vries, A. J. (1972) 'Morphology, coalescence, and size distribution of foam bubbles', in Lemlich, R. (ed.) *Adsorptive Bubble Separation Techniques*. New York and London: Academic Press, pp. 7-31.

Demirbas, A. (2009) 'Thermochemical Conversion of Mosses and Algae to Gaseous Products', *Energy Sources, Part A: Recovery, Utilization, and Environmental Effects*, 31(9), pp. 746-753.

Demirbaş, A. (2006) 'Oily Products from Mosses and Algae via Pyrolysis', *Energy Sources, Part A: Recovery, Utilization, and Environmental Effects*, 28(10), pp. 933-940.

Demirbas, A. and Demirbas, M. F. (2010) *Algae energy algae as a new source of biodiesel*. Springer.

Depraetere, O., Pierre, G., Deschoenmaeker, F., Badri, H., Foubert, I., Leys, N., Markou, G., Wattiez, R., Michaud, P. and Muylaert, K. (2015) 'Harvesting carbohydrate-rich Arthrospira platensis by spontaneous settling', *Bioresource Technology*, 180, pp. 16-21.

Derjaguin, B. V. and Dukhin, S. S. (1961) 'Theory of flotation of small and medium-size particles', *Institution of Mining and Metallurgy 651*, pp. 21–246.

Derjaguin, B. V., Dukhin, S. S. and Rulyov, N. N. (1984) 'Kinetic Theory of Flotation of Small Particles', in Matijević, E. and Good, R. J. (eds.) *Surface and Colloid Science: Volume 13*. Boston, MA: Springer US, pp. 71-113.

DIAO, J., FUERSTENAU, D. W. and HANSON, J. S. (1992) 'Kinetics of coal flotation', *in: SME-AIME Annual Meeting, Phoenix, AZ, vol. 92*.

Díaz-Rey, M. R., Cortés-Reyes, M., Herrera, C., Larrubia, M. A., Amadeo, N., Laborde, M. and Alemany, L. J. (2014) 'Hydrogen-rich gas production from algae-biomass by low temperature catalytic gasification', *Catalysis Today*.

Dickerson, T. and Soria, J. (2013) 'Catalytic Fast Pyrolysis: A Review', *Energies*, 6(1), pp. 514-538.

Dickinson, J. E., Laskovski, D., Stevenson, P. and Galvin, K. P. (2010) 'Enhanced foam drainage using parallel inclined channels in a single-stage foam fractionation column', *Chemical Engineering Science*, 65(8), pp. 2481-2490.

The Different Kinds of Chlorella's Production » Photobioreactor (2011). Available at: https://chlorelle.wordpress.com/2011/04/14/the-different-kinds-of-chlorellas-production/allemagne-016/ (Accessed: April 2015).

Dobby, G. S. (1984) *A FUNDAMENTAL FLOTATION MODEL AND FLOTATION COLUMN SCALE-UP*. McGill University.

Dobby, G. S. and Finch, J. A. (1986) 'A model of particle sliding time for flotation size bubbles', *Journal of Colloid and Interface Science*, 109(2), pp. 493-498.

Dobby, G. S. and Finch, J. A. (1987) 'Particle size dependence in flotation derived from a fundamental model of the capture process', *International Journal of Mineral Processing*, 21(3), pp. 241-260.

Dobby, G. S. and Finch, J. A. (1991) 'Column flotation: A selected review, part II', *Minerals Engineering*, 4(7), pp. 911-923.

Dote, Y., Sawayama, S., Inoue, S., Minowa, T. and Yokoyama, S.-y. (1994) 'Recovery of liquid fuel from hydrocarbon-rich microalgae by thermochemical liquefaction', *Fuel*, 73(12), pp. 1855-1857.

Du, Z., Li, Y., Wang, X., Wan, Y., Chen, Q., Wang, C., Lin, X., Liu, Y., Chen, P. and Ruan, R. (2011) 'Microwave-assisted pyrolysis of microalgae for biofuel production', *Bioresource Technology*, 102(7), pp. 4890-4896.

Duan, P. and Savage, P. E. (2011) 'Hydrothermal Liquefaction of a Microalga with Heterogeneous Catalysts', *Industrial & Engineering Chemistry Research*, 50(1), pp. 52-61.

Eastoe, J. and Dalton, J. S. (2000) 'Dynamic surface tension and adsorption mechanisms of surfactants at the air-water interface', *Advances in Colloid and Interface Science*, 85(2), pp. 103-144.

Edzwald, J. (1993) 'Algae, bubbles, coagulants, and dissolved air flotation', *Water Sci. Technol.*, 27(10), pp. 67-81.

Edzwald, J. K. (2010) 'Dissolved air flotation and me', *Water Res*, 44(7), pp. 2077-106.

Ehimen, E. A., Sun, Z. F. and Carrington, C. G. (2010) 'Variables affecting the in situ transesterification of microalgae lipids', *Fuel*, 89(3), pp. 677-684.

Elena S. Barbieri, V. E. W. H. (2006) 'Dynamics of oxygen production / consumption in Dunaliella salina, Thalassiosira weissflogii and Heterocapsa triquetra circulating within a simulated upper mixed layer*', *Invest. Mar., Valparaíso*, 34(2), pp. 97-108.

Elliott, D. C. (2016) 'Review of recent reports on process technology for thermochemical conversion of whole algae to liquid fuels', *Algal Research*, 13, pp. 255-263.

Elliott, D. C., Biller, P., Ross, A. B., Schmidt, A. J. and Jones, S. B. (2014) 'Hydrothermal liquefaction of biomass: Developments from batch to continuous process', *Bioresource Technology*.

Elliott, D. C., Hart, T. R., Schmidt, A. J., Neuenschwander, G. G., Rotness, L. J., Olarte, M. V., Zacher, A. H., Albrecht, K. O., Hallen, R. T. and Holladay, J. E. (2013) 'Process development for hydrothermal liquefaction of algae feedstocks in a continuous-flow reactor', *Algal Research*, 2(4), pp. 445-454.

Erbil, H. Y. (2006) 'Contact Angle of Liquid Drops on Solids', in *Surface Chemistry*. Blackwell Publishing Ltd., pp. 308-337.

Farid, M. S., Shariati, A., Badakhshan, A. and Anvaripour, B. (2013) 'Using nano-chitosan for harvesting microalga Nannochloropsis sp', *Bioresour Technol*, 131, pp. 555-9.

Faried, M., Samer, M., Abdelsalam, E., Yousef, R. S., Attia, Y. A. and Ali, A. S. (2017) 'Biodiesel production from microalgae: Processes, technologies and recent advancements', *Renewable and Sustainable Energy Reviews*, 79, pp. 893-913.

Fortier, M.-O. P., Roberts, G. W., Stagg-Williams, S. M. and Sturm, B. S. M. (2014) 'Life cycle assessment of bio-jet fuel from hydrothermal liquefaction of microalgae', *Applied Energy*, 122, pp. 73-82.

Fu, Z.-y., Song, J.-c. and Jameson, P. E. (2017) 'A rapid and cost effective protocol for plant genomic DNA isolation using regenerated silica columns in combination with CTAB extraction', *Journal of Integrative Agriculture*, 16(8), pp. 1682-1688.

Fuerstenau, M. C., Jameson, G. J. and Yoon, R. H. (2007) *Froth Flotation: A Century of Innovation*. Littletown, Colorado, USA: Society for Miningm Metallurgy, and Exploration, Inc.

Gai, C., Zhang, Y., Chen, W.-T., Zhang, P. and Dong, Y. (2014) 'Energy and nutrient recovery efficiencies in biocrude oil produced via hydrothermal liquefaction of Chlorella pyrenoidosa', *RSC Advances*, 4(33), p. 16958.

García-Pérez, J. S., Beuckels, A., Vandamme, D., Depraetere, O., Foubert, I., Parra, R. and Muylaert, K. (2014) 'Influence of magnesium concentration, biomass concentration and pH on flocculation of Chlorella vulgaris', *Algal Research*, 3, pp. 24-29.

Garcia Alba, L., Torri, C., Samorì, C., van der Spek, J., Fabbri, D., Kersten, S. and Brilman, W. (2011) *Hydrothermal Treatment (HTT) of Microalgae: Evaluation of the Process As Conversion Method in an Algae Biorefinery Concept*.

Garcia Alba, L., Torri, C., Samorì, C., van der Spek, J., Fabbri, D., Kersten, S. R. A. and Brilman, D. W. F. (2012) 'Hydrothermal Treatment (HTT) of Microalgae: Evaluation of the Process As Conversion Method in an Algae Biorefinery Concept', *Energy & Fuels*, 26(1), pp. 642-657.

Garg, S., Li, Y., Wang, L. and Schenk, P. M. (2012) 'Flotation of marine microalgae: effect of algal hydrophobicity', *Bioresour Technol*, 121, pp. 471-4.

Garg, S., Wang, L. and Schenk, P. M. (2013) 'Effects of algal hydrophobicity and bubble size on flotation separation of microalgae from aqueous medium ', *Chemeca 2013: Australasian Conference on Chemical Engineering* Brisbane, QLD, Australia Institution of Engineers, Australia pp. 1-5.

Garg, S., Wang, L. and Schenk, P. M. (2014) 'Effective harvesting of low surface-hydrophobicity microalgae by froth flotation', *Bioresource Technology*, 159, pp. 437-441.

Garg, S., Wang, L. and Schenk, P. M. (2015) 'Flotation separation of marine microalgae from aqueous medium', *Separation and Purification Technology*, 156, pp. 636-641.

Gerbens-Leenes, W., Hoekstra, A. Y. and van der Meer, T. H. (2009) 'The water footprint of bioenergy', *Proceedings of the National Academy of Sciences*, 106(25), pp. 10219-10223.

Gerçel, H. F. (2002) 'Production and characterization of pyrolysis liquids from sunflower-pressed bagasse', *Bioresource Technology*, 85(2), pp. 113-117.

Gerde, J. A., Yao, L., Lio, J., Wen, Z. and Wang, T. (2014) 'Microalgae flocculation: Impact of flocculant type, algae species and cell concentration', *Algal Research*, 3, pp. 30-35.

Gharai, M. and Venugopal, R. (2016) 'Modeling of Flotation Process—An Overview of Different Approaches', *Mineral Processing and Extractive Metallurgy Review*, 37(2), pp. 120-133.

Ghirardi, M. L., Maness, P. C. and Seibert, M. (2008) 'Photobiological Methods of Renewable Hydrogen Production', in Rajeshwar, K., McConnell, R. and Licht, S. (eds.) *Solar Hydrogen Generation: Toward a Renewable Energy Future*. New York, NY: Springer New York, pp. 229-271.

Gollakota, A. R. K., Kishore, N. and Gu, S. (2018) 'A review on hydrothermal liquefaction of biomass', *Renewable and Sustainable Energy Reviews*, 81, pp. 1378-1392.

Golzary, A., Imanian, S., Abdoli, M. A., Khodadadi, A. and Karbassi, A. (2015) 'A cost-effective strategy for marine microalgae separation by electro-coagulation–flotation process aimed at bio-crude oil production: Optimization and evaluation study', *Separation and Purification Technology*, 147, pp. 156-165.

Gouveia, L. (2011) *Microalgae as a Feedstock for Biofuels*. london: Springer.

Goyal, H. B., Seal, D. and Saxena, R. C. (2008) 'Bio-fuels from thermochemical conversion of renewable resources: A review', *Renewable and Sustainable Energy Reviews*, 12(2), pp. 504-517.

Granados, M. R., Acien, F. G., Gomez, C., Fernandez-Sevilla, J. M. and Molina Grima, E. (2012) 'Evaluation of flocculants for the recovery of freshwater microalgae', *Bioresour Technol*, 118, pp. 102-10.

Greenwell, H., Laurens, L., Shields, R. J., Lovitt, R. and Flynn, K. J. (2010) 'Placing microalgae on the biofuels priority list: a review of the technological challenges ', *Journal of Royal Society Interface*, 7(46), pp. 703-726.

Grierson, S., Strezov, V., Ellem, G., McGregor, R. and Herbertson, J. (2009) 'Thermal characterisation of microalgae under slow pyrolysis conditions', *Journal of Analytical and Applied Pyrolysis*, 85(1), pp. 118-123.

Guan, Q., Wei, C., Ning, P., tian, S. and Gu, J. (2013) 'Catalytic Gasification of Algae Nannochloropsis sp. in Sub/Supercritical Water', *Procedia Environmental Sciences*, 18, pp. 844-848.

Guerrero-Pérez, J. S. and Barraza-Burgos, J. M. (2017) 'A new mathematical model for coal flotation kinetics', *DYNA*, 84, pp. 143-149.

Guilford, W. J., Schneider, D. M., Labovitz, J. and Opella, S. J. (1988) 'High Resolution Solid State (13)C NMR Spectroscopy of Sporopollenins from Different Plant Taxa', *Plant Physiology*, 86(1), pp. 134-136.

Guldhe, A., Singh, P., Kumari, S., Rawat, I., Permaul, K. and Bux, F. (2016) 'Biodiesel synthesis from microalgae using immobilized Aspergillus niger whole cell lipase biocatalyst', *Renewable Energy*, 85, pp. 1002-1010.

Gupta, A. K., Banerjee, P. K., Mishra, A., Satish, P. and Pradip (2007) 'Effect of alcohol and polyglycol ether frothers on foam stability, bubble size and coal flotation', *International Journal of Mineral Processing*, 82(3), pp. 126-137.

Halim, R., Danquah, M. K. and Webley, P. A. (2012) 'Extraction of oil from microalgae for biodiesel production: A review', *Biotechnology Advances*, 30(3), pp. 709-732.

Hamawand, I., Yusaf, T. and Hamawand, S. (2014) 'Growing algae using water from coal seam gas industry and harvesting using an innovative technique: A review and a potential', *Fuel*, 117, pp. 422-430.

Hankey, R. (2018) *Electric power monthly with data for November 2017*. Washington.

Hanotu, J., Bandulasena, H. C. H. and Zimmerman, W. B. (2012) 'Microflotation performance for algal separation', *Biotechnology and Bioengineering*, 109(7), pp. 1663-1673.

Hansen, K. H., Angelidaki, I. and Ahring, B. K. (1998) 'ANAEROBIC DIGESTION OF SWINE MANURE: INHIBITION BY AMMONIA', *Water Research*, 32(1), pp. 5-12.

Hao, W., Yanpeng, L., Zhou, S., Xiangying, R., Wenjun, Z. and Jun, L. (2017) 'Surface characteristics of microalgae and their effects on harvesting performance by air flotation', *International journal of agricultural and biological engineering* 10(1), pp. 125-133.

Heasman, M., Diemar, J., O'Connor, W., Sushames, T. and Foulkes, L. (2002) 'Development of extended shelf- life microalgae concentrate diets harvested by centrifugation for bivalve molluscs – a summary', *Aquaculture Research*, 31(8- 9), pp. 637-659.

Henderson, R. K., Parsons, S. A. and Jefferson, B. (2008) 'Surfactants as Bubble Surface Modifiers in the Flotation of Algae: Dissolved Air Flotation That Utilizes a Chemically Modified Bubble Surface', *Environmental Science & Technology*, 42(13), pp. 4883-4888.

Henderson, R. K., Parsons, S. A. and Jefferson, B. (2009) 'The Potential for Using Bubble Modification Chemicals in Dissolved Air Flotation for Algae Removal', *Separation Science and Technology*, 44(9), pp. 1923-1940.

Henderson, R. K., Parsons, S. A. and Jefferson, B. (2010) 'The impact of differing cell and algogenic organic matter (AOM) characteristics on the coagulation and flotation of algae', *Water Res*, 44(12), pp. 3617-24.

Hidaka, T., Inoue, K., Suzuki, Y. and Tsumori, J. (2014) 'Growth and anaerobic digestion characteristics of microalgae cultivated using various types of sewage', *Bioresource Technology*, 170, pp. 83-89.

Hirano, A., Hon-Nami, K., Kunito, S., Hada, M. and Ogushi, Y. (1998) 'Temperature effect on continuous gasification of microalgal biomass: theoretical yield of methanol production and its energy balance', *Catalysis Today*, 45(1), pp. 399-404.

Hirano, A., Ueda, R., Hirayama, S. and Ogushi, Y. (1997) 'CO2 fixation and ethanol production with microalgal photosynthesis and intracellular anaerobic fermentation', *Energy*, 22(2), pp. 137-142.

Ho, D. P., Ngo, H. H. and Guo, W. (2014) 'A mini review on renewable sources for biofuel', *Bioresour Technol*, 169, pp. 742-9.

Ho, S.-H., Chen, C.-Y. and Chang, J.-S. (2012) 'Effect of light intensity and nitrogen starvation on CO2 fixation and lipid/carbohydrate production of an indigenous microalga Scenedesmus obliquus CNW-N', *Bioresource Technology*, 113, pp. 244-252.

Ho, S.-H., Kondo, A., Hasunuma, T. and Chang, J. (2013) 'Engineering strategies for improving the CO2 fixation and carbohydrate productivity of Scenedesmus obliquus CNW-N used for bioethanol fermentation', *Bioresource Technology*, 143, pp. 163-171.

Hu, Y. R., Wang, F., Wang, S. K., Liu, C. Z. and Guo, C. (2013) 'Efficient harvesting of marine microalgae Nannochloropsis maritima using magnetic nanoparticles', *Bioresour Technol*, 138, pp. 387-90.

Hu, Z., Ma, X. and Chen, C. (2012) 'A study on experimental characteristic of microwave-assisted pyrolysis of microalgae', *Bioresource Technology*, 107, pp. 487-493.

Huang, C., Ruhsing Pan, J. and Huang, S. (1999) 'Collision efficiencies of algae and kaolin in depth filter: the effect of surface properties of particles', *Water Research*, 33(5), pp. 1278-1286.

Huntley, M. and Redalje, D. (2007) 'CO2 Mitigation and Renewable Oil from Photosynthetic Microbes: A New Appraisal', *Mitigation and Adaptation Strategies for Global Change*, 12(4), pp. 573-608.

Im, H., Lee, H., Park, M. S., Yang, J. W. and Lee, J. W. (2014) 'Concurrent extraction and reaction for the production of biodiesel from wet microalgae', *Bioresour Technol*, 152, pp. 534-7.

IMAIZUMI, T. and INOUE, T. (1963) 'Kinetic considerations of froth flotation', *Proceedings of the 6th International Mineral Processing Congress*. Cannes. pp. 581-593.

Ippoliti, D., Gómez, C., del Mar Morales-Amaral, M., Pistocchi, R., Fernández-Sevilla, J. M. and Acién, F. G. (2016) 'Modeling of photosynthesis and respiration rate for Isochrysis galbana (T-Iso) and its influence on the production of this strain', *Bioresource Technology*, 203, pp. 71-79.

Jankowska, E., Sahu, A. K. and Oleskowicz-Popiel, P. (2017) 'Biogas from microalgae: Review on microalgae's cultivation, harvesting and pretreatment for anaerobic digestion', *Renewable and Sustainable Energy Reviews*, 75, pp. 692-709.

Jena, U. and Das, K. C. (2011) 'Comparative Evaluation of Thermochemical Liquefaction and Pyrolysis for Bio-Oil Production from Microalgae', *Energy & Fuels*, 25(11), pp. 5472-5482.

Jenkins, D., Scherfig, J. and Eckhoff, D. W. (1972) 'Application of adsorptive bubble separation techniques to wastewater treatment', in Lemlich, R. (ed.) *Adsorptive Bubble Separation Techniques*. New York and London: Academic Press, pp. 219-242.

Jin, B., Duan, P., Xu, Y., Wang, B., Wang, F. and Zhang, L. (2014) 'Lewis acid-catalyzed in situ transesterification/esterification of microalgae in supercritical ethanol', *Bioresour Technol*, 162, pp. 341-9.

Johnson, M. (2009) *Microalgal biodiesel production through a novel attached culture system and conversion parameters*. VirginiaPolytechnic Institute and State University.

Kadam, K. L. (2002) 'Environmental implications of power generation via coal-microalgae cofiring', *Energy*, 27(10), pp. 905-922.

Kamalanathan, I. D. (2015) *Foam Fractionation of surfactant-protein mixtures*. The University of Manchester.

Kamaroddin, M. F., Hanotu, J., Gilmour, D. J. and Zimmerman, W. B. (2016) 'In-situ disinfection and a new downstream processing scheme from algal harvesting to lipid extraction using ozone-rich microbubbles for biofuel production', *Algal Research*, 17, pp. 217-226.

Kamat, S. S., Williams, H. J., Dangott, L. J., Chakrabarti, M. and Raushel, F. M. (2013) 'The catalytic mechanism for aerobic formation of methane by bacteria', *Nature*, 497(7447), pp. 132-136.

Kang, R., Wang, J., Shi, D., Cong, W., Cai, Z. and Ouyang, F. (2004) *Interactions between organic and inorganic carbon sources during mixotrophic cultivation of Synechococcus sp*.

Katarzyna, L., Sai, G. and Singh, O. A. (2015) 'Non-enclosure methods for non-suspended microalgae cultivation: literature review and research needs', *Renewable and Sustainable Energy Reviews*, 42, pp. 1418-1427.

Kaya, M. and Laplante, A. R. (1986) 'Investigation of Batch and Continuous Flotation Kinetics in a Modified Denver Laboratory Cell', *Canadian Metallurgical Quarterly*, 25(1), pp. 1-8.

Khan, S. A., Rashmi, Hussain, M. Z., Prasad, S. and Banerjee, U. C. (2009) 'Prospects of biodiesel production from microalgae in India', *Renewable and Sustainable Energy Reviews*, 13(9), pp. 2361-2372.

Khoo, H. H., Koh, C. Y., Shaik, M. S. and Sharratt, P. N. (2013) 'Bioenergy co-products derived from microalgae biomass via thermochemical conversion – Life cycle energy balances and CO2 emissions', *Bioresource Technology*, 143, pp. 298-307.

Kim, J., Yoo, G., Lee, H., Lim, J., Kim, K., Kim, C. W., Park, M. S. and Yang, J.-W. (2013) 'Methods of downstream processing for the production of biodiesel from microalgae', *Biotechnology Advances*, 31(6), pp. 862-876.

Knuckey, R., Brown, M., Robert, R. and DMF, F. (2006) 'Production of microalgal concentrates by flocculation and their assessment as aquaculture feeds', *Aquac. Eng.*, 35(3), pp. 300-313.

Koner, S., Pal, A. and Adak, A. (2010) 'Cationic surfactant adsorption on silica gel and its application for wastewater treatment', *Desalination and Water Treatment*, 22(1-3), pp. 1-8.

Kruglyakov, P. M., Karakashev, S. I., Nguyen, A. V. and Vilkova, N. G. (2008) 'Foam drainage', *Current Opinion in Colloid & Interface Science*, 13(3), pp. 163-170.

Kuan, S. H. and Finch, J. A. (2010) 'Impact of talc on pulp and froth properties in F150 and 1-pentanol frother systems', *Minerals Engineering*, 23(11), pp. 1003-1009.

Kulkarni, A. A. and Joshi, J. B. (2005) 'Bubble Formation and Bubble Rise Velocity in Gas−Liquid Systems: A Review', *Industrial & Engineering Chemistry Research*, 44(16), pp. 5873–5931.

Kumaran, K., Lam, M. K., Tan, X. B., Uemura, Y., Lim, J. W., Khoo, C. G. and Lee, K. T. (2016) 'Cultivation of Chlorella vulgaris Using Plant-based and Animal Waste-based Compost: A Comparison Study', *Procedia Engineering*, 148, pp. 679-686.

Kurniawati, H. A., Ismadji, S. and Liu, J. C. (2014) 'Microalgae harvesting by flotation using natural saponin and chitosan', *Bioresour Technol*, 166, pp. 429-34.

Laamanen, C. A., Ross, G. M. and Scott, J. A. (2016) 'Flotation harvesting of microalgae', *Renewable and Sustainable Energy Reviews*, 58, pp. 75-86.

Lam, M. K. and Lee, K. T. (2011) 'Renewable and sustainable bioenergies production from palm oil mill effluent (POME): Win–win strategies toward better environmental protection', *Biotechnology Advances*, 29(1), pp. 124-141.

Lam, M. K. and Lee, K. T. (2012) 'Microalgae biofuels: A critical review of issues, problems and the way forward', *Biotechnology Advances*, 30(3), pp. 673-690.

Lananan, F., Mohd Yunos, F. H., Mohd Nasir, N., Abu Bakar, N. S., Lam, S. S. and Jusoh, A. (2016) 'Optimization of biomass harvesting of microalgae, *Chlorella* sp. utilizing auto-flocculating microalgae, *Ankistrodesmus* sp. as bio-flocculant', *International Biodeterioration and Biodegradation*, 113, pp. 391-396.

Laurens, L. M. L., Quinn, M., Van Wychen, S., Templeton, D. W. and Wolfrum, E. J. (2012) 'Accurate and reliable quantification of total microalgal fuel potential as fatty acid methyl esters by in situ transesterification', *Analytical and Bioanalytical Chemistry*, 403(1), pp. 167-178.

Laurent, E. (2010) *Natural vs. Synthetic Flocculents*. Available at: http://www.algaeindustrymagazine.com/natural-vs-synthetic-flocculents/ (Accessed: April 2015).

Lee, A., Lewis, D. and PJ, A. (2009a) 'Microbial flocculation, a potentially low-cost harvesting technique for marine microalgae for the production of biodiesel', *J. Appl. Phycol.*, 21, pp. 559–567.

Lee, A. F. and Wilson, K. (2015) 'Recent developments in heterogeneous catalysis for the sustainable production of biodiesel', *Catalysis Today*, 242, pp. 3-18.

Lee, A. K., Lewis, D. M. and Ashman, P. J. (2009b) 'Microbial flocculation, a potentially low-cost harvesting technique for marine microalgae for the production of biodiesel', *Journal of Applied Phycology*, 21(5), pp. 559-567.

Lee, A. K., Lewis, D. M. and Ashman, P. J. (2013) 'Harvesting of marine microalgae by electroflocculation: The energetics, plant design, and economics', *Applied Energy*, 108, pp. 45-53.

Leite, G. B., Abdelaziz, A. E. and Hallenbeck, P. C. (2013) 'Algal biofuels: challenges and opportunities', *Bioresour Technol*, 145, pp. 134-41.

Leiva, J., Vinnett, L., Contreras, F. and Yianatos, J. (2010) 'Estimation of the actual bubble surface area flux in flotation', *Minerals Engineering*, 23(11-13), pp. 888-894.

Leroy, S., Dislaire, G., Bastin, D. and Pirard, E. (2011) 'Optical analysis of particle size and chromite liberation from pulp samples of a UG2 ore regrinding circuit', *Minerals Engineering*, 24(12), pp. 1340-1347.

Leung, D. Y. C., Wu, X. and Leung, M. K. H. (2010) 'A review on biodiesel production using catalyzed transesterification', *Applied Energy*, 87(4), pp. 1083-1095.

Li, C., Farrokhpay, S., Runge, K. and Shi, F. (2016) 'Determining the significance of flotation variables on froth rheology using a central composite rotatable design', *Powder Technology*, 287, pp. 216-225.

Li, F. (2012) *MODELING AND CONTROL OF ALGAE HARVESTING, DEWATERING AND DRYING (HDD) SYSTEMS*. Case Western Reserve University.

Li, X., Evans, G. M. and Stevenson, P. (2011a) 'Process intensification of foam fractionation by successive contraction and expansion', *Chemical Engineering Research and Design*, 89(11), pp. 2298-2308.

Li, Y., Chen, Y.-F., Chen, P., Min, M., Zhou, W., Martinez, B., Zhu, J. and Ruan, R. (2011b) 'Characterization of a microalga Chlorella sp. well adapted to highly concentrated municipal wastewater for nutrient removal and biodiesel production', *Bioresource Technology*, 102(8), pp. 5138-5144.

Liang, K., Zhang, Q. and Cong, W. (2012) 'Enzyme-Assisted Aqueous Extraction of Lipid from Microalgae', *Journal of Agricultural and Food Chemistry*, 60(47), pp. 11771-11776.

Lim Jit, K., Chieh Derek Chan, J., Jalak Selah, A., Toh Pey, Y., Yasin Nur Hidayah, M., Ng Bee, W. and Ahmad Abdul, L. (2012) 'Rapid Magnetophoretic Separation of Microalgae', *Small*, 8(11), pp. 1683-1692.

Lin, C.-C. and Hong, P. K. A. (2013) 'A new processing scheme from algae suspension to collected lipid using sand filtration and ozonation', *Algal Research*, 2(4), pp. 378-384.

Liu, J., Zhu, Y., Tao, Y., Zhang, Y., Li, A., Li, T., Sang, M. and Zhang, C. (2013a) 'Freshwater microalgae harvested via flocculation induced by pH decrease', *Biotechnology for Biofuels*, 6(1), p. 98.

Liu, J. C., Chen, Y. M. and Ju, Y.-H. (1999) 'Separation of Algal Cells from Water by Column flotation', *Separation Science and Technology*, 34(11), pp. 2259-2272.

Liu, T., Wang, J., Hu, Q., Cheng, P., Ji, B., Liu, J., Chen, Y., Zhang, W., Chen, X., Chen, L., Gao, L., Ji, C. and Wang, H. (2013b) 'Attached cultivation technology of microalgae for efficient biomass feedstock production', *Bioresource Technology*, 127, pp. 216-222.

Loa, M. (2018, July) *Recent Monthly Average Mauna Loa CO2*. Available at: https://www.esrl.noaa.gov/gmd/ccgg/trends/index.html.

Loganathan, K., Saththasivam, J. and Sarp, S. (2018) 'Removal of microalgae from seawater using chitosan-alum/ferric chloride dual coagulations', *Desalination*, 433, pp. 25-32.

Lohrey, C. (2012) *BIODIESEL PRODUCTION FROM MICROALGAE: CO-LOCATION WITH SUGAR MILLS*. Louisiana State University.

López-González, D., Fernandez-Lopez, M., Valverde, J. L. and Sanchez-Silva, L. (2014a) 'Comparison of the steam gasification performance of three species of microalgae by thermogravimetric–mass spectrometric analysis', *Fuel*, 134, pp. 1-10.

López-González, D., Fernandez-Lopez, M., Valverde, J. L. and Sanchez-Silva, L. (2014b) 'Pyrolysis of three different types of microalgae: Kinetic and evolved gas analysis', *Energy*, 73, pp. 33-43.

López Barreiro, D., Prins, W., Ronsse, F. and Brilman, W. (2013) 'Hydrothermal liquefaction (HTL) of microalgae for biofuel production: State of the art review and future prospects', *Biomass and Bioenergy*, 53, pp. 113-127.

Lu, J., Sheahan, C. and Fu, P. (2011) 'Metabolic engineering of algae for fourth generation biofuels production', *Energy & Environmental Science*, 4(7), pp. 2451-2466.

Lu, K., Li, R., Wu, Z., Hou, K., Du, X. and Zhao, Y. (2013) 'Wall effect on rising foam drainage and its application to foam separation', *Separation and Purification Technology*, 118, pp. 710-715.

Magdalena, J., Ballesteros, M. and González-Fernandez, C. (2018) 'Efficient Anaerobic Digestion of Microalgae Biomass: Proteins as a Key Macromolecule', *Molecules*, 23(5).

Manica, R., Klaseboer, E. and Chan, D. Y. C. (2016) 'The hydrodynamics of bubble rise and impact with solid surfaces', *Advances in Colloid and Interface Science*, 235, pp. 214-232.

Mankosa, M. J., Luttrell, G. H., Adel, G. T. and Yoon, R. H. (1992) 'A study of axial mixing in column flotation', *International Journal of Mineral Processing*, 35(1), pp. 51-64.

Masliyah, J. H. (1979) 'Hindered settling in a multi-species particle system', *Chemical Engineering Science*, 34(9), pp. 1166-1168.

Mata, T. M., Martins, A. A. and Caetano, N. S. (2010) 'Microalgae for biodiesel production and other applications: A review', *Renewable and Sustainable Energy Reviews*, 14(1), pp. 217-232.

McKendry, P. (2002) 'Energy production from biomass (part 2): conversion technologies', *Bioresource Technology*, 83(1), pp. 47-54.

Mercz, T. (1994) *A study of high lipid yielding microalgae with potential for large-scale production of lipids and polyunsaturated fatty acids*. Murdoch University.

Miao, X. and Wu, Q. (2004) 'High yield bio-oil production from fast pyrolysis by metabolic controlling of Chlorella protothecoides', *Journal of Biotechnology*, 110(1), pp. 85-93.

Miettinen, T., Ralston, J. and Fornasiero, D. (2010) 'The limits of fine particle flotation', *Minerals Engineering*, 23(5), pp. 420-437.

Milledge, J. J. (2010) 'The challenge of algal fuel: economic processing of the entire algal biomass', *Condens Matter Mater Eng Newsl*, 1(6), pp. 4-6.

Milledge, J. J. and Heaven, S. (2012) 'A review of the harvesting of micro-algae for biofuel production', *Reviews in Environmental Science and Bio/Technology*, 12(2), pp. 165-178.

Mills, P. J. T. and O'Connor, C. T. (1990) 'The modelling of liquid and solids mixing in a flotation column', *Minerals Engineering*, 3(6), pp. 567-576.

Minowa, T., Yokoyama, S.-y., Kishimoto, M. and Okakura, T. (1995) 'Oil production from algal cells of Dunaliella tertiolecta by direct thermochemical liquefaction', *Fuel*, 74(12), pp. 1735-1738.

Misra, R., Guldhe, A., Singh, P., Rawat, I., Stenström, T. A. and Bux, F. (2015) 'Evaluation of operating conditions for sustainable harvesting of microalgal biomass applying electrochemical method using non sacrificial electrodes', *Bioresource Technology*, 176, pp. 1-7.

Mohan, D., Pittman, C. U. and Steele, P. H. (2006) 'Pyrolysis of Wood/Biomass for Bio-oil: A Critical Review', *Energy & Fuels*, 20(3), pp. 848-889.

Mohd Udaiyappan, A. F., Abu Hasan, H., Takriff, M. S. and Sheikh Abdullah, S. R. (2017) 'A review of the potentials, challenges and current status of microalgae biomass applications in industrial wastewater treatment', *Journal of Water Process Engineering*, 20, pp. 8-21.

Moheimani, N. R., Borowitzka, M. A., Isdepsky, A. and Sing, S. F. (2013) 'Standard Methods for Measuring Growth of Algae and Their Composition', in Borowitzka, M. A. and Moheimani, N. R. (eds.) *Algae for Biofuels and Energy*. Dordrecht: Springer Netherlands, pp. 265-284.

Molina Grima, E., Belarbi, E. H., Acién Fernández, F. G., Robles Medina, A. and Chisti, Y. (2003) 'Recovery of microalgal biomass and metabolites: Process options and economics', *Biotechnology Advances*, 20(7-8), pp. 491-515.

Möllers, K. B., Cannella, D., Jørgensen, H. and Frigaard, N.-U. (2014) 'Cyanobacterial biomass as carbohydrate and nutrient feedstock for bioethanol production by yeast fermentation', *Biotechnology for Biofuels*, 7(1), p. 64.

Montgomery, D. C. (2012) *Design and Analysis of Experiments, 8th Edition*. John Wiley & Sons, Inc.

Moraes, I. D. O., R.D.O.M. Arruda, N.R. Maresca, A.D.O. Antunes, R.D.O. Moraes (2013) 'Spirulina platensis : Process optimization to obtain biomass', *Food Science Technology*, 33, pp. 179-183.

Motasemi, F. and Afzal, M. T. (2013) 'A review on the microwave-assisted pyrolysis technique', *Renewable and Sustainable Energy Reviews*, 28, pp. 317-330.

MUNIR, N., Sharif, N., NAZ, S., SALEEM, F. and F., M. (2013) 'Harvesting and Processing of Microalgae Biomass Fractions for Biodiesel Production (A Review)', *Sci. Tech. and Dev.*, 32(3), pp. 235-243.

Muylaert, K., Bastiaens, L., Vandamme, D. and Gouveia, L. (2017) '5 - Harvesting of microalgae: Overview of process options and their strengths and drawbacks A2 - Gonzalez-Fernandez, Cristina', in Muñoz, R. (ed.) *Microalgae-Based Biofuels and Bioproducts*. Woodhead Publishing, pp. 113-132.

Naik, M., Meher, L. C., Naik, S. N. and Das, L. M. (2008) 'Production of biodiesel from high free fatty acid Karanja (Pongamia pinnata) oil', *Biomass and Bioenergy*, 32(4), pp. 354-357.

Naik, S. N., Goud, V. V., Rout, P. K. and Dalai, A. K. (2010) 'Production of first and second generation biofuels: A comprehensive review', *Renewable and Sustainable Energy Reviews*, 14(2), pp. 578-597.

Nautiyal, P., Subramanian, K. A. and Dastidar, M. G. (2014) 'Production and characterization of biodiesel from algae', *Fuel Processing Technology*, 120, pp. 79-88.

Ndikubwimana, T., Chang, J., Xiao, Z., Shao, W., Zeng, X., Ng, I. S. and Lu, Y. (2016) 'Flotation: A promising microalgae harvesting and dewatering technology for biofuels production', *Biotechnol J*, 11(3), pp. 315-26.

Nguyen-Van, A. (1994) 'The Collision between Fine Particles and Single Air Bubbles in Flotation', *Journal of Colloid and Interface Science*, 162(1), pp. 123-128.

Nguyen, A. V., Ralston, J. and Schulze, H. J. (1998) 'On modelling of bubble–particle attachment probability in flotation', *International Journal of Mineral Processing*, 53(4), pp. 225-249.

Nguyen, A. V. and Schulze, H. J. (2004) *Colloidal science of flotation*. New York: Marcel Dekker, Inc.

Nguyen, A. V., Schulze, H. J. and Ralston, J. (1997) 'Elementary steps in particle—bubble attachment', *International Journal of Mineral Processing*, 51(1), pp. 183-195.

Nguyen, T. L., Lee, D. J., Chang, J. S. and Liu, J. C. (2013) 'Effects of ozone and peroxone on algal separation via dispersed air flotation', *Colloids and Surfaces B: Biointerfaces*, 105, pp. 246-250.

Noraini, M. Y., Ong, H. C., Badrul, M. J. and Chong, W. T. (2014) 'A review on potential enzymatic reaction for biofuel production from algae', *Renewable and Sustainable Energy Reviews*, 39, pp. 24-34.

Nurra, C., Clavero, E., Salvado, J. and Torras, C. (2014) 'Vibrating membrane filtration as improved technology for microalgae dewatering', *Bioresour Technol*, 157, pp. 247-53.

Odd, I. L. (2013) *Aquaculture Engineering*. 2nd edition edn. United Kingdom: John Wiley & Sons, Ltd.

Oh, H.-M., Lee, S. J., Park, M.-H., Kim, H.-S., Kim, H.-C., Yoon, J.-H., Kwon, G.-S. and Yoon, B.-D. (2001) 'Harvesting of Chlorella vulgaris using a bioflocculant from Paenibacillus sp. AM49', *Biotechnology Letters*, 23(15), pp. 1229-1234.

Oilgae *Extraction of Algal Oil by Chemical Methods*. Available at: http://www.oilgae.com/algae/oil/extract/che/che.html.

Ozkan, A. and Berberoglu, H. (2013a) 'Adhesion of algal cells to surfaces', *Biofouling*, 29(4), pp. 469-82.

Ozkan, A. and Berberoglu, H. (2013b) 'Physico-chemical surface properties of microalgae', *Colloids Surf B Biointerfaces*, 112, pp. 287-93.

Pahl, S. L., Lee, A. K., Kalaitzidis, T., Ashman, P. J., Sathe, S. and Lewis, D. M. (2013) 'Harvesting, Thickening and Dewatering Microalgae Biomass', in Borowitzka, M. A. and Moheimani, N. R. (eds.) *Algae for Biofuels and Energy*. pp. 165-185.

Pan, P., Hu, C., Yang, W., Li, Y., Dong, L., Zhu, L., Tong, D., Qing, R. and Fan, Y. (2010) 'The direct pyrolysis and catalytic pyrolysis of Nannochloropsis sp. residue for renewable bio-oils', *Bioresource Technology*, 101(12), pp. 4593-4599.

Papazi, A., Makridis, P. and Divanach, P. (2010) 'Harvesting Chlorella minutissima using cell coagulants', *Journal of Applied Phycology*, 22(3), pp. 349-355.

Park, J. B. K., Craggs, R. J. and Shilton, A. N. (2015) 'Algal recycling enhances algal productivity and settleability in Pediastrum boryanum pure cultures', *Water Research*, 87, pp. 97-104.

Park, W. and Moon, I. (2007) 'A discrete multi states model for the biological production of hydrogen by phototrophic microalga', *Biochemical Engineering Journal*, 36(1), pp. 19-27.

Passos, F., Solé, M., García, J. and Ferrer, I. (2013) 'Biogas production from microalgae grown in wastewater: Effect of microwave pretreatment', *Applied Energy*, 108, pp. 168-175.

Passos, F., Uggetti, E., Carrère, H. and Ferrer, I. (2014) 'Pretreatment of microalgae to improve biogas production: A review', *Bioresource Technology*, 172, pp. 403-412.

Patil, P. D., Reddy, H., Muppaneni, T., Schaub, T., Holguin, F. O., Cooke, P., Lammers, P., Nirmalakhandan, N., Li, Y., Lu, X. and Deng, S. (2013) 'In situ ethyl ester production from wet algal biomass under microwave-mediated supercritical ethanol conditions', *Bioresour Technol*, 139, pp. 308-15.

Peng, W., Wu, Q. and Tu, P. (2000) 'Effects of temperature and holding time on production of renewable fuels from pyrolysis of Chlorella protothecoides', *Journal of Applied Phycology*, 12(2), pp. 147-152.

Perera, F. (2018) 'Pollution from Fossil-Fuel Combustion is the Leading Environmental Threat to Global Pediatric Health and Equity: Solutions Exist', *International Journal of Environmental Research and Public Health*, 15(1), p. 16.

Petruševski, B., Bolier, G., Van Breemen, A. N. and Alaerts, G. J. (1995) 'Tangential flow filtration: A method to concentrate freshwater algae', *Water Research*, 29(5), pp. 1419-1424.

Pezzolesi, L., Samorì, C. and Pistocchi, R. (2015) 'Flocculation induced by homogeneous and heterogeneous acid treatments in Desmodesmus communis', *Algal Research*, 10, pp. 145-151.

Phoochinda, W. and White, D. A. (2003) 'Removal of algae using froth flotation', *Environmental Technology*, 24(1), pp. 87-96.

Phoochinda, W., White, D. A. and Briscoe, B. J. (2005) 'Comparison between the removal of live and dead algae using froth flotation', *Journal of Water Supply: Research and Technology - AQUA*, 54(2), pp. 115-125.

Photobioreactor (2012). Available at: https://en.wikipedia.org/wiki/Photobioreactor (Accessed: April 2015).

Pleissner, D. and Rumpold, B. A. (2018) 'Utilization of organic residues using heterotrophic microalgae and insects', *Waste Management*, 72, pp. 227-239.

Poelman, E., De Pauw, N. and Jeurissen, B. (1997) 'Potential of electrolytic flocculation for recovery of micro-algae', *Resources, Conservation and Recycling*, 19(1), pp. 1-10.

Pradhan, R. R., Pradhan, R. R., Das, S., Dubey, B. and Dutta, A. (2017) 'Bioenergy Combined with Carbon Capture Potential by Microalgae at Flue Gas-Based Carbon Sequestration Plant of NALCO as Accelerated Carbon Sink', in Goel, M. and Sudhakar, M. (eds.) *Carbon Utilization: Applications for the Energy Industry*. Singapore: Springer Singapore, pp. 231-244.

Pragya, N., Pandey, K. K. and Sahoo, P. K. (2013) 'A review on harvesting, oil extraction and biofuels production technologies from microalgae', *Renewable and Sustainable Energy Reviews*, 24, pp. 159-171.

Pranowo, R., Lee, D. J., Liu, J. C. and Chang, J. S. (2013) 'Effect of O3 and O3/H2O2 on algae harvesting using chitosan', *Water Sci Technol*, 67(6), pp. 1294-301.

Prince, M. J. and Blanch, H. W. (1990) 'Bubble coalescence and break- up in air- sparged bubble columns', *AIChE Journal*, 36(10), pp. 1485-1499.

Qari, H., Rehan, M. and Nizami, A.-S. (2017) 'Key Issues in Microalgae Biofuels: A Short Review', *Energy Procedia*, 142, pp. 898-903.

Raheem, A., Prinsen, P., Vuppaladadiyam, A. K., Zhao, M. and Luque, R. (2018) 'A review on sustainable microalgae based biofuel and bioenergy production: Recent developments', *Journal of Cleaner Production*, 181, pp. 42-59.

Raheem, A., Wan Azlina, W. A. K. G., Taufiq Yap, Y. H., Danquah, M. K. and Harun, R. (2015) 'Thermochemical conversion of microalgal biomass for biofuel production', *Renewable and Sustainable Energy Reviews*, 49, pp. 990-999.

Ralston, J., Fornasiero, D. and Hayes, R. (1999) 'Bubble–particle attachment and detachment in flotation', *International Journal of Mineral Processing*, 56(1), pp. 133-164.

Ramachandran, K., Suganya, T., Nagendra Gandhi, N. and Renganathan, S. (2013) 'Recent developments for biodiesel production by ultrasonic assist transesterification using different heterogeneous catalyst: A review', *Renewable and Sustainable Energy Reviews*, 22, pp. 410-418.

Rashid, N., Ur Rehman, M. S., Sadiq, M., Mahmood, T. and Han, J.-I. (2014) 'Current status, issues and developments in microalgae derived biodiesel production', *Renewable and Sustainable Energy Reviews*, 40, pp. 760-778.

Rawat, I., Ranjith Kumar, R., Mutanda, T. and Bux, F. (2011) 'Dual role of microalgae: Phycoremediation of domestic wastewater and biomass production for sustainable biofuels production', *Applied Energy*, 88(10), pp. 3411-3424.

Rawat, I., Ranjith Kumar, R., Mutanda, T. and Bux, F. (2013) 'Biodiesel from microalgae: A critical evaluation from laboratory to large scale production', *Applied Energy*, 103, pp. 444-467.

Rawlings, J. O., Pantula, S. G. and Dickey, D. A. (1998) *Applied Regression Analysis: A Research Tool*. 2nd edn. New York: Springer-Verlag.

Reay, D. and Ratcliff, G. A. (1973) 'Removal of fine particles from water by dispersed air flotation: Effects of bubble size and particle size on collection efficiency', *The Canadian Journal of Chemical Engineering*, 51(2), pp. 178-185.

Reay, D. and Ratcliff, G. A. (1975) 'Experimental testing of the hydrodynamic collision model of fine particle flotation', *The Canadian Journal of Chemical Engineering*, 53(5), pp. 481-486.

Rehn, G., Grey, C., Branneby, C. and Adlercreutz, P. (2013) 'Chitosan flocculation: An effective method for immobilization of E. coli for biocatalytic processes', *Journal of Biotechnology*, 165(2), pp. 138-144.

Reyes, J. F. and Labra, C. (2016) 'Biomass harvesting and concentration of microalgae *Scenedesmus* sp. cultivated in a pilot phobioreactor', *Biomass and Bioenergy*, 87, pp. 78-83.

Reynolds, C. S. (1984) *The ecology of freshwater phytoplankton*. Cambridge, Uk Cambridge University Press.

Rios, S. D., Castaneda, J., Torras, C., Farriol, X. and Salvado, J. (2013) 'Lipid extraction methods from microalgal biomass harvested by two different paths: screening studies toward biodiesel production', *Bioresour Technol*, 133, pp. 378-88.

Robert, C. P. (2012) 'Handbook of Fitting Statistical Distributions with R by Zaven A. Karian, Edward J. Dudewicz', *International Statistical Review*, 80(1), pp. 177-178.

Rodriguez, C., Alaswad, A., Mooney, J., Prescott, T. and Olabi, A. G. (2015) 'Pre-treatment techniques used for anaerobic digestion of algae', *Fuel Processing Technology*.

Rosenberg, M., Gutnick, D. and Rosenberg, E. (1980) 'Adherence of bacteria to hydrocarbons: A simple method for measuring cell- surface hydrophobicity', *FEMS Microbiology Letters*, 9(1), pp. 29-33.

Ross, A. B., Biller, P., Kubacki, M. L., Li, H., Lea-Langton, A. and Jones, J. M. (2010) 'Hydrothermal processing of microalgae using alkali and organic acids', *Fuel*, 89(9), pp. 2234-2243.

Rossignol, N., Vandanjon, L., Jaouen, P. and Quéméneur, F. (1999) 'Membrane technology for the continuous separation microalgae/culture medium: compared performances of cross-flow microfiltration and ultrafiltration', *Aquacultural Engineering*, 20(3), pp. 191-208.

Rubio, J., Souza, M. L. and Smith, R. W. (2002) 'Overview of flotation as a wastewater treatment technique', *Minerals Engineering*, 15(3), pp. 139-155.

Runge, K., Franzidis, J.-P. and Manlapig, E. (2003) *A study of the flotation characteristics of different mineralogical classes in different streams of an industrial circuit*.

Ryu, B.-G., Kim, J., Han, J.-I., Kim, K., Kim, D., Seo, B.-K., Kang, C.-M. and Yang, J.-W. (2018) 'Evaluation of an electro-flotation-oxidation process for harvesting bio-flocculated algal

biomass and simultaneous treatment of residual pollutants in coke wastewater following an algal-bacterial process', *Algal Research*, 31, pp. 497-505.

S. Dobby, G. and A. Finch, J. (1986) *Flotation Column Scale-up and Modelling*.

Saint-Jalmes, A. (2006) 'Physical chemistry in foam drainage and coarsening', *Soft Matter*, 2(10), pp. 836-849.

Salager J. L. (2002) *Surfactants: Types and Uses*. FIRP Booklet, E300-A, Version 2, Merida Venezuela.

Saleh, Z., Stanley, R. and Nigam, M. (2006) 'Extraction of polyphenolics from apple juice by foam fractionation', *International Journal of Food Engineering*, 2, p. Art. 2.

Salema, A. A. and Ani, F. N. (2012) 'Microwave-assisted pyrolysis of oil palm shell biomass using an overhead stirrer', *Journal of Analytical and Applied Pyrolysis*, 96, pp. 162-172.

Salim, S., Bosma, R., Vermue, M. H. and Wijffels, R. H. (2011) 'Harvesting of microalgae by bio-flocculation', *J Appl Phycol*, 23(5), pp. 849-855.

Salim, S., Kosterink, N. R., Tchetkoua Wacka, N. D., Vermuë, M. H. and Wijffels, R. H. (2014) 'Mechanism behind autoflocculation of unicellular green microalgae Ettlia texensis', *Journal of Biotechnology*, 174, pp. 34-38.

Salim, S., Vermuë, M. H. and Wijffels, R. H. (2012) 'Ratio between autoflocculating and target microalgae affects the energy-efficient harvesting by bio-flocculation', *Bioresource Technology*, 118, pp. 49-55.

Sanchez-Silva, L., López-González, D., Garcia-Minguillan, A. M. and Valverde, J. L. (2013) 'Pyrolysis, combustion and gasification characteristics of Nannochloropsis gaditana microalgae', *Bioresource Technology*, 130, pp. 321-331.

Santana, A., Jesus, S., Larrayoz, M. A. and Filho, R. M. (2012) 'Supercritical Carbon Dioxide Extraction of Algal Lipids for the Biodiesel Production', *Procedia Engineering*, 42, pp. 1755-1761.

Sanyano, N., Chetpattananondh, P. and Chongkhong, S. (2013) 'Coagulation-flocculation of marine *Chlorella* sp. for biodiesel production', *Bioresource Technology*, 147, pp. 471-476.

Sastri, S. R. S. (1998) 'Column Flotation: Theory and Practice', *Workshop on Froth Flotation:Recent Trends*. Bhubaneswar.

Sathish, A. and Sims, R. C. (2012) 'Biodiesel from mixed culture algae via a wet lipid extraction procedure', *Bioresour Technol*, 118, pp. 643-7.

Satputaley, S. S., Zodpe, D. B. and Deshpande, N. V. (2017) 'Performance, combustion and emission study on CI engine using microalgae oil and microalgae oil methyl esters', *Journal of the Energy Institute*, 90(4), pp. 513-521.

Satterfield, C. N. (1973) 'Chemical reaction engineering, Octave Levenspiel, Wiley, New York (1972). 578 pages.', *AIChE Journal*, 19(1), pp. 206-207.

Schramm, L. L. and Mikula, R. J. (2012) 'Froth flotation of oil sand bitumen', in Stevenson, P. (ed.) *Foam Engineering: Fundamentals and Applications*. Chichester, UK: Wiley & Sons, Ltd.

Schulze, H. J. (1989) 'Hydrodynamics of bubble-mineral particle collisions', *Mineral Processing and Extractive Metallurgy Review*, 5(1), pp. 43-76.

Schulze, H. J. and Gottschalk, G. (1981) 'Experimental Investigation of the Hydrodynamic Interaction between Particles and a Gas Bubble', *Aufbereitungs-Technik*, 22(5), pp. 254-264.

Shahbazi, B., Rezai, B. and Javad Koleini, S. M. (2010) 'Bubble–particle collision and attachment probability on fine particles flotation', *Chemical Engineering and Processing: Process Intensification*, 49(6), pp. 622-627.

Shakya, R., Adhikari, S., Mahadevan, R., Shanmugam, S. R., Nam, H., Hassan, E. B. and Dempster, T. A. (2017) 'Influence of biochemical composition during hydrothermal liquefaction of algae on product yields and fuel properties', *Bioresour Technol*, 243, pp. 1112-1120.

Sheehan, J., Dunahay, T., Benemann, J. and Roessler, P. (2009) *A look back at the U.S. department of energy's aquatic species program: Biodiesel from algae*.

Shelef, G. A., Sukenik, A. and Green, M. (1984) *Microalgae harvesting and processing: A literature review*. Golden Colorado.

Show, K. Y., Lee, D. J. and Chang, J. S. (2013) 'Algal biomass dehydration', *Bioresour Technol*, 135, pp. 720-9.

Shuit, S. H., Lee, K. T., Kamaruddin, A. H. and Yusup, S. (2010) 'Reactive Extraction of Jatropha curcas L. Seed for Production of Biodiesel: Process Optimization Study', *Environmental Science & Technology*, 44(11), pp. 4361-4367.

Shuping, Z., Yulong, W., Mingde, Y., Kaleem, I., Chun, L. and Tong, J. (2010) 'Production and characterization of bio-oil from hydrothermal liquefaction of microalgae Dunaliella tertiolecta cake', *Energy*, 35(12), pp. 5406-5411.

Singh, G. and Patidar, S. K. (2018) 'Microalgae harvesting techniques: A review', *Journal of Environmental Management*, 217, pp. 499-508.

Sirmerova, M., Prochazkova, G., Siristova, L., Kolska, Z. and Branyik, T. (2013) 'Adhesion of Chlorella vulgaris to solid surfaces, as mediated by physicochemical interactions', *Journal of Applied Phycology*, 25(6), pp. 1687-1695.

Smith, B. T. and Davis, R. H. (2012) 'Sedimentation of algae flocculated using naturally-available, magnesium-based flocculants', *Algal Research*, 1(1), pp. 32-39.

Smith, B. T. and Davis, R. H. (2013) 'Particle concentration using inclined sedimentation via sludge accumulation and removal for algae harvesting', *Chemical Engineering Science*, 91, pp. 79-85.

Smith, R. W., Yang, Z. and Wharton, R. A. (1991) 'Flotation of Chlorella vulgaris with anionic, cationic and amphoteric collectors', *TRANSACTIONS- SOCIETY OF MINING ENGINEERS OF AIME* (290), p. 22.

Soeder, C. J. (1980) 'Massive cultivation of microalgae: Results and prospects', *Hydrobiologia*, 72(1), pp. 197-209.

Somasundaran, P. and Ananthapadmanabhan, K. P. (1987) 'Bubble and Foam Separations - Ore Flotation', in Rousseau, R. W. (ed.) *Handbook of Separation Process Technology*. New York: J. Wiley & Sons, pp. 775-805.

Sompech, K., Chisti, Y. and Srinophakun, T. (2012) 'Design of raceway ponds for producing microalgae', *Biofuels*, 3(4), pp. 387-397.

Song, W., Wang, S., Guo, Y. and Xu, D. (2017) 'Bio-oil production from hydrothermal liquefaction of waste Cyanophyta biomass: Influence of process variables and their interactions on the product distributions', *International Journal of Hydrogen Energy*, 42(31), pp. 20361-20374.

Spolaore, P., Joannis-Cassan, C., Duran, E. and Isambert, A. (2006) 'Commercial applications of microalgae', *Journal of Bioscience and Bioengineering*, 101(2), pp. 87-96.

Steriti, A., Rossi, R., Concas, A. and Cao, G. (2014) 'A novel cell disruption technique to enhance lipid extraction from microalgae', *Bioresour Technol*, 164, pp. 70-7.

Stevenson, P. and Li, X. (2012a) 'Froth phase phenomena in flotation', in Stevenson, P. (ed.) *Foam Engineering: Fundamentals and Applications*. Chichester, UK: Wiley & Sons, Ltd, pp. 227-249.

Stevenson, P. and Li, X. (2012b) 'Pneumatic Foam', in *Foam Engineering*. John Wiley & Sons, Ltd, pp. 145-167.

Stevenson, P. and Li, X. (2014) *Foam Fractionation Principles and Process Design*. Taylor & Francis Group.

Su-Ping, Z. (2003) 'Study of Hydrodeoxygenation of Bio-Oil from the Fast Pyrolysis of Biomass', *Energy Sources*, 25(1), pp. 57-65.

Su, Y., Song, K., Zhang, P., Su, Y., Cheng, J. and Chen, X. (2017) 'Progress of microalgae biofuel's commercialization', *Renewable and Sustainable Energy Reviews*, 74, pp. 402-411.

Suali, E. and Sarbatly, R. (2012) 'Conversion of microalgae to biofuel', *Renewable and Sustainable Energy Reviews*, 16(6), pp. 4316-4342.

Sukenik, A., Bilanovic, D. and Shelef, G. (1988) 'Flocculation of microalgae in brackish and sea waters', *Biomass*, 15(3), pp. 187-199.

Sutherland, K. L. (1948) 'Physical Chemistry of Flotation. XI. Kinetics of the Flotation Process', *The Journal of Physical and Colloid Chemistry*, 52(2), pp. 394-425.

Takisawa, K., Kanemoto, K., Kartikawati, M. and Kitamura, Y. (2013) 'Simultaneous hydrolysis-esterification of wet microalgal lipid using acid', *Bioresour Technol*, 149, pp. 16-21.

Tan, C. H., Show, P. L., Chang, J. S., Ling, T. C. and Lan, J. C. (2015) 'Novel approaches of producing bioenergies from microalgae: A recent review', *Biotechnol Adv*, 33(6 Pt 2), pp. 1219-27.

Tan, X. B., Lam, M. K., Uemura, Y., Lim, J. W., Wong, C. Y. and Lee, K. T. (2018) 'Cultivation of microalgae for biodiesel production: A review on upstream and downstream processing', *Chinese Journal of Chemical Engineering*, 26(1), pp. 17-30.

Tekin, K., Karagöz, S. and Bektaş, S. (2014) 'A review of hydrothermal biomass processing', *Renewable and Sustainable Energy Reviews*, 40, pp. 673-687.

Teo, C. L. and Idris, A. (2014a) 'Enhancing the various solvent extraction method via microwave irradiation for extraction of lipids from marine microalgae in biodiesel production', *Bioresour Technol*, 171, pp. 477-81.

Teo, C. L. and Idris, A. (2014b) 'Evaluation of direct transesterification of microalgae using microwave irradiation', *Bioresource Technology*, 174, pp. 281-286.

Teri, G., Luo, L. and Savage, P. E. (2014) 'Hydrothermal Treatment of Protein, Polysaccharide, and Lipids Alone and in Mixtures', *Energy & Fuels*, 28(12), pp. 7501-7509.

Tian, C., Li, B., Liu, Z., Zhang, Y. and Lu, H. (2014) 'Hydrothermal liquefaction for algal biorefinery: A critical review', *Renewable and Sustainable Energy Reviews*, 38, pp. 933-950.

Tobar, M. and Núñez, G. A. (2018) 'Supercritical transesterification of microalgae triglycerides for biodiesel production: Effect of alcohol type and co-solvent', *The Journal of Supercritical Fluids*, 137, pp. 50-56.

Torri, C., Garcia Alba, L., Samorì, C., Fabbri, D. and Brilman, D. W. F. (2012) 'Hydrothermal Treatment (HTT) of Microalgae: Detailed Molecular Characterization of HTT Oil in View of HTT Mechanism Elucidation', *Energy & Fuels*, 26(1), pp. 658-671.

Udom, I., Zaribaf, B. H., Halfhide, T., Gillie, B., Dalrymple, O., Zhang, Q. and Ergas, S. J. (2013) 'Harvesting microalgae grown on wastewater', *Bioresour Technol*, 139, pp. 101-6.

Uduman, N., Bourniquel, V., Danquah, M. K. and Hoadley, A. F. A. (2011) 'A parametric study of electrocoagulation as a recovery process of marine microalgae for biodiesel production', *Chemical Engineering Journal*, 174(1), pp. 249-257.

Uduman, N., Qi, Y., Danquah, M. K., Forde, G. M. and Hoadley, A. (2010a) 'Dewatering of microalgal cultures: a major bottleneck to algae-based fuels', *Journal of Renewable and Sustainable Energy*, 2(1), p. 012701.

Uduman, N., Qi, Y., Danquah, M. K. and Hoadley, A. F. A. (2010b) 'Marine microalgae flocculation and focused beam reflectance measurement', *Chemical Engineering Journal*, 162(3), pp. 935-940.

Ueno, Y., Kurano, N. and Miyachi, S. (1998) 'Ethanol production by dark fermentation in the marine green alga, Chlorococcum littorale', *Journal of Fermentation and Bioengineering*, 86(1), pp. 38-43.

Ullah, K., Ahmad, M., Sofia, Sharma, V. K., Lu, P., Harvey, A., Zafar, M. and Sultana, S. (2015) 'Assessing the potential of algal biomass opportunities for bioenergy industry: A review', *Fuel*, 143, pp. 414-423.

Ust'ak, S., Havrland, B., Muñoz, J. O. J., Fernández, E. C. and Lachman, J. (2007) 'Experimental verification of various methods for biological hydrogen production', *International Journal of Hydrogen Energy*, 32(12), pp. 1736-1741.

Valdez, P. J., Dickinson, J. G. and Savage, P. E. (2011) 'Characterization of Product Fractions from Hydrothermal Liquefaction of Nannochloropsis sp. and the Influence of Solvents', *Energy & Fuels*, 25(7), pp. 3235-3243.

Vandamme, D. (2013) *Flocculation based harvesting processes for microalgae biomass production*.

Vandamme, D., Beuckels, A., Markou, G., Foubert, I. and Muylaert, K. (2015) 'Reversible Flocculation of Microalgae using Magnesium Hydroxide', *BioEnergy Research*, 8(2), pp. 716-725.

Vandamme, D., Foubert, I., Fraeye, I., Meesschaert, B. and Muylaert, K. (2012) 'Flocculation of Chlorella vulgaris induced by high pH: role of magnesium and calcium and practical implications', *Bioresour Technol*, 105, pp. 114-9.

Vandamme, D., Foubert, I., Meesschaert, B. and Muylaert, K. (2010) 'Flocculation of microalgae using cationic starch', *Journal of Applied Phycology*, 22(4), pp. 525-530.

Vandamme, D., Foubert, I. and Muylaert, K. (2013) 'Flocculation as a low-cost method for harvesting microalgae for bulk biomass production', *Trends Biotechnol*, 31(4), pp. 233-9.

Vandamme, D., Pontes, S. C., Goiris, K., Foubert, I., Pinoy, L. J. and Muylaert, K. (2011) 'Evaluation of electro-coagulation-flocculation for harvesting marine and freshwater microalgae', *Biotechnol Bioeng*, 108(10), pp. 2320-2329.

Vanini, G., Castro, E., Silva Filho, E. and Romão, W. (2013) *Chemical Depolymerization of Post-Consumption Bottle-Grade Poly (ethylene terephthalate) in the Presence of the Cationic Catalyst Cetyl Trimethyl Ammonium Bromide (CTAB)*.

Vardon, D. R., Sharma, B. K., Scott, J., Yu, G., Wang, Z., Schideman, L., Zhang, Y. and Strathmann, T. J. (2011) 'Chemical properties of biocrude oil from the hydrothermal liquefaction of Spirulina algae, swine manure, and digested anaerobic sludge', *Bioresource Technology*, 102(17), pp. 8295-8303.

Vazirizadeh, A., Bouchard, J. and Chen, Y. (2016) 'Effect of particles on bubble size distribution and gas hold-up in column flotation', *International Journal of Mineral Processing*, 157, pp. 163-173.

Velasquez-Orta, S. B., Lee, J. G. M. and Harvey, A. (2012) 'Alkaline in situ transesterification of Chlorella vulgaris', *Fuel*, 94, pp. 544-550.

Vera, M. U. and Durian, D. J. (2002) 'Enhanced Drainage and Coarsening in Aqueous Foams', *Physical Review Letters*, 88(8), p. 088304.

Vijayaraghavan, K. and Hemanathan, K. (2009) 'Biodiesel Production from Freshwater Algae', *Energy Fuels*, 23, pp. 5448–5453.

Wagner, J., Bransgrove, R., Beacham, T. A., Allen, M. J., Meixner, K., Drosg, B., Ting, V. P. and Chuck, C. J. (2016) 'Co-production of bio-oil and propylene through the hydrothermal liquefaction of polyhydroxybutyrate producing cyanobacteria', *Bioresour Technol*, 207, pp. 166-74.

Wahlen, B. D., Willis, R. M. and Seefeldt, L. C. (2011) 'Biodiesel production by simultaneous extraction and conversion of total lipids from microalgae, cyanobacteria, and wild mixed-cultures', *Bioresource Technology*, 102(3), pp. 2724-2730.

Wallis, G. B. (1969) *One Dimensional Two-Phase Flow*. McGraw Hill Higher Education.

Wan, C., Alam, M. A., Zhao, X.-Q., Zhang, X.-Y., Guo, S.-L., Ho, S.-H., Chang, J.-S. and Bai, F.-W. (2014) 'Current progress and future prospect of microalgal biomass harvest using various flocculation technologies', *Bioresource Technology*, (0).

Wan, C., Zhao, X.-Q., Guo, S.-L., Asraful Alam, M. and Bai, F.-W. (2013) 'Bioflocculant production from Solibacillus silvestris W01 and its application in cost-effective harvest of marine microalga Nannochloropsis oceanica by flocculation', *Bioresource Technology*, 135, pp. 207-212.

Wang, C., Pan, J., Li, J. and Yang, Z. (2008) 'Comparative studies of products produced from four different biomass samples via deoxy-liquefaction', *Bioresource Technology*, 99(8), pp. 2778-2786.

Wang, J., Liu, G., Wu, Z. and Zhang, L. (2010a) 'Intensified Effect of Reduced Pressure on the Foam Fractionation Process of Bovine Serum Albumin', *Separation Science and Technology*, 45(16), pp. 2489-2496.

Wang, J., Nguyen, A. V. and Farrokhpay, S. (2016a) 'A critical review of the growth, drainage and collapse of foams', *Advances in Colloid and Interface Science*, 228, pp. 55-70.

Wang, J., Qiu, L. P., Meng, S. L., Fan, L. M., Song, C. and Chen, J. C. (2014) 'Effect of pH on growth and competition of Chlorella vulgaris and Anabaena sp. strain PCC.', *Ecology and Environmental Sciences*, pp. 316–320.

Wang, L. K., Shammas, N. K., Selke, W. A. and Aulenbach, D. B. (2010b) *Flotation Technology*. Totowa, NJ: Humana Press.

Wang, M. and Park, C. (2015) 'Investigation of anaerobic digestion of Chlorella sp. and Micractinium sp. grown in high-nitrogen wastewater and their co-digestion with waste activated sludge', *Biomass and Bioenergy*, 80, pp. 30-37.

Wang, M., Sahu, A. K., Rusten, B. and Park, C. (2013a) 'Anaerobic co-digestion of microalgae Chlorella sp. and waste activated sludge', *Bioresour Technol*, 142, pp. 585-90.

Wang, W., Xu, Y., Wang, X., Zhang, B., Tian, W. and Zhang, J. (2017) 'Hydrothermal liquefaction of microalgae over transition metal supported TiO2 catalyst', *Bioresour Technol*, 250, pp. 474-480.

Wang, Y., Ho, S. H., Cheng, C. L., Guo, W. Q., Nagarajan, D., Ren, N. Q., Lee, D. J. and Chang, J. S. (2016b) 'Perspectives on the feasibility of using microalgae for industrial wastewater treatment', *Bioresour Technol*, 222, pp. 485-497.

Wang, Y., Wu, Z., Li, R. and Zhang, Z. (2013b) 'Enhancing foam drainage using inclined foam channels of different angles for recovering the protein from whey wastewater', *Colloids and Surfaces A: Physicochemical and Engineering Aspects*, 419, pp. 28-36.

Wang, Z., Hou, J., Bowden, D. and Belovich Joanne, M. (2013c) 'Evaluation of an inclined gravity settler for microalgae harvesting', *Journal of Chemical Technology & Biotechnology*, 89(5), pp. 714-720.

Wehner, J. F. and Wilhelm, R. H. (1956) 'Boundary conditions of flow reactor', *Chemical Engineering Science*, 6(2), pp. 89-93.

Wei, P., Cheng, L.-H., Zhang, L., Xu, X.-H., Chen, H.-l. and Gao, C.-j. (2014) 'A review of membrane technology for bioethanol production', *Renewable and Sustainable Energy Reviews*, 30, pp. 388-400.

Weissman, J. C. and Goebel, R. P. (1987) *Design and analysis of microalgal open pond systems for the purpose of producing fuels: A subcontract report* (SERI/STR-231-2840; Other: ON: DE87001164 United States 10.2172/6546458 Other: ON: DE87001164 NTIS, PC A11; 3. NREL English). [Online]. Available at: http://www.osti.gov/scitech/servlets/purl/6546458.

Wen H, L. Y. P., Shen Z, Ren X Y, Zhang W J, Liu J. (2017) 'Surface characteristics of microalgae and their effects on harvesting performance by air flotation', *Int J Agric & Biol Eng*, 10(1), pp. 125–133.

Wiley, P. E., Brenneman, K. J. and Jacobson, A. E. (2009) 'Improved Algal Harvesting Using Suspended Air Flotation', *Water Environment Research*, 81(7), pp. 702-708.

Wiley, P. E., Campbell, J. E. and McKuin, B. (2011) 'Production of biodiesel and biogas from algae: a review of process train options', *Water Environ Res*, 83(4), pp. 326-38.

Willis, R. M., McCurdy, A. T., Ogborn, M. K., Wahlen, B. D., Quinn, J. C., Pease, L. F., 3rd and Seefeldt, L. C. (2014) 'Improving energetics of triacylglyceride extraction from wet oleaginous microbes', *Bioresour Technol*, 167, pp. 416-24.

Wilson, M. A. (2012) *CROSS FLOW FILTRATION FOR MIXED-CULTURE ALGAE HARVESTING FOR MUNICIPAL WASTEWATER LAGOONS*. UTAH STATE UNIVERSITY.

World Energy Statistics (2017) *Global Energy Statistical Yearbook 2017*. Available at: https://yearbook.enerdata.net/renewables/renewable-in-electricity-production-share.html.

Wu, C. H., Chien, W. C., Chou, H. K., Yang, J. and Lin, H. T. (2014) 'Sulfuric acid hydrolysis and detoxification of red alga Pterocladiella capillacea for bioethanol fermentation with thermotolerant yeast Kluyveromyces marxianus', *J Microbiol Biotechnol*, 24(9), pp. 1245-53.

Xia, L., Huang, R., Li, Y. and Song, S. (2017a) 'The effect of growth phase on the surface properties of three oleaginous microalgae (Botryococcus sp. FACGB-762, Chlorella sp. XJ-445 and Desmodesmus bijugatus XJ-231)', *PLoS One*, 12(10), p. e0186434.

Xia, L., Li, H. and Song, S. (2016) 'Cell surface characterization of some oleaginous green algae', *Journal of Applied Phycology*, 28(4), pp. 2323-2332.

Xia, L., Li, Y., Huang, R. and Song, S. (2017b) 'Effective harvesting of microalgae by coagulation–flotation', *Royal Society Open Science*, 4(11), p. 170867.

Xia, W. (2017) 'Role of particle shape in the floatability of mineral particle: An overview of recent advances', *Powder Technology*, 317, pp. 104-116.

Xie, S., Sun, S., Dai, S. Y. and S.Yuan, J. (2013) 'Efficient coagulation of microalgae in cultures with filamentous fungi', *Algal Research*, 2(1), pp. 28-33.

Xiong, J.-Q., Kurade, M. B. and Jeon, B.-H. (2018) 'Can Microalgae Remove Pharmaceutical Contaminants from Water?', *Trends in Biotechnology*, 36(1), pp. 30-44.

Xu, L., Guo, C., Wang, F., Zheng, S. and Liu, C.-Z. (2011) 'A simple and rapid harvesting method for microalgae by in situ magnetic separation', *Bioresource Technology*, 102(21), pp. 10047-10051.

Xu, L., Wang, F., Li, H.-Z., Hu, Z.-M., Guo, C. and Liu, C.-Z. (2010) 'Development of an efficient electroflocculation technology integrated with dispersed-air flotation for harvesting microalgae', *Journal of Chemical Technology & Biotechnology*, pp. 1504-1507.

Xu, R. and Mi, Y. (2010) 'Simplifying the Process of Microalgal Biodiesel Production Through In Situ Transesterification Technology', *Journal of the American Oil Chemists' Society*, 88(1), pp. 91-99.

Xu, R. and Mi, Y. (2011) 'Simplifying the Process of Microalgal Biodiesel Production Through In Situ Transesterification Technology', *Journal of the American Oil Chemists' Society*, 88(1), pp. 91-99.

Xu, X.-Q., Wang, J.-H., Zhang, T.-Y., Dao, G.-H., Wu, G.-X. and Hu, H.-Y. (2017) 'Attached microalgae cultivation and nutrients removal in a novel capillary-driven photo-biofilm reactor', *Algal Research*, 27, pp. 198-205.

Yanfen, L., Zehao, H. and Xiaoqian, M. (2012) 'Energy analysis and environmental impacts of microalgal biodiesel in China', *Energy Policy*, 45(0), pp. 142-151.

Yang, C., Dabros, T., Li, D., Czarnecki, J. and Masliyah, J. H. (2001) 'Measurement of the Zeta Potential of Gas Bubbles in Aqueous Solutions by Microelectrophoresis Method', *Journal of Colloid and Interface Science*, 243(1), pp. 128-135.

Yang, J., Xu, M., Zhang, X., Hu, Q., Sommerfeld, M. and Chen, Y. (2011a) 'Life-cycle analysis on biodiesel production from microalgae: Water footprint and nutrients balance', *Bioresource Technology*, 102(1), pp. 159-165.

Yang, Q. W., Wu, Z. L., Zhao, Y. L., Wang, Y. and Li, R. (2011b) 'Enhancing foam drainage using foam fractionation column with spiral internal for separation of sodium dodecyl sulfate', *J Hazard Mater*, 192(3), pp. 1900-4.

Yang, W., Li, X., Liu, S. and Feng, L. (2014) 'Direct hydrothermal liquefaction of undried macroalgae Enteromorpha prolifera using acid catalysts', *Energy Conversion and Management*, 87, pp. 938-945.

Yang, Y. F., Feng, C. P., Inamori, Y. and Maekawa, T. (2004) 'Analysis of energy conversion characteristics in liquefaction of algae', *Resources, Conservation and Recycling*, 43(1), pp. 21-33.

Yaylayan, V. A. and Kaminsky, E. (1998) 'Isolation and structural analysis of maillard polymers: caramel and melanoidin formation in glycine/glucose model system', *Food Chemistry*, 63(1), pp. 25-31.

Ye, Y. and Miller, J. D. (1988) 'Bubble/Particle Contact Time in the Analysis of Coal Flotation', *Coal Preparation*, 5(3-4), pp. 147-166.

Yen, H.-W. and Brune, D. E. (2007) 'Anaerobic co-digestion of algal sludge and waste paper to produce methane', *Bioresource Technology*, 98(1), pp. 130-134.

Yianatos, J. B. (2007) 'Fluid Flow and Kinetic Modelling in Flotation Related Processes', *Chemical Engineering Research and Design*, 85(12), pp. 1591-1603.

Yoon, R. H. and Luttrell, G. H. (1989) 'The Effect of Bubble Size on Fine Particle Flotation', *Mineral Processing and Extractive Metallurgy Review*, 5(1-4), pp. 101-122.

Yu, G., Zhang, Y., Schideman, L., L. Funk, T. and Wang, Z. (2011) 'Hydrothermal Liquefaction of Low Lipid Content Microalgae into Bio-Crude Oil', *Transactions of the ASABE*, 54(1), p. 239.

Yuan, X.-Z., Shi, X.-S., Yuan, C.-X., Wang, Y.-P., Qiu, Y.-L., Guo, R.-B. and Wang, L.-S. (2014) 'Modeling anaerobic digestion of blue algae: Stoichiometric coefficients of amino acids acidogenesis and thermodynamics analysis', *Water Research*, 49, pp. 113-123.

Zemmouri, H., Drouiche, M., Sayeh, A., Lounici, H. and Mameri, N. (2012) 'Coagulation Flocculation Test of Keddara's Water Dam Using Chitosan and Sulfate Aluminium', *Procedia Engineering*, 33, pp. 254-260.

Zeng, Y., Zhao, B., Zhu, L., Tong, D. and Hu, C. (2013) 'Catalytic pyrolysis of natural algae from water blooms over nickel phosphide for high quality bio-oil production', *RSC Advances*, 3(27), p. 10806.

Zhan, J., Rong, J. and Wang, Q. (2017) 'Mixotrophic cultivation, a preferable microalgae cultivation mode for biomass/bioenergy production, and bioremediation, advances and prospect', *International Journal of Hydrogen Energy*, 42(12), pp. 8505-8517.

Zhang, C., Wang, X., Wang, Y., Li, Y., Zhou, D. and Jia, Y. (2016a) 'Synergistic effect and mechanisms of compound bioflocculant and AlCl3 salts on enhancing Chlorella regularis harvesting', *Appl Microbiol Biotechnol*, 100(12), pp. 5653-60.

Zhang, J., Chen, W. T., Zhang, P., Luo, Z. and Zhang, Y. (2013) 'Hydrothermal liquefaction of Chlorella pyrenoidosa in sub- and supercritical ethanol with heterogeneous catalysts', *Bioresour Technol*, 133, pp. 389-97.

Zhang, X., Amendola, P., Hewson, J. C., Sommerfeld, M. and Hu, Q. (2012) 'Influence of growth phase on harvesting of Chlorella zofingiensis by dissolved air flotation', *Bioresour Technol*, 116, pp. 477-84.

Zhang, X., Hewson, J. C., Amendola, P., Reynoso, M., Sommerfeld, M., Chen, Y. and Hu, Q. (2014) 'Critical evaluation and modeling of algal harvesting using dissolved air flotation', *Biotechnol Bioeng*, 111(12), pp. 2477-85.

Zhang, X., Wang, L., Sommerfeld, M. and Hu, Q. (2016b) 'Harvesting microalgal biomass using magnesium coagulation-dissolved air flotation', *Biomass and Bioenergy*, 93, pp. 43-49.

Zhou, D., Zhang, L., Zhang, S., Fu, H. and Chen, J. (2010) 'Hydrothermal Liquefaction of Macroalgae Enteromorpha prolifera to Bio-oil', *Energy & Fuels*, 24(7), pp. 4054-4061.

Zhou, W., Chen, P., Min, M., Ma, X., Wang, J., Griffith, R., Hussain, F., Peng, P., Xie, Q., Li, Y., Shi, J., Meng, J. and Ruan, R. (2014) 'Environment-enhancing algal biofuel production using wastewaters', *Renewable and Sustainable Energy Reviews*, 36, pp. 256-269.

Zhou, W., Min, M., Hu, B., Ma, X., Liu, Y., Wang, Q., Shi, J., Chen, P. and Ruan, R. (2013) 'Filamentous fungi assisted bio-flocculation: A novel alternative technique for harvesting heterotrophic and autotrophic microalgal cells', *Separation and Purification Technology*, 107, pp. 158-165.

Zhu, L. (2015) 'Microalgal culture strategies for biofuel production: a review', *Biofuels, Bioproducts and Biorefining*, 9(6), pp. 801-814.

Zhu, Y., Albrecht, K. O., Elliott, D. C., Hallen, R. T. and Jones, S. B. (2013) 'Development of hydrothermal liquefaction and upgrading technologies for lipid-extracted algae conversion to liquid fuels', *Algal Research*, 2(4), pp. 455-464.

Zuniga, H. G. (1935) 'Flotation recovery is an exponential function of its rate', *Boln. Soc. Nac. Min., Santiago, Chile*, 47, pp. 83-87.

Zuorro, A., Maffei, G. and Lavecchia, R. (2016) 'Optimization of enzyme-assisted lipid extraction from Nannochloropsis microalgae', *Journal of the Taiwan Institute of Chemical Engineers*, 67, pp. 106-114.

Appendix 1

Most common first order flotation kinetic models

Table A.1: Description of the most common first order flotation kinetic models

No.	Model	Formula	Comment
1.	First order model	$R = R_\infty[1 - e^{-kt}]$	The standard classical first order flotation kinetic model reported to fit the experimental data well when the particle recovery is low. The first order flotation kinetic is the most widely accepted model and is based on theory and experiment which indicate that the collision rate between the bubbles and particles is first order with respect to the number of particles and that the bubble concentration remains constant (bubble concentration >>> number of particles) (Sutherland, 1948).
2.	First order model with rectangular distribution	$R = R_\infty\left\{1 - \frac{1}{kt}[1 - e^{-kt}]\right\}$	The rectangular distribution of floatability was introduced into the classical first order kinetic model to give the model more flexibility and applicability.
3.	Fully mixed reactor model	$R = R_\infty\left[1 - \frac{1}{1 + t/k}\right]$	This model is also described as first order model with exponential distribution of floatability. This model was introduced by Imaizumi and Inoue in 1963 to give the classical first order model added flexibility which enables it to fit the flotation data well (IMAIZUMI and INOUE, 1963).
4.	First order model with sinusoidal distribution	$R = R_\infty\left[1 - \frac{1 - 2kt\frac{e^{-kt}}{\pi}}{\left(1 + \frac{2kt}{\pi}\right)^2}\right]$	The first order model with sinusoidal distribution of floatability was developed by Diao et al. (1992) (DIAO *et al*., 1992).
5.	First order model with gamma distribution	$R = R_\infty\left[1 - \left(\frac{\lambda}{\lambda + t}\right)^P\right]$	This model contains a continuous distribution function (gamma). It was proposed, like others above, to account for the variability in the rate constant.
6.	First order model with triangular distribution	$R = R_\infty\left[1 - \frac{1 + e^{-2kt} - e^{kt}}{(kt)^2}\right]$	This model contains a continuous distribution function (triangular). It was proposed, like others above, to account for the variability in the rate constant.
7.	Modified Kelsall model	$R = R_\infty[(1 - \varphi)(1 - e^{-k_f t}) + \varphi(1 - e^{-k_s t})]$	This model is the modified version of the Kelsall model after adding the effect of ultimate recovery R_∞. It is a first order kinetic model with discretised distribution that incorporates two fractions and two rate constants for slow and fast-floating particles instead of one rate constant. In other words, it describes the recovery as the sum of slow and fast-floating particles.

Note: R: is the flotation recovery at time t (%), R_∞: is the ultimate flotation recovery at infinite time t_∞ (%), k: is the rate constant (min^{-1}), λ: is the inverse of the rate constant in the first order model with gamma distribution, $\lambda = \frac{1}{k}$ (min), P: is the exponential number in the first order model with gamma distribution, φ: the fraction of flotation particles which have slow rate constant, k_f: the rate constant of fast-floating particles, k_s: the rate constant of slow-floating particles.